Function of the Anterior Gradient Protein Family in Cancer

Argyro Fourtouna

Presented for the degree of Doctor of Philosophy at the University of Edinburgh

December 2008

To the memory of my grandfather

Ioannis Fotou

Acknowledgements

I am very grateful to my supervisor Prof. Hupp for taking on the challenge to have me as a Ph.D. student and for always believing in me and finding something positive in my results. I own Ted many thanks for his guidance and remarkable support throughout the whole project and for having so many exciting ideas that motivated me to explore new pathways of knowledge. I also own many thanks to Kathryn for her helpful comments during my project. Many thanks go to Emma and Vikram for being such good friends for all these years and sharing moments inside and outside science. Thank to you David Lleres for endless conversations about fluorescent microscopy and for valuable advice. Thanks also to a great lab of friends whose support was invaluable Jenny, Jen, Lisa, Sarah, Corina, Magda, Bart, Euan, Angeli, Craig, Yao, Nicky, Erin, Hannan, Suzanne, Jew-Kwang, as well as past members Ben, David, Ashley, Maura, Lindsay, Mirjam, Liz and Nathalie. I am also very grateful to Shirley and Jade for their great technical support. Thank you to Andrea, for always taking care of administrative problems and bureaucracy so that we would only have to worry about science. I am very grateful to Euan for introducing me to the fascinating field of peptide technology. Many thanks go to my friends who always stood by me and support me for all these years abroad, Savvas, Panagiotis, Kostas Kir, Kostas Krik., Manos, Giannis, Deri and most of all Georgia for being an excellent flatmate but most of all for being a great friend. I have no words to express my gratitude to my family for supporting me in all the scientific-related or not problems. Ευχαριστώ πολύ μπαμπάκα, μανούλα, γιαγιά και μπέμπη γιατί χωρίς εσάς δεν θα είχα καταφέρει τίποτε. Thank you to Nikos for being such a great support and for always understanding and believing in me. I am very grateful to Breast Cancer Campaign for the generous funding I received.

Declaration

I hereby declare that I am the author of this thesis and that I performed all the work described herein, except where specifically stated. All sources of information have been acknowledged by means of reference.

Argyro Fourtouna 8/12/08

Summary

Proteomic technologies verified Anterior Gradient 2, AGR-2, as a protein over-expressed in human cancers, including breast, prostate and oesophagus cancers, with the ability to inhibit the tumour suppressor protein p53. *AGR-2* gene is a hormone responsive gene with an unexpected induction by the anti-cancer drug tamoxifen highlighting the proto-oncogenic role of this protein. Anterior Gradient-2 encodes one protein that gives rise to two forms· the full length and the mature one. Full length bears a leader sequence that leads the protein to secretion. Localization studies of both forms of AGR-2 were performed using fluorescence microscopy and subcellular fractionation, in order to determine in which compartment the protein functions. Localization mutants of the mature and full length protein determined the exact sequence required for certain localization patterns. Once localization was confirmed, the mechanism of how Anterior Gradient-2 localization within the cell can inhibit p53 was initiated. Furthermore, novel peptide aptamers that bound to the protein were cloned into GFP vectors and their effect on AGR-2 was investigated. AGR-3, another member of the family, was also examined in terms of localization and function in MCF-7 cells. Yeast two hybrid analysis has identified potential nuclear and cytoplasmic binding partners for AGR-2, essential for the upstream or downstream regulation of the AGR-2 pathway. In conclusion, we present data showing models of how the Anterior Gradient protein family might function as drug-resistance survival factor in cancer as well as a p53 inhibitor, suggesting a multi-potent role of its members when it comes to trafficking, cellular localization and activation or inhibition pathways in cancer.

Abbreviations

a.a	amino acids
AGD	amoebic gill disease
AGR-2	anterior gradient 2
AGR-3	anterior gradient 3
AIF	apoptosis inducing factor
Akt	alias of protein kinase B (PKB)
ANF	anterior neural folds
AP-1	activator protein 1
Apaf-1	apoptosis protease-activating factor 1
APC	adenomatous polyposis coli
apg	autophagy related gene
Apo1	alias of CD95, Fas
Apo3	alias of DR3
Apo3L	Apo3 ligand
APS	ammonium persulfate
AR	androgen receptor
ARF	alias for cyclin-dependent kinase inhibitor CKDN
ASOs	anti-sense oligonucleotides
Asp	Asparagine amino acid
ATCC	American tissue culture collection
Atg	autophagy gene
ATM	ataxia telengiectasia
ATN	adenine nucleotide translocator
ATR	ataxia telengiectasia and Rad3 related
ATRIP	ATR interacting protein
Bad	Bcl2-associated agonist of cell death
BAI1	brain-specific angiogenesis inhibitor 1
BAIAP3	BAI1-associated protein 3
Bak	Bcl2-antagonist/killer 1
BAT3	HLA-B associated transcript 3
Bax	Bcl2-associated X protein
Bcl-2	B-cell lymphoma 2
BCMP11	Breast cancer membrane protein 11
Bid	BH3 interacting domain death agonist
Bim	Bcl2-like 11 apoptosis facilitator
Bip	alias of hspA5
BMP	bone morphogenic protein

bp	base pair
BRCA1	breast cancer 1, early onset
BSA	bovine serum albumin
B&W	black and white
CAK	cyclin-activating kinase
Caspase	cysteine asaprtate protease
CBP	CREB binding protein
CDK 4/6	cyclin-dependent kinase 4/6
CDH6	cadherin 6
CDKN 1/2A	cyclin-dependent kinase inhibitor 1/2A
cDNA	complimentary DNA
C/EBP	CCAAT/ enhancer binding protein
Ced-3	cell death abnormality family member
CGH	Comparative Genome Hybridization
Chk1/2	checkpoint homolog
CHUK	conserved helix-loop-helix ubiquitous kinase
CKAP2	cytoskeleton-associated protein 2
Cop-1	caspase-1 dominant-negative inhibitor pseudo-ICE
CRUK	Cancer Research United Kingdom
CSS	charcoal stripped serum
Cys	cysteine
Da	daltons
Dabco	1,4-Diazabicyclo[2.2.2]octane solution
DAG1	alpha dystroglycan
DAPI	4’,6-Diamidino-2 phenylindole dihydrochloride
DAPK	death-associated protein kinase
DBD	DNA-binding domain
DCA	deoxycholic acid
DDR	DNA damage response pathway
DISC	death-inducing signalling complex
DLG1	discs, large homolog 1
DMSO	dimethyl sulphoxide
DNA-PK	DNA-dependent protein kinase
DR3/4/5	death receptor 3/4/5
dsb	double strand break
dsRNA	double-stranded RNA
DTT	Dithiothreitol solution
Drp	dynamin-related protein
E2	estradiol

E2F	E2F transcription factor
ECACC	European collection of cell cultures
ECL	enhanced chemiluminescence
EDTA	ethylene diamine tetra acetic acid
EGF	epidermal growth factor
EGP	enhanced GFP
EGFR	epidermal growth factor receptor
ER	endoplasmic reticulum
ERα	estrogen receptor alpha
ERBB2	v-erb2 erythroblastic leukemia viral oncogene homolog 2
ERK	alias of MAPK1
ERp	endoplasmic reticulum resident proteins
ERR	oestrogen receptor-related receptor
EST	expressed sequence tag
FADD	FAS-associated death domain
FAS	TNF receptor superfamily, member
FBS	fetal bovine serum
FCS	foetal calf serum
FISH	fluorescent in situ hybridization
FOXA	forkhead box protein
FP	fluorescent protein
FRET	fluorescence resonance energy transfer
GADD54	growth arrest and DNA-damage-inducible
GFP	green fluorescent protein
GI	gastro-intestinal
GIT1	G protein-coupled receptor kinase interactor 1
Gob-4	alias of AGR-2
GR	glucocorticoid receptor
GRH	gonadotrophin releasing hormone
GSTM4	glutathione S-transferase M4
GTFIIH	general transcription factor IIH, polypeptide 4
HCC	hepatocellular carcinoma
hCG	human choriogonadotropin
HDAC	histone deacetylase
HDM	human homolog of mouse doubles minute 2
HER2	herstatin, herceptin 2, alias of ERBB2
HERC2	hect domain and RLD2
HIC-1	hypermethylated in cancer 1
HIF-1	hypoxia inducing factor 1

HIP1R	huntingtin interacting protein 1 related
HRP	horseradish peroxidase
Hsp	heat shock protein
HUWE1	HECT, UBA and WWE domain containing 1
ICE	alias of caspace 1, interleukin 1-B converting enzyme
IF	immunofluorescence
IH	immunohistochemistry
IGF-1	insulin growth factor-1
IGF-1R	insulin growth factor-1 receptor
IkB	alias of CHUK
IKK	IκB kinase kinase
IL-1	interleukin-1
IPTG	Isopropylβ-D-1thiogalactopyranosidine
IR	ionising radiation
IXL1	alias of MED29
JNK	alias for MAPK8
KCT3	keratinocytes associated transmembrane protein
KIBRA	alias of WWC1
LC3	alias of MAP1LC3A
LRBA	LPS-responsive vesicle trafficking, beach and anchor containing
MAST1	microtubule associated serine/threonine kinase 1
MAP	multiple antigenic peptides
MAP1LC3A	microtubule-associated protein 1 light chain 3 alpha
MAPK	mitogen-activating protein kinase 1
Mdm2	mouse double minute 2
Mdm	mitochondrial distribution and morphology protein
MED29	mediator complex subunit 29
MEF	mouse embryonic fibloblast
Mfn 1/ 2	mitofusin protein 1/ 2
Mmm	maintenance of mitochondrial morphology protein
MOMP	mitochondrial outer membrane permeabilization
mRNA	messenger RNA
MRC	mitochondrial respiratory chain
MS	mass spectrometry
MTs	microtubules
mtDNA	mitochondrial DNA
MTT	methylthiazoletetrazolium
MYBBP1A	v-myb myeloblastosis viral oncogene homolog
MYBBP1A	MYB binding protein

NB	neuroblastoma
NCBI	National Centre for Biotechnology Information
NEAA	non-essential amino acids
NES	nuclear export signal/sequence
NF-κB	nuclear factor kappa B
NLS	nuclear localization signal/sequence
NuMA	nuclear protein associated with the mitotic apparatus
Opa1	optic atrophy protein 1
PAGE	polyacrylamide gel electrophoresis
$P^{14}ARF$	alias for CDKN2A
PARG1	PTPL1-associated RhoGAP 1
PBS	phosphate buffered saline
PBS-T	phosphate buffered saline tween
PCNA	proliferating cell nuclear antigen
PCR	polymerase chain reaction
PDI	protein disulfide isomerase
PF	parafolmadehyde
Pfu	plaque forming units
PI3K	phosphatidyl inositol 3 kinase
PIKK	phosphoinositide-3-kinase-related kinase
Pirh-2	alias fof RCHY1
PKC	protein kinase C
PM	plasma membrane
PPM1D	protein phosphatase 1D magnesium-dependent, delta isoform
PR	progesterone receptor
Prod1	proximal distal determination
PS	phospatidylserine
PSA	prostate specific antigen
PSME1	proteasome (prosome, macropain) activator subunit 1 (PA28 alpha)
PTEN	phosphatase and tensin homolog
Puma	Bcl2 binding component 3
qRT-PCR	quantitative real-time PCR
RAR	retinoic acid receptor
Rb	retinoblastoma
RCHY1	ring finger and CHY zinc finger domain containing 1
RFP	red fluorescent protein
RGB	red green blue
RIP140	nuclear receptor interacting protein 140

R.L.U	Relative Light Units
RNA	ribonucleic acid
ROI	reactive oxygen intermediate
ROS	reactive oxygen species
RU	relative units
RUVBL2	RuvB-like 2
SELEX	Systematic Evolution of Ligands by EXponential enrichment
Ser	serine amino acid
shRNA	short hairpin RNA
Siah-1	seven in absentia homolog 1
siRNA	small interfering RNA
SDS	sodium dodecyl sulphate
SPTBN1	spectrin, beta, non-erythrocytic 1
ssDNA	single strand DNA
STAT	signal transducers and activators of transcription
TBP	TATA-binding protein
TCA	trichloracetic acid
TFIIH	alias of GTFIIH
TGF	transforming growth factor
TLN1	talin 1
TNF	tumour necrosis factor
TNFR	TNF receptor
TRAIL	TNF-related apoptosis-inducing ligand
TRAPP	transport protein particle
tRNA	transfer RNA
Trx	thioredoxin
UPR	unfolded protein response
US	United States
UV	ultra-violet
VDAC	voltage-dependent anion channel
VEGF	vascular endothelial growth factor
VTCs	vesiculotubular clusters
v/v	volume/volume
w/v	weight/volume
WAF1	alias of CDKN1
Wip-1	alias for PPMID
WT1	Wilm’s tumour 1
WWC1	WW and C2 domain containing 1
Y2H	Yeast-two-hybrid

List of contents

List of figures

List of tables

Chapter 1

Introduction

1.1 Cancer: a multistep process

1.1.1 History of cancer

Hippocrates first described cancer. He called benign tumours *oncos*, Greek for swelling, and malignant tumours *carcinos*, Greek for crab or crayfish. This name comes from the appearance of the cut surface of a solid malignant tumour, with *the veins stretched on all sides as the animal the crab has its feet, whence it derives its name* (as described by Paul of Aegina, 7th century of AD) [342]. He later added the suffix -*oma*, Greek for swelling, giving the name *carcinoma*. Since it was against Greek tradition to open the body, Hippocrates only described and made drawings of apparently visible tumors on the nose, skin and breasts [342]. Through the centuries it was discovered that cancer could occur anywhere in the body. Today, the Greek term carcinoma is the medical term for a malignant tumour derived from epithelial cells, which cover more than 86% of all tumours. Cancers of glandular tissue are called adenocarcinomas (e.g breast) and the ones that derive from mesoderm cells (e.g muscle, bones) are termed as sarcomas [461]. It is Celsus who translated *carcinos* into the Latin *cancer*, also meaning crab. Galen used "*oncos*" to describe *all* tumours, the root for the modern word oncology, modern Greek for swelling [342].

Cancer is a class of diseases in which a number of cells exhibit uncontrolled proliferation, growth, invasion in adjacent tissues and sometimes metastasis to other sites in the body. These three malignant properties differentiate malignant tumours from benign ones which do not invade or metastasize [461]. According to WHO 2007, cancer is responsible for 13% of all deaths worldwide (*www.who.int/topics/cancer/en/*) with lung, stomach, liver, colon and breast cancer accounting for most of these deaths. Cancer development is a multi-step process involving different and variable activation and inactivation pathways. The transformation of a ‘normal’ cell to a cancerous one requires a cascade of mutated genes, oncogenes, tumor suppressor genes and other genes modulating cell cycle,

which are being silenced or overexpressed. There are many different kinds of cancer (more than 100 have already been classified) associated with almost every cell type, establishing cancer as a multistage and widely spread 'disease' [461]. In 2000, after detailed analysis, Hanahan and Weinberg defined six hallmarks of most, if not all, cancers summarised in Figure 1.1.

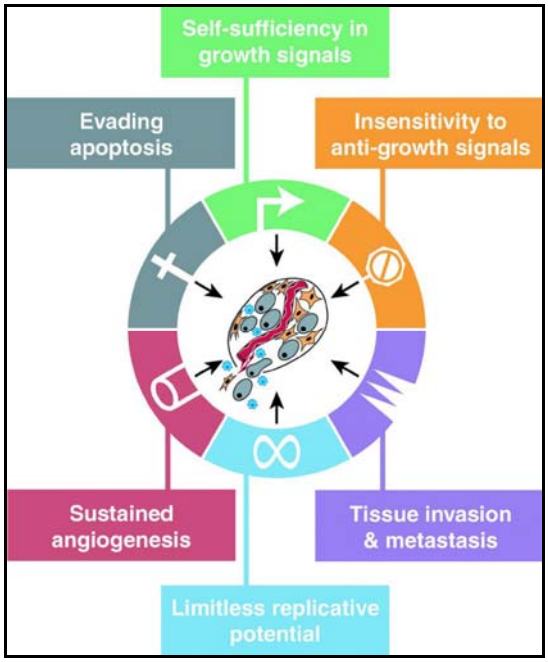

Figure 1.1: Acquired capabilities of cancer. Most if not all cancers have acquired the same set of functional capabilities during their development (Image adapted from [245]).

Most cancers are caused by genetic abnormalities due to the effect of carcinogens, UV, radiation, chemicals, tobacco smoke or viruses (responsible for 15% of all cancers, *www.who.int/topics/cancer/en/*). Genetic abnormalities, including DNA mutations, also involve inheritance of certain cancer-promoting oncogenes or cancer-protecting tumour suppressor genes. Cancer is usually classified according to the tissue from which the cells originate, the primary tumor, as well as the normal cell type they most resemble in terms of location and histology [342]. Diagnosis usually requires medical tests such as blood tests, X-rays, endoscopy and computed

tomography, CT, scans. Histological examination of a tissue biopsy or surgery specimen by a pathologist follows and the histological grade of the tumour along with other characteristics is classified and prognosis is being determined. The prognosis of cancer patients is most influenced by the type of cancer, as well as the stage, or extent of the disease. In addition to histological grading, the presence of specific molecular markers can also be useful in establishing prognosis, as well as in determining individual treatments. Cancer can be treated by surgery, chemotherapy, radiotherapy, immunotherapy, monoclonal antibody therapy, or even combination of some methods (Figure 1.2). The choice of therapy depends upon the location and grade of the tumour and the stage of the disease, as well as the general state of the patient and these characteristics determine cure. As research develops, treatments are refined for different types of cancer. There has been significant progress in the development of targeted therapy drugs that act specifically on molecular abnormalities in certain tumours, and which minimize damage to normal cells. Monoclonal antibody therapy targeted strategy in which the therapeutic agent is an antibody which specifically binds to a protein on the surface of the cancer cells. Examples include the anti-HER2/neu antibody trastuzumab (Herceptin) used in breast cancer [417, 620], and the anti-CD20 antibody rituximab, used in a variety of B-cell malignancies [113]. Targeted therapy can also involve small peptides as "homing devices" which can target and bind to cell surface receptors or other molecules that play a role in cancer [9, 429]. Small molecule targeted therapy drugs can also belong to inhibitors of enzymatic domains on mutated, overexpressed, or otherwise critical proteins within the cancer cell. Prominent examples are the tyrosine kinase inhibitors imatinib and gefitinib.

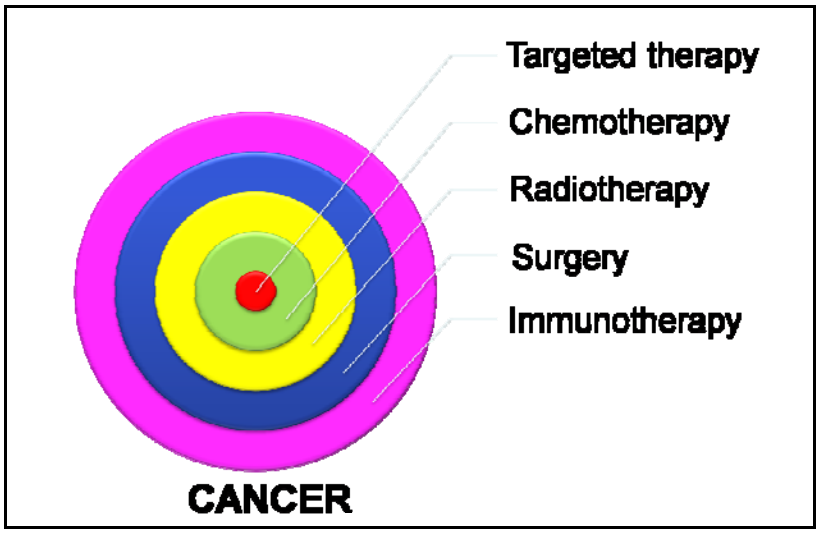

Figure 1.2: Therapeutic approaches to cancer. Several different methods are followed to cure cancer and sometimes more than one of the above methods is applied.

1.1.2 Hormone dependent cancers

Hormone dependent cancers include prostate, ovarian and breast cancer. Prostate cancer is the commonest non-skin cancer in men. Sex hormones such as androgens and estrogens play a vital role when it comes to the differentiation and the progression of prostate cancer as well as the other hormone-dependent cancers [132, 215, 319]. Ovarian cancer is the first leading cause of death from gynaecological malignancies [73, 116]. In the last 30 years much has been achieved when it comes to endocrine treatment and therapy [226]. An important benefit of these therapies is their low toxicity compared to chemotherapy and radiation, providing less severe side effects and a better quality of life for cancer patients. Some ERα-positive tumours fail to respond to endocrine therapy or become resistant in time. Moreover, a third of all breast cancer patients has ERα-negative tumours and therefore is less prone to endocrine therapy [389]. In that case a more aggressive form of combinational therapy is followed, combining radiation and chemotherapy with taxanes, anthracyclines, anti-tumour antibiotics, gonadotrophin-releasing hormone

agonists, retinoids, rexinoids, vitamin D derivatives and more recently platins which are platinum-based drugs [92, 182, 378].

1.1.2.1 Breast cancer

Breast cancer is amongst the most frequent types of human cancer, especially in women (*www.who.int/topics/cancer/en/*). Various factors have been implicated in the development and progression of breast cancer [307]. Reproductive hormones, such as estrogens, play a vital role in the progression of breast cancer. In particular, breast cancer incidence is decreased by late menarche, early first childbirth or early menopause whereas the risk of developing breast cancer is increased by pregnancy, shorter period of breastfeeding, lower parity and administration of estrogens, such as the contraceptive pill [472]. Other known risk factors for the development of breast cancer are age, ethnicity, estrogen exposure, abnormal proliferation of the tissue within the breast (atypical hyperplasia or lobular carcinoma *in situ*), radiation exposure, family history/ genetic predisposition, and lifestyle factors, such as obesity, alcohol consumption, and lack of exercise [421]. Despite the high incidence of breast cancer, the survival rate is relatively higher than in other forms of cancer, if diagnosed early [369]. In Scotland, the relative survival rate in female breast cancer at eight years after diagnosis, for patients diagnosed in the period 1987-93 was increased due to various therapies used such as with radiotherapy, chemotherapy and surgical removal [578].

After diagnosis of breast cancer, treatment depends upon the disease stage and pathologic features such as steroid and growth factor receptors status and tumor grade [174, 585]. Disease stage is determined by tumor size, the number and location of lymph nodes involved, histological grade and the presence or absence of distant metastatic disease and the tumour is evaluated from stage 0-IV scaling up severeness. For the purpose of diagnosis, prognosis and response to therapy, breast cancer is divided into two main types based on the hormone receptor status (Estrogen receptor,

ERα, positive or negative) and origin of the epithelial cells (basal or luminal). Basal or luminal types are immunohistologically distinguished by the type of cytokeratins expressed in each one [549, 594]. Luminal-like tumours are the most commons ones and have gene expression patterns that resemble the ones in the luminal epithelial cells that line the duct and are characterized by cytokeratins 8 and 18 [238, 549, 594]. Basal-like tumours resemble the gene expression pattern found in basal epithelial cells in the normal mammary gland and are characterised by expression of cytokeratins 5/6 and 17 [466, 549, 550, 594] and are ERα-ve. Interestingly, the last expression patterns mentioned are common in BRCA1 hereditary mutation carriers [203]. According to their gene expression profile there are five types of breast cancer tumours universally used within the scientific community to classify breast cancer and predict, to some extent, their clinical outcome and determine treatment [466, 549, 550]. These types are divided into two ERα+ subtypes that are classified as luminal A (ERα+ve/PR+ve/HER2-ve) and luminal B (ERα+ve/PR+ve/HER2+ve/HER1+ve) [549, 550] and three ERα -ve (basal) subtypes which are further subclassed as HER2 overexpressing, "normal-like" (unclassified) and triple negative (EGFR+ve, ERα-ve, PR-ve and HER2-ve) [118, 430] and should be treated as different diseases [466, 481, 482]. It is indicative that 2/3 of women aged <50 years will have ERα^+ breast cancer and more than 80% of women aged >50 years are ERα^+ [21]. The most favourable type of breast cancer in terms of treatment and clinical outcome is the luminal A type, followed by the luminal B one whereas the worst types are the basal ones [594]. Histological grading in breast cancers is based on the evaluation of 3 features: (i) the percentage of tubule formation, (ii) the degree of nuclear polymorphism and (iii) the mitotic count in a defined field area [56, 280]. The grading criteria were unified by Elston and Ellis, who designed a modification of the Bloom and Richardson grading system, namely the Nottingham combined histologic grade [173]. This system was based on the semiquantitative evaluation of the three morphologic features mentioned above and was established as a universal one [173]. Another potential marker for breast cancer is the progesterone receptor, PR. PR is an ERα-related gene and there is evidence

that PR^+ tumours respond better to Tamoxifen treatment but these findings are not universal [38]. PR is synthesized by tumour cells that are stimulated by estrogens through interaction with ER*α*. Because the presence of PR reflects a functional ER*α* pathway, smaller benefit from tamoxifen for $ER\alpha^+/PR^-$ tumors compared with $ER\alpha^+/PR^+$ tumors would be expected [24]. However, the increased need for novel biomarkers, indicative of the follow-up treatment of different types of breast and not only cancers, has lead to new approaches in research. Biomarkers therefore, are useful tools for cancer detection. They can predict who is likely to develop cancer (*BRCA1* mutation status) and/or detect the disease at an early stage (mammographic image). They can indicate a particular stage in the disease guide treatment decisions (circulating tumor cells, pathological response, $HER2^+$, $ER\alpha^+$, PR^+), and, importantly, aid in the identification of novel targets for therapy [598].

Existing therapies predominantly target proliferation either with ionizing radiation, cytotoxic agents, or inhibition of estrogen receptor and HER2 growth factor signaling pathways. Combining these treatments together with radiortherapy, surgery and chemotherapy has contributed to the improved survival rate in breast cancer. Clinical application of targeted therapy is based on the identification of credentialed markers that are biologically relevant to the disease [151]. Cancer cells exhibit significant genetic and molecular differences [598]. The target should have specific characteristics including clinical relevance, reproducibility between patients, to be easily measurable and minimum toxicity. Potential targets for maximum efficiency include characteristics of malignancy such as uncontrolled proliferation, insensitivity to drugs, lack of apoptosis and senescence, genomic instability, metastatic potentials and angiogenesis.

Tamoxifen and aromatase inhibitors are the most commonly-used drugs against breast cancer. Tamoxifen citrate treatment has long been considered the gold standard due to its efficacy and safety and was first approved in 1977 by the US Food and Drug Administration. It binds to ER*α* and inhibits the growth of tumour cells. It has been widely used for three decades as the standard treatment for node-positive and node-negative breast cancers [163]. It is an orally active selective ER*α*-

modulator and it is used in pre- and post-menopausal women. When bound to the ERα it forms a nuclear complex that decreases DNA synthesis and halts the cells in G_1 or G_0 phase of the cell cycle, acting as a cytostatic rather than cytotoxic drug. Tamoxifen itself is a pro-drug and has to be metabolized by cytochrome P450 to its active form 4-hydroxytamoxifen and des-N-methyl-4-hydroxytamoxifen [141, 297, 298] that antagonize estrogens' binding to their receptor [609]. This active metabolite possesses a 30- to a 100- fold higher efficiency in inhibiting estrogen-dependent cell proliferation [69, 122, 297, 493]. Aromatase inhibitors, in turn, are anti-estrogen agents that target the aromatase enzyme in the final step of most of estrogen production and block oestrogen synthesis. They have been developed as first- (aminoglutethimide), second- (formestane) and third-generation inhibitors minimizing their side-effects [82]. The third generation aromatase inhibitors include letrozole (non-steroidal), exemestane (steroidal) and anastrozole (non-steroidal), which are equally or more efficient to tamoxifen inhibiting aromatization with a 98% efficiency and also exhibit a better toxicity profile. ERα-negative cancers are more difficult to treat and require combinational therapy including radiation, chemotherapy and surgery [541]. Last but not least Herceptin, as mentioned before, is a humanized monoclonal antibody against the extracellular domain of HER2-receptor and promotes G_1arrest and stops proliferation. It has been suggested that the drug induces some of its effect by downregulation of HER2 leading to disruption of the receptor dimerization and PI3K signalling [30]. Further improvements in therapy must attack other hallmarks of malignancy and will undoubtedly be accompanied by better means of individual patient selection for such therapies while selectively promote elimination of cancer cells [151]. Despite all the different approaches used to achieve therapy, they all come to one goal: induce cell cycle arrest or apoptosis (programmed cell death) of cancer cells [167]. Cell death consists of apoptosis (Type I), autophagic cell death (Type II), and necrosis (Type III) (Figure 1.3).

1.2 Cell death

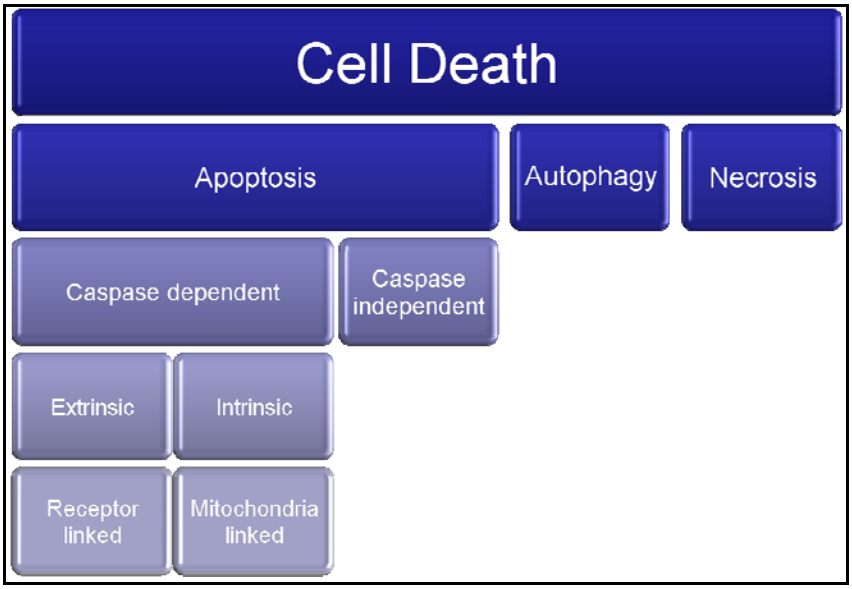

Figure 1.3: Overview of cell death pathways. Cell death consists of three main pathways which are further sub-classed in different categories (described in 1.2.1-1.2.3)

1.2.1 Apoptosis

Apoptosis plays an important role in cell maintenance, development and tissue homeostasis. Cells undergo apoptosis through two major pathways, the intrinsic pathway that involves the mitochondria and the extrinsic pathway that involves cell death receptors (overview of cell death in Figure 1.3). In either case the leftovers of the dead cell are packaged into apoptotic bodies which are recognised by neighbouring cells or macrophages and cleared out by phagocytosis.

Apoptosis was first observed by Walther Flemming in 1885 who called it chromatolysis because the nucleus was gradually disappearing. Apoptosis as we know it, was later studied and described in detail by Kerr and co-workers in 1972 [309] and involves a series of morphological and biochemical features that are distinctive of this type of cell death. Hallmarks of apoptosis consist of membrane blebbing, cell shrinkage, cell surface exposure of phosphatidylserine, loss of mitochondrial membrane potential, nuclear fragmentation (karyorhexis from the

greek ‘karyon’:nucleus and ‘rhexis’: disruption) chromatin condensation and large-scale DNA fragmentation finally leading to phagocytosis of the ‘dead’ cell by macrophages or neighbouring cells and so protecting tissues from inflammatory injury due to toxic contents of the dying cells [627]. Apoptosis is totally different from necrosis, since the last one is the consequence of extreme damage of the cell microenvironment leading to loss of membrane integrity, blebbing and therefore strong inflammatory response of the damaged tissue [349]. Apoptosis consists of two pathways, the extrinsic and the intrinsic (Figure 1.3) which both end up at the formation of the apoptosome which is the last step of programmed cell death.

1.2.1.1 Extrinsic apoptotic pathway

The extrinsic pathway is initiated when death-inducing ligands bind to cell surface receptors, called death-receptors, and stimulate a cascade of events leading to the apoptotic characteristics mentioned above. Death receptors belong to the tumour necrosis factor gene superfamily and contain similar and variable in numbers cysteine-rich domains that are exposed to the cell surface to be recognised by their ligands [236], as well as a cytoplasmic death domain that ensures signal cytotoxicity and enables the receptors to directly initiate the apoptotic response [285, 571]. The best characterized death receptors include TNFR, DR3 (Death Receptor 3, also called Apo3), DR4, DR5 and Fas (also called Apo1, CD95). The ligands that activate these receptors belong to the TNF gene superfamily [236, 546] and include TRAIL (binds to DR4 and DR5) [372, 454, 455, 520], TNF (binds to TNFR), CD95 ligand (binds to Fas) and Apo3L, ligand, (binds to DR3) [114]. Once bound to its ligand the receptor oligomerises and triggers the recruitment of FADD, FAS-associated death domain, and caspase 8, forming a death-inducing signalling complex (DISC). The initiator caspase 8 then activates the effector caspases 3, 6 and 7 [27].

Caspases were first discovered after genetic analyses of the nematode *C.elegans* from the ced-3 gene that encodes a homologue of the interleukin-1$_\beta$ processing

enzyme [645]. Ced-3 gene is abundant during embryogenesis where most of programmed cell death happens and was proposed to act as a cysteine protease that controls cell death by proteolytic activation or inactivation of substrates [645]. In the same study it was also revealed that specific mutations in the conserved region irreversibly inhibited the 131 programmed cell death processes that would otherwise occur during the hermaphrodite development. When Ced-3 was overexpressed in Rat-1 mammalian cells, it was able to induce apoptosis [404]. A number of similar type apoptosis-inducing proteins were termed as 'caspases' (cysteine aspartate-specific proteases) [17]. The 'c' reflects a cysteine protease mechanism and the 'aspase' refers to their ability to cleave after aspartic acid which is the most characteristic feature of this family. Individual family members were distinguished by an arabic numeral following after the 'caspase' term, which indicated the date of its publication. Fourteen mammalian caspases have been identified and cloned so far and they all contain a prodomain followed by p20 large and p10 small subunits. They are first synthesized as inactive precursors, then proteolytically cleaved at internal caspase recognition sites to active enzymes during apoptosis and in turn cleave substrates at Asp-Xxxx motives [580]. Based on their function caspases are classified into three categories. The first one consists of inflammatory caspases -1, -4, -5, -11, -12, -13 and -14 which are involved in inflammation after bacterial infection or change, entry of intracellular pathogens in the ionic cellular environment and bear an activation and recruitment domain [385]. The second category includes the initiator caspases which possess large prodomains with either death-effector domain, in the case of caspases-8 and -10, or a caspase activation and recruitment domain, caspases-2 and -9, respectively. Initiator caspases are involved in the interaction with upstream adaptor molecules to initiate apoptotic response [580]. The third category contain the effector caspases -3, -6 and -7 which are characterized by short prodomain and cleave variable cellular substrates after upstream caspases' activation [93, 192, 237, 269, 426, 567, 610]. Initiator caspases are autoproteolyticaly activated when brought to close distance, a model called 'the close proximity model' [425, 543, 554]. The model suggested that pro-caspases, although inactive, shown low activity which is

sufficient to induce cleavage of another molecule of the same pro-caspase and thus activate it when brought to close distance, in an autoprocessing manner [509]. The cleavage takes place in a short domain between the large and the small subunits of the catalytic domain in Asp $_{297}$ which is the highly conserved amino acid that directs cleavage specificity in this domain [655]. The above model was later refined by 'the proximity induced dimerization model' which suggests that dimerization induces auto-activation [64, 146]. In this model, initiator caspases are activated when inactive monomers dimerize within macromolecular structures such as DISC and apoptosome [64, 146]. Effector caspases are proteolytically cleaved and activated at Asp-X sites by active initiator caspases suggesting the possibility of autocatalytic activation [580].

1.2.1.2 Intrinsic apoptotic pathway

The intrinsic pathway is initiated by various intrinsic apoptotic stimuli such as UV damage, drugs, X-rays, oxidative stress or starvation. The key event is what is called mitochondrial outer membrane permeabilization (MOMP) which is controlled by the pro-apoptotic Bcl-2 family members such as Bad, Bid, Bak and Bax. The function of these proteins involves the formation of pores in the outer mitochondrial membrane from where cytochrome c is being released to the cytoplasm [41]. Basanez and co-workers, 1999, supported the instabilization of the phospholipid bilayers of the outer mitochondrial membrane and the disruption of the permeability barrier as a potential mechanism that leads to the formation of these pores, the so called apoptotic pores [41]. When this large pores are formed, Bax enters the inner mitochondrial membrane and destabilizes it, leading to (i) loss of the mitochondrial electrochemical potential, (ii) activation of the permeability transition pore and (iii) mitochondrial swelling [325, 388, 459, 542, 596]. Once MOMP is initiated a whole cascade of either releasing of molecules or mitochondrial loss of function begins. Cytochrome c is being released rapidly from their inner membrane compartment into the cytosol

where it binds to Apaf-1 and activates procaspase-9 through oligomerization, creating, an intracellular DISC-like complex known as the apoptosome [366]. The apoptosome then activates the executioner caspases -3, -6 and 7 [356, 659]. *In vivo* studies in Apaf-1, caspase-9 or caspases 3 deficient MEFs showed that the aforementioned molecules are essential to apoptosis and in their absence no apoptotic response is achieved [96, 242, 330, 356, 642], and is sometimes accompanied by lethality or defective development [242, 330]. After caspase -3 activation, the two pathways converge and a whole cascade of protein activation and deactivation begins.

Besides mitochondria, ER is another major player in the intrinsic apoptotic pathway. Oxidative stress, Ca^{++} ionophores, toxic reagents or inhibitors of ER glycosylation such as tunicamycin, blocking of ER-Golgi transport [365], depletion of intracellular Ca^{++} levels [152, 357] can induce the Unfolded Protein Response, UPR, and affect the quality control mechanism which ensures that only the correct folded proteins are processed along the secretory pathway and that prefolded and misfolded proteins are degraded so that they cannot cause any harm to the cell [395, 523, 587]. The UPR pathway controls transcription of genes encoding ER-resident protein chaperones that regulate folding, assembly and modification of cellular proteins [323]. During UPR the upregulation of these chaperones increases the folding capacity of this organelle. If UPR persists, then ER-associated protein degradation occurs and leads to apoptosis. What is more, Ca^{++} , which is stored to the ER, is released to the cytosol during apoptosis and uptaken by the mitochondria and triggers cytochrome c release which in turns induces more Ca^{++} release and a positive feedback loop is created, thus triggering dramatic caspases activation [490, 519]. Interestingly, pro-apoptotic Bcl-2 family members participate in ER targeting by interrupting ER and mitochondria crosstalk [437, 519, 658]. Bax/Bak mediate ER stress-induced apoptosis by ensuring Ca^{++} homeostasis in the ER [437, 519, 658]. ER-stress causes conformational changes and oligomerization of the aforementioned proteins on the ER membrane and jeopardise membrane integrity. On the other hand, overexpression of either Bax or Bak causes accumulation of the protein in the ER or mitochondria

and induces caspase-independent Ca^{++} release and accumulation to the mitochondria, a process depending on the Bcl-2 family members [437]. In ER-mediated apoptosis, ER-targetted Bak induces caspase-12 cleavage [658] and then caspase-12 is being released from the ER to the cytosol, where in cleaves procaspase-9 and triggers caspases-3 activation leading to the formation of the apoptosome.

1.2.1.3 Apoptosome as the last step before total extinction

The last step of apoptosis includes packaging of the dead cell content into cavities, called apoptosomes. Apoptosomes then release signals to phagocytes uptaken by rertain receptors, for the phagocytosis to begin so that the extracellular environment is clear of the unwanted leftovers and no inflammation is induced around the dying cells. Phagocytes can be 'professional' such as the macrophages or 'amateurs' such as fibroblasts, neutrophils, melanoma cells, other types of epithelial cells, Sertoli cells, Jurkat T cells, tumour cells or vascular smooth muscle cells [49, 183, 184, 260, 422]. Phagocytes receptors include CD14, lectins or integrins [399].

Amongst these signals is phosphatidylserine, which normally faces the cytoplasmic side of the cell membrane, but in a cell undergoing apoptosis is exposed to the external surface of the cell membrane [183, 184, 422]. In non-apoptotic cells, phospholipids are distributed in an asymmetric way in the cell membrane with cholide-containing lipids in the outer membrane and amino-phospholipids in the inner leaflet. The first category of cholide-containing lipids includes phosphatydilcholine and sphingomyelin and the second category of amino-phospholipids includes phosphatidylethanolamine and phospatidylserine, PS, [183, 184]. Loss of phospholipid asymmetry and exposure of PS to the outer leaflet of the cell membrane is a universal apoptotic phenomenon and was first identified in apoptotic lymphocytes by Fadok and co-workers in 1992 [183, 184]. PS is then recognised in a stereospecific manner by phagocytes [183, 184]. It has been known that macrophages can recognise cells which have lost membrane asymmetry [195]

but it has been also supported that they specifically recognise negatively charged liposomes and especially PS [16, 195]. Other 'eat me' signals include changes in membrane sugars that are being recognised my macrophage-lectins [547]. Lectins and their receptors are produced in large quantities during the early infection stage and are involved in pathogen recognition by identifying bacterial surfaces as well as helping to neutralization of foreign bodies and other pathogens in the host organism.

1.2.2 Autophagy

Autophagy (from the greek word *auto*:self and *phagy*:feed which literary means to 'eat oneself') is a conserved catabolic process that degrades long-lived proteins, organelles and bulk cytoplasm, recycling it back as metabolic precursors. Autophagy has been associated with both cell survival and cell death. Short-lived proteins are degraded by the ubiquitin-proteosome pathway but analysing this process remains beyond the aims of this project. Cells can undergo autophagy in response to extracellular stress, such as nutrient starvation, high temperature, hypoxia, high population density [134, 223], intracellular stress, such as accumulation of damaged or extra organelles that are no longer required, and even under normal physiological conditions where massive cell elimination is required such as neuronal degeneration, insect metamorphosis [435, 503], organogenesis and tissue remodelling, in *Drosophila* salivary gland, [137, 348]. Autophagy is considered a survival mechanism of the cells in times of stress and especially famine because at that point the cellular constituents are degraded to ensure sufficient energy production. Two types of autophagy have been identified in eukaryotic cell, macro-autophagy and micro-autophagy [562]. These two modes differ to the pathway by which cytoplasmic material is delivered to the lysosomes but share the same characteristics when it comes to packing and degradation of the unwanted contents. Micro-autophagy is characterised by direct engulfment of the cytoplasm to the lysosomes whereas macro-autophagy utilizes the formation of double-membrane vacuoles that lead portions of the cytoplasm to the lysosomes (Figure 1.4). We will focus on

macro-autophagy, which will be from now on be referred as autophagy, because it is the most common type of autophagy from yeast to mammals.

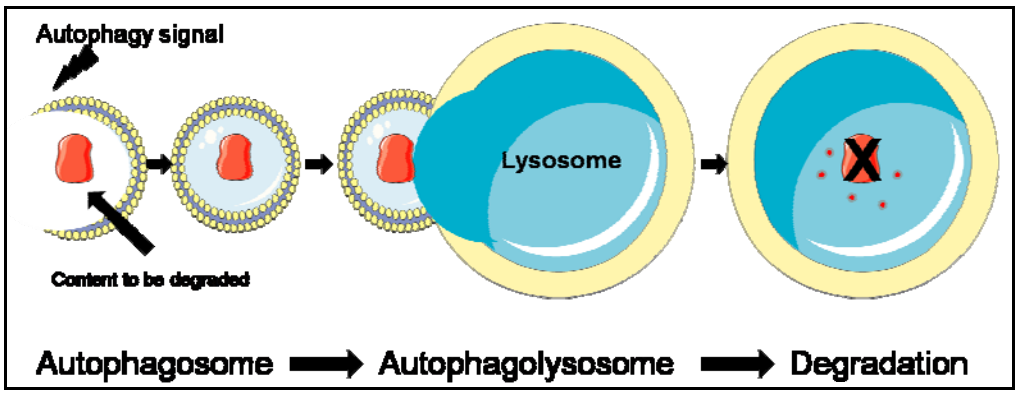

Figure 1.4: Formation of autophagosome. Induction results in the formation of a double-membraned autophagic vacuole that encloses cytoplasmic components that need to be degraded. The autophagic vacuole then docks against the lysosome, to form an autophagolysosome and the fusion of the outer autophagic vacuole membrane with the lysosome releases the inner membrane-bound cytoplasmic components into the lysosome where degradation occurs (designed by Servier Tools Medical Art Software).

A morphological characteristic of autophagy is the rearrangement of subcellular membranes and the formation of autophagosomes (Figure 1.4), cytoplasmic double membrane vacuoles that contain bulk cytoplasm and/or cytoplasmic organelles such as mitochondria and ER [53]. The origin of the double-membrane was believed to come from rough ER, as several protein markers used as immunological probes for all the types of cell membranes (Golgi, endosomes and plasma) failed to label these vacuoles whereas antisera against several integral ER membrane proteins did [159]. Nevertheless, recent studies revealed that autophagic vacuoles are formed *de novo* through nucleation, assembly and elongation of small membrane structures [566] which are called pre-autophagosomal structures and contain many apg proteins (apg genes is a subset of what was later called ‘ atg’ genes in nomenclature [316] and included apg (autophagy)-aut (autophagy)-cvt (cytoplasm-to-vacuole targetting)

genes. No ER, Golgi or late-endosomal markers were detected [312]. After engulfing bulk cytoplasm/ organelles, the autophagosomes fuse to lysosomes to form an autolysosome and their contents are degraded and recycled (Figure 1.4) [31, 300]. Key pH-sensitive lysosomal enzymes called hydrolases are used to digest the unwanted cargo [608]. Lysosomal permeases then release the digested material back to the cytosol for macromolecular synthesis and/or bioenergetics.

Autophagic cell death is considered as the type II cell death. It is distinctive from apoptosis in terms of morphological changes as well as biochemical ones. Genes and proteins that regulate autophagy were first studied in yeast but some of their mammalian orthologues have also been characterised. An autophagosome-associated protein microtubule-associated protein II light chain (LC3) has been used as a popular marker for this type of cell death. The shift in localization of LC3 from the cytoplasm to the membrane of the autophagosomes is indicative of autophagy [300]. Two forms of LC3 are produced post-translationally in cells by proteolytic cleavage at the C-terminus, cytosolic type I and membrane-bound type II, [300]. The two forms have different molecular weights. Another popular marker for autophagy is Beclin-1, which is the mammalian orthologue of the yeast apg6 (autophagy related gene) protein that is involved in the early steps of autophagic vacuoles formation. Several atg-deficient yeast strains have indicated that these genes are essential for sporulation, survival during starvation and differentiation after starvation in yeast [518, 590]. Similar mutation studies in the sole amoeba *Dictyostelium discoideum* also showed that orthologues of the yeast atg genes were essential for viability and formation of a multicellular organism (a well-characterised mechanism of this amoeba to overcome famine, where a lot of amoebas are clustered together and form multicellular structures) during nutrient starvation [450]. However, a very surprising result in Beclin-1 haploinsufficient mice was that the animals, as they age, displayed a pronounced increase in the incidence of lymphoma and carcinoma of the lung and liver [480]. In addition, mammary tissues in these animals displayed hyperproliferative, pre-neoplastic changes in response to Beclin-1 deletion. Beclin-1 deficiency in mice results in embryonic lethality due to inability of

undergoing remodelling and differentiation of ventral ectoderm and extensive cell death indicating a potential pro-survival role of autophagy [646]. In the same study, it was shown that although the protein is not essential for apoptosis, as Beclin-1 $^{-/-}$ ES cells showed normal apoptotic response after UV and serum withdrawal compared to the control wt ones, it is important to regulate autophagy because in the same cells autophagic response to nutrient deprivation was totally abnormal. If autophagy was a cell suicide mechanism then the Beclin-deficient cells would have been resistant to cell death. Apart from suggesting a cell survival role of autophagy the above experiment also explains the behaviour of tumour cells that utilize autophagy in a regular basis [646]. Indeed, when cancer cells face nutrient depletion, for example after blood supply is disrupted, they use autophagy as an energy mechanism until new blood vessels are formed and nutrient supply is restored. Evidence also exist that Beclin-1 regulates the degradation of proteins [166]. Overexpression of a Beclin-1 binding protein located primarily in the Golgi apparatus, CAL (CFTR associated ligand, also known as PIST), reduces the rate of appearance and halflife of CFTR (cystic fibrosis transmembrane conductance regulator) chloride channel in the plasma membrane [110]. Thus, a Beclin 1-containing protein complex may regulate the trafficking and turnover of other plasma membrane proteins that are involved in signal transduction and/or nutrient acquisition. Interestingly, Beclin-1 is mapped on the 17q21 locus, 150kb centromeric of BRCA1 gene, which is monoallelically deleted in a lot of cancers including ovarian (75%) [12, 164, 500], breast (50%) [209, 505] and prostate cancer (40%) [211], suggesting tumour-suppressing potentials. This tumour-suppressing role was refined by FISH analysis of 22 breast cancer cell lines that revealed a percentage of 41% Beclin-1 allelic deletion [12] along with protein expression data from a different team that showed total protein loss or attenuation in breast cancers [359]. Transfection of Beclin-1 into a transformed breast carcinoma cell line decreased its tumourigenic potential in nude mice, further supporting the aforementioned data.

In plants, autophagy gene mutations, in the atg genes, do not have implications on the plant life cycle but do induce shorter life cycle that results in earlier senescence,

under normal conditions. Under carbon or nitrogen depletion these mutant plants show enhanced chlorosis (state where the plants becomes yellow due to chlorophyll degradation) [143, 243].

Is autophagy a survival or a cell death mechanism then? Much debate has been going on in the field. In favour of the survival role, researchers support that since autophagy provides the cell with amino-acids and other essential molecules it can be adapted as a supporting energy-producing mechanism in times of nutrient deprivation [62]. Liver, for example, is totally dependent on autophagy after amino acid deprivation and total energy production for the whole organism depends on that exact mechanism. What is more, damaged or excess organelles, like mitochondria, ER, peroxisomes, are removed by the autophagy pathway, maintaining the cellular homeostasis. By removing damaged mitochondria, autophagy protects the cell from the release of pro-apoptotic molecules that would trigger apoptotic response, as well as limiting the exposure of cellular DNA to genotoxic stresses such as free radicals [350]. It was also shown that ionizing radiation or certain drugs can induce the formation of acidic vesicular organelles in breast cancer cells that lack caspase-3, such as MCF-7 [26]. The same autophagy induction is observed in prostate and colon cancer after irradiation [452]. In this radiation-induced autophagy, the autophagy inhibitor bafilomycin A_1, an H^+-ATPase inhibitor, induced apoptosis in cancer cells, suggesting a protective role for autophagy in terms of apoptosis escape [452].

Research in the last decade has revolutionized our knowledge on the molecular mechanisms involved in autophagy. Novel functions for autophagy genes have been unraveld, implicated in yeast sporulation, multicellular development of Dictyostelium [320], insect metamorphosis, organogenesis, neuro-differentiation and early plant senescence. All these processes share a common need for a competent catabolic pathway that degrades and recycles unwanted intracellular material through different developmental stages across several different species. To date there is no ultimate proof that autophagy is required to maintain cell survival. Autophagy is a self-limited process and cells dependent on this mechanism are capable of

maintaining bioenergetics until a point when their internal resources will be exhausted and finally die of necrosis.

1.2.3 Necrosis

Apoptosis is different from necrosis or oncosis (derived from the Greek word 'oncos' which means swelling, type III cell death) in which the cells suffer from a major insult such as osmosis, extreme physico-chemical stress, detergent stress, freezing-thawing cycles, mechanical stress and die abruptly after losing membrane integrity and swelling. The term oncosis was first proposed by Von Recklinbauer in 1910 to mean cell death by swelling [377]. The cellular contents are released into the surrounding environment and alert the innate immune system due to the presence of proinflammatory molecules in the necrotic spot. Necrosis is characterised by rapid cytoplasmic vacualization and swelling, irreversible changes in the nucleus including karyolysis and pyknosis dut not DNA fragmentation and organised chromatic condensation. Necrosis was believed to be uncontrolled but recent studies came to reveal that it is tightly regulated as it can include signs of controlled processes such as mitochondrial dysfunction, ATP-depletion [102, 349, 583], proteolysis and early membrane rupture [102]. In addition, it was also shown that inhibition of proteins with a role in apoptosis (caspases) [599] or autophagy (atg encoded proteins) [320] can favour necrotic death [86, 102]. Therefore, programmed necrosis can be tightly upregulated by several pathways which are characteristic of the other types of cell death, and it can be set as a default death pathway after inhibition of apoptosis or autophagy. Under normal physiological conditions this type of cell death occurs during tissue development (e.g. the death of chrondrocytes controlling the longitudinal growth of bones) [491] and in adult tissue homeostasis (e.g. in intestinal epithelial cells) [39]. Whereas apoptotic cells, that undergo budding, are engulfed completely by phagocytes with the formation of tight fitting phagosomes [229, 230], necrotic cells (which swell) are internalized by a macro-pinocytotic mechanism,

meaning that only parts of the cell are taken up by phagocytes through multiple broad membrane ruffles directed towards the necrotic material [326, 584]. In negative terms, necrosis is characterized by the absence of caspase activation, cytochrome c release and DNA fragmentation [327] and it can be discriminated from apoptosis by microscopy, time-lapse or DIC, flow cytometry, transmission electron microscopy and accurate biochemical methods although a very detailed and multi-disciplinary approach combining several biomarkers, such as PS, caspases, cytochrome c that are distinctive of apoptosis, along with morphological characteristics is required.

Other types of cell death include mitotic catastrophy, anoikis, excitotoxicity, Wallerian degeneration and cornification of the skin but analysing all these different types remains beyond the objectives of this project.

1.3 Tumour suppressor genes and oncogenes

Cancer is a complex genetic disease, arising from accumulation of mutations that promote clonal selection of cells with increasingly aggressive behaviour [188]. The two groups of genes believed to be mainly involved in cancer development are oncogenes and tumour suppressor genes. Oncogenes are genes that when mutated they express more protein-product that usual or have amplified activity and therefore act in a dominant manner and initiate carcinogenesis [460]. In this class belong genes that positively regulate cell growth, proliferation such as growth hormone receptors, growth hormones themselves [370, 460], inhibitors of cell death, such as Bcl-2, [370], stimulators of cell proliferation, such as c-Myc, [370], and also cell cycle genes such as cyclins [81]. Tumour suppressor genes on the other hand, encode proteins that have inhibitory effects in tumour formation and progression [460]. Tumour suppressor genes restrict unusual cell proliferation and include many cell cycle genes, cell death-regulators etc [615]. These genes induce apoptosis and/or cell

cycle arrest in malignant cells [445]. Mutations in these key-regulator genes can lead to cancer.

1.3.1 p53- a tumour suppressor gene

One of the most highly involved genes in the progression of most cancers, as well as breast cancer, is the p53 tumor-suppressor gene. p53 was first described in 1979 and thought to be an oncogene by virtue of its ability to cooperate with mutant Ras genes in transforming primary rodent fibroblasts [343, 447]. The gene is found to be mutated or absent in almost half of human cancers [34, 91, 258, 392, 432] due to its unique post-translational responsiveness that involves a broad range of signals. Genotoxic and non-genotoxic, stimuli such as hypoxia/anoxia and activation of cell cycle/growth signalling cascades, may drive p53 expression and lead to uncontrolled cell proliferation and therefore cancer through transcriptional activation of multiple genes that control cell cycle.

1.3.1.1 p53 structure

The homotetrameric tumor suppressor p53 consists of folded core and tetramerization domains, each of 393 residues [581] (Figure 1.5). Each chain has three functionally distinct domains: the N-terminal domain where the transcription activation domain lays along with a proline rich domain. This N-terminal domain contains major, residues 1-42, and minor, residues 45-56, transactivation domains (Figure 1.5). The transcriptional activation of p53 is modulated through binding of target molecules to this N-terminus on the transcription activation domain [136]. This domain is followed by a highly conserved sequence-specific DNA binding domain, residues 98-296, also termed as the core domain, that aids p53 to act as a transcription factor, and a complex C-terminal region containing tetramerization motifs, residues 319-363, linked to the core domain by an intrinsically disordered

sequence, as well as a domain exerting negative regulation on DNA-binding activity, residues 364-393 [136]. The C-terminal part of the protein contains a sequence unspecific DNA-binding regulatory domain [10]. The C-terminal domain neither interacts with other regions of p53 nor has an effect on the conformation of the molecule but interestingly C-terminal p53 deletions prevent the interaction of the protein to the p21-cyclin dependent kinase inhibitor [464]. The inactive form of the protein, highly unstable, adopts a conformation in which the C-terminal domain mediates interactions of the DNA-binding domain with its target [276]. Hupp and colleagues demonstrated that phosphorylation, antibody interaction or deletion of the C-terminus could facilitate DNA binding using inert bacterially expressed p53 [275].

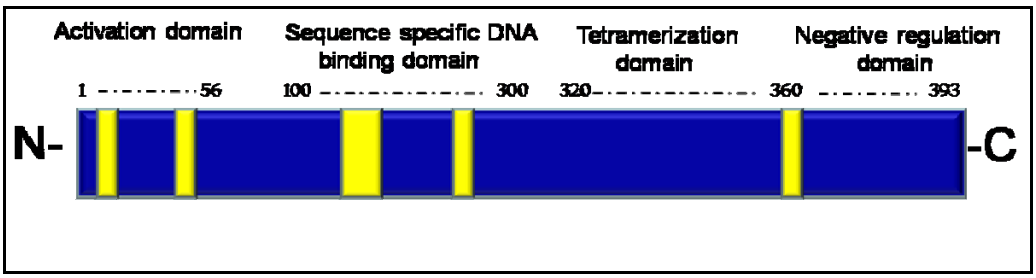

Figure 1.5: Graphical representation of p53 protein structure. The N-terminal activation domains, the core DNA-binding domain and the C-terminal tetramerization domain are all depicted in the diagram.

1.3.1.2 p53 and its various roles

The p53 protein plays a vital role in cell proliferation, genome stability, accurate chromosome segregation, cell cycle progression [602, 647] and protection from DNA damage by ionizing radiation, oxidative stress or hypoxia. The gene is also involved in the regulation of the cell cycle arrest and apoptosis. When p53 is active then the apoptotic pathway is enhanced, whereas when p53 is mutated or absent the apoptotic pathway is inhibited. It has been shown that p53-/- cells cannot undergo apoptosis and malignant transformation is being established [52, 392].

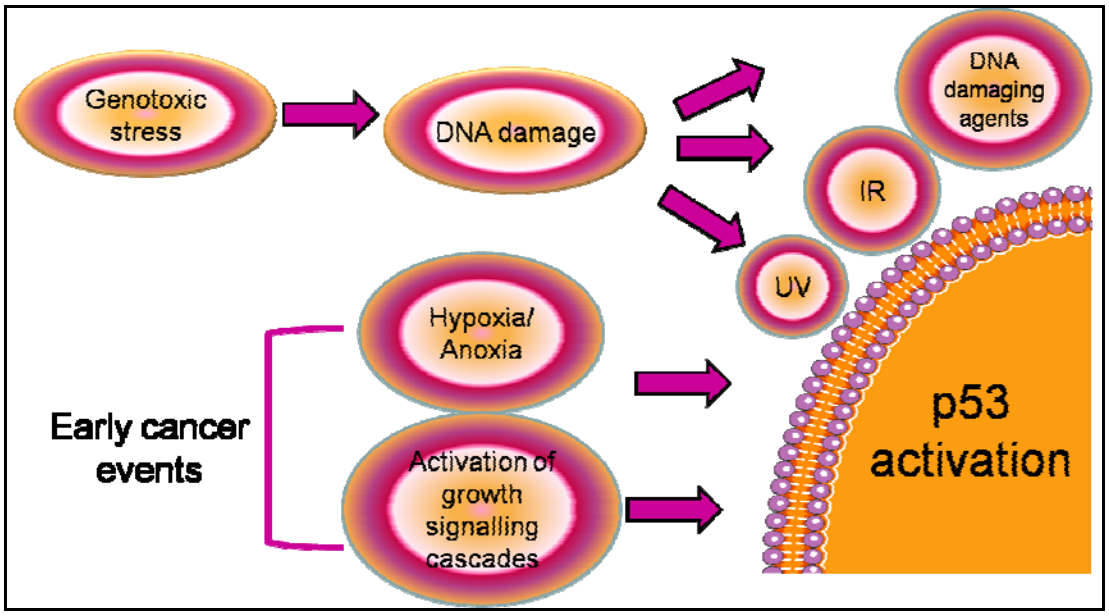

Figure 1.6: p53 activation by various stimuli. Genotoxic stress includes UV exposure, ionizing radiation (IR) and other DNA-damaging agents. Non-genotoxic stress is summarized in hypoxic/anoxic and induced growth signalling conditions which are characteristic of cancer development (Designed by Servier Medical Art Tools software).

p53 can act as a transcription factor by binding to TFIIH (nucleotide excision repair mechanism) complex. As far as the cell cycle is concerned, p53 affects G_1 block [392] by transcriptional activation of the p21WAF1 gene [168] as well as regulating G_2/M block after DNA damage [8, 559]. p53 binds to DNA as a tetrameric protein [121, 324] and is capable of directly inhibiting DNA replication by interacting with a single-stranded DNA-binding protein complex required for DNA unwinding during replication [392].

Maltzman and Czyzyk ,1984, were the first to discover that UV or even UV-mimetic chemical carcinogens activate p53 in mouse cells [380]. This discovery was much later supported, 1991, by Kastan and co-workers that demonstrated that p53 was essential for cell cycle arrest after genotoxic stress such as DNA damage or irradiation [303] (Figure 1.6). The first role found for p53 was the regulation of gene expression as a sequence specific transcription factor [308]. The so called ‘guardian

of the genome' is sensing and reacting to DNA damage by the ATM/ATR and Chk1/Chk2 pathway. It is the main regulator of the DNA damage response pathway (DDR pathway) activated by DNA bases modifications, DNA double or single strand breaks after exposure to genotoxic agents or ionizing radiation or even replication stress during S phase in the case of ssDNA. The aforementioned DNA lesions such as oxidative lesions or bulky adducts, are being repaired by the nucleotide excision repair and base excision repair pathways through the ATR/ATRIP pathway (ATM and Rad3-related kinase /ATR interacting protein) which is activated after replication stress and DNA damage and especially after ssDNA formation [126, 185, 661]. ATM and DNA-PKcs respond mainly to DNA double-strand breaks, whereas ATR is activated by single stranded DNA and stalled DNA replication forks. In particular, ionizing radiation, radiomimetic agents and other dsDNA damage agents activate mainly the ATM pathway, whereas, UV and UV-mimetic agents, such as cisplatin, promote base damages and stimulate the ATR pathway [126, 185, 661]. When the above pathways are deficient then the lesion is converted into a DNA double strand break and the DDR pathway takes control by activating ATM [293]. Along to ATM, the DNA-dependent protein kinase is being activated and leads to p53 phosphorylation on serine 15 and 37 [506]. On the other hand, ATM activation leads to direct or indirect p53 phosphorylation on serine 6, 9, 15 (direct), 20, 37(direct), 46 and Thr 18 as well as phosphorylation of other checkpoint kinases [36, 253, 506] such as Chk2 which phosphorylate p53 on serine 20 [103, 255, 530]. Interestingly, all three of the phosphoinositide 3-kinase-related kinases (PIKK) ATM, ATR and DNA-PK, as well as Chk1 and Chk2 can also phosphorylate downstream targets with important roles in cell cycle checkpoints and DNA repair [185]. p53 phosphorylation reduces binding of mdm-2 ubiquitin transferase to the p53 molecule which then enables replacement of the ubiquitin molecules by acetylation, resulting in p53 stabilization [413]. Mdm-2 binds to the N-terminal transcriptional activation domain of p53 and disrupts its interaction with the general transcription machinery, as well as promote its nuclear export and proteosomal degradation [106, 197, 413]. After activation, p53 acts as a suppressor or activator of various genes and can translocate

to the mitochondria to induce apoptosis or localize directly in the nucleus and promote DNA repair [45, 384, 511].

p53 is also activated by non-genotoxic stress such as hypoxia/anoxia and activation of growth signalling pathways (Figure 1.6). Hypoxia/anoxia refers to the low presence (less that 1.5%) or total absence of O_2, respectively. Under hypoxic conditions p53 activates genes involved in G_1 arrest, such as GADD45, through nuclear translocation of p53 [227]. The exact mechanism in which p53 is being induced is yet to be determined. Interestingly, the prevalent hypotheses implicate changes in the mitochondrial permeability and release of mitochondrial dependent ROS that create an oxidizing signal in the cytosol [99], induction of transcription factors such as the hypoxia-inducible factor Hif-1α that might bind p53 leading to its stabilization and modulation of proline hydroxylation [20, 90, 99]. It should be noted that it is difficult to exclude any DNA damage implications, as hypoxia has been shown to induce certain endonucleases in vitro from chronically anoxic fibroblasts but no increase in cellular DNA strand breaks was measured [501].

In conclusion, genotoxic stress leads to rapid and high-levelled accumulation of p53 which in turn activates a series of genes participating in apoptosis, while on the other hand, non-genotoxic stress induces a long-lasting moderate accumulation of p53 with activation of cell cycle inhibitory genes (Figure 1.7). The two processes mentioned before are not fundamentally different as the first one leads to total extinction of the dysfunctional cell through apoptosis whereas the second leads to permanent or not cell cycle arrest from the pool of the replicating population depending on the dose, duration and type of the stress applied to the particular cell each time.

Genomic instability is a major cause of cancer [379] with mice with germline deficiencies in p53 are curtailed by cancer [145]. p53 heterozygotes mice develop neoplasms by the first 6-8 months of age including sarcomas, ovarian choriocarcinoma and lymphomas whereas p53-deficient mice develop various primary neoplasms in terms of cell type, malignancy and early onset, indicating the essential role of p53 in tumour suppression and progression [145]. Moreover, the absence of the p53 gene or the functional protein predisposes the organism to

develop cancer at a young age with most well-known the Li-Fraumeni syndrome, which involves germline mutations on the p53 gene [379].

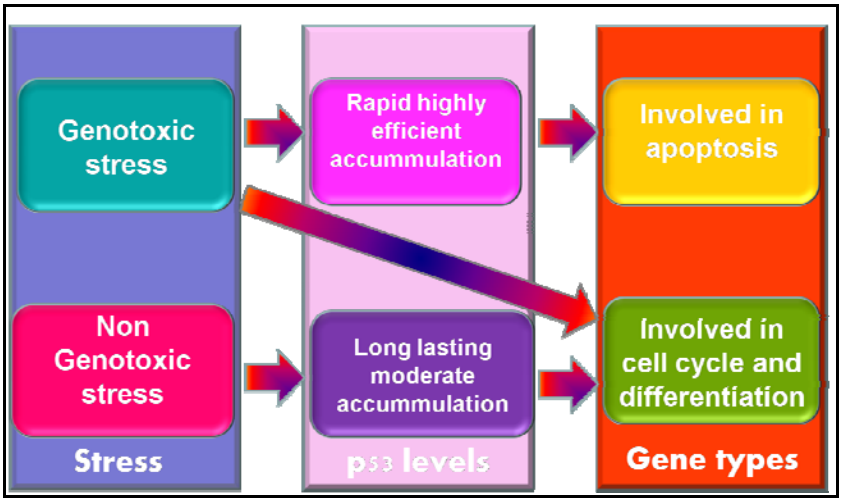

Figure 1.7: Summary of different types of stress. Genotoxic stress (UV exposure, ionizing radiation and DNA-damaging agents) compared to non-genotoxic stress (hypoxic/anoxic and induced growth signalling conditions) and different types of p53 activation effects.

1.3.1.3 p53, estrogens and hormone-dependent cancers

The structure and the function of the human breast tissue are under the regulation of various hormones such as steroids, progesterone and estradiol. Most of the above hormones, along with other signalling molecules, are implicated in the transformation of a normal tissue into cancerous and are also related to tumour response to treatment. Mutations in the p53 gene are implicated in various cancers with breast and ovarian cancer amongst them. Notably breast cancers, maintain the wild-type p53 gene indicating that other epigenetic or genetic events can inactivate p53 pathway and promote cancer progression [657]. In breast cancer, p53 is inactivated between a 0-40% inactivation rate in non-invasive breast cancers and 20-50% rate in invasive ones [135]. p53 mutations are associated with a decrease in disease-free period and shorter overall survival after systemic treatment of lymph

node-positive patients [54, 55, 540]. On the other hand, overexpression of p53 protein in the nucleus is an indicator of poor prognosis [540] and therefore it can be postulated that p53 plays a role in the progression of breast cancer from a hormone-dependent phenotype to a more aggressive hormone-unresponsive phenotype [23].

When it comes to estrogens and p53, it has been established that estrogen treatment in ERα-negative and -positive cancer resulted in elevated levels of phosphorylated Rb, an inhibitor of the E2F mitogenic transcription factors [277] and negative regulator of G_1 re-entry [352]. Rb phosphorylation is controlled by cyclins cdk-4 and -6 complex who act in favour of G_1 transition after mitogenic stimuli [352]. A noticeable difference between the ERα-positive and -negative cell lines was that in the first ones hyperphosphorylation of pRb occurred earlier than in the negative ones. In both cases medium containing E_2 was essential for the hyperphosphorylation of the protein [277, 420] but this effect was selective only for E_2 and not other steroids [420]. Further supporting these data, recent studies of MCF-7 xenografts in mice came to reveal [130] that tumours derived from MCF-7 overexpressing an inactive mutant of p53, after hormone stimulation, developed a characteristic metastatic phenotype with increased tumour growth, higher tumour histopathology grade, poorer differentiation whereas its molecular characteristic included centrosome amplification, loss of nuclear ERα expression, increased expression of Mdm-2 oncoprotein which induces ERα degradation [160], Rb hyperphosphorylation, lack of p21 which is a cdk inhibitor, premature expression of cyclin E and A (promoters of G_1-S transition and initiators of DNA replication [278]) and resistance to the antiestrogen tamoxifen [130]. All the above features resemble the triple negative tumours $ER\alpha^-PR^-HER^-$ and suggest a model for the development of $ER\alpha^-$ phenotype from $ER\alpha^+$ tumours.

Further supporting the above model comes the fact that p53 upregulates ERα, which is an estradiol-activated transcription factor, suggesting that specific p53 mutations in breast tumours may contribute not only to oncogenesis and drug resistance, as in the case of doxorubicin [540], but also to a more aggressive phenotype associated with the loss of ERα expression [23]. Loss of ERα expression involves a mechanism with

p53 abrogation, deregulation of cdk2 activity and centrosome amplification as mentioned above [130]. In a p53-null mouse model for mammary tumorigenesis, cancer cells arising from ERα-positive breast carcinomas develop loss of ERα expression [396], and as known tumours with no ERα display more aggressive phenotype [23], proposing that abrogation of p53 function may accelerate the development of phenotypic heterogeneity in breast cancer.

It is worth mentioning that apart all the above functions, p53 is implicated in the transcriptional activation and inactivation of various genes of other hormone-responsive tumours, such as WT-1, which act as an anti-oncogenic protein in Wilm's tumours and is responsible for gonadal dysgenesis in ovarian and Sertoli cells of the testis [582]. The ability of gonadotropins to prevent granulose cells apoptosis has been related with the activity of Bax and bcl-2 which are regulated by p53 [582]. In vivo treatment with gonadotropin in ovarian cells resulted in reduction of the p53 mRNA levels and bax protein, as verified by immunohistochemical experiments showing p53 restrained in the nucleus. Moreover, recent experiments showed that estrogen treatment also involve mdm-2 protein as well as TNF. As far as the TNF is concerned it was demonstrated that estrogen treatment resulted in resistance of MCF-7 to the cytotoxic action of TNF.

1.3.1.4.p53 and Tamoxifen

Cytostatics, radiation and tamoxifen can induce apoptosis via p53 dependent or independent pathways [52]. Benefits of chemotherapy with the anti-estrogen tamoxifen have been widely demonstrated and related to most of the ERα-positive breast cancers [420]. However, the molecular basis for the drug's activity and its association to the cell cycle has not yet been clearly established. Several molecular and cellular mechanisms have been proposed as contributors to the acquisition of this resistant phenotype including loss of ERα, selection of ERα mutants, shift in metabolism toward the accumulation of estrogenic metabolites, altered growth factor

production from breast cancer cells towards other targets, ligand-independent ERα-mediated transcription, active recruitment of corepressor or coactivator proteins to produce a mixed transcriptional phenotype based on the antagonist's DNA-binding properties, among others [568, 621]. Only two mechanisms will be analysed in this thesis involving, (i) HER2 association and (ii) a novel cdk/centrosome pathway. Tumours overexpressing HER2 are resistant to antiestrogen therapy and have lower clinical response [67, 248, 268]. HER2 overexpression in MCF-7 cells results in enhanced activity of mitogen-activated protein kinase MAPK [335]. MAPK has been shown to phosphorylate Ser_{118} in the ERα which is required for full activity of its activating function, leading to steroid-independent activation of ERα with loss of the inhibitory effect of tamoxifen on ERα-mediated transcription [78, 531]. Moreover, MAPK has been suggested to alter ERα association with corepressors [335] and therefore tamoxifen can no longer recruit those corepressors to the AF-2 region in the hormone-binding domain of the ERα to block ERα-mediated transcription [287, 568]. The second mechanism has been recently developed and suggests an alternative tamoxifen-resistant pathway focused on antitumor effects of the drug due to the expression of cyclin-dependent kinase inhibitors, especially p21(WAF1) which in turn are regulated by a decrease in wild-type p53 [279]. Different mechanisms may be responsible for antiestrogen resistance and that can explain studies in patients diagnosed with breast cancer and treated with adjuvant tamoxifen which supported that elevated p53 levels are associated with poorer survival [170]. Other studies demonstrated that there is no correlation between p53 levels and response to tamoxifen treatment [25], although it is clear that this era is not yet fully characterised. Since all these therapeutic approaches act through genomic damage and can therefore induce apoptosis and because p53 can respond to genomic instabilization and promote apoptosis [640], it can be hypothesized that an intact p53 would predict sensitivity to therapy [169].

1.3.1.5 UV damage, breast cancer and p53-dependent apoptosis

In response to a wide variety of apoptotic stimuli, cells immediately activate a defensive response characterized by mitochondrial activation, manifested by rapid up-regulations of multiple mitochondrial respiratory chain (MRC) proteins and enhanced MRC activities such as oxygen consumption. In the meantime, Bcl-2 proteins undergo dynamic alterations in an attempt to keep the cells alive [100]. Proteins in the Bcl family control cell death by altering the permeability of the outer mitochondria membrane in response to exogenous or endogenous stimuli, such as UV or due to oxidative phosphorylation (intrinsic apoptotic pathway thoroughly analysed in section 1.2.1.2). In short after UV damage, (i) cytosolic cytochrome c is being released, (ii) complex consisting of Apaf-1, dATP and pro-caspase-9 is being formed [240, 242, 366], (iii) activation of caspase-3 and caspase-7 follows, (iiii) caspase-3 then cleaves pro-caspase 9 to its active form creating a positive feedback loop [555]. Caspase-9, is required for p53-mediated apoptosis [504, 548].
Interestingly, a variation of this mechanism exists in MCF-7 breast cancer cells. In these cells endogenous cytochrome c is being released in the cytosol but is unable to induce pro-caspase-9 cleavage [543, 553], whereas exogenous cytochrome or a cell-free system from MCF-7 lysates is able to induce pro-caspase-9 activation in a dose-dependent manner [60, 190]. These data support the hypothesis of a cytosolic cytochrome-c inhibitor present in MCF-7 cells. On an independent study, Blanc and co-workers revealed that absence of caspase 3 leads to delayed cytochrome c release and defects in pro-caspase 9 activation [60]. In the same study it was also found that caspase-3 reconstitution in MCF-7 cells (caspase-3 deficient) enables cytochrome c release to the cytosol and pro-caspase 9 cleavage. Interstingly, in pro-caspase-3 reconstituted MCF-7 cells cytochrome c was capable of inducing caspase-3 activity but after incubation at 37°C, suggesting additional defects in cytochrome c-mediated caspase activation pathway.

1.3.1.6 p53 and subcellular redistribution

Normal p53 undergoes cell cycle-dependent translocation. In growth-stimulated synchronous populations of 3T3 cells newly synthesised p53 stays in the cytoplasm during G_1 phase, translocates to the nucleus prior to G_1-S transition where it remains till initiation of DNA synthesis and then recycled back into the cytoplasmic compartment [524]. DNA damage leads to the accumulation of p53 in the nucleus where it acts as a transcription factor and transactivates a myriad of target genes implicated in apoptosis, cell cycle arrest and DNA repair [168]. The tetramerization domain and the exposed nuclear localization signal are necessary for nuclear import and retention, and thus activation of the p53 protein whereas residues Arg $_{306}$ and Lys $_{305}$ are implicated in cytoplasmic localization of the protein. Cytoplasmic localization of p53 has been observed in breast tumours as well as other neoplasms, embryonic stem cells [334] and undifferentiated neuroblastomas [410]. Cytoplasmic retention of p53 results in severe functional defects in the p53-mediated G_1 checkpoint response [411] after DNA damage but studies in NB cells showed that when the cytoplasmic capacity is exceeded due to p53 overflow (excess DNA damage), p53 enters the nucleus where it is transcriptionally active [411]. The same study suggested a rather interesting mechanism to explain this cytoplasmic localization of p53 which included the presence of a molecular chaperone that binds to the protein and is present in limited amounts in the cytoplasm. This speculation was supported by the presence of distinct p53-associated punctate structures in the cytoplasm. Once all of the available binding sites of this anchor protein-chaperone are occupied, p53 is no longer trapped and is free to move. Hsp70 proteins utilize this mechanism of cytoplasmic retention when bound upon their targets (steroid receptors or kinases) but once the ligand binds to the receptor then the last one is released and enters the nucleus where it activates transcription [411].

The relationship between hormonal stimuli and the pattern of p53 expression may be quite complex as suggested by the absence of cytoplasmic p53 in 50% of normal breast samples but this may be due to the presence of different hormonal levels in

each patient at the time of the surgery [334]. Experiments with the MCF-7 breast cancer cell line, which contains p53wt gene [499] have demonstrated that the protein is being mislocalized after estradiol treatment [351, 408]. In particular, cells grown in charcoal stripped serum had p53 in the nucleus and the cytosol, whereas after estrogen treatment most of the p53 protein was detected in the cytoplasm instead of the nucleus. In p53-mutated breast cancer cells, nuclear translocation does not occur [351]. The above results suggest that estrogen treatment may mediate p53 inactivation and prevent p53-mediated growth arrest [525, 526]. In normal ovarian epithelial tissue, DNA damage along with hCG treatment has resulted in elevated levels of nuclear p53 [334]. Nuclear exclusion is therefore, a non-mutational mechanism for attenuating p53 suppressor function but other ways of inhibiting the protein are via its interaction by certain inhibitor proteins. Only a few p53 inhibitors, have been identified so far with the most well characterised being mdm-2.

1.3.1.7 p53 and mdm2

A variety of positive and negative feedback loops between p53 and a series of other genes have been described in literature. All these loops provide a means to connect p53 with a series of diverse signal transduction pathways and orchestrate cell growth and division as well as backing up the cell in case of a system's malfunction. Each of these loops consists of a series of proteins whose activity or rate of synthesis is affected by p53 activation and this in turns results in the adaptation of p53 activity. Of these, seven are negative feedback loops that modulate down p53 activity (mdm-2, Cop-1, Pirh-2, p73 delta N, cyclin G, Wip-1 and Siah-1) and three are positive feedback loops (PTEN-AKT, p14/19 ARF and Rb) that positively modulate p53 activity [249]. Interestingly, six of these feedback loops act through mdm-2 (mdm-2, cyclin G, Siah-1, p14/19 ARF, AKT and Rb) to modulate p53 activity.
The mdm-2 gene was originally cloned as a cellular oncogene amplified on a mouse double-minute chromosome from a transformed derivative of 3T3 cells cDNA

library [84]. In the same study, in situ hybridization mapped mdm-2 on chromosome 10, regions C1-C3. The crystal structure of the 109-residue amino-terminal domain of mdm-2 that binds to a 15-residue transactivation domain peptide of p53 revealed that mdm-2 has a deep hydrophobic cleft on which the p53 peptide binds as an amphipathic α helix [336]. What is more, mdm-2 encodes a putative nuclear localization signal and is characterized by an acidic domain often found in transactivators [262]. The amino-terminal domain of p53 is rich in negatively-charged acidic amino acids that are required for the transactivation function of the protein and therefore influence the p53-dependent transcription machinery [106]. A genetic analysis of p53 and mdm-2 mutations, of the targeted amino acids to alanine, that block this protein complex has identified critical amino-acid residues in each protein that are important for this binding interaction [205, 361]. The interaction was tested by Y2H and site-directed mutagenesis *in vitro* as well as the p53 transcriptional control *in vivo* by transient transfection in mammalian cells [205]. These same amino-acid residues have been shown to make these protein contacts in the crystal structure of the amino-terminus of HDM-2 (the human protein) and a peptide from the amino-terminus of p53 [336]. Residues phenyalanine 19, tryptophan 23 and leucine 26 of p53 form the major contacts in the mdm-2 hydrophobic pocket. Phosphorylation of residues serine 20 and possibly serine 15 should weaken these contacts, and peptides and drugs that compete with these contacts block the p53-mdm-2 complex and promote apoptosis in cells [315].

Mdm-2 forms a complex with p53 and down regulates its ability to activate transcription [37, 328, 413, 625] (Figure 1.8), therefore affecting p53 stability [328] as well as growth inhibition [196], G_1 arrest and apoptosis [107]. The p53-mdm-2 protein complex was originally detected in a cell line containing a temperature-sensitive p53 protein, which behaved like the wild-type p53 protein at 32°C and a mutant p53 protein at 37°C -39°C [387, 413]. The p53-mdm-2 complex was readily detected at 32°C and only poorly observed at 37°C -39°C even though it was clear that mdm-2 bound well to mutant p53 protein [254], undoubtedly indicating that mdm-2 synthesis is being controlled by the presence of wild type p53 [625]. Mdm-2

is an E3 ubiquitin ligase which keeps p53 levels low in undamaged cells. It binds p53 and targets it for ubiquitin-mediated proteosomal degradation, therefore inhibiting its tumour suppressor function [261, 328]. There is evidence to suggest that mdm-2 shuttles p53 from the nucleus to the cytoplasm [497] where mdm-2 interacts with p300 resulting in the breakdown of p53 [235] and also accelerating p53 degradation by the proteosome. Mdm-2 also regulates p53 by blocking the ability of p53 to bind to the transcriptional machinery creating a negative auto-feedback loop whereby p53 upregulates mdm-2 [625]. On the other hand, $p14^{ARF}$ stabilizes p53 by inhibiting mdm-2 thus helps maintaining a steady state level of p53 in undamaged cells (Figure 1.8). Interestingly, mdm-2 knockout mice are lethal 6 days after fertilization at the blastocyst developmental stage. This may be triggered by hypoxia caused at this stage, activating p53 in the absence of mdm-2 and leading to apoptosis. Consistent with this analysis is the observation that a p53/mdm-2 double knockout mouse is viable and is born as normal as a p53 knockout mouse [296, 414].

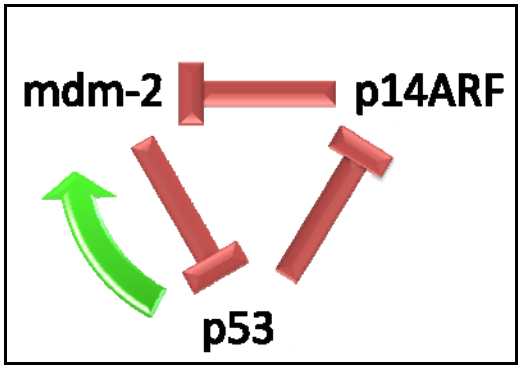

Figure 1.8: p53/mdm-2/p14ARF loop. Arrows denote stimulatory interactions, whereas horizontal bars instead of arrowheads indicate inhibitory influences (described in 1.3.1.7).

Recently, it has been revealed that this p53-mdm2 autoregulatory loop triggers an oscillatory effect with the two proteins' levels increasing and decreasing over time under mathematical precision like a 'digital clock' [338] (Figure 1.9). The oscillatory reaction includes release of well-timed quanta of p53 in discrete pulses after stress

[338]. Digital behaviour may require a damage checkpoint functioning when p53 levels are low and releasing the next pulse only if the damage is still present. Interestingly, the higher the damage the more pulses of p53 are being triggered whereas the pulses' size and shape remains unaffected. By releasing quanta of p53 after a certain period of time, the cells are able to repair their DNA without risking the dreadful consequences of excessive p53 that leads to cell death.

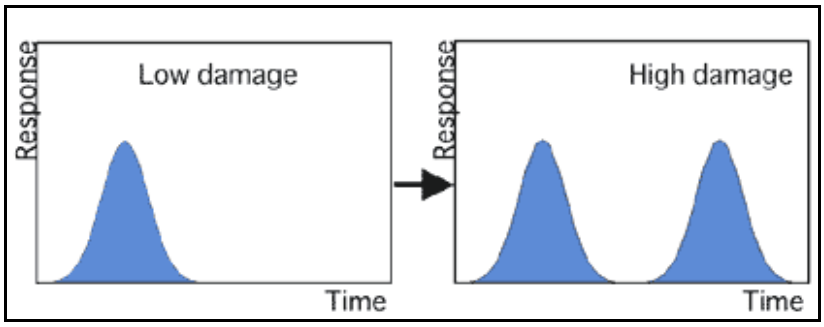

Figure 1.9: Digital behaviour of p53-mdm-2 loop. Digital systems show an increased number of pulses with increasing signal, but the pulse size and shape do not depend on the signal strength (adapted from [338]).

The mdm-2 gene has been amplified in many cancers. In more detail, the protein is overexpressed in 30-40% of sarcomas, in many leukemias and glioblastomas [76, 443] which are characterised by escape from p53-regulated growth control. The wild type p53 gene should be intact, although the p53 protein is apparently inactive, so that drugs that disrupt the p53-hdm-2 complex should activate p53. In addition, many other cancers appear to express the hdm-2 gene product at high levels even when the hdm-2 gene is not amplified. In these types of cancers blocking hdm-2 activity or releasing p53 from this complex could well promote apoptosis selectively in the cancer cells. Therefore, the p53-mdm-2 complex and the mdm-2 ubiquitin ligase activity have become a major drug target for some cancers. Nutlins, or else cis-imidazoline derivatives, are novel non-peptidic mdm-2 antagonists that disrupt the physical interaction between p53 and mdm-2 [19, 623].

1.3.1.8 p53 and other inhibitors

Apart from mdm-2 other p53 inhibitors have been identified including iASPP which regulate the ability of p53 to bind promoter elements of proapoptotic target genes. The ASPP family consists of two pro-apoptotic family members, (i) ASPP1 and ASPP2 [510], both of which bind to p53 and aid transcription of pro-apoptotic genes, (ii) and one anti-apoptotic family member, iASPP, which binds to p53 and represses its apoptotic transactivation potential [46, 51, 633], plus binding to the NF-κB subunit p65 to inhibit its transcriptional activity [633]. It is worth mentioning that one mechanism by which wild-type p53 is tolerated in human breast carcinomas is through loss of ASPP activity [51]. iASPP expression is upregulated in human breast carcinomas expressing wild-type p53 and normal levels of ASPP. Overexpression of iASPP confers resistance to the cytotoxic effects of ultraviolet radiation and to cisplatin-induced p53-mediated apoptosis while silencing of the protein leads to p53-dependent apoptosis [51]. Another group of p53 inhibitors includes histone deacetylases HDACs. Histone deacetylases are chromatic-modified enzymes that facilitate a closed chromatin structure and therefore transcriptional repression [439]. HDACs inhibit p53 through the p21 pathway [362, 439, 495] but analysing this pathway remains beyond the focus of this project. Recently, another gene was added to the list of p53 inhibitors, termed AGR-2 which belongs to the Anterior Gradient protein family [474].

1.3.2 Anterior Gradient 2

1.3.2.1 Anterior Gradient 2 in *Xenopus* development

The *h*AGR-2 (human Anterior Gradient 2, also known as HAG2, AG2, GOB4) gene is the human homologue of the *Xenopus laevis* cement gland gene *x*AG-2. AGR-2 was first described in 1997 by virtue of expression in *Xenopus* eggs, where the

protein was reported to be secreted. In *X.laevis* the *x*AG family is highly expressed in the ectoderm during the early stages of the embryo development, but certain members of the *x*AG family, such as AG-1, AG-2 and AG-3 are downregulated as development progresses [3]. *x*AG-2 is involved in the anterior specification of the *Xenopus* embryonic ectoderm giving rise to forebrain and cement gland. Its expression is induced by signals deriving from the Specmann's organizer and a certain concentrations of the protein is being required in order to induce differentiation [3]. In frog embryo, *x*AG-2 protein is expressed in the cement gland, a mucus secreting organ that facilitates the attachment of the embryo to a solid sterigma, essential for the feeding and growth of the embryo whereas in adult frog, the gene encodes a protein highly expressed in the lung primordium and the pharynx [3]. Recently, another *x*AG-2 homologous gene, named *X*Agr-2, was identified in *Xenopus* embryos, which in addition to the cement gland, was found to be expressed in the otic vesicles, specifically in the ventromedial region that later develops to the cochlea, and notochord, especially in the tailbud and neurula stages [436]. This XAgr-2 gene had greater sequence homology to the *h*AGR-2 and *m*AGR-2 than *x*AG-1and *x*AG-2 (Figure 1.10). *X*Agr-2 was identified as a target of the *x*Anf-1, for Xenopus anterior neural folds, gene that is a novel homeobox gene essential for the development of the telencephalon [649].

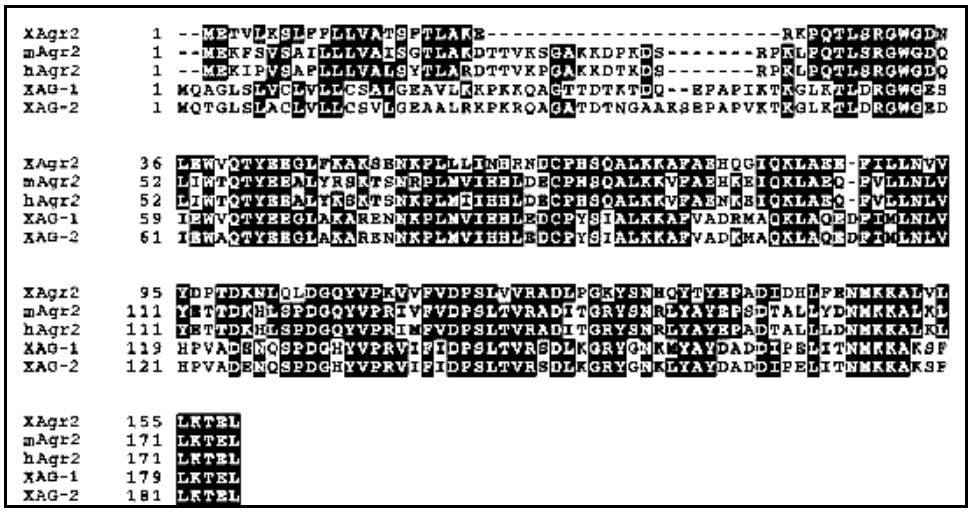

Figure 1.10: Alignment of the Agr homologous genes. XAgr2 has a higher homology to mouse and human Agr-2 genes than to the XAG-1 and XAG-2 genes (adapted from [436]).

1.3.2.2 Anterior Gradient 2 in adult salamander

Recent studies identified AGR-2, termed as *n*AG, as a key player in limb regeneration in adult salamander. The regeneration occurs only if there is simultaneous regeneration of the severed nerves [331]. The limb blastemal cells of the salamander regenerate the structures remote to the level of amputation, and the surface protein Prod-1 is a key player in this process. Prod-1 is a cell surface protein expressed in a proximal-to-distal gradient in the newt limb regeneration blastema and is critical determinant of their proximodistal identity. Prod-1 is expressed at the cell surface as a glycosylphosphatidylinosotol (GPI)–anchored protein of the Ly^6/CD59 superfamily and mediates cell-to-cell interaction and positional identity [415]. Its expression is graded (Proximal > Distal) in both normal and regenerating limbs and is regulated by retinoic acid [415]. *n*AG was found to interact with Prod-1 after Y2H and co-immunoprecipitation analyses and promote cell division [331]. *n*AG was found to be essential to rescue nerve dependence but not to enhance nerve regeneration. When *n*AG was expressed, it induced formation of *n*AG-positive glands in the wound epidermis and secreted *n*AG acted directly on the limb [331]. Understanding how vertebrates such as the newt can re-grow body parts may explain why mammals have limited re-growth abilities and have major effects in regenerative medicine. In humans, *h*AGR-2 was found to interact with the C4.4 protein that is a GTI-anchored protein and has two Lys^6-type domains and is associated with metastasis [199]. C4.4 and Prod-1 both have small Cys-rich domains and their interaction with AGR-2 suggests a conserved pathway of protein complexes.

1.3.2.3 Anterior Gradient 2 homologues in other vertebrates

In the zebrafish, *Danio rerio*, AGR-2 is expressed in most organs such as epidermis, otic vesicles, pharynx, esophagus, olfactory bulbs, pneumatic duct, gills, swim bladder, and the goblet cells of the mid-intestine [532]. zAGR-2 contains a putative

similar sequence to *x*AG-2 and the gene was found as a duplicate with identical nucleic acid and amino acid sequences in chromosomes 7 and 19. Interestingly, the cleavage site was predicted between Gly^{20} and Lys^{21}, suggesting that the zebrafish homologue may encode a secreted protein similar to the *Xenopus* and human homologues [3]. Recent studies by Morrison and co-workers, revealed that AGR-2 is upregulated in the Atlantic salmon, affected with the amoebic gill disease, an ectoparasitic condition that creates reduced appetite, lethargy, respiratory distress and loss of equilibrium in fish [418]. These AGR-2 mRNAs were cloned, sequenced and shown to be predominantly expressed in epithelial-rich tissue of the gills, intestine and brain in healthy fish [418], a pattern of expression consistent with the role of the protein in *Xenopus* [532]. Interestingly, p53 mRNA was downregulated in the same AGD lesions that AGR-2 was high, consistent with data from human cell lines that propose AGR-2 as a p53 inhibitor [474]. AGR-2 mRNA is downregulated during *Mycobacterium marinum* insfection in zebrafish [397] Other genes found to be downregulated in the same model were muscle-specific genes, MHC genes, Major Histocompatibility Complex, and other genes that reflected the general disease state of the animal, which is widely used as a human tuberculosis model and reveals new insights for mycobacterial pathogenesis. Interestingly, similar profile studies concerning the transcriptome response of the salmon fish after *Aeromonas salmonicida* exposure that stimulates acute bacterial response, revealed that AGR-2 was amongst the genes downregulated in the gills [386]. The gills are regarded as a primary site of infection and are shown to be immunologically active as they have high numbers of antibody-secreting cells [150]. Both independent studies suggested a role of AGR-2 in inflammatory response especially after bacterial expression but the exact mechanism is yet unidentified.

Mouse AGR-2 (also called Gob4) is expressed mainly in the adult stomach, intestines, and colon and localized in mucus-secreting cells of the intestine, named goblet cells, as verified by in situ hybridization [318]. Goblet cells are part of the small intestine epithelium and are thought to derive from stem cells in the basal region of a crypt. Same analysis detected the protein in the lower crypt region cells

of the colon and in mucous neck cells of the stomach. Amino-acid sequence analysis revealed that Gob-4 is similar to xAGR-2, with a 46% homology. Both, human and mouse genes encode a protein of 175a.a and have a similarity of 98.3% [612]. *m*AGR-2 also bears a putative signal sequence like *h*AGR-2 and the most likely cleavage site was predicted between Ala^{20} and Lys^{21} [318]. At nucleotide level *m*AGR-2 and *h*AGR-2 share 87% homology [577].

Major differences among anterior gradient homologues in vertebrates are caused by length variations in the N-terminal region, 22-45 residues long, and low sequence similarity in this region [532] (Figure 1.11). Phylogenetic analyses in this variable N-terminal region revealed that zebrafish AGR-2 is clustered with homologues from the Atlantic salmon (*s*AGR-2) and pufferfish (*t*AGR-2) and this group also included the human and mouse anterior gradient 2 genes. The same study also revealed that human and mouse AGR homologues (HAGR-3, mAGR-3) are clustered together with the *Xenopus X*AG-1 and *X*AG-2 genes, suggesting a closer relationship between these genes (Figure 1.11). The aforementioned results proposed a model supporting the existence of one anterior gradient 2 gene in teleosts and that human AGR-2 and AGR-3 are the products of a tandem duplication event due to adjacent chromosome mapping [199] which also may be the case for mouse and *Xenopus* anterior gradient 2 genes.

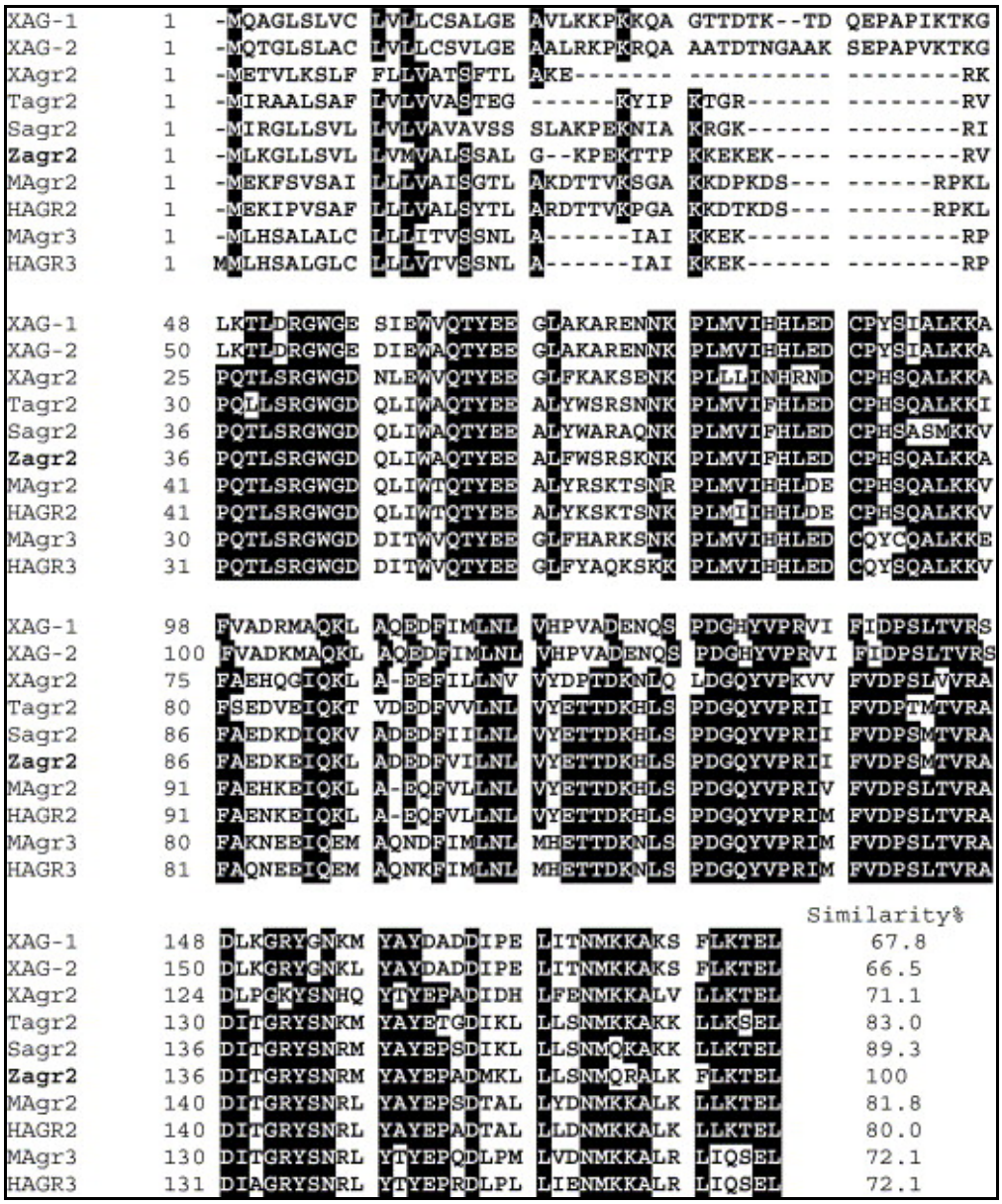

Figure 1.11: Alignment of the amino acid sequence of zebrafish *agr2* with other anterior gradient 2 homologues from the pufferfish, Atlantic salmon, *Xenopus*, human, and mouse. Identical amino acid sequences which are greater than or equal to seven are shown in black boxes. Gaps are introduced as represented by dots to optimize the alignment. The percentage of amino acid similarity between zebrafish agr2 and each homolog is shown. Sequences are pufferfish Tagr2 *Tetraodon nigroviridis*, Atlantic salmon Sagr2 *Salmo salar*; human HAGR2 and HAGR3, mouse MAgr2 and MAgr3, zebrafish Zagr2 this study and *Xenopus* XAG-1 XAG-2 and XAgr2 (adapted from [532])

1.3.2.4 The human *h*AGR-2

The *h*AGR-2 gene was mapped to chromosome band 7p21.3 [470]. The gene was first described in the MCF-7 breast carcinoma cell line, and found to be co-expressed with the Estrogen Receptor α, in ERα-positive cell lines [612] [577] and also upregulated under hypoxic, serum deprived or stress conditions [662]. The same study also revealed that in ERα-negative tumours the protein's expression was associated with PgR expression. Four putative oestrogen response elements have been discovered in the AGR-2 promoter and have been suggested to play a role in the oestrogen-dependent expression of AGR-2 in breast cancers [273]. Recent reports demonstrate that AGR-2 enhances colony formation in clonogenic assays, attenuates p53-dependent gene expression, and suppresses ATM-mediated p53 phosphorylation at Ser^{15} and Ser^{356} after DNA damage, proposing a p53-inhibitory role for the protein in the premalignant metaplastic epithelium, called Barret's oesophagus [474].

The protein is expressed in some normal tissues such as liver, heart, placenta, stomach and kidneys apart from cancer ones [650]. AGR-2 encodes a protein that gives rise to two different isoforms, the full length and the mature one [3, 650]. The full length protein contains a leader signal peptide that is processed to yield the mature protein. The main difference in these two forms of the protein is that the full length one contains the leader sequence targeting the protein to secretion, whereas the mature form does not bear this sequence. This N-terminal hydrophobic leader sequence is predicted to be cleaved between Ala^{20}/Lys^{21} giving rise to a 17,949Da mature protein. AGR-2 is a 19,797Da protein and is under regulation by the proteosome [474]. Staining of primary breast tissues from patients showed cytoplasmic and membranous staining of the protein [282].

More recently AGR-2 has been identified as a novel member of the protein disulfide isomerase family consisting of protein disulfide isomerases (PDIs) and ER proteins (ERps) [467]. The active motif of such proteins is a CXXC domain, also contained in thioredoxins and therefore termed the Tx domain [194]. AGR-2 has homology to ERp18/19 (Figure 1.13), and while it does not contain a CXXC motif, it does have a

CXXS domain which was recently identified in two other ERp proteins [22] and shown to have lower activity that the original CXXC motif. AGR-2 and AGR-3, another member of the AGR family, also show conserved intron position with respect to protein sequence when compared to Erp18/19 as well as exon boundaries [468]. Such data suggest that AGR-2 may have evolved from PDI/ERps but no longer retains its characteristic function.

1.3.2.5 AGR-2 in secretory cells

In *Xenopus* oocytes AGR-2 is found in the secretory cement gland where it regulates its differentiation as well as ectodermal patterning throughout the different developmental stages [3]. The gene has 91% similarity to the Gob-4 gene in mice, which is highly expressed in mucous-secreting goblet cells of the intestine [318]. Moreover, upregulation of the gene in Barret's epithelium, a condition which is characterised by an increased number of goblet cells in the lower oesophagus [484, 485] along with protein's expression data in mucus-secreting cells and endocrine organs [652] further support the list of secretory cells that overexpress the protein. Recently, AGR-2 has been identified as a candidate gene for inflammatory bowel syndrome under the control of goblet cell-specific transcription factors FOXA1 and FOXA2 [652]. Pilot studies involving the AGR-2 protein fused to a C-terminal GFP revealed that is also secreted from HeLa cells [364] consistent to secretory data from androgen-inducible prostate cancer cell lines [650]. The same study revealed that AGR-2 was overexpressed in the secretory epithelial cells of the prostate gland, it encodes two proteins and the shortest isoform is secreted upon androgen treatment although both transcripts were induced by dose-dependent treatment with testosterone, diethylstilbestrol and 17-beta estradiol.

1.3.2.6 AGR-2 in metastasis, tumour growth and cell survival

Anterior Gradient-2 was found to be overexpressed in metastatic cancer cell lines [364] as well as in the circulating tumour cells in the peripheral blood of advanced metastatic cancer patients [544] and was therefore recommended as a potential detection and characterization marker for these cells. A strong correlation between AGR-2 expression, the presence of metastasis and patient survival has been observed in a group of tamoxifen-treated patients with ERα-positive breast cancers and elevated levels of AGR-2 that exhibited a statistically significant poorer survival rate and higher incidence of metastasis, than those without AGR-2 mRNA [364]. AGR-2 has also been implicated to interact with a metastasis gene that encodes glycosylphosphatidylinositol-anchored protein C4.4A [199], which is upregulated in several types of metastatic cancers. Furthermore, studies in SEG-1 esophageal adenocarcinoma cells further supported the role of AGR-2 in metastasis and cell migration [611]. In these studies media from SEG-1-AGR-2 cells was transfused into SEG-1 KD1 cells that were AGR-2 deficient (due to retroviral shRNA) and induced migration by a 2.5 fold factor, as measured by in vitro migration assays.

Recent studies have shown that AGR-2 increases the growth rate of mouse fibroblast NIH3T3 cell line by in vitro assays that included the formation of discrete foci or compromising anchorage independent growth in soft agar [611]. Stable cells expressing AGR-2 showed up to 7-fold increase in colonies compared to NIH3T3 control cells consistent with the protein's role in enhancing colony formation in H1299 cells [474]. These xenographs of NIH3T3 AGR-2-positive cells in mice were 15-fold larger in size 21 days after implantation. This is also related to data indicating that AGR-2 transfection enhances the level of attachment of AGR2-negative cell lines to an extracellular matrix [611].

Interestingly, experiments mimicking the tumour microenvironment in terms of low oxygen and growth factors status, showed AGR-2 upregulation under these conditions [662]. The same study also revealed that this upregulation occurs through a MAPK/ERK-dependent pathway, by treating with certain inhibitors of signalling

pathways such as JNK, p38, PI3K and ERK1/2, which are involved in anti-apoptotic cell response [239, 489]. Therefore, a survival role for AGR-2 under physiological stress conditions that promote selection of more aggressive types of tumour cells was supported. This conclusion is consistent with the findings that AGR-2 acts as a p53 inhibitor in response to UV damage, which is a type of stress, and rescues cells from death [474]. These stress-induced experiments were performed in ERα-negative cell lines and showed independence of ERα status for AGR-2 induction, supporting the observation that 20% of ERα-negative cancers show elevated AGR-2 expression and revealing a new model of action, regardless of the ERα status [199]. On the other hand, ERα- positive cells growing in estrogen depletion have lower levels of AGR-2 than cells growing in the presence of estrogens suggesting that ERα status is essential to AGR-2 function and further affects survival and tumour behaviour in these cell types [282] (summary of 1.3.2.6 depicted in Figure 1.12).

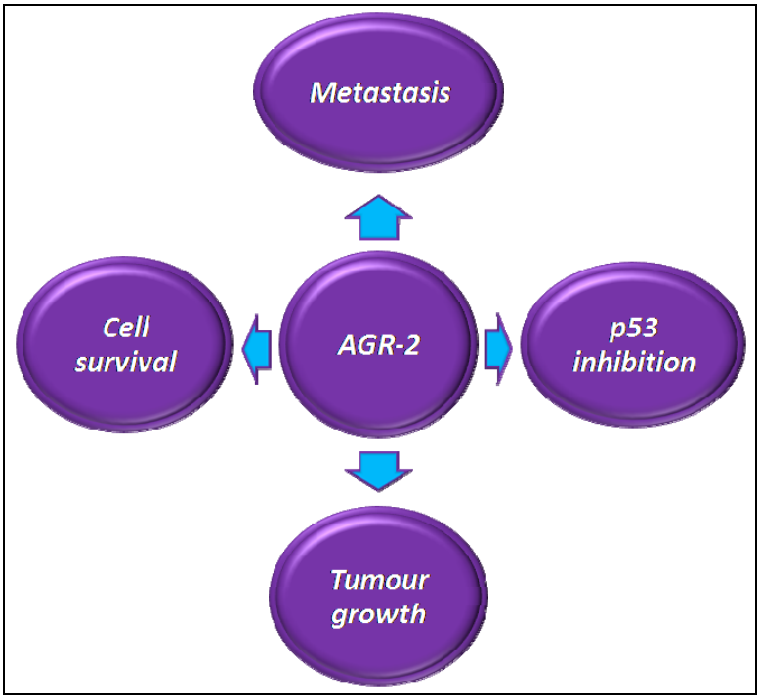

Figure 1.12: Schematic diagram of AGR-2 roles in human cancer. Human AGR-2 is implicated in cell survival, metastasis, tumour growth and p53 inhibition in cancer cells. The exact mechanism of action has not yet beed characterised.

1.3.3 Anterior Gradient 3

Human anterior gradient-3 (AGR-3) was discovered several years after AGR-2 by a group researching unknown human and mouse genes [561]. The gene, named Breast Cancer Membrane Protein 11 (BCMP11) was also identified during proteomic analysis of purified membrane proteins of breast tumour derived cell lines, shown to localise to endosomes of T47D breast cancer cells and implicated as being secreted [4]. Around the same time Fletcher and co-workers also found BCMP11 and reported its homology with AGR-2, leading to the name being altered to AGR-3, in line with it being a member of the anterior gradient family [199]. *h*AGR-3 and *h*AGR-2 share a 71% sequence identity and they are both candidate members of the thierodoxin superfamily of proteins due to the characteristic CXXS motif and also the high degree of homology with ERp18/19 [468] (Figure 1.13). AGR-3 is a 19,176Da protein and proposed to have an N-terminal signal sequence, which is predicted to be proteolytically cleaved between Ala^{23}/Ala^{24} resulting in a mature protein of 16,822Da. Both *h*AGR-2 and *h*AGR-3 genes comprise seven coding exons with similar exon/intron boundaries, which along with the high similarity and close genomic locality suggest that they arose from a gene duplication event [199]. The majority of differences between the two genes are found within the predicted hydrophobic leader sequence. AGR-3 also shows a correlation with ERα expression in samples derived from breast cancer patients and processed with RT-PCR [199] but the exact role of the protein is yet undefined. As well as being implicated in breast cancer, AGR-3 is also upregulated in patients with inflammatory bowel disease, albeit to a lesser extent than AGR-2 [652]. AGR-3 also binds to the C4.4 metastasis associated protein and alpha-dystroglycan (DAG-1) and the minimum binding domains, as identified by overlapping contigs, were restricted to the extracellular part of DAG-1 (alpha dystroglycan chain) or C4.4a consistent with the secretory nature of the *h*AGR proteins [199].

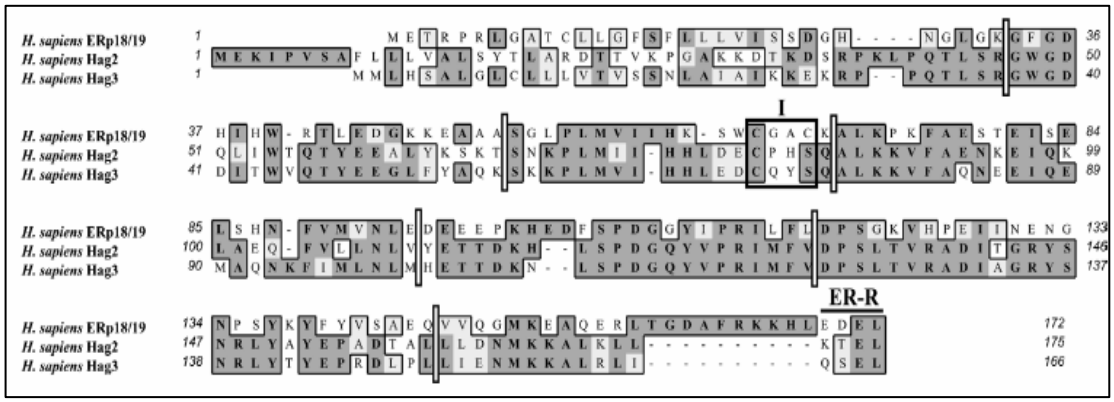

Figure 1.13 Homology between anterior gradient proteins and ERp18/19 Sequence identity between AG-2, AG-3 and ERp18/19.Highlighted areas indicate regions of homology between the proteins (adapted from [468]).

1.4 PDI family of proteins

Since AGR-2/AGR-3 both are novels members of the PDI family, separate attribute to this family should be made. Endoplasmic reticulum contains a broad network of chaperones that facilitate the correct folding and processing of the proteins targeted to secretion. The protein disulfide isomerases, PDIs, play an important role as they catalyse formation, reduction and isomerization of disulfide bonds, depending on the redox environment, and thereby stabilizing intermediate conformations during protein maturation in the lumen of the ER [522]. In particular, PDIs are involved in the proper folding, formation and reshuffling of the disulfide bridges of the proteins synthesized in the rough ER, imported in the lumen of this structure and destined to be secreted or incorporated in the cell membrane [593]. Interestingly, several of these proteins that reside in the ER in normal cells, have been shown to accumulate at the cell surface in cancer cells as part of larger molecular complexes [18] and may affect antigen presentation [131].

It has also been supported by literature that certain members of the PDI family act in other cellular compartments apart from the endoplasmic reticulum. In non-ER locations they are present in lower amounts and it has been suggested that a less oxidative environment, compared to the ER, alters their function [593]. Proteins of this family have also been reported of being secreted from hepatocytes, platelets, aortic endothelial cells [267] and pancreatic exocrine cells. Reports of their presence in the cytosol involve ERp57 mainly [354] as well as other members such as Erp49 but remain beyond the aims of this project. Protein disulfide isomerase activity has been detected in the mitochondria as well, especially at the membrane level and not the matrix, and a protein was purified but the molecular weight was much smaller than the PDIs one and an anti-PDI antibody could not recognize it [487]. Moreover, the protein was suggested to have a role in the mitochondrial membrane permeability by reducing protein disulfides and affecting redox regulation. When it comes to the nuclei, it is noteworthy that ERp57 and PDI are present in the nuclei, either by direct detection of the protein [213] or by *in vitro* evidence that these proteins influence processes at the DNA level, such as DNA binding to transcription factors or structural nuclear proteins. PDIs facilitates the binding of NFκB and AP-I to DNA [120]. The above observations were not free of criticism due to the peripheral localization of the ER around the nucleus and possible cross-contamination of the one compartment to the other in vitro. Immunohistochemical proof of nuclear localization of ERp57 followed in Hela and 3T3 cells and was verified by DNA-protein cross linking experiments [124]. In conclusion, the PDI family includes proteins with diverse mobility and localization patterns, activating different pathways and triggering various reactions, depending on their distribution and the redox environment.

The active binding motif of the proteins is the CXXC, which is also characteristic of another protein family, the thioredoxins (Txs). For that reason this motif is referred to as a Tx-domain motif [206]. Members of the PDI contain up to four Txs motifs [15, 193]. Another characteristic motif that most of the PDIs harbour is the H/KDEL

ER retrieval signal, or derivatives of the last such as QEDL, KTEL, RTEL etc in different species [468] but this motif is analysed in chapter 3.1.1.3.

1.5 Objectives of project

AGR-2 and AGR-3 enhance colony survival and cell growth of cancer cells but the exact pathway of their oncogenic activity needs to be refined. As AGR-2 and AGR-3 are over-expressed in breast cancers, this thesis examines by molecular biological, immunochemical, and microscopic techniques (i) the localization of each AGR-2/3 protein intracellularly to aid in defining the function of both proteins and whether they compensate for each other (chapters 3 and 4), (ii) developing proof-of-concept peptide-inhibitors towards AGR-2 to determine whether p53 function can be rescued (chapter 5), and (iii) formulate a model that describes potential pathways in which AGR2/3 proteins can mediate their pro-oncogenic effects in cancer (chapter 6). The data demonstrate that AGR-2 and AGR-3 carry out distinct functions in cells based on compartmentalization and that the proteins can have distinct effects on inhibiting the p53-Bax pathways in cancer.

Chapter 2

Materials and Methods

2.1 Reagents and Materials

All chemicals were puschased from Sigma or BDH unless otherwise stated. Tissue culture and other plasticware were obtained from Nunc or TPP.

2.2 Cell culture

2.2.1 Cell lines and cell culture

All cells were kept in a humidified Hera incubator equipped with CO_2 gas cylinders. No antibiotics were used in any of the cell lines.

Cell line	Description	Growth conditions	Culture media
MCF-7	Human, breast adenocarcinoma, Estrogen receptor +/+	5% CO_2, 37 °C	DMEM, 10%FBS
LCC1	Human, breast adenocarcinoma, Estrogen receptor +/+, MCF-7 derived	5% CO_2, 37 °C	Modified DMEM -L-Glu, -Pyruvate, 5% Charcoal stripped FBS*, 1%L-Glutamine
LCC9	Human, breast adenocarcinoma, Estrogen receptor +/+ MCF-7 derived	5% CO_2, 37 °C	Modified DMEM -L-Glu, -Pyruvate, 5% Charcoal stripped FBS*, 1%L-Glutamine
MDA-MB 231*	Human, breast adenocarcinoma, Estrogen receptor -/-	5% CO_2, 37 °C	DMEM, 10%FBS

Table 2.1: Cell lines used. Brief description of their origin, growth conditions and the media used for culturing (*kindly provided by Dr. Hrstka, Czech Republic).

DMEM: Dulbecco-s Minimal Essential Media, containing Puryvate, L-Glutamine, 4500mg/L Glucose and Phenol Red.
ModifiedDMEM: Dulbecco-s Minimal Essential Media, withoutPuryvate, L-Glutamine, Glucose and Phenol Red.
FBS:Fetal Bovine Serum
*Charcoal stripped FBS obtained from LSI

2.2.2 Media and supplements

Media (GIBCO) was supplemented with fetal bovine serum (FBS, GIBCO) at 10%, unless otherwise stated. LCC1 and LCC9 cell lines were grown in DMEM without L-Glutamine and Pyruvate, plus 5% charcoal stripped fetal bovine serum and 1% L-Glutamine to ensure absence of endogenous steroids and growth factors.
No antibiotics were used in any of the cell lines. Media was stored at 4 °C and heated at 37 °C prior to use. Fetal bovine serum and charcoal stripped serum aliquots were kept at -20 °C and thawed at 37 °C prior to use. Trypsin-EDTA, 0.05%, was kept at 4 °C and warmed at room temperature before use.

2.2.3 Subculturing, storage and recovery of cells

Freezind media
Fetal bovine serum supplemented with 10% (v/v) DMSO

Cells were sub-cultured 2-3 times per week in 10cm diameter culture dishes in sterile conditions. The media was discarded and the cells were washed with 10ml sterile PBS. Trypsinization of cells followed with 3ml Trypsin-EDTA solution and incubation for 1-3 minutes at the 37 °C incubator, when the cells start to detach from the dish. Subsequent dilutions, varying from 1:2 to 1:10 depending on the time and

type of the experiment, were applied. The final volume per 10 cm diameter dish was 10ml in any condition. Cells grown in 25-cm diameter dish were cultured in 25ml media whereas cells grown in 100mm diameter dish in 2ml media.

To prepare cells for storage a 10cm diameter culture dish with 80-95% confluent cells was trypsinized as normal and the cells collected were diluted in 10ml finale volume media and centrifuged in sterile Falcon tubes at 1000rpm, 5min, at room temperature. The cell pellet was gently resuspended in ice cold freezing media, 5ml, and transferred to cryotubes (Nunc) at 1ml/tube. The cells were frozen down gradiently in Nalgene^{TM} Cryo freezing containers and then transferred to -80 °C. Twenty-four hours after, the vials were transferred at cryoboxes in liquid nitrogen.
Same conditions applied in cells growing in the 100mm or 25cm culture dishes with the only difference of the volumes added in each step, summarized below:
100mm dish: 1ml Trypsin-EDTA and 1ml media, then centrifuge and resuspend in 2ml freezind media. 1ml of cell/vial.
25m dish: 6ml Trypsin-EDTA and 14ml media, then centrifuge and resuspend in 10ml freezing media. 1ml of cell/vial.

To recover the cells from liquid nitrogen storage, each vial was incubated at the 37°C waterbath till half of the volume is thawed. By pippeting, the rest of the frozen stock was thawed and the cells were transferred in a 100mm diameter culture dish containing fresh media. Cells were left to reach 80% confluency and then transferred to a 10cm culture dish.

2.2.4 Transient transfections

Cells were counted using a Haemocytometre and plated out at 2-4x10^5 cells/well(according to the Lipofectamine^{TM} 2000 (InVitrogen) protocol, into 6-well plates with 2ml of the appropriate medium for each cell line. Cells were incubated overnight at 37 °C, in 10% CO_2 or 5%CO_2 depending on the cell line used, to 90% confluence. DNA/liposome complexes were prepared separately according to the manufacturer's protocol. For each DNA to be transfected 5µg of plasmid DNA ligated to the gene of interest, were diluted in OptiMEM(GIBCO) up to 100µl. The Lipofectamine^{TM} 2000 reagent (InVitrogen) was diluted in OptiMEM as well 1:10 dilution. The Lipofectamine/OptiMEM suspension was combined with the DNA/OptiMEM one. Following a 20min incubation at room temperature, 200µl of the DNA/Lipofectamine were added to each well, and incubated overnight at 37 °C. Cells were harvested after 24h unless otherwise stated. Protocol was adjusted to smaller or larger cell volumes and numbers according to the protocol.

2.3 Microbiological techniques

All microbiological techniques were carried out under aseptic conditions

2.3.1 Growing bacterial cultures

Luria- Bertani (LB) broth

1% (w/v) Tryptone

0.5% (w/v) Yeast extract

1% (w/v) NaCl

Sterilised by autoclaving at 121°C for 20min

Selective antibiotics

Ampicillin (Sigma) at 100µg/ml

Kanamycin (Sigma) at 30µg/ml

Filter-sterilised

3ml LB media containing the appropriate antibiotic was inoculated with a colony of bacteria from a stock plate or from a glycerol stock and incubated for 8h at 37 °C at 225rpm. This starter culture was then transferred to a 250ml LB media plus antibiotic culture at 1:1000 dilution and incubated overnight under the conditions mentioned above. Culture flask capacities were at least 4x the volume of the culture being grown to allow sufficient aeration.

2.3.2 Glycerol stocks

Glycerol stocks of bacterial cells were prepared by adding 125µl of bacterial culture to 875µl of sterile glycerol, 80% v/v, in a cryovial (NUNC) and snap freeze in liquid nitrogen. The cells were then stored at -80 °C.

2.3.3 Agar bacterial culture dishes

LB agar
1% (w/v) Tryptone
0.5% (w/v) Yeast extract
1% (w/v) NaCl
1.5% (w/v) agar powder
Sterilised by autoclaving at 121°C for 20min

LB agar was liquefied by heating in a microwave oven, maximum heat, 5min. The agar was left to cool down at room temperature and when hand-warmed the antibiotic was added and then poured into 90mm diameter Petri dishes (Sterilin) and left to solidify. Prior to use the dishes were left at 37 °C for 1h to dry out. If no transformation followed, the dishes were kept at 4 °C, sealed with parafilm till use and no longer than 3 weeks.

2.3.4 Preparation of competent cells

2.3.4.1 Heat shock method

Transformation buffer I (TFBI)	**Transformation buffer II (TFBII)**
30Mm Potassium acetate	10mM MOPS
100mM RbCl	75mM $CaCl_2$
10mM $CaCl_2$	10mM RbCl
50mM $MnCl_2$	15% (v/v) Glycerol
15% (v/v) Glycerol	
Adjust to pH 5.8 with dilute acetic acid sterilize by filtration	Adjust to pH 6.8 with NaOH and sterilize by filtration

A starter culture of DH5α bacterial cell was set by inoculating 2-3ml LB broth with glycerol stock of bacteria in a 15ml sterile Falcon tube and shake overnight at 37 °C at 225rpm. This culture was diluted 1:200 in LB broth and incubated until OD_{600nm} reached 0.3 (Logarithmic growth phase, Figure 2.1). Cells then were centrifuged at 8000rpm for 5min at 4 °C, the pellet was resuspended in ice-cold TFBI, 16ml TFBI/50ml culture, and the incubated on ice for 30min. After a second centrifuge at 1000rpm, at 4 °C for 5min, the pellet was resuspended in 4ml TFBII and incubated on ice for another 30min. DH5α cells were then snap-frozen in liquid N_2, in 100 µl aliquots and stored at -80 °C till use.

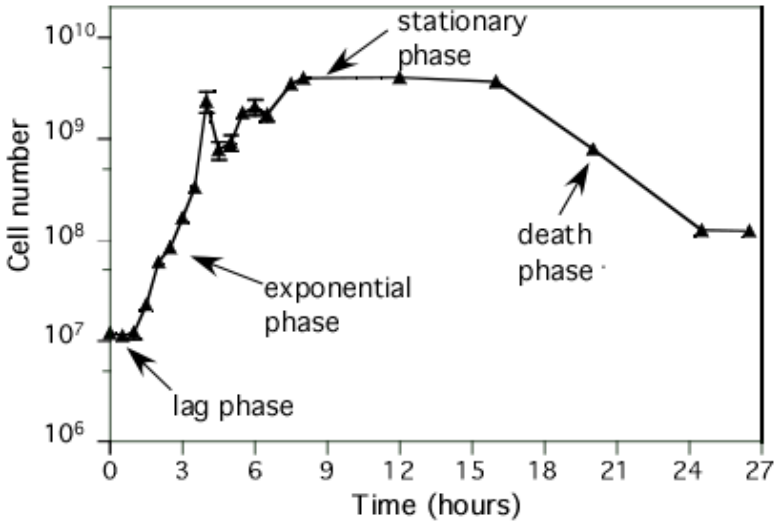

Figure 2.1: Bacterial growth curve. *E.coli* strain K grown in minimal media supplemented with glycose.The four phases of growth are depicted: lag (i), exponential (ii), stationary (iii) and death phase (iv) are shown (chart adapted from *www.bact.wisc.edu*).

2.3.5 Transformation of bacteria

2.3.5.1 Heat shock method

100 µl of competent cells, thawed on ice, were mixed gently with 0.05-0.5µg of the desired plasmid DNA. The cells were incubated on ice for 30min, then heat shocked at a 42°C waterbath for 1.5min and incubated on ice again for an extra 5min. 500µl of sterile LB was added and the cells were left to grow at a 37 °C waterbath for 1h before plating out on LB agar plates containing the selective antibiotic and being left overnight at a 37 °C incubator.

2.3.5.2 KCM method

2YT media	**KCM buffer II (KBII)**
1.6% (w/v) Bacto-Tryptone	100mM KCl
1% (w/v) Yeast extract	30mM $CaCl_2$
0.5% (w/v) NaCl	50mM $MgCl_2$
Adjust to pH 7.0 with NaOH	

Competent cells (100µl) were thawed on ice and 10.05-0.5µg of the desired plasmid DNA was added to 20µl of 5xKBII and sterile H_2O was added up to a final volume of 100µl. Bacterial cells were then added to the diluted DNA mix and incubated on ice for 20min and then at room temperature for another 10min. 1ml of 2YT buffer was added to the mix and the culure was left to grow at a 37 °C water bath for 1h. Cells were then plated out onto an agar plate containing the appropriate antibiotic incubated at 37 °C overnight.

2.4 Plasmid DNA

2.4.1 Amplification of plasmid DNA

A single colony of bacteria containing the plasmid was used to inoculate a 3ml starter LB culture containing the selective antibiotic and incubated at 37 °C at 225rpm for 8h. This culture was then transferred in a 1:1000 dilution in 250ml LB plus antibiotic and left to grow overnight at 37 °C at 225rpm, in a 2L sterile flask.

2.4.2 Purification of plasmid DNA

2.4.2.1 Maxi-prep DNA

DH5α cells from a 250ml culture were collected after centrifuge at 6000rpm/20min at 4 °C (in a Sorvall-spin centrifuge). Plasmid DNA was then isolated and purified using the Qiagen Maxi^{TM} kit according to the manufacturer's protocol. The DNA was resuspended in endotoxin-free TE buffer, unless otherwise specified, and stored at -20 °C.

2.4.2.2 Mini-prep DNA

Cells from a 5ml culture mentioned above, were collected after centrifuge at 6000rpm/20min at 4 °C. Plasmid DNA was then isolated and purified using the Qiagen Mini^{TM} kit according to the manufacturer's protocol. The DNA was resuspended in endotoxin-free TE buffer, unless otherwise specified, and stored at -20 °C.

2.4.3 Quantification of plasmid DNA

2.4.3.1 Spectrometry

Plasmid DNA was diluted in 1:100 in ddH_2O into glass DNA cuvettes and absorbance of DNA at 260nm was measured by spectrometer (DigiLab HitachiU2800). Blank measurements were made by ddH_2O only. Alternatively,

concentration was measured by NanoDrop, by adding 1µl of undiluted DNA and measuring absorbance at 260nm.

2.5 SDS-PAGE

2.5.1 Preparation of cell lysates

2.5.1.1 Cell lysis

Urea lysis buffer
8M Urea
10x Triton
5M NaCl
20mM HEPES, pH 8.0
1M DTT
Buffer prepared prior to use

1% Triton X-100 lysis buffer
50mM HEPES pH 8.0
0.1mM EDTA
150Mm NaCl
1x Protease inhibitor mix
1% (v/v) Triton-X
10mM NaF
2mM DTT

CHAPS lysis buffer
150 mM NaCl,
10 mM HEPES, pH 7.4
1.0% (w/v) CHAPS
1:100 dilution of Protease Inhibitors Cocktail
Buffer prepared prior to use

RIPA lysis buffer
50mM Tris HCL pH 7.5
150mM NaCl
1% Nonidet p40 (IGEPAL)
0.5% sodium deoxycholate
0.1% SDS
1x Protease inhibitor mix
Buffer prepared prior to use

Protease Inhibitor cocktail	**SDS sample buffer (5x)**
Complete mini protease Inhibitor cocktail tablets supplied by Roche	0.25M Tris pH 6.8 10% (w/v)SDS 50% (w/v) Glycerol 0.025% (w/v)Bromophenol blue 0.05M DTT (added just prior to use)

Cells were washed twice with ice old PBS and scraped with 1ml/10cm dish, or 500 µl/100mm dish, PBS into sterile microcentrifuge 1.5ml tubes and then centrifuged at 4000 rpm for 5min at 4 °C. The supernatant was discarded and the pellet was resuspended in lysis buffer, 100 µl/100mm dish or 500 µl/10cm dish, and kept on ice for 30min, exemptions apply to Urea and CHAPS lysis where the incubation time was 1h instead of 30min. After incubation, the cell lysate was centrifuged at 13.000rpm for 15min at 4 °C to precipitate nuclei and non-lysed cells. The supernatant was further processed to protein quantification by Bradford or stored at -20 °C.

2.5.1.2 Subcellular fractionation of proteins

For the subcellular extraction of the cellular compartments the ProteoExtract® Subcellular Proteome Extraction Kit (Calbiochem®) was used. The cells were grown in 6-well plates at a seeding density of 10^6 cells/ml. Twenty-four hours post-transfection the cells were harvested in ice cold 1x PBS and centrifuged at 4000rpm, 4 ^{o}C. The supernatant was discarded and the cell pellet was transferred to new pre-cooled Eppendorf tubes and snap-frozen in liquid N_2 unless processed for fractionation. The protocol followed was the one adjusted for frozen cell pellets according to the manufacturer's instruction. Four different composition buffers ensured high quality cytosolic, membrane, nuclear and cytoskeleton extracts. All

extraction buffers contain protease inhibitors and all steps were carried out at 4 ^{o}C unless stated. All fractions were stored at -80 ^{o}C and analysed by immunoblotting

2.5.1.3 Protein quantification

BIORAD Bradford Reagent was diluted 1:5 in ddH_2O and filter-sterilized. 1µl of each sample was added in 200µl of 1x Bradford into a 96-well plate (NUNC) and incubated at room temperature for 5min. The 96-well plate was then shaken by using an ordinary plate-shaker (Jencons) for less than 1min to allow mix of the samples. The absorbance of the samples at 595nm was measured with the Powerwave XS^{TM} Microplate Spectrophotometer (Biotek) and the exact concentration, µg/µl, according to the Standard curve was calculated by using the KC-Junior programme. The protein standard curve for the Bradford method is created by diluting BSA, 1mg/ml BSA stock solution (≤96% pure grade, A-7638 Sigma) in ddH_2O at a final concentration of 0.5-1-2-4-8 µg/µl, w/v, and measuring absorbance at 595nm.There should be a linear relationship between absorbance and protein concentration.

To determine the protein concentration of urea cell lysates, the BCA^{TM} Assay kit (Pierce, Perbio Science) in a 96-well plate was used. Absorbance at 562nm was measured with the Powerwave XS^{TM} Microplate Spectrophotometer (Biotek) and the exact concentration, µg/µl, w/v, according to the Standard curve, standard concentration samples provided in the kit, was calculated by using the KC-Junior programme.

All samples were measured in triplicates to ensure as minimum deviation as possible.

2.5.2 Preparation of gels and separation of proteins by SDS-PAGE

SDS-Running Buffer 10x

192mM Glycine

25mM Tris

0.1%(w/v) SDS

Transfer buffer 10x

192 mM Glycine

25 mM Tris

20% (v/v) Methanol

10 x Phosphate Buffered Saline (PBS)

1.37 M NaCl

0.1 M Na_2HPO_4

0.027 M KCl

0.018 M KH_2PO_4

adjusted to pH 7.4 with HCl

1x PBS-Tween (PBS-T)

1x PBS

0.1% (v/v) Tween -20

Blocking Buffer 1x

1x PBS-T

5 %(w/v) low fat dry Milk (Marvel)

Stacking gel – 5 % (per 1 ml)

30 % Acrylamide mix* 0.17 ml

1.5 M Tris (pH 6.8) 0.13 ml

10 % SDS 0.01 ml

10 % Ammonium peroxidisulphate 0.01 ml

TEMED (Sigma) 0.001 ml

dH_2O 0.68 ml

Separating gel – 10% (per 5 ml)

30 % Acrylamide mix* 1.7 ml

1.5 M Tris (pH 8.8) 1.3 ml

10 % SDS 0.05 ml

10 % Ammonium peroxidisulphate 0.05 ml

TEMED (Sigma) 0.002 ml

dH_2O 1.9 ml

Separating gel – 15 % (per 5 ml)
30 % Acrylamide mix* 2.5 ml
1.5 M Tris (pH 8.8) 1.3 ml
10 % SDS 0.05 ml
10 % Ammonium peroxidisulphate 0.05 ml
TEMED (Sigma) 0.002 ml
dH_2O 1.1 ml

* Acrylamide mix (National Diagnostics; Ultrapure Protogel) consists of 30 % (w/v) acrylamide and 0.8 % (w/v) bis-acrylamide.

SDS-polyacrylamide gels, 10% or 15%, were prepared in glass plates cleaned with 70% ethanol. The separating gel was left to polymerise at room temperature overlaid with water to straighten the top of it. The water was then removed and the stacking gel was added along with a equivalent comb, 10- or 15- well and 0.75mm or 1.5mm thickness size, respective to the number and amount of the samples to be assayed. After polymerization, the combs were removed and the glass plates with the gels were adjusted in the appropriate tank filled with 1x SDS running buffer.
SDS sample buffer (5x) was added to the lysates, 10-20μg of total protein,the mixtures were spinned at 13.000rpm for 1min and heated up to 95°C in a thermal block for 1min immediately prior to loading. 5μl of pre-stained protein standards, low range or high range (Biorad) depending on the protein sizes and gel type, were loaded in the first lane as size markers. Electrophoresis separation was performed at 100V for 60-90min till the bromophenol blue dye reached the end of the gel.

2.5.3 Detection of separated protein

2.5.3.1 Immunoblotting

ECL Solution 1	**ECL Solution 2**
100 mM Tris pH 8.5 2.5 mM Luminol 0.4 mM p-coumaric acid	100 mM Tris pH8.5 0.02 % (v/v) H_2O_2

Following electrophoresis on the SDS-PAGE gel, proteins were transferred to nitrocellulose membranes (Hybond-C, Amersham) in tanks filled with transfer buffer and ensuring low temperature by ice-blocks present in the tank. Electroblotting was performed at 300mA for 100min. After transfer protein blots were ink stained (Pelikan) and washed 3x with PBS-T for 5min to remove excess ink. Membranes were then blocked by washing in PBS/0.1% Tween-20/+5% (w/v) milk (dried skimmed, Marvel), at room temperature on an orbital shaker for 1h. The primary antibody was added and diluted in 5% milk in PBS-Tween (0.1% v/v), and incubated overnight at 4 °C (Table 2.2). Following 3x5min washes in PBS-Tween, the appropriate secondary antibody conjugated to horse radish peroxidase was added and the blot was incubated for 1h at room temperature (RT). Blots were then washed 4x15min in PBS-Tween and visualized by enchanced chemiluminesence (ECL). Membranes were covered in ECL 1+2 (1:1 v/v ratio), left at room temperature for 3min and after removal of excess ECL by tissue, exposed to Hyperfilm for the appropriate time (Kodak) and then developed (Mediphot 937).

2.5.3.2 Immunobloting of phosphorylated antibodies

According to the manufacturer's protocol (Cell Signalling).

2.5.3.3 Coomassie brilliant blue staining

Destain 1

50 % (v/v) Methanol

10 % (v/v) Acetic acid

Coomassie brilliant blue stain

50 % (v/v) Methanol

10 % (v/v) Acetic acid

0.2 % (w/v) Coomassie Blue R-250

Destain 2

7.5 % (v/v) Methanol

10 % (v/v) Acetic acid

Gels were transferred to a dish containing Destain 1 for >5min and then placed into another dish containing Coomassie Blue Stain. The duration of the staining procedure depended on the strength of the staining required (5min to 12h) and in some cases the stain was preheated to 45 ºC to increase staining even further. Gels were then placed in a dish containing Destain 2. A folded tissue was used to absorb excess dye and Destain 2 was renewed as needed. Destaining was performed until the bands became visible and the background staining was removed. Gels were air-dried in between DryEase MiniCellophane^{TM} sheets (Invitrogen) in a DryEase GelDrying^{TM} system (Invitrogen).

2.5.3.4 Stripping nitrocellulose membranes

Antibodies bound to membranes were removed by stripping the blots with 0.1N NaOH, when blots needed to be reprobed for similar size proteins or with antibodies raised in the same species. Blots were first washed with H_2O for 5min at room temperature and then with PBS-T for 5min. 0.1N NaOH was added to the blots for 10min on a orbital shaker. The membranes were then washed 3x in PBS-T for 3min each lapse and blocked in 5%milk in PBS-T for 1h before adding the primary antibody diluted in 5%milk+PBS-T as normal.

kDa	Antibody	Type	Company	Dilution
50	β-actin	Mouse monoclonal	Sigma	1:4000
53	p53 DO1	Mouse monoclonal	Moravian Biotechnologies	1:1000
53	p53 DO12	Mouse monoclonal	Moravian Biotechnologies	1:1000
53	p53 P-Ser^{15}	Mouse polyclonal	Cell signalling	1:1000
21	Bax	Mouse monoclonal	InVitrogen	1:1000
20	Bid	Mouse monoclonal	InVitrogen	1:1000
21	Bcl-2	Mouse monoclonal	InVitrogen	1:1000
20	Bax 6A7	Mouse monoclonal	InVitrogen	1:1000
16	Cytochrome c	Mouse monoclonal	Calbiochem	1:1000
20	AGR-2	Mouse monoclonal	Abnova	1:1000
19	AGR-3	Mouse monoclonal	Moravian Biotechnologies	1:1000
70	Hsp70	Mouse monoclonal	Stressgen	1:1000
17	LC3	Mouse monoclonal	Cell Signalling	1:500
116/89c	PARP	Mouse monoclonal	Cell Signalling	1:1000
	HA	Mouse monoclonal	Sigma	1:1000
-	FLAG	Mouse monoclonal	Sigma	1:1000

Table 2.2 List of antibodies for immunoblotting.

2.6 DNA amplification

2.6.1 Polymerase chain reaction

2.6.1.1 Primer design

A primer is a short synthetic oligonucleotide which is used in many molecular techniques from PCR to DNA sequencing. These primers are designed to have a sequence which is the reverse complement of a region of template or target DNA to which we wish the primer to anneal. Primers for the amplification of the AGR-2 gene (NCBI accession number NM_006408), from a DNA template, AGR-2 in pDEST 3.2, were designed with a length of 39-40bp recognizing the start and the end of the gene (Figure 2.2, Table 2.3). Restriction enzyme recognition sites were integrated in the 5' of each of the primers to enable ligation to the desired vectors, AcGFP-N_1 and DsRed Express N_1. The primers had a melting temperature of 76-82°C and a G+C content between 46-50% of the total primer sequence. No primer dimers were formed according to the Sigma-Aldrich primer design tool (*www.sigmaaldrich.com*). Last but not least, all the primers started (5') with a GC to increase the efficiency of priming and were PAGE- purified. Extra bases were integrated where required to keep the gene in frame.

The same reverse primer was used for the *wt* gene amplification whereas different reverse primers were used for the KTEL deletion (Δ_{KTEL}) and the KDEL mutants (T-D mutation). To sum up, at the end of the amplification 6 fragments were amplified: mature AGR-2_{wt}, full length AGR-2_{wt}, mature AGR-2_{KDEL}, full length AGR-2_{KDEL}, mature AGR-$2_{\Delta KTEL}$, full length AGR-$2_{\Delta KTEL}$. Each one of them was subcloned into the AcGFP-N_1 and DsRed ExpressN_1 vectors.

```
 1     atggagaaaa  ttccagtgtc  agcattcttg  ctccttgtgg  ccctctccta
cactctggcc
61     agagatacca  cagtcaaacc  tggagccaaa  aaggacacaa  aggactctcg
acccaaactg
121   ccccagaccc  tctccagagg  ttggggtgac  caactcatct  ggactcagac
atatgaagaa
181   gctctatata  aatccaagac  aagcaacaaa  cccttgatga  ttattcatca
cttggatgag
241   tgcccacaca  gtcaagcttt  aaagaaagtg  tttgctgaaa  ataaagaaat
ccagaaattg
301   gcagagcagt  ttgtcctcct  caatctggtt  tatgaaacaa  ctgacaaaca
cctttctcct
361   gatggccagt  atgtccccag  gattatgttt  gttgacccat  ctctgacagt
tagagccgat
421   atcactggaa  gatattcaaa  tcgtctctat  gcttacgaac  ctgcagatac
agctctgttg
481 cttgacaaca tgaagaaagc tctcaagttg ctgaagactg aattgtaa
```

Figure 2.2: The AGR-2 cDNA sequence (NCBI NM_006408). The leader sequence is highlighted in red. The mature form of the protein contains no leader sequence and starts from site 61aga whereas the full length form starts from the 4gag site. The KTEL encoding sequence is highlighted in blue at position 517act.

Primers for the N-terminal Fluorescent vectors

Name	T_m	Restriction enzyme	Sequence
mAGR2 forward	81.8°C	*XhoI*	GCAAGG *CTCGAG* **ATG AGA GAT ACC ACA GTC AAA CCT GGA**
AGR2*wt* reverse	77.3°C	*EcoRI*	GCAAGG *GAATTC* **CAA TTC AGT CTT CAG CAA CTT G**
flAGR2 forward	79.1°C	*XhoI*	GCAAGG *CTCGAG* **ATG GAG AAA ATT CCA GTG TCA**
KTEL deletion reverse	76.2°C	*EcoRI*	GCAAGG *GAATTC* **CAG CAA CTT GAG AGC TTT C**
KDEL reverse	78.2°C	*EcoRI*	GCAAGG *GAATTC* **CAA TTC *ATC* CTT CAG CAA CTT G**

Table 2.3: AGR-2 primers. Highlighted in bold are AGR-2 codon sequences whereas in italics are the restriction enzyme recognition sites.

2.6.1.2 Hot-start Taq polymerase amplification

PCR Master mix/reaction	**Cycling conditions**
1xPCR buffer (Qiagen)	Taq activation:95°C for 15min,
1mM dNTPs (Promega)	Denaturation:95°C for 30sec,
0.5mM $MgCl_2$(Qiagen)	Annealing: 53.6°C for 30sec,
0.1μM forward and reverse primers	Elongation:72°C for 1min
5% (v/v) DMSO	Cycle to step 2 x30 times,
1μg DNA template	72°C x 5min.
HotstarTaq™ DNA polymerase	4 °C for t_∞
5units/reaction (Qiagen)	
ddH_2O up to a final volume of 50 μl	

In order to ensure maximum yield of amplification for each product, different annealing times, varying from 50-70°C, along with elongation times between 30sec-3min, were tried. Different concentration of $MgCl_2$ and DMSO covering a range between 0.1-3mM and 1-10% (v/v) per reaction respectively, ensured maximum primer efficiency. 100ng of DNA template were used as initial concentration.

2.6.1.3 PFU polymerase reaction

The reason for trying PFU® Turbo amplification was that unlike *Taq* DNA polymerase, highly thermostable *Pfu* DNA polymerase possesses 3' to 5' exonuclease proof-reading activity that enables the polymerase to correct nucleotide-misincorporation errors. This means that *Pfu* DNA polymerase-generated PCR fragments will have fewer errors than *Taq*-generated PCR inserts. All reactions performed in a DNA Engine Dyad™ machine.

PCR Master mix/reaction

1x cloned PFU® buffer (Stratagene)
1mM dNTPs (Promega)
0.5mM $MgCl_2$ (Qiagen)
0.1µM forward and reverse primers
5% (v/v) DMSO
1µg DNA template
PFU® Turbo DNA polymerase 2.5 units/reaction (Stratagene)
ddH_2O up to a final volume of 50 µl

Cycling conditions

Taq activation:95°C for 15min,
Denaturation:95°C for 30sec,
Annealing: 53.6°C for 30sec,
Elongation:72°C for 1min
Cycle to step 2 x30 times,
72°C x 5min.
4 °C for t_∞

2.6.1.3 PFU Turbo polymerase amplification

PfuTurbo® properties list

- Ideal for high-fidelity amplification
- 3'-5' exonuclease activity provides a low error rate
- One of the most thermostable DNA polymerases known
- Lack of extendase activity means no unwanted 3' overhangs
- Optimal for blunt-end PCR cloning
- Optimum temperature near 75°C
- 95% active after 1-hour incubation at 98°C

2.6.2 Site Directed Mutagenesis

2.6.2.1 Primer Design

To mutate specific tyrosines to phenylalanines, the QuickChange mutagenesis XL kit (Stratagene) was employed according to the manufacturer's instructions. Primers were designed according to the guidelines laid out in the QuickChange™ Site

Directed Mutagenesis Kit Manual (Stratagene) (Table 2.4). Oligonucleotides were purchased from Sigma-Genosys, PAGE purified and reconstituded in sterile dd H_2O. The Quick Change Site Directed mutagenesis kit was used in order to reconstitute the original *wt* form of the AGR-2 DNA and correct the mutations integrated from the PCR reaction, referring to simple aminoacid substitutions or in frame reconstitution of the gene. Starting with two antiparallel primers carrying codons for the required substitutions (purchased from InVitrogen), vectors containing AGR2 DNA were PCR-amplified by *Pfu* DNA polymerase according to the manufacturer's protocol. The incorporation of oligonucleotide primers generates a mutated plasmid containing staggered nicks.

Name	**T_m**	**Sequence**
Forward wt AGR2 Inframe	82°C	AAG TTG CTG AAG ACT GAA TTG **CGA** ATT CTG CAG TCG ACG
Reverse wt AGR2 Inframe	82°C	CGT CGA CTG CAG AAT **TCG** CAA TTC AGT CTT CAG CAA CTT
Forward Δ_{KTEL} AGR2 Inframe	81.9°C	AAA GCT CTC AAG TTG CTG **CGA** ATT CTG CAG TCG ACG
Reverse Δ_{KTEL} AGR2 Inframe	81.9°C	CGT CGA CTG CAG AAT **TCG** CAG CAA CTT GAG AGC TTT
Forward KDEL AGR2 Inframe	82.8°C	AAG TTG CTG AAG GAT GAA TTG **CGA** ATT CTG CAG TCG ACG
Reverse KDEL AGR2 Inframe	82.8°C	CGT CGA CTG CAG AAT **TCG** CAA TTC ATC CTT CAG CAA CTT
Forward KTEL-KAEL AGR2	80.8°C	CTC AAG TTG CTG AAG **GCT** GAA TTG CGA *ATT* CTG CAG
Reverse KTEL-KAEL AGR2	80.8°C	CTG CAG AAT TCG CAA TTC **AGC** CTT CAG CAA CTT GAG
Forward AGR2_AAC-AGC	73.7°C	C TA TAT AAA TCC AAG ACA AGC ***AAC*** AAA CCC TTG ATG ATT ATTC

Reverse AGR2_AAC-AGC	73.7°C	GAAT AAT CAT CAA GGG TTT ***GTT*** GCT TGT CTT GGA TTT ATA TAG
Forward Aptamer stop	84.9°C	CAT CTG CCG ACG ***TGA*** ATT TAT TAT GGT CCG CCG GGG
Reverse Aptamer stop	84.9°C	CCC CGG CGG ACC ATA ATA AAT ***TCA*** CGT CGG CAG ATG
Forward Aptamer 22Y-A	89.9°C	CTG CCG ACG ACG ATT TAT ***GCT*** GGT CCG CCG GGG TGA
Reverse Aptamer 22Y-A	89.9°C	TCA CCC CGG CGGACC ***AGC*** ATA AAT CGT CGT CGG CAG

Table 2.4: Site-Directed mutagenesis primers. Muatted sequences are shown in bold.

2.6.2.2 Site Directed mutagenesis reaction

The QuickChange mutagenesis XL kit (Stratagene) was employed according to the manufacturer's instructions. The 68°C step was adjusted to the size of the plasmid-to-be amplified and the number of cycles was 16 for a single amino acid change or 18 for multiple amino acid changes.

2.6.2.3 *DpnI* digestion

The product was then digested with *Dpn I* endonuclease, specific for methylated and hemimethylated DNA, hence the parental DNA template was digested (since DNA originating from *E. coli* is usually *dam* methylated). The nicked vector DNA carrying the desired mutations was proliferated in *Epicurian coli* XL1-Blue supercompetent

cells (Stratagene). Plasmid DNA was isolated (using Qiagen High Speed kit) and sequenced.

2.6.3 DNA Sequencing

2.6.3.1 Primer design

Sequencing primers were designed with a length of around 20-30 bp spaced over the MCS of each vector and a melting temperature of around 65.8-70°C. The oligonucleotides were HPLC purified (Sigma-Aldrich) and reconstituted in sterile ddH_2O (Table 2.5).

Name	**T_m**	**Sequence 5'-3'**
Forward AcGFP-N_1	63.1°C	AAAATCAACGGGACTTTCCA
Reverse AcGFP-N_1	70°C	GCCGCTCACGCTGAACTTGT
Forward DsRed Express-N_1	65.8°C	TTTGTTTTGGCACCAAAATCAA
Reverse DsRed Express-N_1	67.9°C	TGAAGCGCATGAACTCCTTGAT3'

Table 2.5: DNA sequencing primers.

2.6.3.2 Sequencing analysis

Sequencing reaction

20ul of each primers (10uM)

5ul of DNA isolated by Qiagen Maxi™ kit or

10ul DNA isolated by Qiagen Mini™ kit

The DNA template along with the primers was sequenced in the Medical Research Council- Human Genetics Unit by experienced researchers (MRC-HGU, IGMM centre, University of Edinburgh).

2.6.4 PCR purification of amplified DNA

The PCR products designated to sub-cloning into different vectors were purified immediately after amplification using the QIAquick PCR purification kit (Qiagen) to ensure removal of primers, nucleotides, enzymes, mineral oil, salt and other impurities from DNA samples

2.6.5 Annealing of single strand oligos for aptamer construction

Single-strand Oligos (Sigma-Genosys), dissolved into nuclease free water (Promega) into a final concentration of 100μM, were mixed, forward and reverse oligo, and 2μM of each was diluted in 10mM Tris-HCl, pH6.8. The mixture was heat-shocked at 85°C for 10min, cooled to room temperature for 1h, incubated at 37°C for 15min for the oligos to anneal and left at room temperature for another 10min. The concentration of the final annealed double-strand oligo was determined by spectrometry at 260nm (Digilab Hitachi). Annealing efficiency was tested by

polyacrylamide gel electrophoresis and annealed oligos were digested and cloned into the appropriate vector, as described.

2.7 Agarose and polyacrylamide gel electrophoresis for DNA

2.7.1 Agarose gel electrophoresis of DNA fragments above 300bp

50x TAE (Tris-Acetate EDTA)
2M Tris pH 6.8,
0.1M $Na_2EDTA.2H_2O$
4% Acetic acid (v/v)
Adjust pH to 8.5

6x DNA loading buffer
0.25% Bromophenol blue (w/v)
0.25% Xylene cyanol (w/v)
15% Ficoll 400 (w/v)

TAE buffer was diluted (50x) to 1x and 1% (w/v) ultrapure agarose was added. The solution was heated in a microwave oven until the agarose is completely dissolved and left to cool down to handwarm under the hood. Ethidium Bromide EtBr was added to a final concentration of 5% (w/v). The solution was then poured into a horizontal electrophoresis gel tray with a 10-well or bigger comb inserter and left to solidify. When solid, the agarose gel was submerged in a horizontal electrophoresis tank filled in 1xTAE buffer. DNA loading buffer (6x) was added to the samples (3μl of site-directed mutagenesis DNA or 10μl of PCR amplified DNA) to 1x and then loaded onto the gel. 1kb DNA ladder was also loaded at 5μl volume. Electrophoresis at 100V at room temperature followed till adequate separation was achieved and then the bands were visualized by UV light using a CHEMI Genius^2 BioImaging System^{TM} (Syngene) and the Genesnap^{TM} tool with an ethidium bromide filter and transilluminator. The images were captured with a Sony UP-D895MD.

2.7.2 Polyacrylamide gel electrophoresis of small DNA fragments

10x TBE (Tris-Acetate EDTA)
2M Tris pH 6.8,
0.1M $Na_2EDTA.2H_2O$
4% Acetic acid (v/v)
Adjust pH to 8.5

50% polyacrylamide gel
50% polyacrylamide (v/v)
50% 1xTBE (v/v)
300 µl Ammonium Pelsulfate (APS)
10 µl TEMED

17% polyacrylamide gel
17% polyacrylamide (v/v)
83% 1xTBE (v/v)
300 µl Ammonium Pelsulfate (APS)
10 µl TEMED

Polyacrylamide gels have smaller pore sizes than agarose gels and allow precise separations of molecules from 10–1500bp. Due to the small size of the aptamers, the agarose gel was no option and for that reason a polyacrylamide gel approach was adopted. The 50% polyacrylamide gel was poured first and left to become solid in vertical glass plates. The 17% gel was poured above the 50% and 15-well comb was inserted and left to become solid. When solid, the gel was submerged in a vertical electrophoresis tank filled in 1xTBE buffer. DNA loading buffer (6x) was added to the samples (1µl of DNA diluted in 20µl ddH_2O) to 1x and then loaded onto the gel. 100bp DNA ladder(Biorad) was also loaded at 3µl/lane volume. Electrophoresis at 110V at 4 °C for 6h followed till adequate separation was achieved. The gel was then washed in 1x TBE supplemented with 5% EtBr for 6h. The bands were visualized by UV light using a CHEMI $Genius^2$ BioImaging System^{TM} (Syngene) and the Genesnap^{TM} tool with an ethidium bromide filter and transilluminator. The images were captured with a Sony UP-D895MD.

2.8 Restriction enzyme digestion and ligation

2.8.1 Restriction enzyme digestion

Single Restriction enzyme reaction
1xNEB/Roche buffer (1:10 v/v) supplemented with
100μg/ml Bovine Serum Albumin (BSA, New England Biolabs) where required
1μg of DNA
1unit of restriction endonuclease

Double Restriction enzyme reaction
1xNEB/Roche buffer (1:10 v/v) supplemented with
100μg/ml Bovine Serum Albumin (BSA, New England Biolabs) where required
2μg of DNA
1unit of each restriction endonuclease

Negative Restriction enzyme reaction
1xNEB/Roche buffer (1:10 v/v) supplemented with
100μg/ml Bovine Serum Albumin (BSA, New England Biolabs) where required
1μg of DNA
no restriction endonuclease

Restriction enzyme digestion of the vector and the DNA-insert is required after PCR amplification. The restriction endonucleases recognize specific sequences to digest. As far as the insert is concerned the adequate restriction enzymes were chosen according to the Multiple Cloning Site (MCS) of the vector to be inserted in. The DsRed-Express N_1 and the AcGFP-N_1 plasmids have an identical MCS and so the mature and full length wt and mutants AGR-2 fragments contained the same *EcoRI/XhoI* sites on the 5'-3' end respectively (Table 2.6).
Single, containing only one of the enzymes, and double, with both of the enzymes, reactions were performed in the vector. The single restriction enzyme reaction ensured the functionality of the enzyme as the linear DNA runs slower than the

circular when electrophorised onto a 1% agarose gel. Most of the enzymes used were purchased from NEB and the maximum efficiency buffer (1, 2, 3 or 4) was chosen according to the NEBbuffer chart *(www.neb.com)*. When enzymes from different companies needed to be used, the compatibility of the buffers was compared according to their composition. When *EcoRI* (NEB) was combined with *XhoI* (Roche) the buffer from Roche was used which had the same composition as buffer 1 from NEB. Incubation times at 37 °C varied between 1-16h.

Restriction endonuclease	**Company**	**Recognition site**	**Activation temperature**
BamHI	New England Biolabs	5′...G▼GATCC...3′ 3′...CCTAG▲G...5′	37 °C
BglII	New England Biolabs	5′...A▼GATCT...3′ 3′...TCTAG▲A...5′	37 °C
EcoRI	New England Biolabs	5′...G▼AATTC...3′ 3′...CTTAA▲G...5′	37 °C
EcoRV	New England Biolabs	5′...GAT▼ATC...3′ 3′...CTA▲TAG...5′	37 °C
DpnI	New England Biolabs	CH_3 5′...GA▼TC...3′ 3′...CT▲AG...5′ CH_3	37 °C
XhoI	Roche	5′...C▼TCGAG...3′ 3′...GAGCT▲C...5′	37 °C

Table 2.6: Restriction enzymes.

2.8.2 DNA gel purification

After incubation at 37°C, the entire DNA was run on a 1%, w/v, agarose gel in TAE buffer supplemented with 5% EtBr, after diluting it in 1x DNA loading buffer (6x).

Low temperature melting agarose (Sigma) was used for electrophoresis. The gel was then run at 100V for 1h and the bands were visualized and excised under UV light (Flowgen). The resulting agarose fragments containing the digested DNA were transferred to sterile Eppendorf 1.5ml tubes and weighed. The Gel Extraction kit (Qiagen) was used to extract and purify the digested DNA.

2.8.3 Dephosphorylation of recessed 5'ends or blunt ends

Dephosphorylation reaction	**Formula for the amount of CIAP needed**
1x Alkaline Phosphatase Calf Intestinal (CIAP) buffer (10x, Promega) CIAP (0.5U/pmols of ends, Promega) Digested DNA Sterile H_2O up to 100μl	$\frac{\mu g \text{ of vector to be phopshorylated} \times 3.04}{\text{size of vector (Kb)}}$

Dephosphorylation is the essential process of removing phosphate groups from an organic compound (as ATP) by hydrolysis. The opposite process is phosphorylation. Dephosphorylation of a DNA template, usually a vector plasmid, is essential when it comes to ligating a phosphorylated digested insert to a digested vector, as it increases the ligation ability of each other. After addition of the phosphatase, the reaction was incubated at a 37 °C waterbath for a time of 15min and then at 56 °C heated stage for another 15min. A second aliquot of the enzyme was added (0.5U/pmols of ends) and the incubation times at both temperatures were repeated. The higher temperature ensures accessibility of the recessed end. 0.5M EDTA, pH8.0, was used to stop the reaction. Unless processed to ligation directly the sample was stored at -20 °C for further application.

2.8.4 Ligation of DNA in the appropriate vector

2.8.4.1 Ligation of DNA in the appropriate vector

Ligation reaction	**Formula for the vector:insert ratio**
1x Ligation Buffer (10x Promega) 10-100ng vector DNA xng insert 10units of T_4 ligase (10u/ μl , Promega) ddH_2O up to 10μ	$\frac{\mu g \text{ of vector} \times \text{size of insert (Kb)}}{\text{size pf vector (Kb)}} \times \text{ratio } \frac{\text{insert}}{\text{vector}}$

After digestion the vector plasmid and the DNA-insert were ready to be ligated. The above reaction was incubated at 4 °C in Eppendorf tubes, overnight. For each ligation different ratios insert:vector were applied each time, varying between 1:1 and 5:1, according to the size of the insert when compared to the vector.

2.8.4.2 Transformation of the ligated mixture into competent cells

After ligation 1-10μl of the mixture was added to 100μl of DH5α cells or 20-50μl XL-Blue supercompetent cells (Stratagene) and the heat-shock transformation method was applied. The transformed bacteria were then plated out in LB-agar plates bearing the selective antibiotic for each plasmid and incubated overnight at 37°C.

2.9 Co-immunoprecipitation assay

IP Wash buffer A
1%NP40
25mM Tris pH.7
0.4M KCl
Keep at 4 °C

IP Wash buffer B
0.1% NP40
25mM Tris pH.7.5
150mM KCl
Keep at 4°C

IP Lysis buffer
IP Wash Buffer A
1M DTT (7µl per 7ml buffer),
1 tablet protease inhibitor (per 7ml lysis buffer)

Protease Inhibitor cocktail
Complete mini protease Inhibitor cocktail tablets supplied by Roche

Cells were cultured for 24h, in a 10cm plate at 37 °C until reached 80-95% confluence. Twenty-four hours post-plating, the cells were rinsed twice with 10ml sterile ice cold 1xPBS, and harvested in 1ml sterile ice cold PBS. The eluate was then centrifuged at 13000rpm, 4 °C and the pellet was resuspended in IP Lysis buffer (500µl/10cm dish). The suspension was incubated at 4 °C for 30min on a rotary shaker and following centrifugation at 13000rpm, snap frozen in liquid N_2 unless processed for co-immunoprecipitation on the same day. 30µl of Protein G Fast Flow beads (SantaCruz) per reaction were washed 5x in IP wash buffer B, at 4 °C with rotation and centrifuged at 3000rpm for 1min each time and in the final step resuspended in 50µl IP Wash buffer B. 500µg -1mg of protein, as measured by Bradford method, were incubated overnight at 4 °C with 1ml IP Buffer B plus 1M DTT and protease inhibitors in the presence of 50µl of beads (SantaCruz) and 2µl of the appropriate primary antibody. The protein plus beads-primary antibody complex was recovered by centrifugation for 1min at 13000rpm and washed 6x with 1ml IP Wash buffer B buffer on a rotary shaker. The third time wash was for 15 min instead of 5 min and the last centrifuge was at 13000 rpm instead of 6000rpm. The pellet was

resuspended in 75µl of sample buffer (5x) containing DTT. Samples were boiled at 90 °C for 1min prior to SDS-PAGE analysis.

2.10 Fluorescence analysis

2.10.1 Immunofluorescence analysis

2.10.1.1 Antibodies for fluorescent microscopy

Antibody	Specificity	Type	Dilution	Company
Anti-PDI	PDI protein, ER marker	mouse monoclonal	1:1000	Abcam
Anti-Golgin	Golgin protein, Golgi marker	mouse monoclonal	1:500	Abcam
Anti-AGR2	AGR-2 protein	mouse monoclonal	1:1000	Abnova
Anti-AGR3	AGR-3 protein	mouse monoclonal	1:1000	Moravian Biotechnologies
Anti-HA	HA epitope tag	mouse monoclonal	1:1000	Sigma
Anti-FLAG	FLAG epitope tag	mouse monoclonal	1:5000	Sigma

Table 2.7: Primary antibodies list for immunofluorescent microscopy.

Antibody	Specificity	Excitation colour
Alexa 594	Goat anti-mouse	red
Alexa 488	Goat anti-mouse	green

Table 2.8: Secondary antibodies list. All antibodies were Alexa conjugated, Molecular Probes, InVitrogen.

2.10.1.2 Immunofluorescence analysis for endogenous proteins

Wash buffer

1x PBS

0.01% Tween-20

Fixatives

4% Parafolmadehyde (w/v) or

100% Methanol (v/v) or

1: 1 Methanol: Acetone (v/v)

Permeabilization buffer

1x PBS

0.5% Triton-X100 (v/v)

Freshly prepared each time

Antibody solution

1% Bovine Serum Albumin (w/v)

1x PBS

Filter sterilized

Stored at 4°C

Blocking solution

3% BSA (w/v)

1x PBS

Filter sterilized

Stored at 4 °C

Cells were seeded at a density of $0.13x10^6$ cell/ ml and plated in sterile four-chambered slides (NUNC). Twenty-four hours post-plating the medium from the cells was removed and the slides were washed 2x in sterile PBS. 4% PF, 200µl/per chamber, was added for 15min as a fixative and 3x washes in sterile 1x PBS followed. Cells were also fixed in ice cold methanol or a mixture of methanol:acetone (1:1, v/v) for 5min, and air-dried in order to specify the optimal fixing method. This fixation method does not require a permeabilization step. Parafolmadehyde fixed cells were permeabilised in freshly prepared 0.5% (w/v) TritonX-100 in 1xPBS, and slides were washed 3x with 1x PBS for 10min. Following washes with 1x PBS, nonspecific sites were blocked for 1h with 3% (w/v) BSA/PBS in room temperature under shaking. After 3 washes in 1xPBS, the plastic chambers from each slide were removed by forceps and cells were incubated

overnight with the primary antibody diluted in 1% (v/v) BSA/PBS at 4 °C (200µl/chamber). Different antidoby dilutions were used in order to define the best concentration that ensured low background staining and higher epitope binding.
Twenty-four hours post-incubation, the slides were washed 5x in 0.1% (v/v) PBS-Tween and incubated with the secondary antibody conjugated to Alexa for 30min at room temperature (200µl/chamber). After the secondary antibody incubation cells were washed 3x in 0.1% (v/v) PBS-Tween and the cells were mounted with Fluorescent Mounting Media (DakoCytomation) under a 1.5mm glass coverslip (LabTek)

2.10.1.3 Immunofluorescence analysis for transfected proteins

Same protocol as 2.10.2.2 followed with the only modification in the transfecting step. Transfections were performed with the Lipofectamine reagent (InVitrogen). Cells were seeded at a density of $0.13x10^6$ cell/ml and plated in sterile four-chambered slides (NUNC). Twenty-four hours post-plating the growth media from the cells was removed and fresh media was added. Cells were transfected with 1µg/ml total DNA. In co-transfections, 0.5µg/ml DNA along with 0.5µg/ml pDEST 3.2 control DNA was added to ensure a total amount of 1µg/ml per chamber. The slides were then processed as described previously.

2.10.2 Nuclear staining for fluorescent microscopy

2.10.2.1 Epifluorescence microscopy nuclear staining

DAPI or 4', 6-diamidino-2-phenylindole is a fluorescent stain that binds strongly to DNA. Since DAPI will pass through an intact cell membrane, it was used to stain fixed cells (4% parafolmadehyde, ethanol/acetone fixed). DAPI is excited with ultraviolet light (UV). When bound to double-stranded DNA its absorption

maximum is at 358nm and its emission maximum is at 461nm. This emission is fairly broad, and appears blue/cyan. DAPI will also bind to RNA, though it is not as strongly fluorescent. Its emission shifts to around 500nm when bound to RNA Apart from labelling cell nuclei, the most popular application of DAPI is in detection of mycoplasma or virus DNA in cell cultures.
At the last step before mounting the fixed cells, DAPI stain was added to the DAKO Cytomation mounting media at a concentration of µl per 1ml media. No incubation time was required and the slides were ready for observation immediately.

2.10.2.2 Confocal fluorescence microscopy nuclear staining

TO-PRO 3 stain is a useful counterstain and dead cell indicator, with long-wavelength red fluorescence, excites at 633nm, easily distinguished from fluorescein and rhodamine fluorescence.
TOPRO 3 solution (1mM, InVitrogen) was diluted 1:1000 in 37°C pre-warmed PBS and added to each chamber of the slide, at approximately 200µl per chamber. The slides were then incubated at a 37°C dark incubator and washed 3x in PBS-T, room temperature warm, each for 5min, on a vertical shaker. The PBS was then discarded and the slides were mounted with DAKO Cytomation mounting media. Unless directly processed to imaging, the slides were kept at 4°C, covered in foil to ensure no light conditions and fading of the signal.

2.10.2.3 Live cell imaging nuclear staining

mCherry (kan^R) plasmid pBS34 (kindly provided by Dr. Lierres, University of Dundee) was added to the cells at the 37 °C incubator under normal Lipofectamine transfection conditions and cells visualised by LEICA SP5 confocal microscope.

2.10.3 Live cell imaging analysis

Cells designated to live cell imaging analysis were directly grown at 4-chamber glass slides (NUNC) after seeded at a density of $0.13x10^6$ cell/ ml. Twenty-four hours post-plating, CO_2 independent growing media (GIBCO), containing no phenol red was added to the cells and slides were adjusted to an inverted Leica SP-5 confocal microscope (Leica), equipped with a temperature controlled chamber. Distribution and localization of the protein of interest was exported and analysed as AVI file by the Leica Application Suite software.

2.11 ELISA analysis

AGR-2 and AGR-3 peptides were coated in a 96-ELISA plate in 0.1M $NaHCO_3$ (pH 8.6) and incubated overnight at 4 °C. Templates were washed 6x PBS-T (0.1%) in a final volume of 200µl/well and blocked by 4% BSA/PBS-T (w/v) for 1h on a rotary shaker. Primary antibodies diluted in 3% BSA/PBS-T (1:1000, v/v) were added and incubated at 4 °C overnight. The plate was then washed 6x PBS-T (0.1%) in a final volume of 200µl/well and HRP-conjugated anti-mouse secondary antibodies, diluted in 3% BSA/PBS-T, were added on a rotary shaker for 1h, at room temperature. ECL1/2 (1:1, v/v) was added (50µl/well) and emission was measured in RLU under a luminometer (Fluoroscan Ascent FL Labsystems).

Chapter 3

Localization of AGR-2

3.1 Introduction

3.1.1 Protein trafficking within the cell

3.1.1.1 Sequences defining the localization of proteins

Signal sequences play a vital role in targeting as well as in protein topogenesis by orienting themselves in the translocon [244], and the membrane [250, 552, 607]. Cleavable signals for secretory proteins were found to expose their C-terminal cleavage site to signal peptidase on the luminal surface of the ER membrane and the N-terminus towards the cytosol [217]. A major factor that determines orientation is the distribution of charged amino acids on either end of the hydrophobic sequence due to electrostatic interactions with charges at or near the translocon [217]. The more positively charged flanking sequence is usually found on the cytosolic side of the membrane in both prokaryotic and eukaryotic cells [250]. Another important factor which might affect protein topogenesis is the folding of N-terminal sequences, whereas the size of this sequence does not seem as a limiting factor [139].
Various models were suggested to explain the protein translocation and orientation when it comes to ER [217, 456, 527]. Some of them are quite contradictory but they all come to one conclusion: the flanking charges are vital in determining protein translocation and orientation. One of the most common ER retention sequence is the KDEL (HDEL in yeast) sequence.

3.1.1.2 Endoplasmic Reticulum and protein trafficking

In order to understand the role of AGR-2, it is essential to study the secretory pathway where the two different isoforms of the AGR-2 protein are involved. In the secretory pathway, proteins travel from the Endoplasmic Reticulum (ER) where they

are synthesised through the Golgi apparatus and then are redirected to secretion, plasma membrane, and towards secretory and endocytic organelles (Figure 3.1). The biosynthetic pathway is balanced by the opposite-way pathway that includes endocytosis of extracellular molecules as well as recycling of intracellular proteins [601]. Trafficking is being accomplished by fusion vesicles or connecting tubules. Most proteins are retained in the ER until they are correctly folded and assembled. Besides allowing post-translational modifications such as protein-folding, glycosylation, disulfide bond formation, proline-hydroxylation, and tyrosine sulfation, the secretory machinery has to fulfill another important task, namely the distribution of correctly folded proteins to their final destination [57]. Misfolded proteins are retrotranslocated to the cytosol, in a process involving ER chaperones and key-proteins of the import machinery, and degraded by the proteasome, most times by polyubiquitination [66]. Correctly folded proteins leave the ER, 'exit sites', and selectively exported by COPII vesicles to the Golgi apparatus [171] (Figure 3.1). Once the COPII vesicles have detached from the ER and formed vesiculotubular clusters (VTCs) with the microtubules, the COPII coat is replaced by the COPI coat. COPI vesicles are formed in the *cis*-Golgi compartment and mediate the formation of return vesicles back to the ER (Figure 3.1) through a retrograde pathway. Finally, the *trans*-Golgi network, from which cargo moves to the plasma membrane (PM) and through endosomes to lysosomes serves as a location for the rerouting of some misfolded proteins that are to be degraded [171]. Secretory proteins usually enter the ER post-translationally. In terms of the machinery involved, secretory transport can be dissected into at least four distinct steps: ER import/quality control, ER to Golgi transport, intra-Golgi transport/ER retrieval and post-Golgi transport [57]. Their translocation depends on the N-terminal signal peptide. This signal peptide is removed by a signal peptidase post-translationaly while the protein is exiting the ER [601]. If a protein contains a stop-transfer signal then translocation is halted and the hydrophobic regions are inserted into the membrane and join transmembrane domains [601].

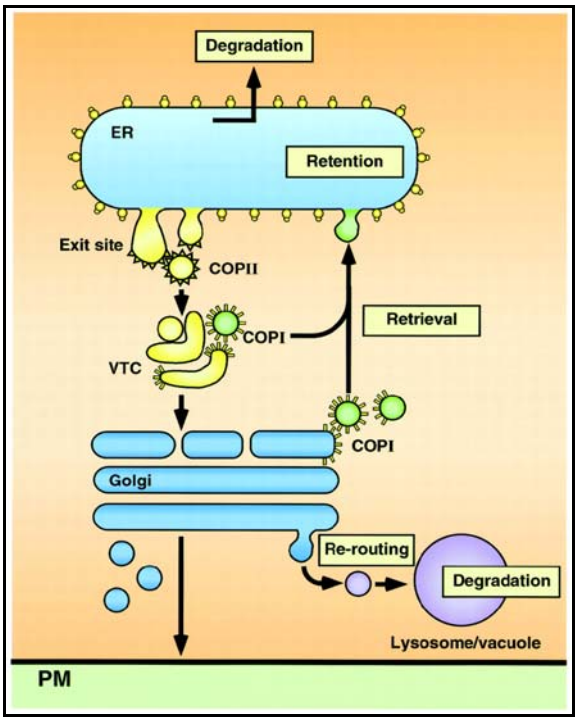

Figure 3.1 : Schematic overview of the organelles of the secretory pathway. Synthesized proteins enter the pathway at the ER and are subjected to repeated sorting and transport between membrane organelles until they arrive at their designated destination. PM:plasma membrane, ER:endoplasmic reticulum, VTC:vesiculotubular cluster. (for detailed explanation consult 3.1.1.2, adapted from [171])

3.1.1.3 KDEL sequence as an ER-retrieval sequence

The ER, as mentioned above, contains a number of resident proteins whose roles include: protein and lipid modification, processing of N-linked glycans, vesicle formation, protein sorting and transport [246]. Proteins that are transported along the secretory pathway are membrane proteins, soluble lysosomal/vacuolar proteins and secreted proteins [57, 171] as mentioned above. Soluble ER proteins include chaperones and components of the quality control machinery [171]. The localization of these proteins in the ER or the processing to the Golgi is established by certain retention or retrieval mechanisms involving specific sequence motifs within the

polypeptide chain [573]. ER-residency is achieved in two ways: (i) prevention of residents from entering newly forming transport vesicles and (ii) retrieval of those residents that escape [573]. The latter mechanism is directed by discrete retrieval motifs. One of the most thoroughly studied and best characterized sequence responsible for ER-retention is the KDEL sequence (HDEL in yeast) present in soluble ER-resident proteins [353, 631] in their C-terminus. It is a tetrapeptide sequence consisting from K-D-E-L, Lysine-Aspartic acid-Glutamic acid-Leucine, and recognized by specific receptors, named KDEL receptors, in post-ER compartments (Figure 3.2) that return the proteins to the ER. This retrograde transport triggers the formation of the COPI-coated vesicles mentioned above that transport the protein from the Golgi back to the ER [57, 171].

ER-retrieval sequences ensure return of proteins that have left the compartment in which they reside. It is noteworthy that apart from the KDEL motif, ER-residency is achieved by direct retention involving association and interaction of protein subunits into large complexes through their transmembrane or luminal domains [433, 446]. The aforementioned subunits escape packaging through preventing being exported from the ER. The ER-resident lumen proteins, known as reticuloplasmins, are conserved between eukaryotic cell types from plants, animals and fungi. Examples of these proteins include the molecular chaperones BiP, HSP and PDIs (analysed in chapter 1.4). Apart from the KDEL motif, many ER transmembrane proteins contain a dilysine motif (KKXX) at their C-terminal cytoplasmic tail that ensures ER-retention and not ER-retrieval.

Interestingly, plants utilize two ER-retention sequences, HDEL and KDEL. In some proteins, such as the SH-EP (cysteine protease) superfamily, the KDEL sequence is being post-translationally removed [441]. The removal of the KDEL sequence from SH-EP in homologous *Vinus mungo* cells and in heterologous SF-9 cells is so far unique amongst the retention sequence-bearing proteins that have been described [441]. Several studies have shown partial or enhanced retention within the ER/nuclear envelope that usually ends up to trafficking to the endomembrane system, indicating that the KDEL sequence itself is not sufficient to ensure complete

retention within the ER [138]. However, in the above studies the exact fate of the retention signal was not established and the possibility of post-translational processing masking its effects still remains.

3.1.1.4 The KDEL receptor mediates ER retrieval

The KDEL receptor (Figure 3.2), also known as ERD2, is a Golgi/intermediate compartment-located integral membrane protein [231] that carries out the retrieval of escaped ER-proteins bearing a C-terminal KDEL sequence [83]. The receptor recognizes and binds to this KDEL tetrapeptide. It consists of a seven-transmembrane domain protein with a short 12-13 amino acid tail at the C-terminus, orientated towards the cytosol that is responsible for the retrieval of ER-proteins from the Golgi complex [586]. Phosphorylation of the KDEL receptor at serine 209 (in the consensus site KKLSL) is necessary for its function [83]. The retrieval of the KDEL-bearing proteins by the receptor happens through retrograde traffic mediated by COPI-coated transport vesicles [83] (Figure 3.1). The receptor has high affinity for this tetrapeptide and after release of the protein to the ER, is recycled back to the Golgi for further cycles of retrograde transport. The pH difference between the ER and the Golgi has been proposed to be responsible for the different affinity exhibited by the receptor towards different kinds of proteins, enabling binding of KDEL proteins in the Golgi and release upon to the ER [622].

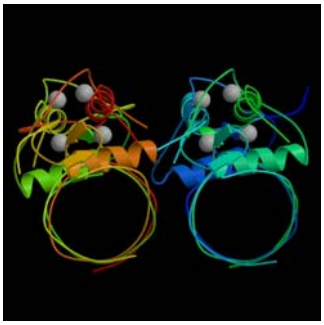

Figure 3.2: Structure of the KDEL receptor. This receptor is responsible for retrieval of KDEL-proteins back to the ER. (picture adapted from *www.georgetown.edu,* June 2006).

3.1.2 Fluorescent microscopy as a localization tool

One of the most commonly used techniques to detect intracellular protein localization and trafficking, and the one used thoroughly throughout the whole project, is fluorescence microscopy. Fluorescence imaging is a useful method for studying the localization or concentration of molecules to subcellular loci, as it is non-invasive, of high sensitivity and specificity. Fluorescence occurs when light absorbed by a molecule is emitted after a very short period (approximately 10^{-8}s) following light absorbance. Emitted light is always produced at a longer wavelength than absorbed (named Stokes shift) due to a small dissipation of energy during the excited state [175, 476]. This shift is of course crucial for the detection of fluorescence as it makes it possible to discriminate between the excitation and the emission signal. Fluorescence is gaining more and more ground over the recent years, resulting in many different techniques that stem from the same principle: emission and excitation of fluorophores when light activation occurs.

Neither Y2H, nor MS provide data on the interaction of proteins in their native environment. The development of highly sophisticated equipment along with the wide use of fluorescent proteins in cell biology, enabled researchers to study protein interactions in vivo, even transient ones. Most of these methods are based on the excitation of a donor-fluorescent fused molecule and an acceptor-fluorescent fused one followed by fluorescent measurements. Fluorescense Resonance Energy Tranfer [406], Bioluminescence Energy Transfer [628], Fluorescence Correlation Spectroscopy, Fluorescence Lifetime Imaging [390] and co-localization assays are only very few of the techniques that fall into this category [476] (Table 3.1).

Bioluminescent RET is similar to FRET, but in this case the candidate protein is fused to a bioluminescence luciferase and the potential binding partners to a GFP protein. When the two proteins interact, the luciferase and the GFP are brought close enough for resonance energy transfer to happen, and therefore the bioluminescence emission is shifted [628]. Both methods offer no limitations when it comes to the localization of the proteins, compared to the Y2H, but are dependent on the

orientation and conformation of the binding partners. Moreover, cell type specific interactions can be detected, as both systems utilize fluorescence change and this is feasible to any model. On the other hand, because the fluorophore/ luciferace tags are fused to ends of potentially interacting proteins and because resonance energy transfer requires distance between 10-100 Å, some interactions may not be detectable despite occurring because the fluorophore/luciferase do not come in close distance. It is also possible to test the kinetics of interaction *in vivo* [628].

3.1.2.1 Fluorescent techniques for imaging

Following is a brief summary of the techniques widely used in fluorescent microscopy for variable studies concerning protein trafficking, secretory pathways, protein interactions [476] (Table 3.1)

Immunofluorescence	Visualization of protein distribution in fixed cells. Usually nonquantitative.
Directly labelled proteins	Visualization of protein distribution in fixed or living cells. Quantification is less difficult than that of antibody binding as epitope accessibility is not an issue.
Time-lapse imaging (non-quantitative)	Change in location of a protein in a living cell over time. Motion/dynamics ofvisible organelles and structures in living cells.
Time-lapse imaging (quantitative)	Change in location of a protein in a single living cell over time. Typically used to determine kinetics of transfer of a bolus of protein between organelles. Varying degrees of sophistication can be applied ranging from determination of general timescale to fitting mathematical models based on systems of differential equations

Fluorescence Recovery after Photobleaching (FRAP)	Determines ability of a protein to diffuse within a single membrane or within cytosol, effectively a probe of local environment. Also commonly used to visualize kinetics of exchange of a protein between two compartments in cases where the trafficking of the protein cannot be effectively synchronized. The two compartments can be organelles of the secretory pathway or an organelle and cytosol.
Fluorescence Resonance Energy Transfer (FRET)	Locates particular protein–protein interactions inside cells. Requires a fluorescent tag on each of the proteins. FRET is sensitive to the exact distance between these fluorescent tags and will fail if they are too far apart.
Fluorescence Correlation Spectroscopy (FCS)	FCS can determine diffusion coefficients, degree of clustering of a molecule and molecular concentrations. It can have advantages over FRAP for fast-diffusing (i.e., cytosolic) proteins and when the fluorescent protein is a mix of fast-diffusing and slow-diffusing species. Requires a specialized apparatus. Data analysis non-trivial.
Fluorescence Cross-Correlation Spectroscopy (FCCS)	FCS variant used to detect complexes between two proteins each carrying a different fluorescent tag. Unlike FRET the technique is insensitive to the precise location of the fluorophores on the interacting proteins.
Image Correlation Spectroscopy (ICS)	Same uses as FCS but can be implemented with standard confocal microscope capable of rapid image acquisition. Can give some spatial resolution as well as directional information in the case of protein flow. However less capable than FCS of analyzing fast (i.e., cytoplasmic) diffusion.
Image Cross-Correlation Spectroscopy (ICCS)	ICS-based technique to detect interaction between two proteins tagged with different fluorophores. Requires a confocal microscope capable of rapid simultaneous acquisition of two channels. Current generation confocal microscopes are generally capable of this. However specialized mathematical expertise and custom computer software is needed.

Fluorescence Lifetime Imaging Microscopy	Primarily used as a sensitive technique to detect FRET. Requires specialized equipment that is not yet generally available.
Total Internal Reflection Microscopy (TIRF)	Detects events occurring very close to the cell surface (e.g. vesicle fusion). Can also be used to visualize single fluorescent molecules on or very near the cell surface.

Table 3.1: List of different fluorescent-based techniques and applications. Right panel refers to the definition and the left panel explains the exact application of each technique (adapted after [476]).

3.1.2.2 Directly labelled proteins

Direct labelling of the target protein was used in this project to visualize different proteins in subcellular compartments. In this method, the cells are transfected with plasmids encoding the gene of interest fused with a fluorescent protein (green, yellow, cyan and red are the most widely used, Table 3.2). The fused gene is the introduced into the cells where it is being expressed fused to the FP protein and its localization is detected by fluorescent microscopy using the excitation and emission wavelengths specific for each fluorescent probe (Table 3.2).

Endogenous fluorescent proteins are usually found in many cnidarians [301, 535] including many jellyfishes and corals as energy-transfer acceptors in bioluminescence. FPs fluoresce *in vivo* upon receiving energy from either a luciferase-oxyluciferin excited-state complex or a Ca^{+2}-activated phosphoprotein [475]. Fluorescence in these species serves reproductive and survival purposes and is genetically controlled. The emission and excitation wavelengths vary from colour to colour and depend to each protein (Table 3.2).

Colour	Excitation	Emission
Green	395 nm	509 nm
Red	558 nm	583 nm
Cyan	434 nm	475 nm
Yellow	513 nm	527 nm

Table 3.2: Excitation and emission wavelengths of each of the 4 most widely used fluorescent proteins (information adapted from *www.BDbiosciences.com*)

Although fluorescent proteins are quite useful in research, they also have drawbacks and features that can reduce their quality as reporter genes. For that reason most of the fluorescent proteins than are used in biology are developed and optimized so variants are being selected [43]. Each variant has different spectra of characteristics, leading to enhanced fluorescence emission. The insertion of different promoters to drive expression of the gene of interest, usually under cytomegalovirus promoter, and mutations to the sequence are also used to increase their efficiency and stability as molecular markers. The most commonly used fluorescent proteins are the Green Fluorescent Protein (GFP) and the Red Fluorescent Protein (RFP) along with their optimized variants.

3.1.2.3 Green Fluorescent Protein

The Green-Fluorescent Protein (GFP) has become an important reporter for monitoring gene expression and protein localization within cells [660]. Prasher and co-workers, 1992, were the first to clone the green fluorescent protein found in the medusa *Aequorea Victoria* [475]. The protein consists of a β-barrel with 11 anti-parallel strands, capped at both ends, and a coaxial helix, with the chromophore

forming from the central helix in the internal cavity [448] (Figure 3.3). When GFP is expressed it yields green fluorescence when excited by ultraviolet (UV) or blue light. To utilize their fluorescence in molecular biology, many variants of the GFP protein are constructed. These variants aim to reduce GFPs disadvantages and increase its useful characteristics (summarized in Table 3.3). One of these variants is the AcGFP-N_1 fluorescent protein that will be used in the current project.

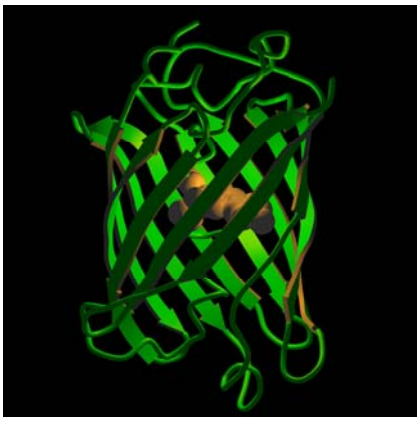

Figure 3.3: Structure of the GFP protein. The barrel-like structure of GFP. The fluorophore is the one retained in the internal cavity (adapted from *www.tsienslab.usbc*, December 2005)

Green Fluorescent Protein	
Pros	**Cons**
Stable variant	Low fluorescent intensity in blue light
Species-independent	Poor expression in some mammalian cell lines
Non-invasively monitored	Low sensitivity
Direct measurement of transfection efficiency	Lag in the development of fluorescence after protein synthesis
No need of substrates or cofactors	Not very high half life

Table 3.3: Advantages and Disadvantages of the Green Fluorescent Protein (GFP) widely used in fluorescence microscopy.

The $AcGFP_1$ variant derives from the jellyfish *Aequora coerulescens* and is a novel alternative to monomeric GFP. $AcGFP_1$ is an engineered fluorescent mutant of the wild-type protein with 94% homology to enhanced-GFP, EGFP a bioengineered GFP with enhanced fluorescent abilities, at the amino acid level. The plasmid that contains this variant (obtained from BD Biosciences) features an open reading frame in which the coding sequence has been optimized for expression in human cells. This optimization increases the translational efficiency of the $AcGFP_1$ mRNA and results in higher expression levels. The $AcGFP_1$ protein is stable and can be detected without cofactors or substrates. The last feature makes it a valuable tool for transfections and immunofluorescent microscopy. The protein can be fused to the N- or C- terminus of the protein, characterised as AcGFP-C_1 and AcGFP-N_1 in respect to which terminus of the GFP the target gene is fused.

3.1.2.4 DsRed and its variants

Another fluorescent protein, which emits red fluorescence and that will be used widely, is the DsRed protein, a variant of the Anthozoan reef coral *Discosoma sp.* fluorescent protein [391]. Reef corals consist of a variety of colours. These corals have the ability to tolerate different intensities of light depending on the depth they are into [508]. Fluorescent proteins, yellow and red, of these corals have the ability to protect them from intense light exposure in shallow water but on the other hand, they enhance availability and absorption of light in deep water [508]. Anthozoa animals do not have bioluminescent properties unlike *Aequorea victoria*, suggesting that in Nature fluorescent proteins are not always linked to bioluminescence.

The fluorescence excitation and emission maxima of the protein are at the wavelengths 558nm and 583nm, respectively which are well separable from that of GFP and therefore attracts great interest as an expression marker and fusion partner for multicolor cellular imaging [382]. DsRed, 28kDa size, is a tetramer and this structure is essential for the fluorochrome's maturation [637]. It is also believed that

this tetrameric configuration provides the needed photoprotective character to the corals [637]. Each DsRed monomer has an 11-stranded α-can tertiary structure (Figure 3.4) similar to that of GFP. These monomers units interact with each other via hydrophobic and hydrophilic interactions to form a tetrameric unit [637]. The advantage of DsRed compared to GFP is that the first one's fluorescent spectra is unaffected by pH (in the range 5–12 [33]) and its orange-red emission (wavelength maximum 583nm) is spectrally distant from green cellular autofluorescence. These properties should make DsRed a better choice as a label in some applications compared with GFP. However DsRed has some drawbacks including, slow maturation, strong oligomerization to form a tetrameric structure, and a tendency to aggregate which can limit its applications [33, 85, 406, 537]. Modifications of DsRed to improve its properties and create monomeric, faster-folding, more efficient and photostable variants are underway with the help of molecular evolution and genetic engineering and therefore many new forms of DsRed are now available [85, 537].

Figure 3.4: The structure of the DsRed tetramer. The X-ray crystal structure of DsRed was prepared using DSViewer Pro Accelrys Software (adapted from [537]).

3.1.3 Objectives of chapter

Anterior Gradient 2 is present intracellularly in two isoforms. The full length which has a cleavable N-terminal signal peptide designating the protein to secretion and the mature form without this signal peptide. Both forms bear the same putative ER-retention C-terminal tetrapeptide. No evidence exists whether one isoform is predominant compared to the other in a cancer cell. This chapter investigates the localization of endogenous AGR-2 in a panel of breast cancer cell lines. Moreover, fluorescent-tagged AGR-2_{wt} and different mutants are examined in an attempt to fully characterize the distribution of the protein based on specific sequences present in either of the two isoforms. Co-localization data with different subcellular organelles and chemical fractionation of subcellular compartments are shown, further defining the variable localization patterns of the wild type proteins and mutants and therefore initiating the characterization of the protein's function.

3.2 Results

3.2.1 Localization of endogenous AGR-2

3.2.1.1 Subcellular localization of endogenous AGR-2 in breast cancer panel

Subcellular fractionation of endogenous AGR-2 protein was performed by the S-PEK kit (Calbiochem) according to the manufacturer's protocol, in order to study the localization of the endogenous AGR-2 in MCF-7, LCC1 and LCC9 cell lines at the protein level. LCC1 and LCC9 cell lines are MCF-7-derived and show different resistance to Tamoxifen and other antiestrogens, with the LCC9 cells being totally resistant to the drugs. The monoclonal antibody recognized a single band of approximately 20kDa. The migration of the protein onto the gel matched the predicted protein molecular weight (Figure 3.5).

The AGR-2 band was present in the cytosolic (F_1), cell membrane (F_2) and nuclear fractions (F_3) of all cell lines but differences in the expression levels were observed (Figure 3.5.A). No AGR-2 was detected in the cytoskeletal fractions (F_4) in any of the cell lines. In MCF-7 cells, AGR-2 was expressed in higher levels in the cytosolic and cell membrane/organelles fraction, whereas nuclear AGR-2 was less dominant. On the other hand, in LCC1 cells the protein was more cytosolic and nuclear and less in the cell membrane/organelles fraction. In LCC9 cells, AGR-2 was highly nuclear and cytosolic, following the same pattern as in LCC1 cells, but with slightly more elevated nuclear levels. To sum up, the LCC1 and LCC9 cell panels appeared to express cytosolic and nuclear AGR-2 in higher levels that the MCF-7, whereas MCF-7 showed elevated AGR-2 levels in the cytoplasm and lower levels in the nucleus compared to the other cell lines.

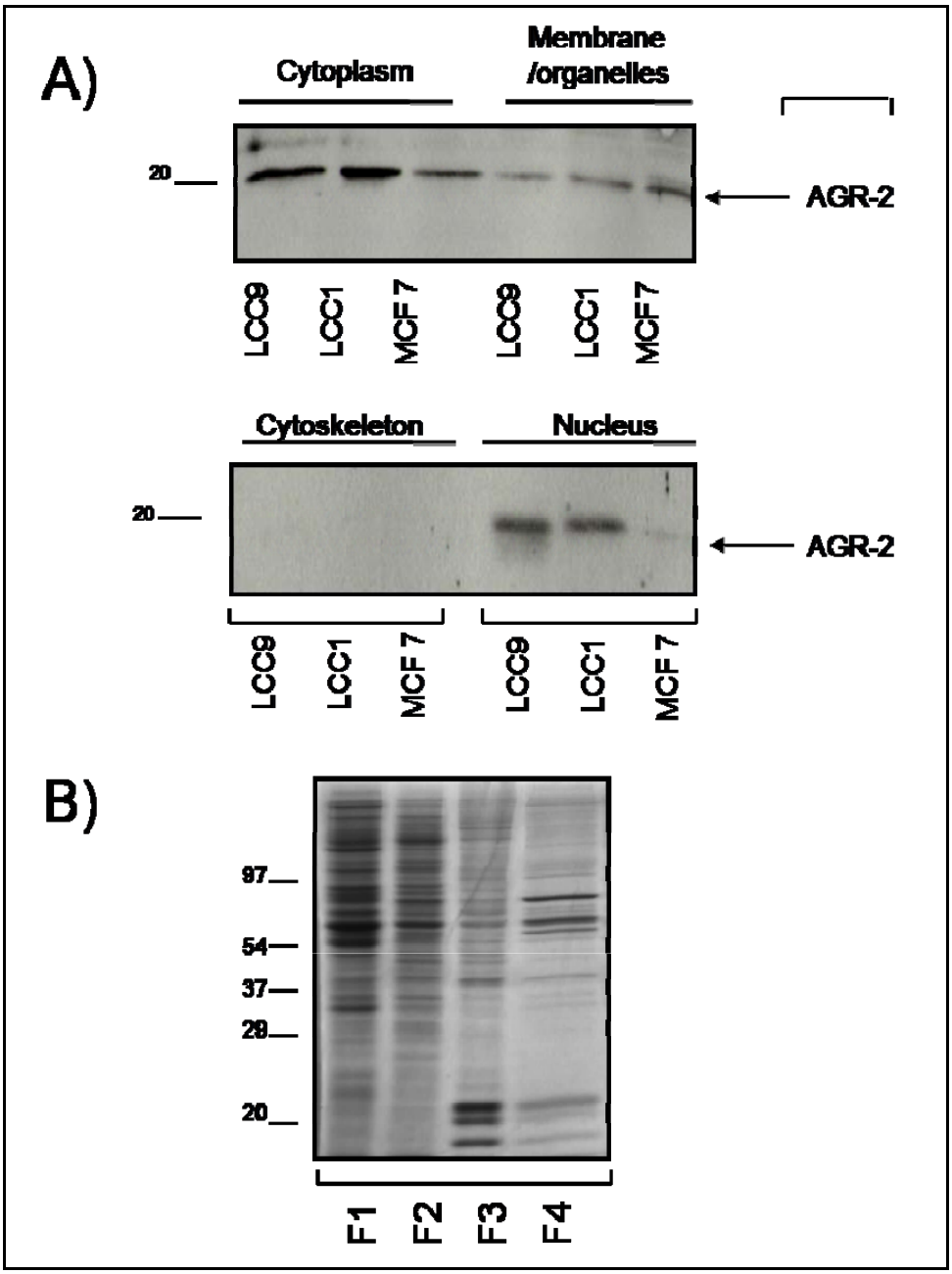

Figure 3.5: Intracellular localization of endogenous AGR-2 in breast cancer cell lines. A) MCF-7 (lanes 3 and 6) LCC1 (lanes 2 and 5) and LCC9 (lanes 1 and 4) were processed using fractionation methodologies into F_1 (cytosolic), F_2 (membrane/organelles), F3 (nuclear), and F_4 (cytoskeletal), as indicated. The distribution of endogenous AGR-2 protein (~ 18 kDa) was determined by immunoblotting. B) Representative coomassie blue staining used as a control for fractionation.

Immunofluorescent data after staining for endogenous AGR-2 with rabbit polyclonal antibody (Moravian Biotechnologies) showed cytoplasmic distribution of the protein with strong perinuclear staining (Figure 3.6). No nuclear signs of AGR-2 were detected. The same motif was repeated in MCF-7, LCC1 and LCC9 cells. MDA-MB 231 negative control cells had no signs of endogenous protein, as expected. Furthermore, immunostaining with a mouse monoclonal antibody against AGR-2 followed similar distribution patterns in MCF-7 cells, with the only difference that this antibody was able to detect nuclear AGR-2 as shown by the white arrows (Figure 3.7). The protein was again detected in the cytoplasm with strong perinuclear staining. Cells grown in the absence of FCS for two days showed no change in the localization motives (Figure 3.7, panels D-F). Same observation was made with cells irradiated with $50J/m^2$ and left to grow for six hours before immunostained for AGR-2 (Figure 3.7, panels G-I). Another striking difference when compared to the rabbit polyclonal antibody was that the monoclonal one showed a rather reticulum-like distribution pattern of the protein, with few granules distributed around the nucleus whereas the polyclonal one showed diffuse localization pattern but no signs of perinuclear distribution were present.

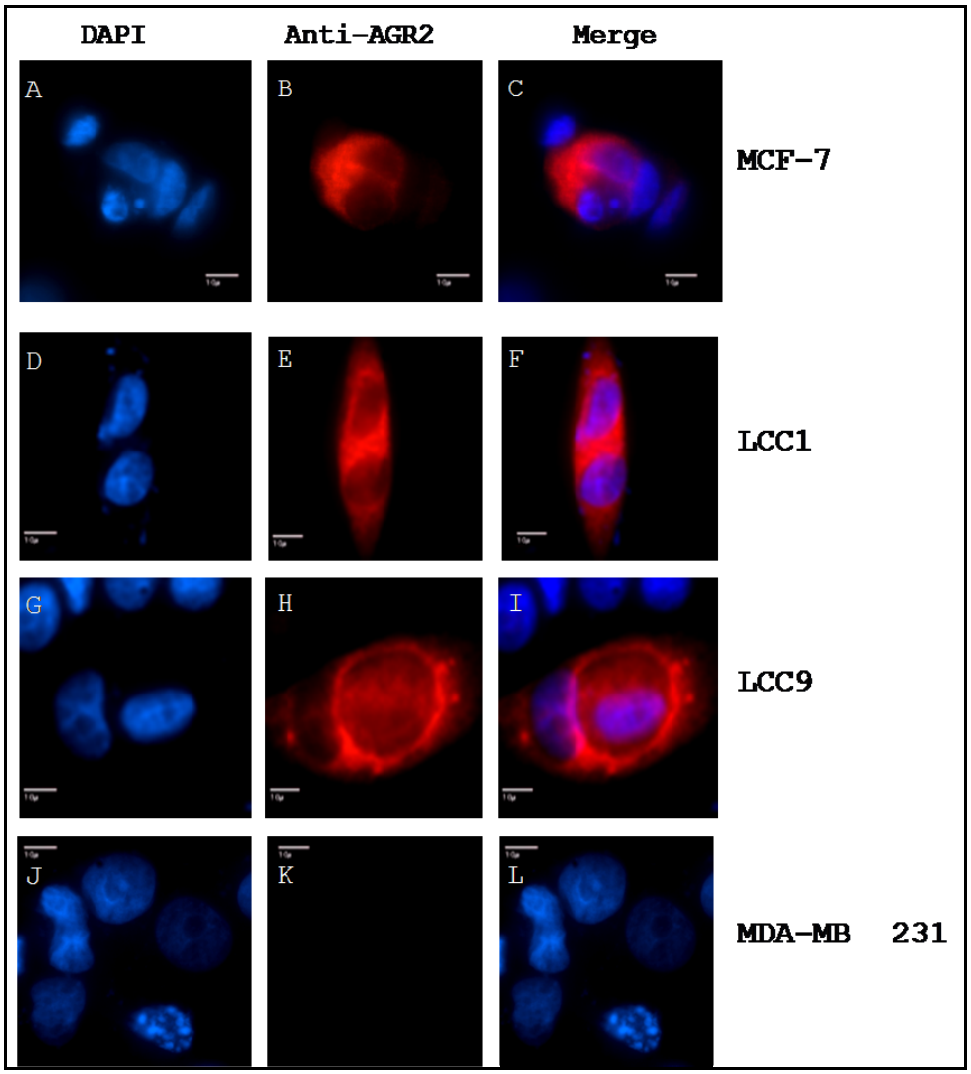

Figure 3.6: Intracellular localization of endogenous AGR-2 using fluorescent microscopy. Fluorescent images of endogenous AGR-2 in MCF-7 (panels A-C), LCC1 (panels D-F), LCC9 (panels G-I), AGR-2 positive, breast carcinoma cells, visualized by fluorescence microscopy. MDA-MB 231 (panels J-L), AGR-2 negative, cells were used as a negative control for unspecific antibody binding. After fixation the protein was visualized using anti-AGR2 antibody and Alexa-conjugated secondary antibody was applied (Alexa-594, Molecular Probes). Nuclei were visualized by DAPI. Images captured by Sony Cool Snap 3.2 (Anti-AGR2: panels B, E, H and K, DAPI: A, D, G and J, merge: C, F, I and L) by Zeiss Axionplan microscope. Same exposure times used for all images. Figure showing representative of 3 independent experiments. Scalebar represents 10µm.

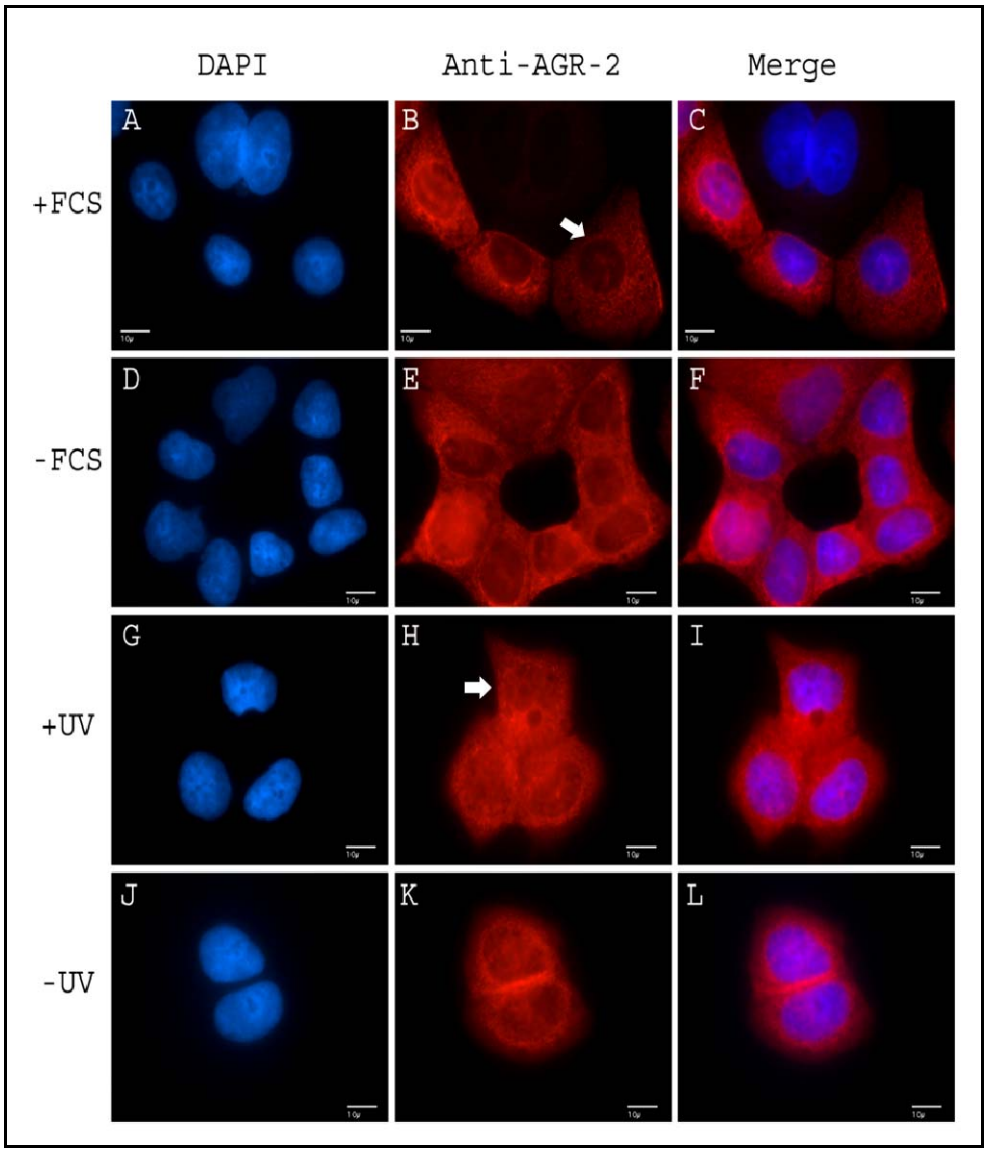

Figure 3.7: Intracellular localization of endogenous AGR-2 in MCF-7 using fluorescent microscopy and commercial anti-AGR2 antibody. Fluorescent images of endogenous AGR-2 in MCF-7 cells grown in the presence of FCS (panels A-C), absence of FCS (panels D-F), UV irradiated panels G-I) and non-UV irradiated (panels J-L). After fixation the protein was visualized using monoclonal anti-AGR2 antibody (Abnova) and Alexa-conjugated secondary antibody was applied (Alexa-549, Molecular Probes). Nuclei were visualized by DAPI. Images captured by Sony Cool Snap 3.2 (Anti-AGR2: panels B, E, H and K, DAPI: A, D, G and J, merge: C, F, I and L) by Zeiss Axionplan microscope . Same exposure times used for all images.). Scalebar represents 10μm.

3.2.2 Localization of transfected mature and full length AGR-2 wt.

3.2.2.1 Immunofluorescence verified AGR-2 localization

MCF-7 (Figure 3.8), LCC1 (Figure 3.10), LCC9 (Figure 3.11) and MDA-MB 231(Figure 3.9) cells were transfected with:

- Mature AGR-2wt pDEST 3.2, V-5 tagged,(Gateway)
- Full length AGR-2wt pDEST 3.2, V-5 tagged, (Gateway)
- pDEST 3.2 vector only (Gateway)

Untransfected cells were also used for detecting endogenous AGR-2 and as a comparing control. Twenty four hours post-transfection cells were incubated with a rabbit polyclonal anti-AGR-2 antibody (Moravian Biotechnologies). In all the cell lines tested, including the AGR-2-negative MDA-MB 231 cell line (Figure 3.9), both full length and mature transfected cells exhibited the same localization patterns (Figures 3.8-3.11). The protein was detected in the cytoplasm distributed in a diffused pattern whereas no signs of membrane staining were present. No difference in proteins' localization between the different cell lines was observed. In particular, cells transfected with the full length form of the protein,, showed no membrane staining, with most of the signal detected in the cytosolic area in all cell lines. Cells expressing the mature form of the protein that bears no leader sequence, excited most of the red light in the cytoplasm. As far as the endogenous AGR-2 is concerned, it is noteworthy that the pattern was the same as in the transfected ones, with the protein being detected in the cytoplasm and slightly in the nucleus, rather than in other cell compartments in LCC1 and LCC9 cels. The above data are consistent with the results from subcellular fractionation, which showed AGR-2 predominantly in the cytosolic fraction (Figure 3.5), although differences in the nuclear fraction were observed amongst cell lines. The cytosolic localization of AGR-2 was also confirmed by immunohistochemistry experiments in breast cancer tissues (kindly provided by R. Nenutil, Czech Republic) from ductal and lobular carcinomas (Figure 3.12).

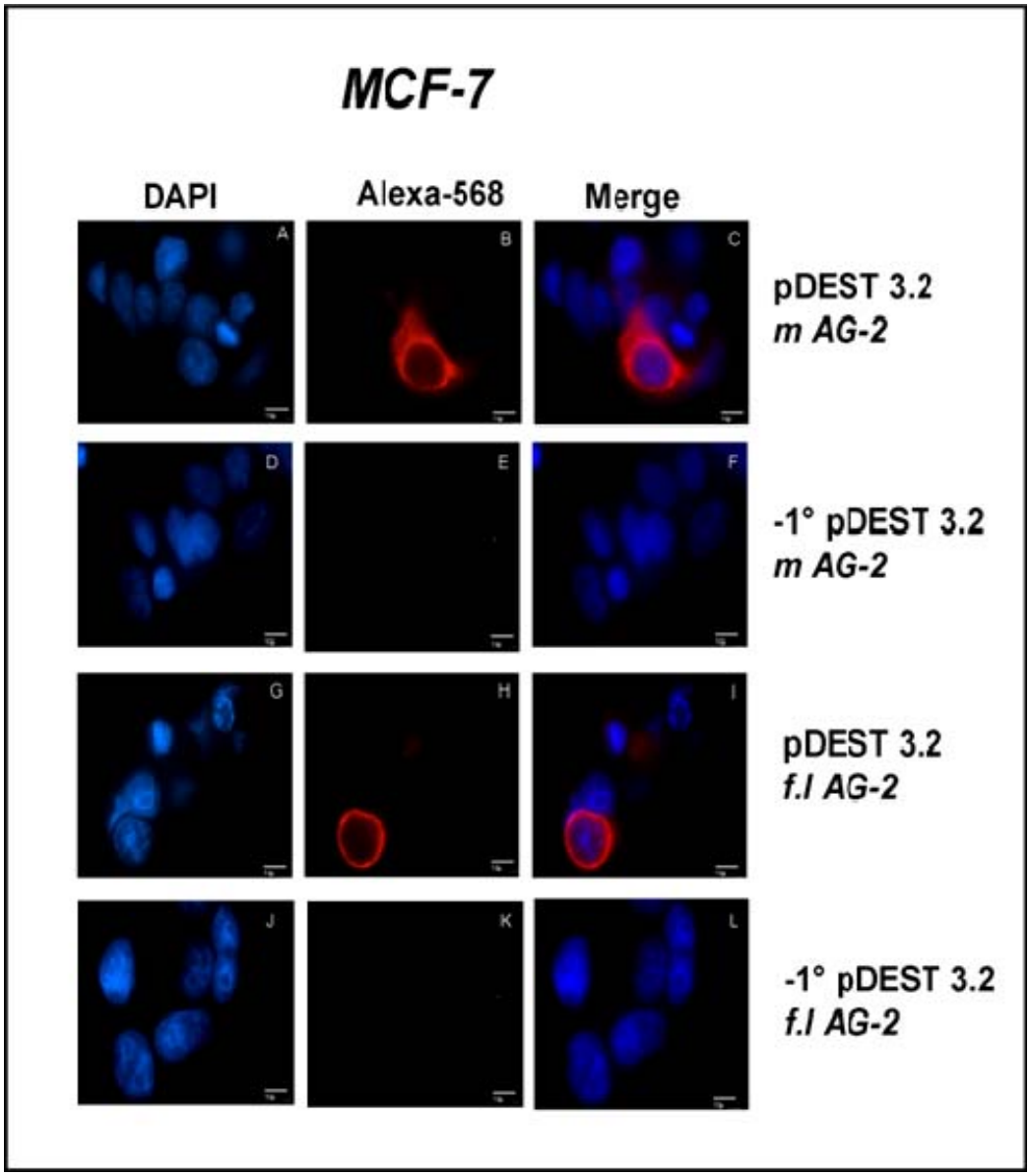

Figure 3.8: Intracellular localization of transfected mature and full length AGR-2 using fluorescent microscopy in MCF-7. Fluorescent images of the mature (panels A-C) and full length (panels G-I) AGR-2pDEST-3.2 constructs. MCF-7 cells were transfected with the constructs and visualized by fluorescence microscopy. Minus primary antibody controls were included (panels D-F, J-L). Protein was visualized by Alexa-conjugated antibody (Alexa-594, Molecular Probes). Nuclei were visualized by DAPI. Images captured by Sony Cool Snap 3.2 (red:panels B, E, H and K, DAPI panels A, D, G and J merge:panels C, F, I and L) under a Zeiss microscope. Same exposure times used for all images (scalebar:10μm).

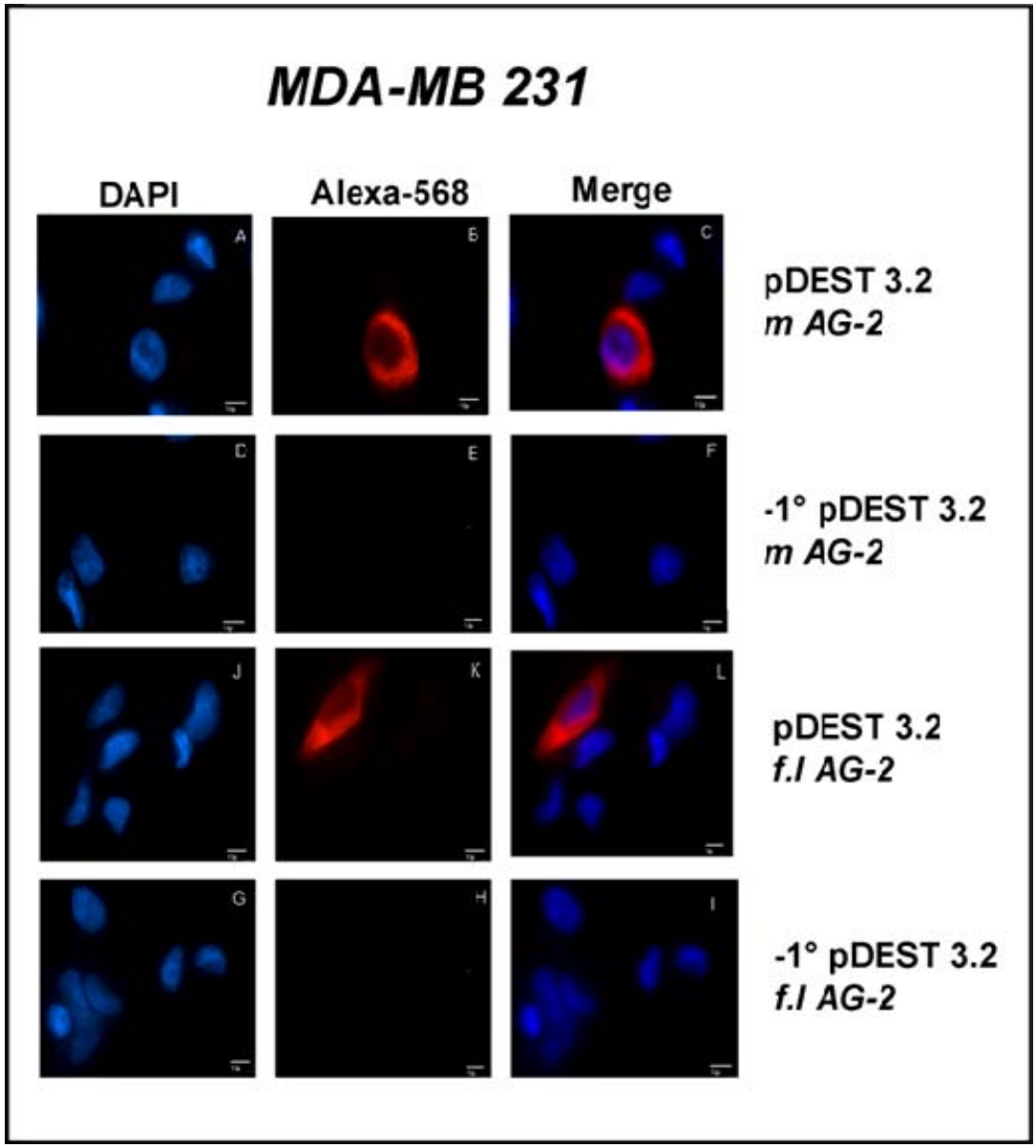

Figure 3.9: Intracellular localization of transfected mature and full length AGR-2 using fluorescent microscopy in MDA-MB 231. Fluorescent images of the mature (panels A-C) and full length (panels G-I) AGR-2pDEST-3.2 constructs. MDA-MB 231, AGR-2 negative, cells were used as a control for antibody binding. Minus primary antibody controls were included (panels D-F, G-I). Protein was visualized by Alexa-conjugated antibody (Alexa-594, Molecular Probes). Nuclei were visualized by DAPI. Images captured by Sony Cool Snap 3.2 (red:panels B, E, H and K, DAPI panels A, D, G and J merge:panels C, F, I and L) under a Zeiss microscope. Same exposure times for all images. Scalebar represents 10μm.

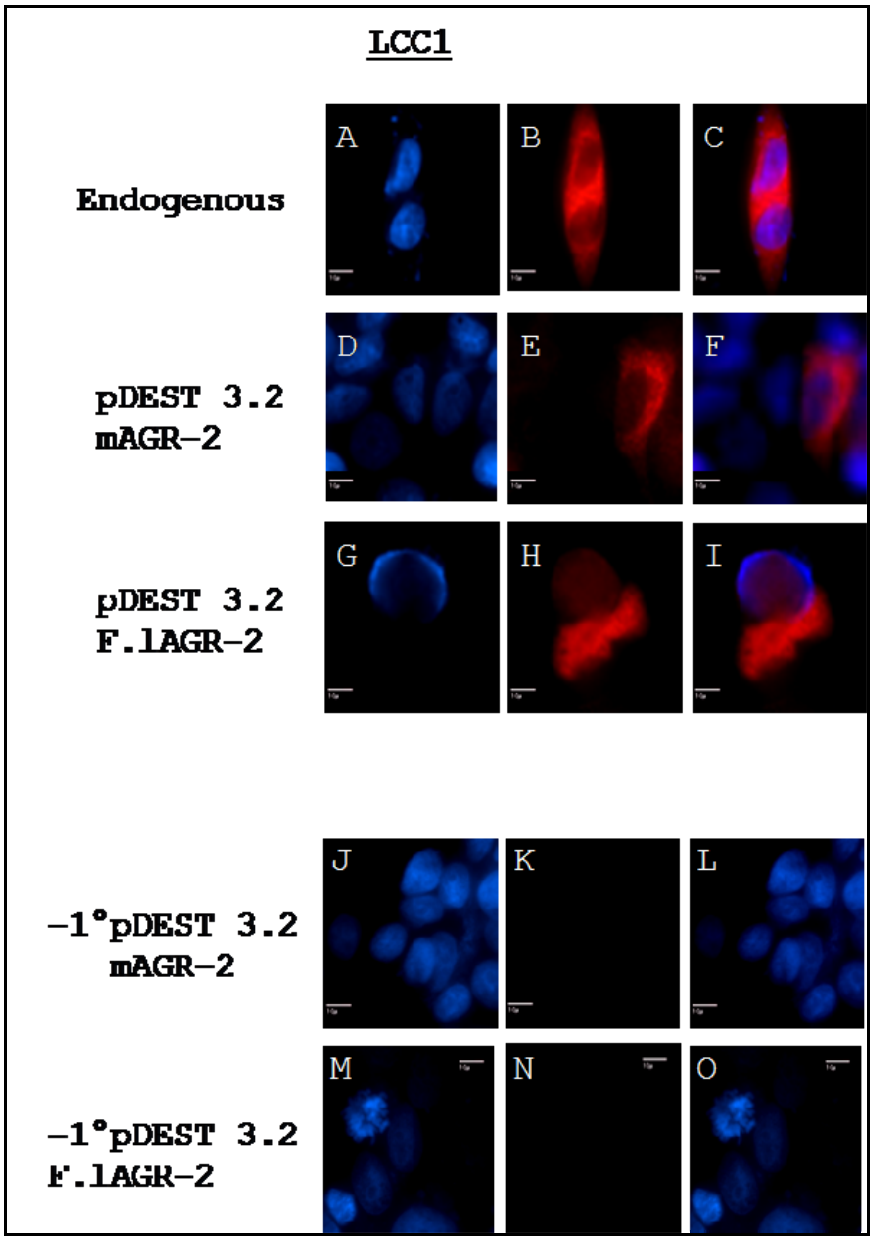

Figure 3.10: Intracellular localization of endogenous and transfected mature/full length AGR-2 using fluorescent microscopy in LCC1. Fluorescent images of the endogenous (panels A-C) mature (panels D-F) and full length (panels G-I) AGR-2pDEST-3.2 constructs. Minus primary antibody controls were included (panels J-L and M-O). Protein was visualized by Alexa-conjugated antibody (Alexa-594). Nuclei were visualized by DAPI. Images captured by Sony Cool Snap 3.2 (red:panels B, E, H, K and N, DAPI panels A, D, G, J and M, merge:panels C, F, I, L and O) under a Zeiss microscope. Same exposure times for all images. Scalebar represents 10µm.

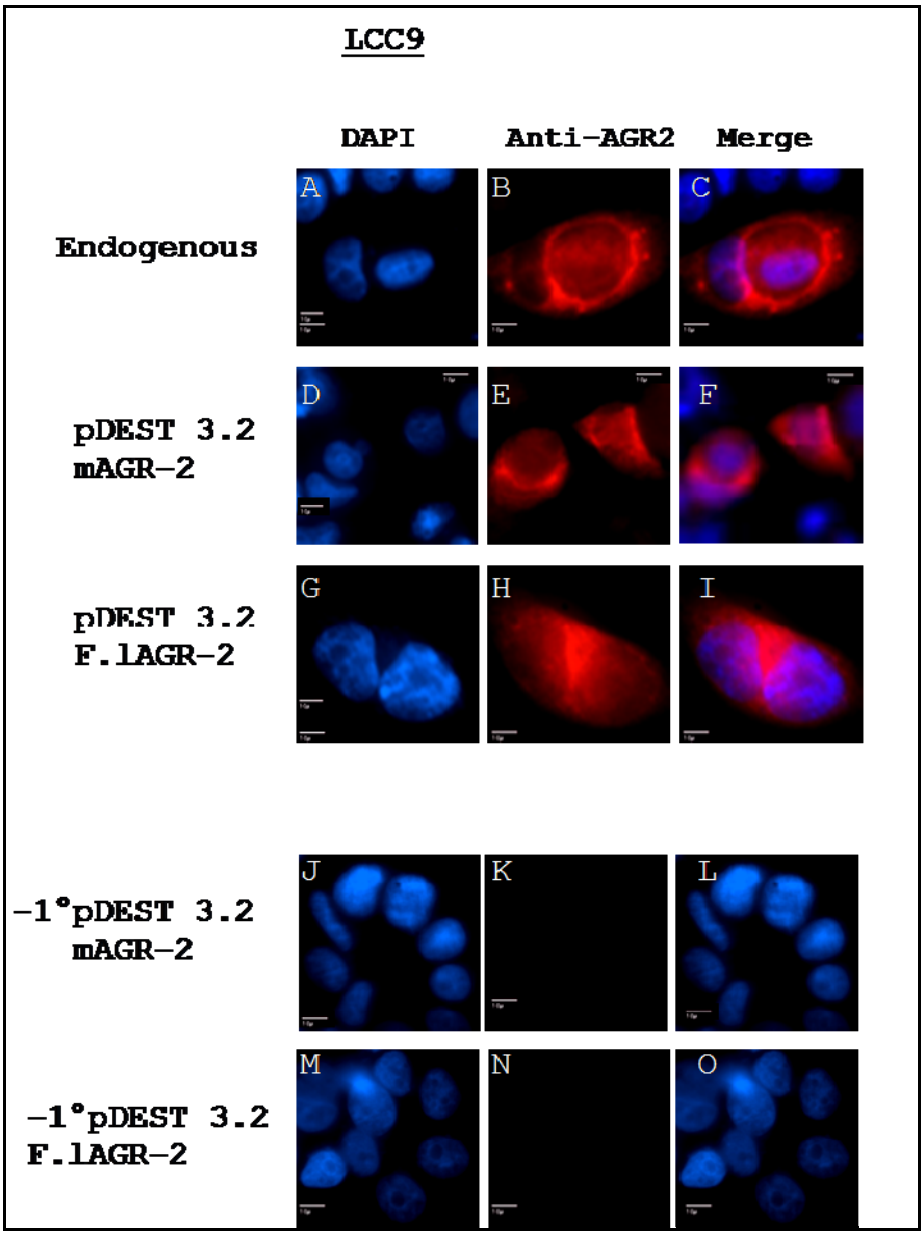

Figure 3.11: Intracellular localization of endogenous and transfected mature/full length AGR-2 using fluorescent microscopy in LCC9. Fluorescent images of the endogenous (panels A-C) mature (panels D-F) and full length (panels G-I) AGR-2pDEST-3.2 constructs. Minus primary antibody controls were included (panels J-L and M-O). Protein was visualized by Alexa-conjugated antibody (Alexa-594). Nuclei were visualized by DAPI. Images captured by Sony Cool Snap 3.2 (red:panels B, E, H, K and N, DAPI panels A, D, G, J and M, merge:panels C, F, I, L and O) under a Zeiss microscope. Same exposure times for all images. Scalebar represents 10µm.

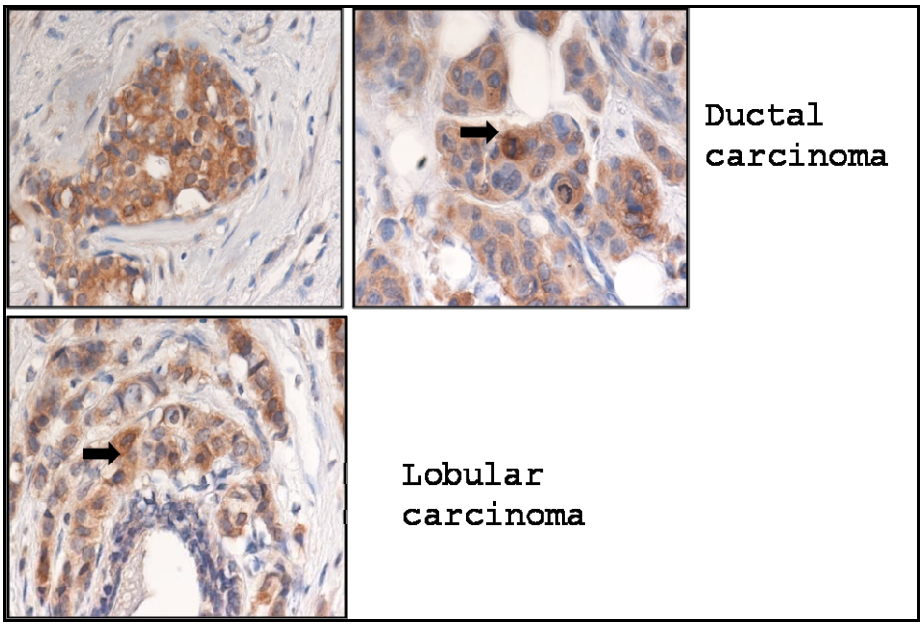

Figure 3.12: Immunohistochemistry of breast cancer tissues. Breast cancer sections showing the cytosolic localization of Anterior Gradient 2. Ductal and lobular carcinoma refer to different types of breast cancer regarding the type of the cells affected. The black arrows indicate the location of the protein (kindly provided by Dr. Nenutil).

3.2.3 Mature and full length AGR-2 fused to Green and Red Fluorescent vectors

3.2.3.1 Cloning of mature and full length AGR-2 GFP/RFP

AGR-2 exists in two isoforms: one full-length isoform with an N-terminal hydrophobic leader sequence (FL or F.l or f.l-AGR2) and a mature form with the N-terminus removed by proteolytic processing (m-AGR2) (Figure 3.13.A). The mature isoform is the one capable of inhibiting p53 transactivation function and capable of inducing cell survival in clonogenic assays [474]. AGR-2 has been previously suggested to reside extracellularly as part of a secretory pathway that promotes cell

migration or metastasis [199, 650]. To build further on our knowledge of the AGR-2 pathway, we examined AGR-2 subcellular localization using two approaches (i) RFP-tagged AGR-2 tested by confocal microscopy and (ii) subcellular chemical extraction methodologies into cytosolic, membrane/organelle, nuclear, and cytoskeletal fractions. To study the different localization of AGR-2 due to the leader sequence as well as the role of its KTEL sequence as a potential ER-retention sequence, a number of fluorescent-conjugated constructs were cloned (Figure 3.13):

1. Full length AGR-2wt in pAcGFP-N_1. This fuses the fluorescent protein to the C-terminus of full length AGR-2. Includes the AGR-2 signal sequence and the KTEL C-terminal tetrapeptide.
2. Mature AGR-2wt in p pAcGFP -N_1. This fuses the fluorescent protein to the C-terminus of mature AGR-2. Does not include the AGR-2 signal sequence but only the KTEL tetrapeptide.
3. Full length AGR-2$\mathbf{\Delta_{KTEL}}$ in pAcGFP-N_1. This fuses the fluorescent protein to the C-terminus of full length AGR-2 minus the last four amino acids that make up the putative ER retention sequence. Still includes the signal sequence.
4. Mature AGR-2$\mathbf{\Delta_{KTEL}}$ in pAcGFP-N_1This fuses the fluorescent protein to the C-terminus of mature AGR-2 minus the KTEL tetrapeptide. Does not include the AGR-2 signal sequence.
5. Full length AGR-2 **KDEL** in pAcGFP-N_1. This fuses the fluorescent protein to the C-terminus of full length AGR-2 but bears the C-terminal KDEL ER-retention sequence instead of KTEL. Still includes the AGR-2 signal sequence.
6. Mature AGR-2 **KDEL** in pAcGFP-N_1. This fuses the fluorescent protein to the C-terminus of mature AGR-2 but bears the C-terminal KDEL ER-retention sequence instead of KTEL. Still includes the AGR-2 signal sequence.

The same constructs will be cloned to the DsRed Express-N_1 vector in order to be fused to a red fluorescent protein, for co-localization experiments (Figure 3.13).

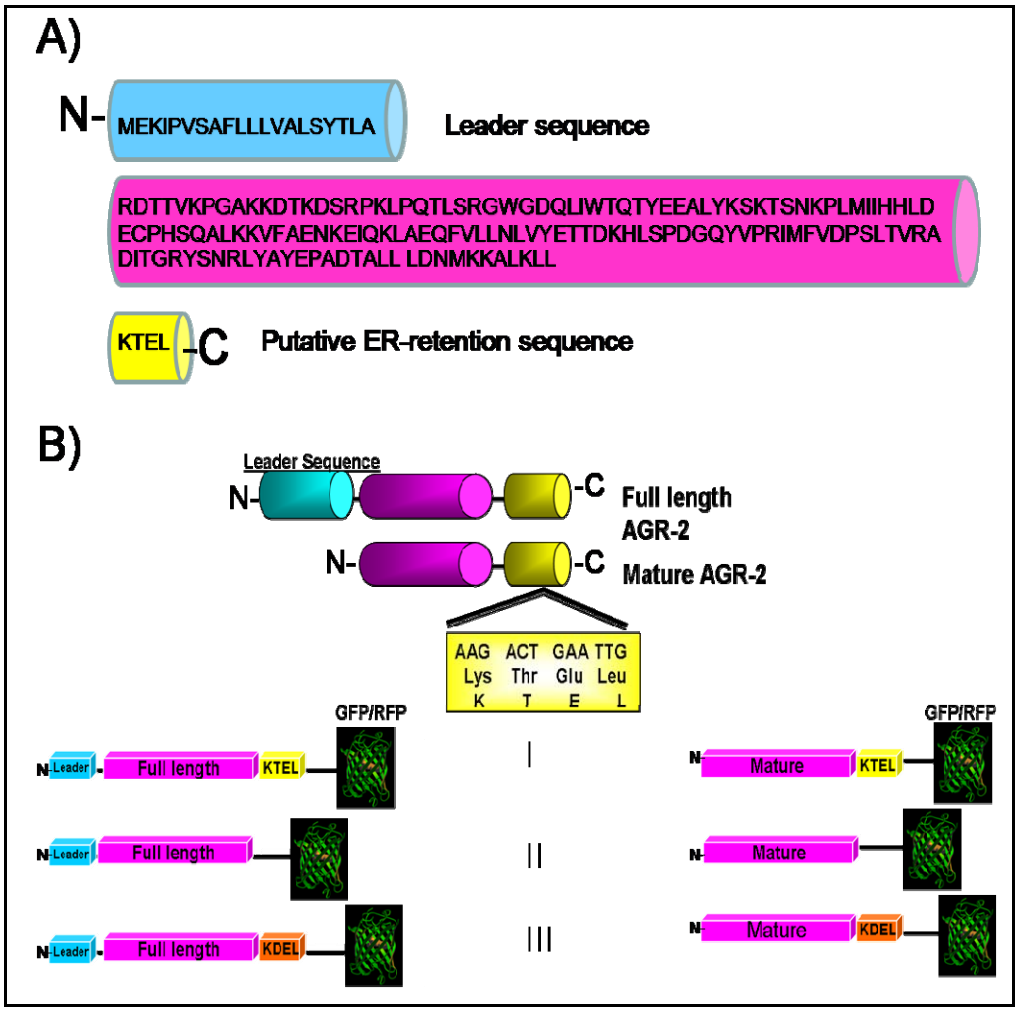

Figure 3.13: Representative diagram of the clones fused to green or red fluorescent protein. A) Detailed amino acid composition of AGR-2. B) Different mutants of the wt protein (BI). Mutation of the KTEL sequence (BIII) as well as complete deletion of the sequence (BII) are shown. The GFP/RFP fusion tags are integrated in the C-terminus of the constructs. Leader sequence shown in blue and KTEL in yellow. Mutant KDEL sequence is depicted in orange.

The full length and mature AGR-2 fused to GFP or RFP were tested by microscopy (fl. and m. respectively). The full length constructs, that contain the leader sequence, were all granular-shaped and distributed within the cytoplasm (Figure 3.15, panels A-C). Full length wt protein showed intense granular appearance (Figure 3.15 panel A) but within the whole cytoplasm whereas the fl.KDEL RFP mutant had intense

perinuclear granular appearance (Figure 3.15 panel B). The fl.Δ_{KTEL} RFP mutant had the exact same granular appearance as the previously described constructs but with a more diffused pattern (Figure 3.15 panel C) when compared to the wt and KDEL ones. As far as the mature protein is concerned (Figure 3.15 panels D-F), the wt form was highly nuclear and also distributed in a diffused way within the cytoplasm with only a few granules detected (Figure 3.15 panel D). The m.KDEL RFP mutant was also nuclear and cytosolic but more granules were detected compared to the wt one (Figure 3.15 panel E). The m.Δ_{KTEL} mutant had no signs of nuclear allocation and was distributed within the cytoplasm (Figure 3.15 panel F). This last mutant was highly unstable, as the fluorescent signal bleached after a short time and when that was not the case, it emitted very low fluorescence when compared to the AcGFP-N_1 empty vector control (Figure 3.14). AcGFP-N_1 (Figure 3.14 panels D-F) and DsRed-N_1 (Figure 3.14 panels A-C) empty vector transfected cells were included in the experiment and showed non-specific distribution as they were detected everywhere within the cells.

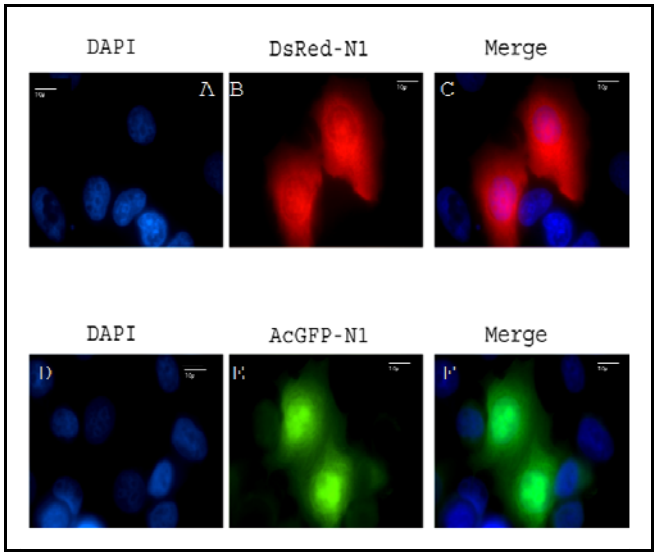

Figure 3.14: Subcellular distribution of pAcGFP-N_1 and DsRed Express-N_1. MCF-7 cells were single transfected with pAcGFP-N_1 (panels D-F) and DsRed Express-N_1 (panels A-C) and analysed by microscopy. DAPI (panels A and D). Images visualized by Zeiss Axionplan microscope and captured by a photometric CoolSnap HQ camera. Figure showing representative of 5 independent experiments. Scalebar represents 10μm.

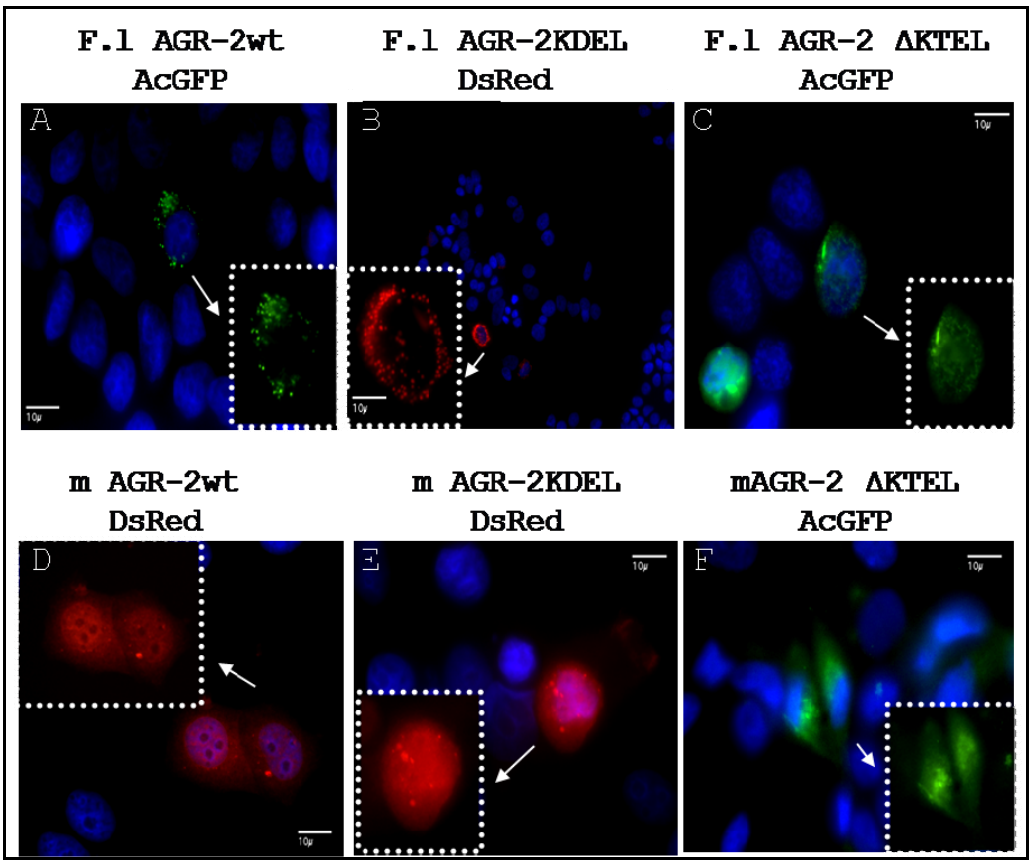

Figure 3.15: Intracellular localization of mature and full length AGR-2 GFP/RFP using fluorescent microscopy Merge images of MCF-7 carcinoma cells transfected with full length (panels A-C) or mature (panels D-F) AGR-2wt RFP/GFP constructs and visualized by fluorescence microscopy. KDEL (panels B and E) and KTEL deletion (Δ_{KTEL}) (panels C and F) fluorescent mutants of both isoforms are also depicted. Small images included in white frames of each photo show the localization of each construct without DAPI staining. Images visualized by Zeiss Axionplan microscope and captured with the photometric CoolSnap HQ camera. Same exposure times applied for all images. Figure showing representative of 5 independent experiments. Nuclei were visualized by DAPI. Scalebar represents 10μm.

3.2.3.2 Co-localization of the mature and full length AGR-2 RFP constructs with ER and Golgi

The transfection of the "inactive" full length AGR-2wt RFP, that bears the KTEL sequence, expression vector results in largely cytosolic RFP-protein expression, which in turn co-localizes to a relatively high degree with the endoplasmic-reticulum marker protein PDI (Figure 3.16-3.17 panels A-D). DAPI along with brightfield microscopy independently verified this co-localization (Figure, 3.16-3.17 panels A-D). Quantitation of Fl AGR-2wt RFP revealed that ~33% of cells showed essentially complete, 100%, co-localization of AGR-2 with the endoplasmic-reticulum (Figure 3.22 panel B first column), whilst ~67% of cells showed less that 100% AGR-2 co-staining with the endoplasmic-reticulum (Figure 3.22 panel A). These results indicate that this isoform is not apparently expressed extracellularly and that it is largely an ER- localized isoform. Moreover, this form was not strictly co-localized to the ER indicating the dynamic nature of the protein, as it was also detected in the cytoplasm of transfected cells. Co-staining for the Golgi compartment showed no clear sign of co-localization (Figure 3.18 panels A-D).

The transfection of full length AGR-2 KDEL RFP containing the point mutation in the C-terminal domain, exhibited a more pronounced co-staining with the endoplasmic-reticulum (Figure 3.16-3.17 panels E-H) totally consistent to the presence of the KDEL ER-retention sequence which is typical of many of the ER-resident proteins. Quantitation revealed that approximately 79% of cells exhibited complete ER localization and 21% of cells exhibited less than 100% ER localization (Figure 3.22 panel B second column) so there was higher co-localization rate when compared to the wt RFP isoform that has the KTEL sequence (Figure 3.22 panel B first column). Brightfield was consistent to nuclear localization data (Figure 3.16-3.17 panels A).Thus, mutation of the KTEL sequence also resulted in ER sequestration of the protein and no evidence was seen of extracellular or plasma membrane localization (Figure 3.16-3.17 panels E-H). The divergence of the highly conserved KTEL sequence of AGR-2 away from the canonical KDEL endoplasmic-

reticulum retention sequence presumably lowers the affinity of AGR-2 for the endoplasmic-reticulum receptor protein and allows AGR-2 to exit the endoplasmic-reticulum at a higher rate. Again, no Golgi co-localization was detected, although these two compartments show high affinity to each other and collaborate in the secretory pathway (Figure 3.18 panels E-H). Transfection of the deletion mutant full length AGR-2Δ_{KTEL} RFP resulted in a less distinct co-staining with the endoplasmic reticulum, (Figure 3.16-3.17 panels I-L) although a percentage of 37% of the cells exhibited total co-localization (Figure 3.22 panel B third column). Interestingly 63% of the cells showed less that 100% co-localization (Figure 3.22 panel B third column) to the ER. These non-co-localization levels for the full length AGR-2Δ_{KTEL} RFP were much lower than the KDEL mutant and a bit less than wt construct, as expected, due to the absence of the KTEL sequence (Figure 3.22 panel B). No Golgi co-staining was again observed (Figure 3.18 panels I-L).

The transfection of the "active" mature AGR-2wt RFP expression vector results in a qualitatively different distribution than the full-length isoform of AGR-2, although extracellular or plasma membrane expression was again not observed. Mature AGR-2wt RFP exhibited both nuclear and diffuse cytosolic expression (Figure 3.19 panels A-D) with only relatively small amounts of co-localization with the endoplasmic-reticulum compartment (Figure 3.19 panels A-D). Interestingly, the protein was excluded from the nucleoli of the cells. Co-localization percentages varied amongst cells, so to enable graphical representation and grouping the 10% rate was chosen as a reference point for all graphs. Quantitation revealed that approximately 34% of cells showed nuclear and cytosolic expression with no endoplasmic-reticulum localization, whilst 66% of cells exhibited nuclear and cytosolic distribution but with less than 10% of granular endoplasmic-reticulum co-localization (Figure 3.22 panel A first column).

Similar to the full-length AGR-2KDEL RFP mutant, the transfection of the mature AGR-2KDEL RFP expression vector resulted in increased retention of AGR-2 in the endoplasmic reticulum (Figure 3.19 panels E-F) but qualitatively different distribution than the full-length isoform of AGR-2 (Figure 3.16-3.17 panels E-H),

although extracellular expression was again not observed. Mature AGR-2KDEL RFP exhibited little nuclear and diffuse cytosolic expression (Figure 3.19 panels E-F). The expression of mature AGR-2KDEL RFP was confined predominantly to granular endoplasmic reticulum with 43% of cells showing more than 10% endoplasmic reticulum co-localization while the rest of the cells had less that 10% co-localization rate (Figure 3.22 panel A second column). Nevertheless, all the cells had distinct granules within the cytoplasm which were more in number and density that in the wt form of the protein (Figure 3.19 panels A-D). Together, these data indicate that the N-terminal leader sequence of AGR-2 shifts the equilibrium of AGR-2 towards the ER whilst the C-terminal sequence is required for entry of AGR-2 into nuclear pools. Interestingly, the mature AGR-2 Δ_{KTEL} GFP mutant was characterised by total absence of granules within the cytoplasm and all the cells showed diffused cytosolic distribution as well as dimly nuclear localization of the protein (Figure 3.19 panels I-L). It is worth mentioning, that this construct behaved in a rather unstable way and was bleached after a few exposures under the microscope whereas the GFP vector was highly steady and durable even after very long exposures (Figure 3.21 A-H. No Golgi co-staining was observed in none of the mature constructs (Figure 3.20 panels I-P). Control AcGFP-N_1 (Figure 3.21 panels I-P) and DsRed-N_1 (Figure 3.22 panels A-H) empty vector transfections were performed as well for every localization marker tested (Figure 3.21, ER: panels A-D and I-L, Golgi: panels E-H and M-P). Both FPs showed non-selective distribution patterns and were detected everywhere in the cells, including the nucleoli, although very few DsRed-transfected cells excluded the protein from the nucleoli but these were not more that 5% of all population (representative photo shown in Figure 3.22 panel B).

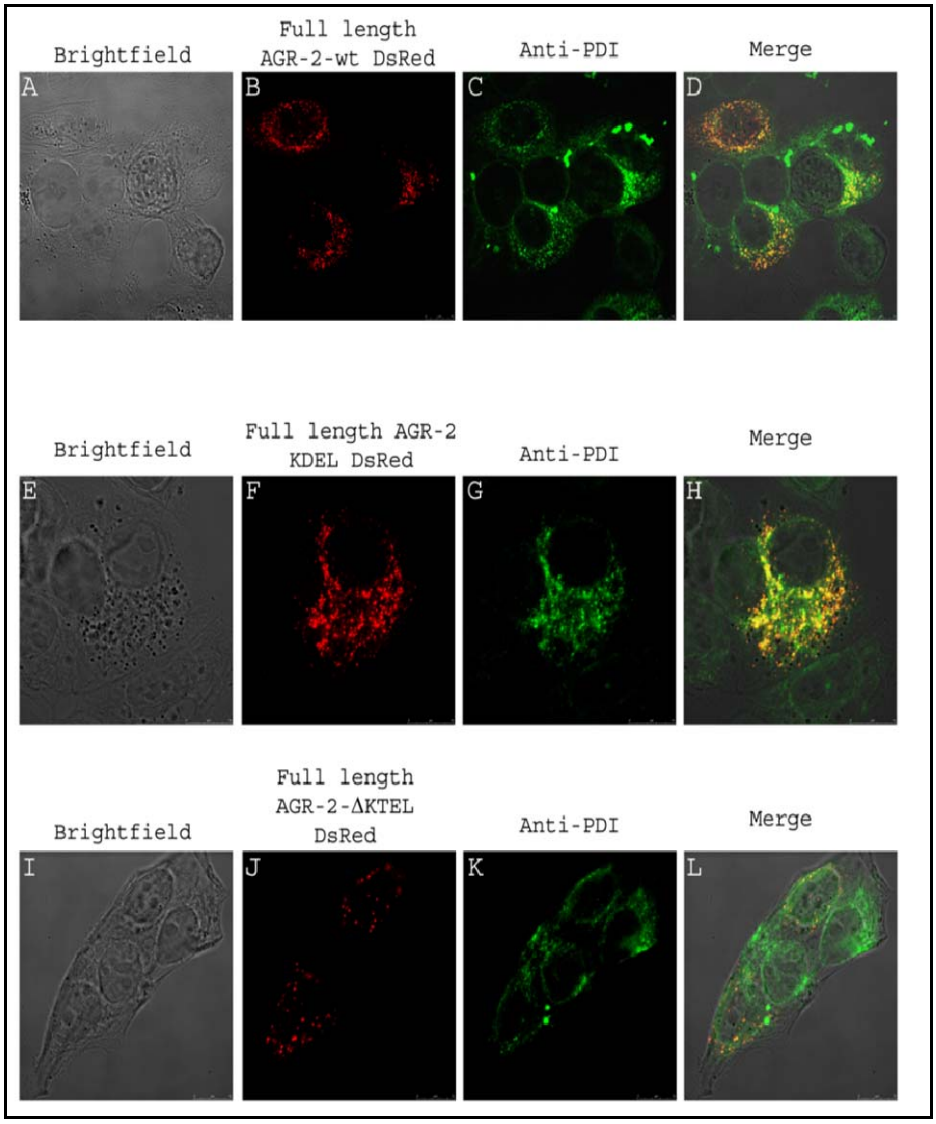

Figure 3.16: Intracellular localization of full-length AGR-2 RFP in respect to the endoplasmic reticulum. MCF-7 cells were transfected with the indicated vector expressing full-length AGR-2wt RFP (panels A-D), full-length RFP-tagged AGR-2 containing a mutation in the C-terminal KTEL motif (AGR-2^{T173D}) (panels E-H) or full-length RFP-tagged AGR-2 with no KTEL sequence (Δ_{KTEL}) (panels I-L). After fixation of cells, the endoplasmic reticulum was visualized using an anti-PDI-specific antibody. The brightfields are shown in panels A , E and I; AGR-2 localization is highlighted in panels B, F and J; PDI expression is depicted in panels C, G and K, and the extent of co-localization of AGR-2 and PDI was determined by merging the respective images (D, H and L) using a Leica SP5 confocal microscope. Figure is representative of at least 5 independent experiments.

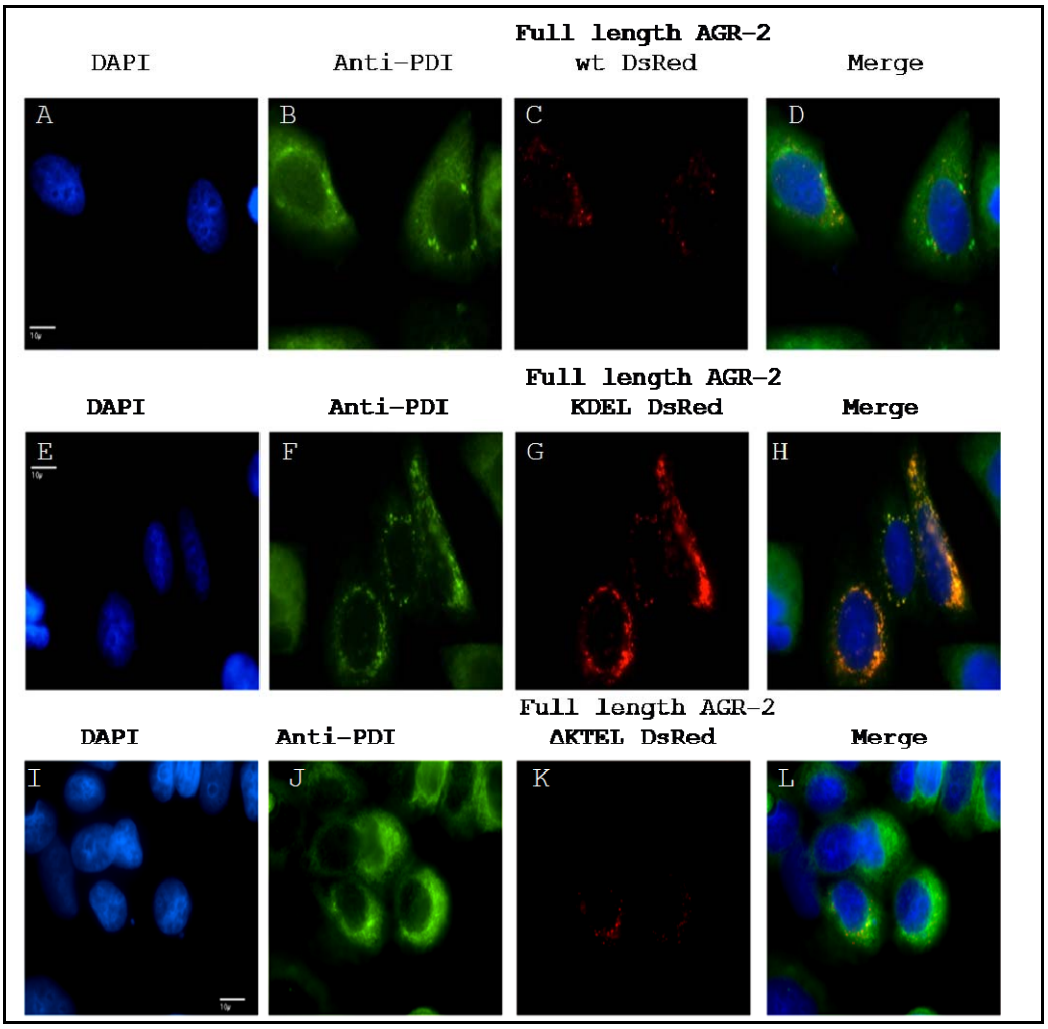

Figure 3.17: Intracellular localization of full-length AGR-2 RFP in respect to nuclear markers and ER. MCF-7 cells were transfected with the indicated vector expressing full-length AGR-2wt RFP (panels A-D), full-length RFP-tagged AGR-2 containing a mutation in the C-terminal KTEL motif (AGR-2^{T173D}) (panels E-H) or full-length RFP-tagged AGR-2 with no KTEL sequence (Δ_{KTEL})(panels I-L). After fixation of cells, the endoplasmic reticulum was visualized using an anti-PDI-specific antibody. DAPI is shown in panels A, E and F, AGR-2 localization is highlighted in panels B, F and J; PDI expression is depicted in panels C, G and K, and the extent of co-localization of AGR-2 and PDI was determined by merging the respective images (D, H and L) using a Zeiss microscope equipped with spectral separation filters. Figure is representative of at least 5 independent experiments. Scalebar represents 10µm.

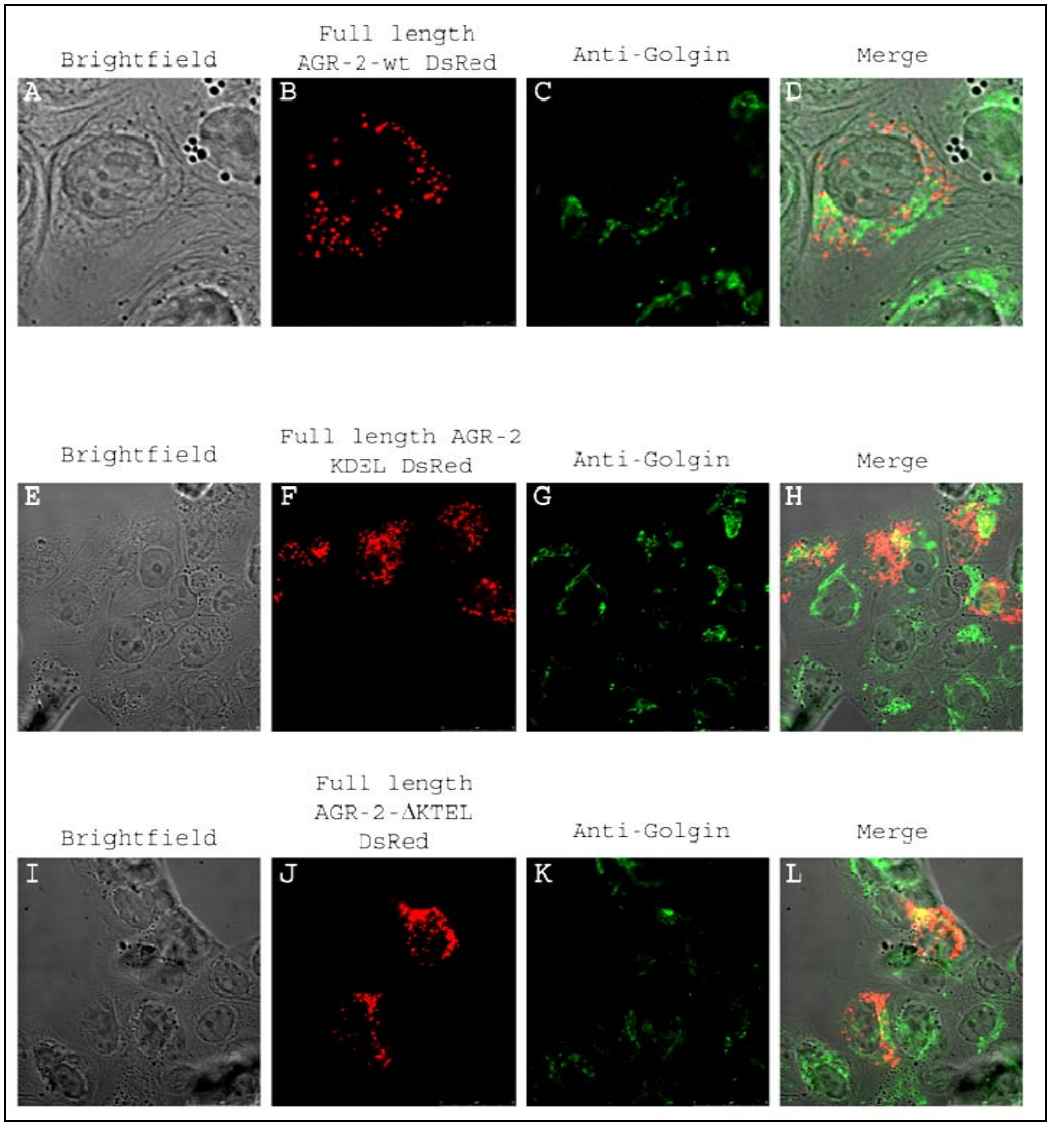

Figure 3.18: Intracellular localization of full-length AGR-2 RFP in respect to the Golgi compartment. MCF-7 cells were transfected with the indicated vector expressing full-length AGR-2wt RFP (panels A-D), full-length RFP-tagged AGR-2 containing a mutation in the C-terminal KTEL motif (AGR-2^{T173D}) (panels E-H) or full-length RFP-tagged AGR-2 with no KTEL sequence (ΔKTEL) (panels I-L). After fixation of cells, the Golgi compartment was visualized using an anti-Golgin-specific antibody. The brightfields are shown in panels A , E and I; AGR-2 localization is highlighted in panels B, F and J; Golgin expression is depicted in panels C, G and K, and the extent of co-localization of AGR-2 and Golgin was determined by merging the respective images (D, H and L) using a Leica SP5 confocal microscope. Figure is representative of at least 5 independent experiments.

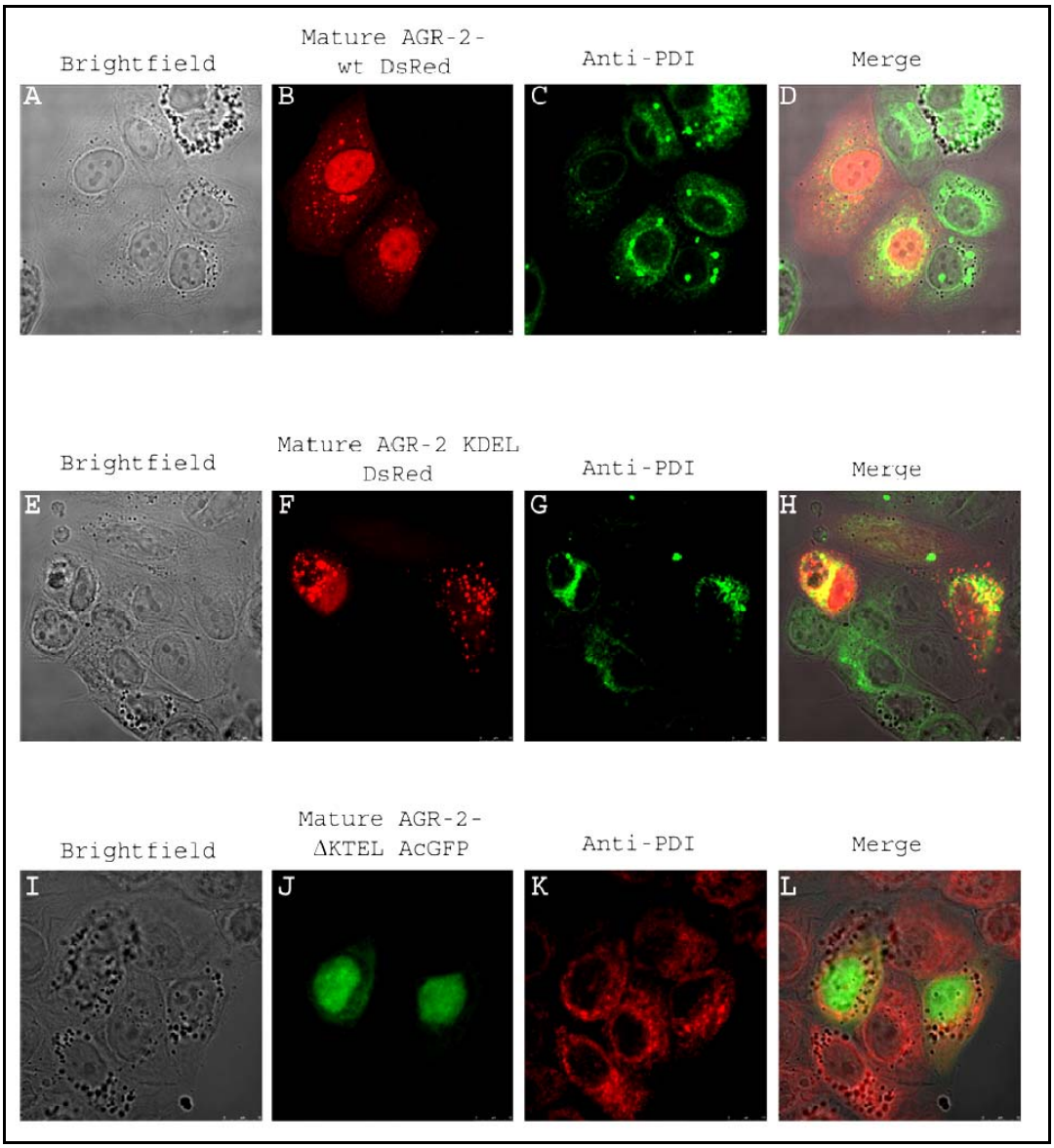

Figure 3.19: Intracellular localization of mature AGR-2 RFP in respect to the endoplasmic reticulum. MCF-7 cells were transfected with the indicated vector expressing mature RFP-tagged AGR-2wt (panel s A-D), mature AGR-2 RFP containing a mutation in the C-terminal KTEL motif ($AGR2^{T173D}$) (panel s E-H), or mature GFP-tagged AGR-2 without the C-terminal KTEL tetrapeptide (Δ_{KTEL}) (panels I-L). After fixation of cells, the endoplasmic reticulum was visualized using an anti-PDI-specific antibody (C, G, and K). The extent of co-localization of AGR-2 and PDI was determined by merging the respective images (D, H, and L) using a Leica confocal microscope. Figure is representative of at least 5 independent experiments.

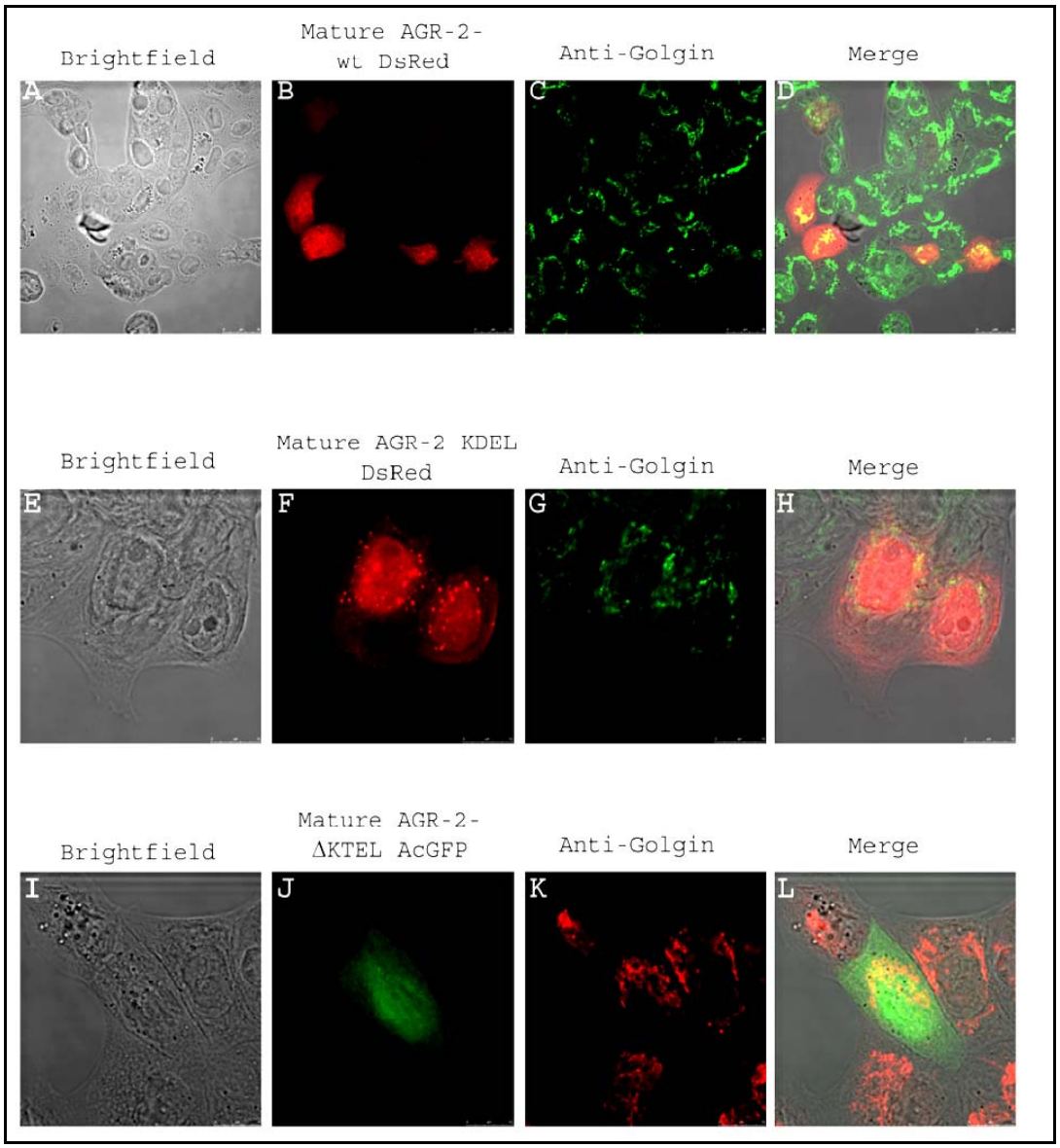

Figure 3.20: Intracellular localization of mature AGR-2 RFP in respect to the Golgi compartment. MCF-7 cells were transfected with the indicated vector expressing mature RFP-tagged AGR-2wt (panels A-D), mature AGR-2 RFP containing a mutation in the C-terminal KTEL motif ($AGR2^{T173D}$) (panel s E-H), or mature GFP-tagged AGR-2 without the C-terminal KTEL tetrapeptide (Δ_{KTEL}) (panels I-L). After fixation of cells, the Golgi was visualized using an anti-Golgin-specific antibody (C, G, and K). The extent of co-localization of AGR-2 and PDI was determined by merging the respective images (D, H, and L) using a Leica confocal microscope. Figure is representative of at least 5 independent experiments.

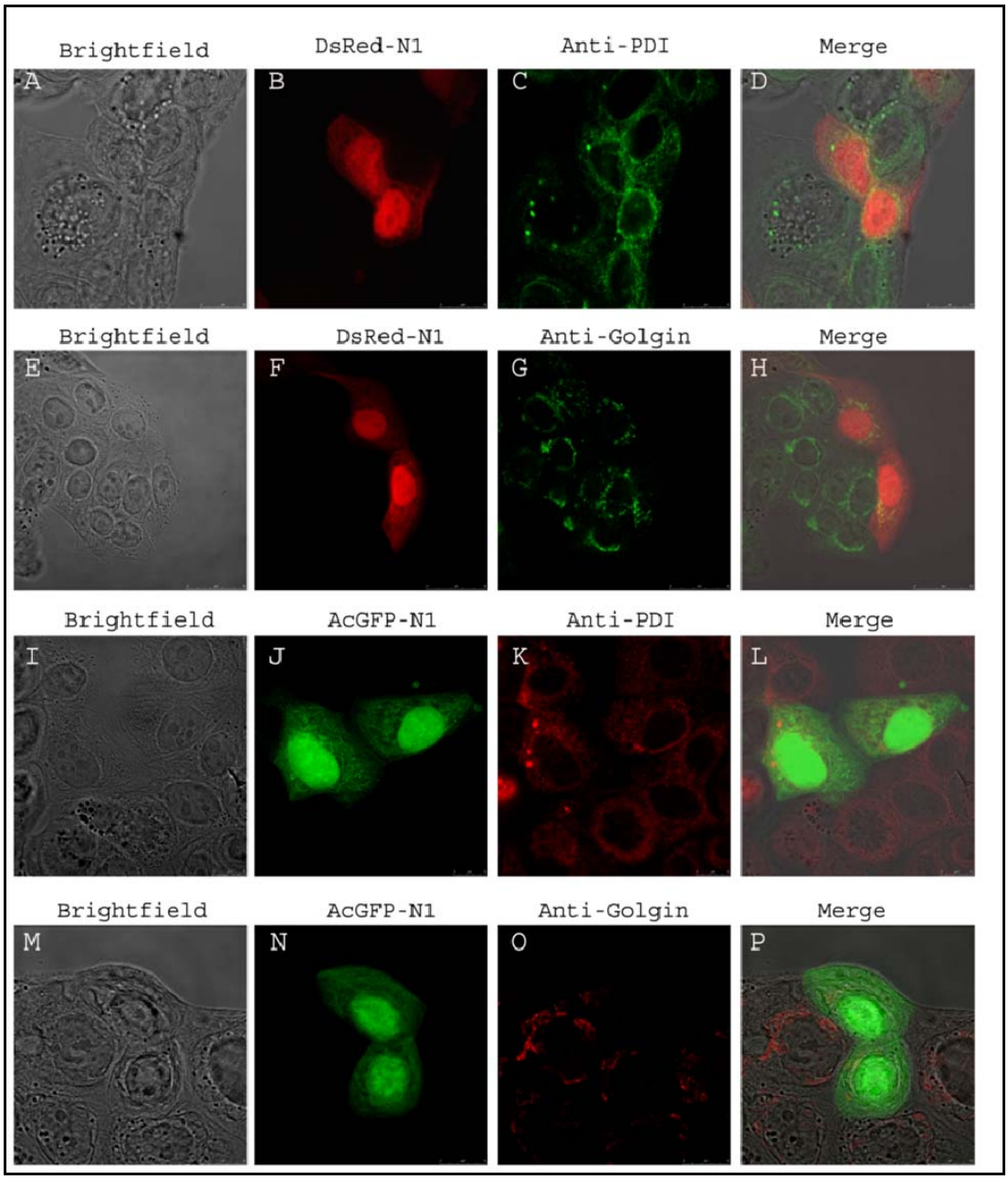

Figure 3.21: Intracellular localization AcGFP-N_1 and DsRed-N_1 control vectors. MCF-7 cells were transfected with the indicated vector DsRed-N_1 (panels A-H) or AcGFP-N_1 (panels I-P) expressing only the fluorescent protein without any additional proteins fused to its C-terminus. After fixation of cells, the endoplasmic reticulum was visualized by anti-PDI-specific antibodies (panels C and K) and the Golgi using an anti-Golgin-specific antibody (panels G and O). Images taken by a Leica SP5 confocal microscope. Figure is representative of at least 5 independent experiments.

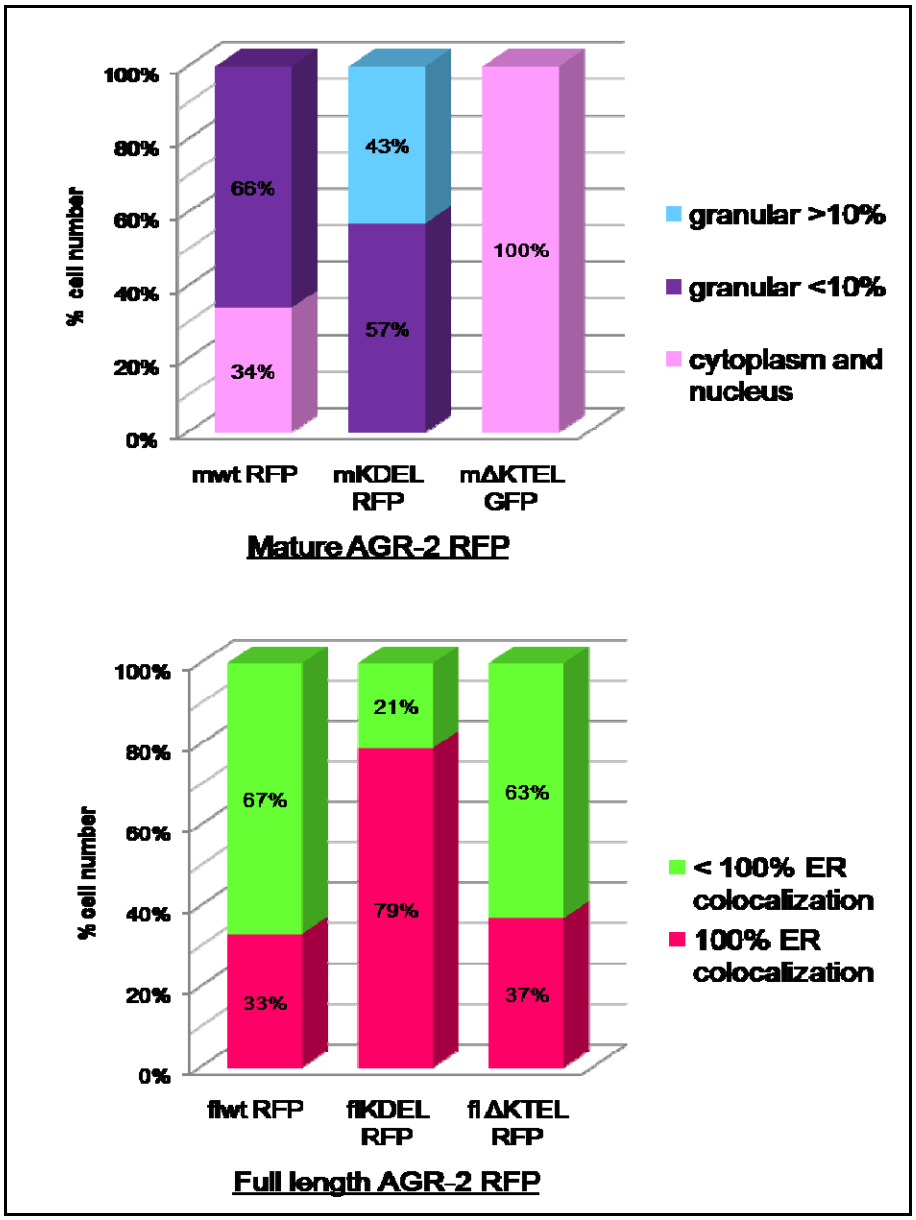

Figure 3.22: Graphical representation of the co-localization extent of each mature or full length RFP/GFP construct, wt KDEL and ΔKTEL. MCF-7 cells transfected with each of the constructs and blotted against the ER, were tested for co-staining rate. Co-localization rate defined by the LEICA SP5 Application Suite in a total of 1000 nuclei.

3.2.3.3 Mitochondrial localization of the full length AGR-2wt and Δ_{KTEL} fluorescent clones

To further investigate whether the full length wt and Δ_{KTEL} AGR-2 RFP clones were co-localized with other organelles apart from the endoplasmic reticulum and the Golgi compartment, the mitochondria network was tested (Figure 3.23 panels A-H). The full length AGR-2KDEL RFP mutant was not tested because it showed almost total co-localization with the ER (Figure 3.22 B second column, Figure 3.16 panels E-F). Mitotracker Green is a green fluorescent dye that stains the mitochondria of the cells. Mitochondria, in MCF-7 cells, are distributed around the nucleus in a string-alike reticulum and usually take up most of the cytoplasm. The wt RFP form of the full length protein did not co-localize with the mitochondria and interestingly it showed a rather peri-mitochondrial distribution (Figure 3.23 panels A-D). The same pattern was followed by the KTEL deletion RFP mutant (Figure 3.23 panels A-D). The protein was detected around and on the top of mitochondria, on an anterior-posterior orientation axis, but no co-localization was observed. Control DsRed-N_1 vector-only transfected cells emitted red fluorescence in the nucleus and within the cytoplasm and small co-staining with the mitochondria was observed, with only a few co-localization areas stained in yellow, as expected by a non-specific FP (Figure 3.23 panels I-L).

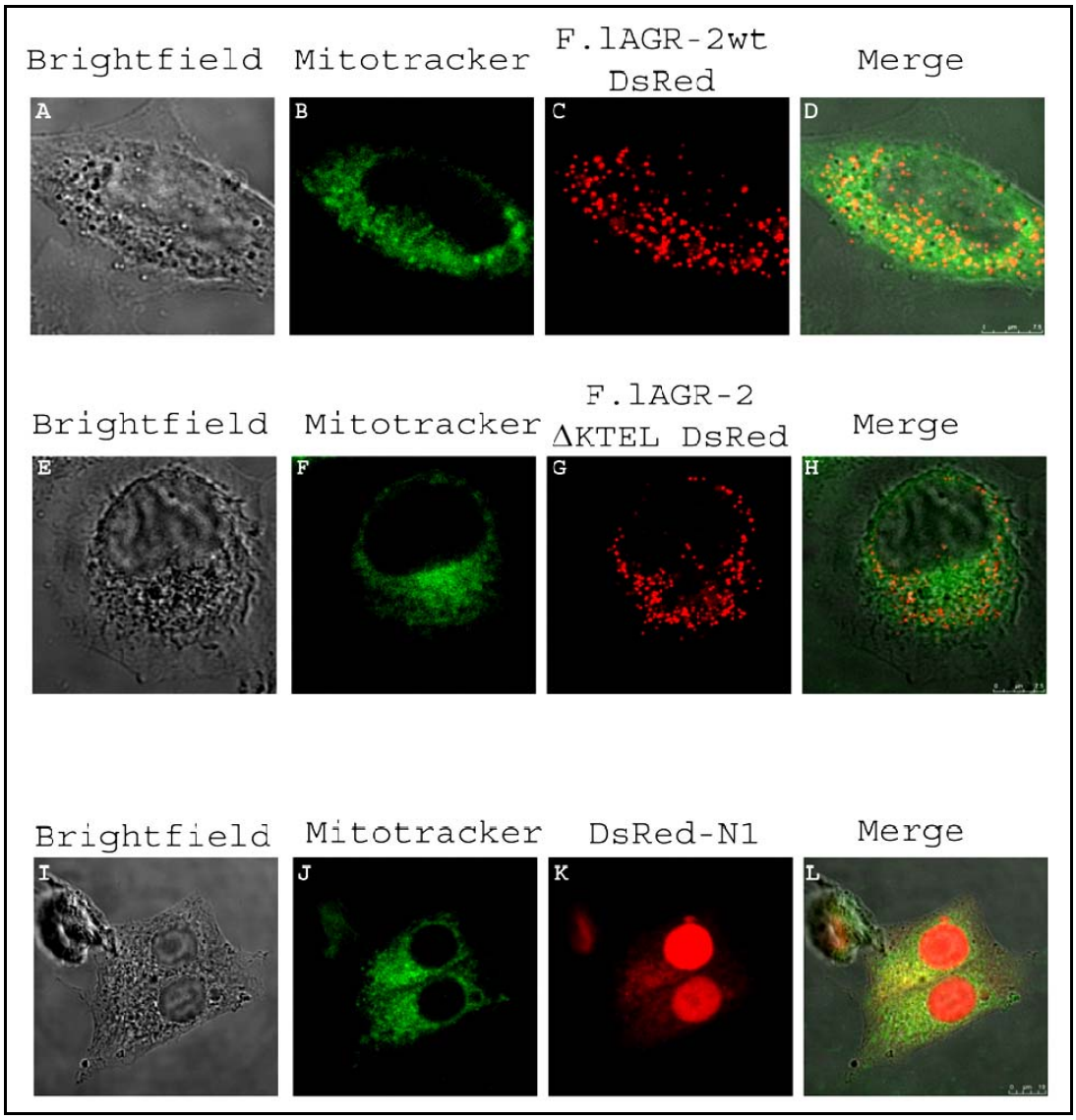

Figure 3.23: Intracellular localization of full-length AGR-2 RFP in respect to the mitochondria network. MCF-7 cells transfected with full-length AGR-2wt RFP (panels A-D), full-length RFP-tagged AGR-2 without the C-terminal KTEL motif (Δ_{KTEL}) (panels E-H) or DsRed-N_1 vector control (panels I-L). Before fixation, Mitotracker Green was added to the cells to visualize mitochondria (panels B, F and J). Brightfields are shown in panels A, E and I; AGR-2 RFP localization is highlighted in panels C, G and K; Mitotracker is depicted in panels B, F and J, and the extent of co-localization of AGR-2 and Mitotracker was determined by merging the respective images (D, H and L) using a Leica SP5 confocal microscope. Figure is representative of at least 3 independent experiments.

3.2.3.4 Subcellular fractionation of the fluorescent constructs

We next complemented the confocal microscopy by examining the localization of the endogenous AGR-2 and transfected AGR-2 RFP using subcellular chemical extraction methodologies in order to determine whether (i) the C-terminus of AGR-2 permits nuclear entry of the AGR-2 isoform and (ii) endogenous AGR-2 can enter the nucleus. Two different exposures are shown for quantification purposes (Figure 3.24 right and left panels). In more detail, mature AGR-2wt RFP resulted in a relatively different distribution when compared to the endogenous protein, with AGR-2wt RFP highly expressed in the F_1 cytosolic and F_3 nuclear fractions when compared to the F_2 cell membrane and organelles fraction (Figure 3.24 A). The mutation to KDEL resulted in confinement of the mature AGR-2KDEL RFP protein to the cytosolic and membrane fractions and lower expression in the nuclear F_3 (Figure 3.24 B). These data again are relatively consistent with the microscopy (Figure 3.19 panels A-H), which indicated that the mature-AGR-2wt RFP can be diffuse cytosolic and nuclear, but mutation of the KTEL to KDEL shifts the equilibrium to a more confined compartmentalization outside the nucleus although nuclear localization is still present but in much lower levels than in the wt form of the protein (Figure 3.19 panels E-H). This difference was quantified and depicted in Figure 3.25. As a control, the endogenous AGR-2 protein appears as only one band, at ~18kDa, and detected in three fractions: the F_1 cytosolic, the F_2 membrane/organelles and the F_3 nuclear fractions (Figure 3.24 panels A-C bottom lane) resembling the siatridution of the mature AGR-2wt RFP protein. Total deletion of the KTEL sequence resulted in strictly cytosolic localization but in very low levels (Figure 3.24 C), further supporting the fluorescent microscopy data, which suggested a rather unstable cytosolic form of the protein (Figure 3.19 panels I-L).

The transfection of RFP-tagged full length AGR-2wt resulted in a distribution into the cytosolic, membrane/organellar fraction, nuclear, and cytoskeletal fractions (Figure 3.24 A). The full length AGR-2wt RFP when compared to the mature form of the protein showed higher organelles/membrane F_2 expression levels (Figure 3.24

A), further supporting the fluorescent microscopy data that the full length isoform strongly co-localizes to the endoplasmic reticulum (Figure 3.22 A-B first columns). The mutation to KDEL resulted in confinement of the full-length AGR-2 RFP protein to the cytosolic and membrane/organelles fractions (Figure 3.24 B). These data are relatively consistent with the microscopy, which indicated that mutation of the KTEL to KDEL shifts the equilibrium to a more confined compartmentalization (Figure 3.22 B). This full length KDEL RFP mutant had much higher cytosolic and membrane distribution that the equivalent mature one which is presumably due to the presence of the leader sequence that supposed to designate the protein to secretion (Figure 3.24 B). The full length AGR-2wt RFP followed the same patterns when it came to the first three fractions with very strong presence of the protein in F_2 fraction which is the one representing the cell membrane and organelles extract (Figure 3.24 A). The full length deletion mutant AGR-2Δ_{KTEL} RFP showed lower expression levels in F_1 cytosolic and F_2 membrane/organelles fractions when compared to the full length wt and KDEL mutant, as expected (Figure 3.24 C). This mutant is the one that has the lowest co-localization rate to the endoplasmic reticulum (Figure 3.22 B third column) and, as shown by Western blotting here, the lowest expression levels in the cytosolic and membrane/organelles fraction compared to the wt and KDEL RFP mutants (Figure 3.24 A-C).

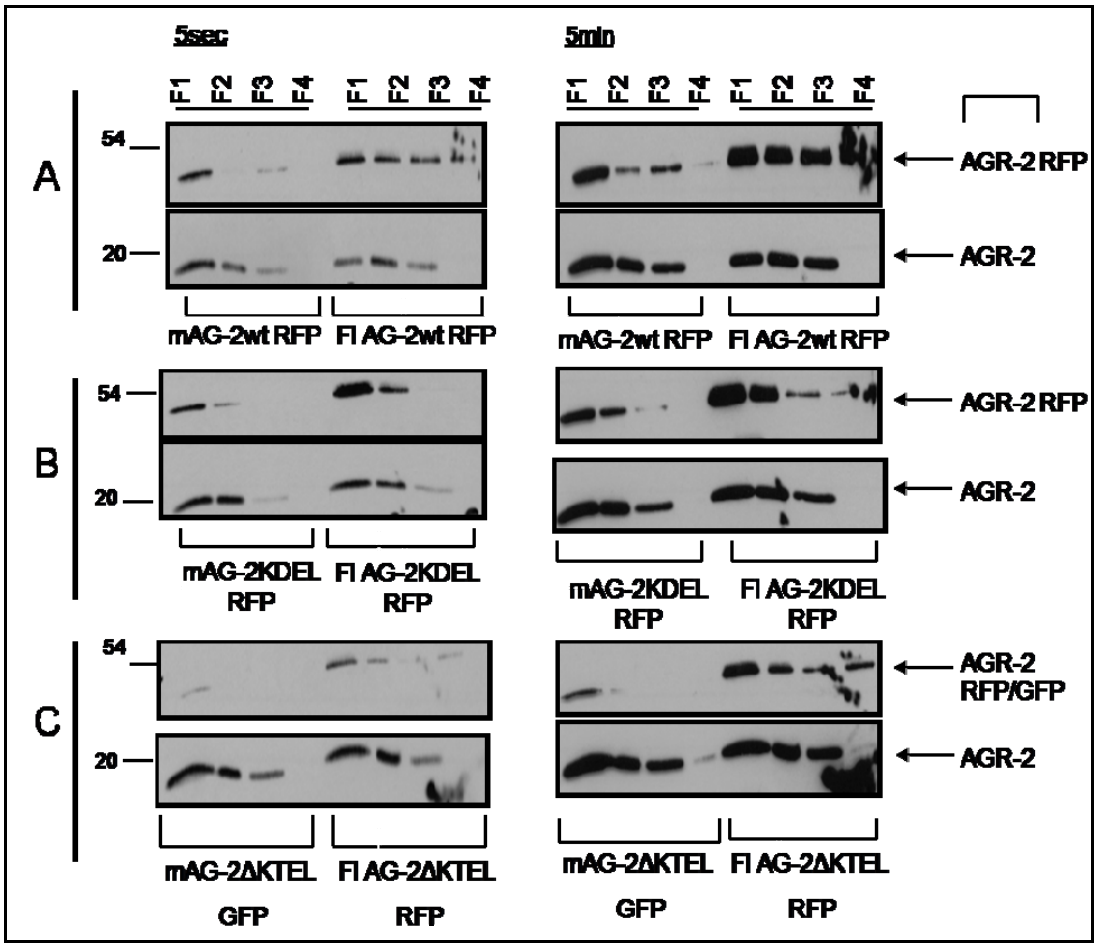

Figure 3.24: Intracellular localization of AGR-2 RFP isoforms using chemical fraction. MCF-7 cells were transfected with the indicated vector expressing mature or full length AGR-2wt RFP (panel A), mature/full-length AGR-2 RFP containing a mutation in the C-terminal KTEL motif ($AGR2^{T173D}$) (panel B), mature/full length GFP/RFP-tagged AGR-2 without the C-terminal KTEL tetrapeptide (Δ_{KTEL}) (panel C) respectively. The cells were processed using fractionation methodologies into F_1 (cytosolic), F_2 (membrane/organelles), F_3 (nuclear), and F_4 (cytoskeletal) as indicated. The distribution of the RFP-tagged AGR-2 isoform (top section, ~ 50 kDa) or endogenous AGR-2 protein (bottom section, ~ 18 kDa) was determined by immunoblotting. Different exposure times are depicted. Figure is representative of 3 independent experiments.

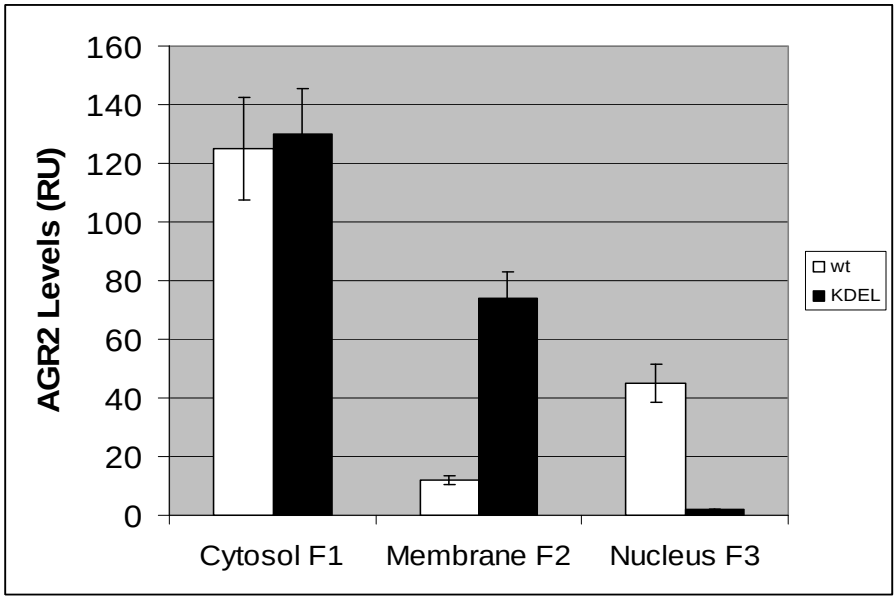

Figure 3.25: Quantitation of RFP-tagged mature AGR-2wt and mature AGR-2 KDEL isoforms distribution into nuclear and cytosolic fractions.

3.2.4 Localization of wt/KDEL and Δ_{KTEL} AGR-2 RFP constructs in an AGR2-negative cell line

To further characterize the distribution differences between the mature and full length wt-KDEL and Δ_{KTEL} RFP constructs, MDA-MB 231 breast cancer cells were used. This cell line is Estrogen Receptor α /AGR2-negative and is normally used as a negative control. MCF-7 cells have high levels of endogenous AGR-2 and so the pathways that the protein participates are active. On the other hand, MDA-MB 231 do not have endogenous protein and are useful in investigating the localization differences of the mutants in a cell system deficient in AGR-2.

Interestingly, mature AGR-2wt RFP was detected in the cytosolic, nuclear and cytoskeleton fraction (Figure 3.26 B). No membrane/organelle distribution was observed. AGR-2 was highly expressed in the nuclear fraction and also detected in the cytoskeleton but in much lower levels. Mutation of the KTEL sequence to KDEL

shifted the equilibrium to the cytosolic and membrane/organelles fractions although nuclear localization was still retained (Figure 3.26 B). Interestingly, the expression levels of the mature AGR-2KDEL RFP protein in the membrane and organelles fraction was induced and reached similar levels to the cytosolic and nuclear expression of the protein, when compared to the equivalent wt form. Deletion of the KTEL sequence in the C-terminus restored the localization patterns to the cytosolic and nuclear fractions and interestingly the cytosolic distribution of this mutant was relatively more intense when compared to the wt protein patterns (Figure 3.26 B), whereas nuclear AGR-2 was expressed in a much lesser extent when the KTEL sequence was deleted.

As far as the full length constructs is concerned, the full length AGR-2wt RFP was distributed in the first three fractions and was more intense in the cytosolic and nuclear fraction (Figure 3.26 C). Moreover, the membrane/organelles fraction showed relatively higher AGR-2 expression levels when compared to the mature wt that had undetectable protein levels (Figure 3.26 B and C). However, the full length isoform had lower nuclear AGR-2wt RFP that the mature one. The cytoskeleton fraction also had low but detectable levels of AGR-2. Mutation of the KTEL sequence to KDEL induced the protein's expression levels in all fractions and especially in the membrane/organelles fraction (Figure 3.26 C). The cytosolic and nuclear levels were elevated as well compared to the wt form of the full length isoform. The induction of full length AGR-2 RFP after KDEL mutation, resembled the pattern observed when the mature AGR-2wt RFP was mutated to KDEL in the same cell line, where the same mutation caused elevation of AGR-2 levels in all the fractions apart from the cytoskeleton one (Figure 3.26 B and C). Deletion of the last four KTEL amino acids resulted in total loss of the protein from the nuclear fraction and further engaged it to the cytosolic and membrane fractions (Figure 3.26 C). The membrane/organelles fraction had much higher protein levels when compared to the wt form. Control untransfected and vector only samples showed no signs of the protein, as expected (Figure 3.26 A).

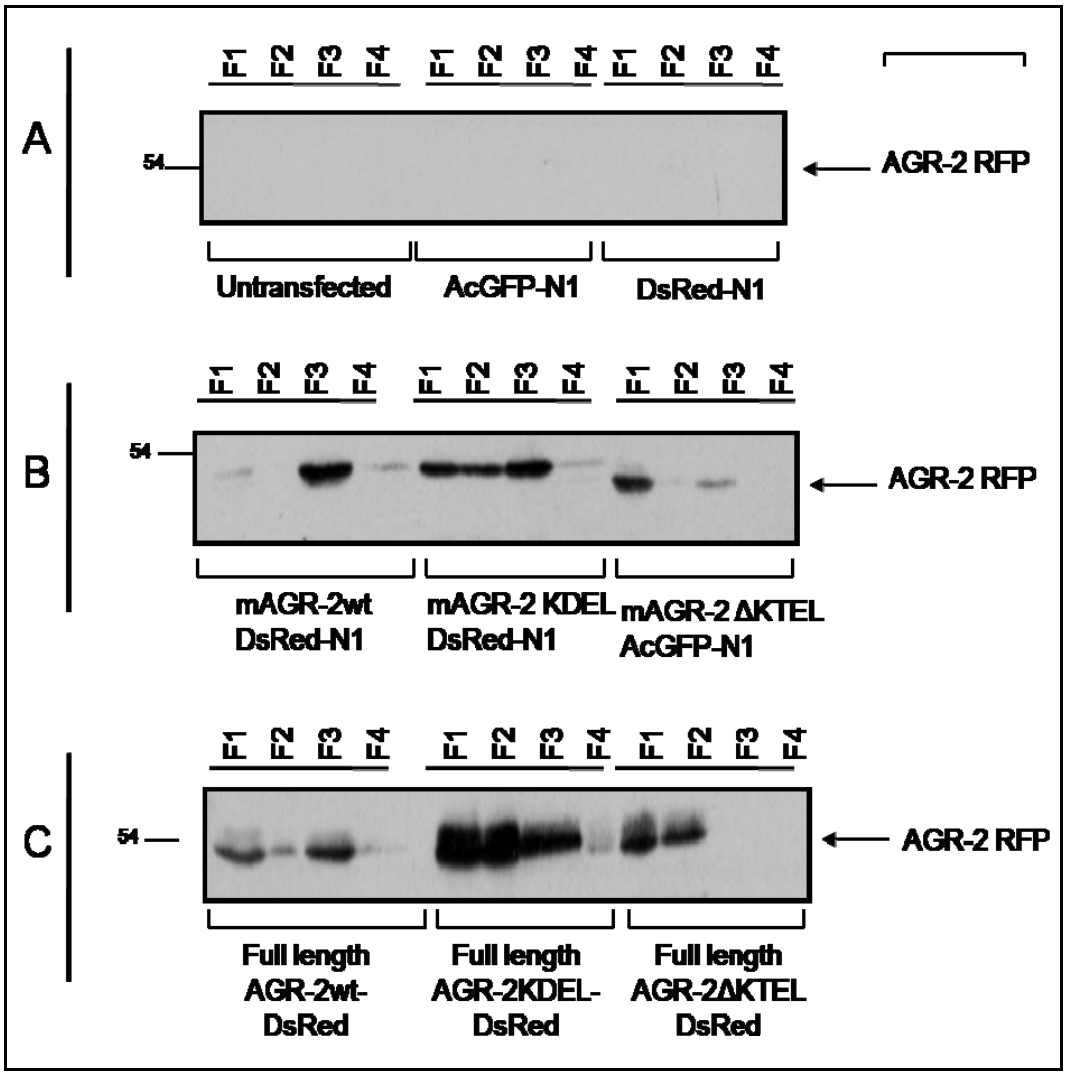

Figure 3.26: Intracellular localization of AGR-2 isoforms using chemical fraction in an AGR-2 negative cell line. MDA-MB 231 cells were transfected with the indicated vector expressing full-length AGR-2wt RFP, full-length AGR-2 RFP containing a mutation in the C-terminal KTEL motif ($AGR2^{T173D}$), full length RFP-tagged AGR-2 without the C-terminal KTEL tetrapeptide (Δ_{KTEL}) (panel C) and mature AGR-2 RFP, mature AGR-2 RFP containing a mutation in the C-terminal KTEL motif ($AGR2^{T173D}$)/ mature GFP-tagged AGR-2 without the C-terminal KTEL tetrapeptide (Δ_{KTEL}) (panel B). Control vector AcGFP-N_1 and DsRed-N_1 transfections were included in the experiment (panel A). The cells were processed using fractionation methodologies into F1 (cytosolic), F2 (membrane/organelles), F3 (nuclear), and F4 (cytoskeletal) as indicated. The distribution of the RFP-tagged AGR2 isoform (top section, ~ 50 kDa) was determined by immunoblotting.

3.2.5 Mature and Full length AGR-2KAEL RFP

Since the last four amino acids are essential to AGR-2 activity [474] and also the KTEL sequence plays an important role in maintaining nuclear localization we further mutated this sequence to KAEL. This substitution was chosen in order to further define the role of the threonine, T, which was the one mutated to aspartic acid, D, and affected the full length protein's localization towards the endoplasmic reticulum (Figure 3.22 B). A neutral mutation of this threonine to alanine will assist in determining the importance of this amino acid to localization of the protein. Site-directed mutagenesis on the mature and the full length AGR-2wt RFP that bears the KTEL sequence was applied. Subcellular fractionation of different cellular compartments revealed that presence of the KAEL mutated sequence highly induced the expression of mature AGR-2KAEL RFP mutant in the cytoplasm whereas reduced it in the membrane/organelles and nuclear fractions, when compared to the AGR-2wt RFP construct (Figure 3.27 A). Nuclear reduction was much stronger compared to the organellar one. As far as the full length AGR-2 is concerned, presence of the KAEL sequence did not significantly alter the distribution of the protein in the cytosolic and membrane/organelles fraction (Figure 3.27 B). On the other hand, the nuclear fraction was again affected, with the KAEL mutant's expression levels being reduced compared to the wt control (Figure 3.27 A). What is more, KAEL presence in the C-terminus of the mature and the full length form of the protein as well, lead to increase of AGR-2 in the cytoskeleton fraction F_4. Endogenous AGR-2 control expression levels remained unaltered in all the samples (Figure 3.27 A and B).

To further evaluate the KAEL mutant, fluorescent microscopy was performed (Figure 3.28). ER and Golgi markers were used to test for co-staining (Figure 3.28 panels C/G and K/O, respectively). Mature AGR-2KAEL RFP was again nuclear with some granules distributed within the cytosol but very low endoplasmic reticulum co-localization was observed. Only a few granules co-stained with the anti-PDI marker with less than 5% co-localization rate (Figure 3.28 panels E-H). The full

length AGR-2KAEL RFP vector had granular appearance and distributed within the cytosol but under a perinuclear pattern. The mutant was localized around the endoplasmic reticulum in a spherical way and some co-staining was detected (Figure 3.28 panels A-D). Neither mature nor full length AGR-2KAEL RFP mutants co-localized with the Golgi marker (Figure 3.28 panels I-P). Interestingly, the full length AGR-2KAEL RFP vector followed a characteristic distribution pattern around and adjacent to the Golgi compartment (Figure 3.28 panels I-L).

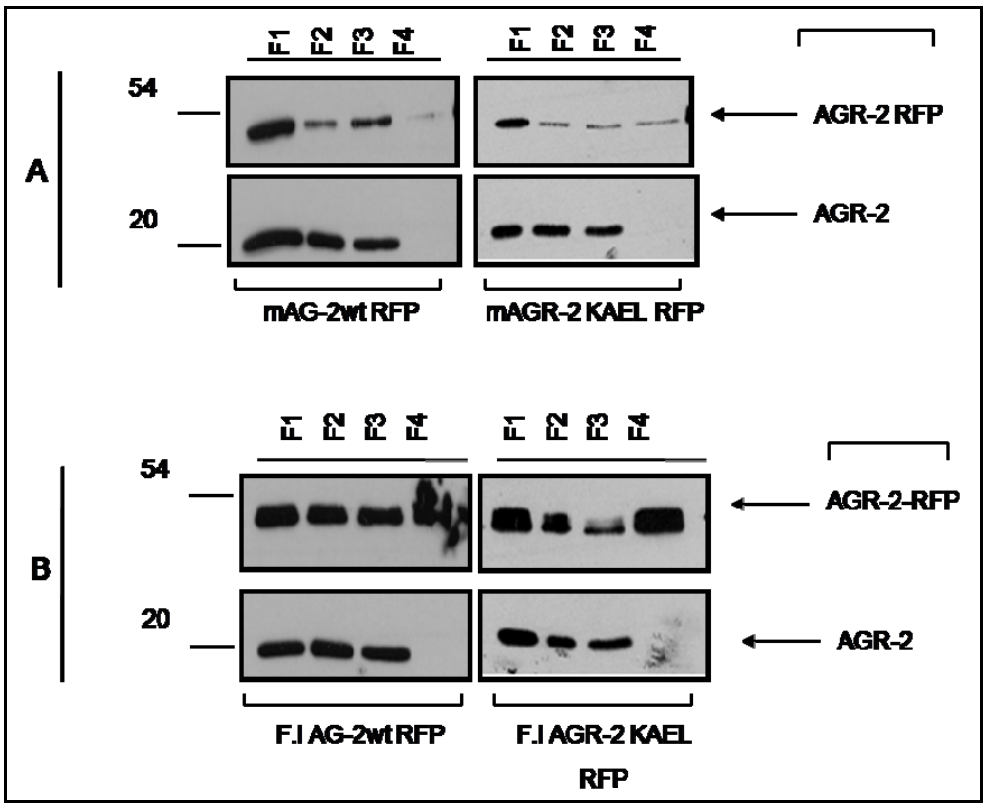

Figure 3.27: Intracellular localization of mature and full length AGR-2 RFP KAEL mutants by chemical fraction. MCF-7 cells were transfected with vectors expressing full-length AGR2wt RFP /Fl AGR-2 RFP containing a mutation in the C-terminal KTEL motif ($AGR2^{T173A}$) (panel B) or mature AGR-2wt/mAGR-2 RFP containing a mutation in the C-terminal KTEL motif ($AGR2^{T173A}$) (panel A). The cells were processed using fractionation methodologies into F_1 (cytosolic), F_2 (membrane/organelles), F_3 (nuclear), and F_4 (cytoskeletal) as indicated. The distribution of the RFP-tagged AGR2 isoform (top section, ~50 kDa) or endogenous AGR-2 protein (bottom section, ~ 18 kDa) was determined by immunoblotting.

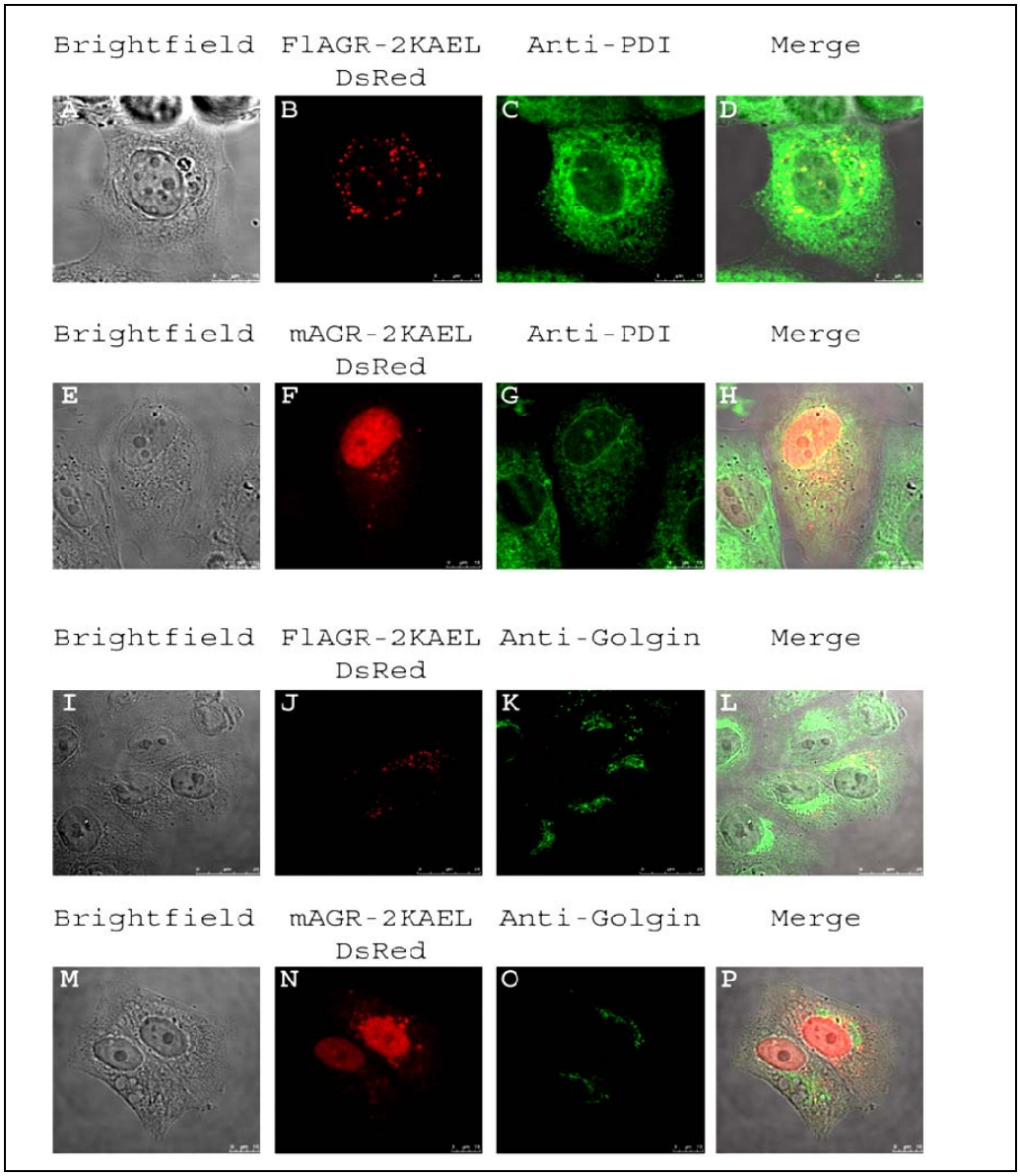

Figure 3.28: Intracellular localization of of mature and full length AGR-2KAEL RFP mutants by confocal microscopy. MCF-7 cells were transfected with the indicated vector expressing full length RFP-tagged AGR-2 containing a mutation in the C-terminal KTEL motif ($AGR2^{T173A}$) (panel A-D and I-L) or mature AGR-2 RFP with the same mutation in the C-terminal KTEL motif ($AGR2^{T173A}$) (panel E-H and M-P). After fixation of cells, the endoplasmic reticulum was visualized using an anti-PDI-specific antibody (panels C and G) whereas the Golgi compartment by an anti-Golgin-specific antibody (panels K and O). The extent of co-localization of AGR-2 and PDI was determined by merging the respective images (D, H, L and P) using a Leica confocal microscope.

3.3 Discussion

3.3.1 MCF-7 and MCF7-derived cells show different AGR-2 distribution

Localization studies are a useful tool when it comes to defining the role of many proteins. Proteins must be localized in the same subcellular compartment to cooperate toward a common physiological function. The position of a protein, most of times, determine its role, as transcription factors are distributed in the nucleus [368], secretory proteins in the cytoplasm, transporters in the cytoplasm as well, receptors in the cell membrane and so on, although the equilibrium is highly dynamic and changes according to environmental or not conditions. There are no studies up to present that suggest a principal form of the protein within the cell and the antibodies used recognise both forms, full length and mature as well. Since there is no way to discriminate between these two forms, the staining pattern observed is a combination of these both, cytoplasmic, perinuclear and nuclear. Endogenous AGR-2 in MCF-7 cells was distributed in a diffuse cytoplasmic way totally coherent to immunostaining data from cancer tissues [199](IH data presented here, Dr Nenutil) that showed the protein to be present in the cytoplasm (Figure 3.6). Monocolonal antibody immunostaining, detected the protein in the cytoplasm as well as in the perinuclear space and some signal was emitted from the nucleus as well (Figure 3.7). Subcellular fractionation of different cellular compartments (Figure 3.5) showed expression of the protein predominantly in the cytosol, less in membrane/organelles fraction and traces of the protein detected in the nuclear fraction coherent to the microscopy data.
MCF7-derived cell lines that show different resistance to Tamoxifen and ICI 182,780 have the same distribution patterns (Figure 3.6) but different expression levels of the protein in each compartment (Figure 3.5). LCC9 cells, which are totally resistant to Tamoxifen and the steroidal anti-oestrogen ICI 182,780 [75], show high nuclear levels of AGR-2 but the exact mechanism conferring this resistant phenotype is yet

unclear as many molecular mechanisms that vary between these cell lines are undefined. Interestingly, these data were consistent with high total protein expression levels and estrogen-independence in the LCC9, as performed by a separate group although Tamoxifen treatment induced AGR-2 expression [270]. The anti-oestrogen ICI 182/780 disrupts ERα shuttling from the nuclei to the cytoplasm by blocking its nuclear uptake [133]. It is proposed that these cells prevent ICI 182/780-induced effect on ER turnover or even alter events downstream the ER thereby bypassing effects on receptor turnover [75]. Interestingly, LCC9 have elevated PgR protein expression levels when grown without estrogenic supplementations although the ER levels remain unchanged compared to the MCF-7 cells. In addition, other considerable variations in gene expression including p21, p27, cyclin A, cyclin D_1, cyclin E and CDK4 and other genes implicated in tumourigenesis and regulation of oestrogen and anti-oestrogen cell cycle, were observed after SNP (Single Nucleotide Polymorphisms) and CGH (Comparative Genome Hybridization) analysis between LCC9 and MCF-7 [295], suggesting that AGR-2 might belong to the same category of differentially expressed genes and affect Tamoxifen resistance. LCCI on the other hand, have essentially comparable ER and PgR levels when compared to the parental MCF-7 cell line [75]. In our studies LCC1 showed intermediate nuclear expression levels of the protein comparable to MCF-7 (Figure 3.5) although studies have shown that the protein is elevated in LCCI cells as well [270]. Amplification or deletion of gene copies, alterations in transcriptional and translational regulation may contribute to altered protein production. Protein function or rate of degradation may be altered by changes in post-translational modifications. Alterations in the levels and activity of cellular proteins may be responsible for the development of tamoxifen or anti-oestrogen resistance. AGR-2 is a strong candidate protein for this resistance, since it was found to be associated with patient cell survival and response to anti-oestrogens while at the same time our data have supported that the protein is localized in different compartments and show variable expression levels in cell lines that have different response to anti-cancer drugs, consistent to previous studies [270]. Moreover, the protein is overexpressed in ER^+ cancers which are the ones that have

better clinical outcome compared to ER^- ones and is upregulated by Tamoxifen [270] but downregulated by aromatase inhibitors [374]. MCF7-derived cell lines that have different resistance to anti-oestrogens and show different AGR-2 localization patterns are an ideal system to start exploring the mechanisms conferring resistance and lead the way to a targeted therapy with better clinical outcome. Of course, more studies need to be conducted to further elucidate anti-oestrogen resistance and AGR-2 expression.

3.3.2 Endoplasmic reticulum retention is predominantly controlled by the N-terminal leader sequence in the full length AGR-2 RFP

Presence of a cleavable signal sequence, at position A^{20}-R^{21}, in AGR-2 leads the protein to secretion [3]. In general, signal sequences define whether proteins should be secreted or incorporated into a cytoplasmic membrane. Signal sequences have common features in their sequences but lack in primary structural homology [119]. Nonetheless, they share common properties including a positively charged N-terminal region (usually Lysine or Arginine but Histidine is sometimes an option, AGR-2 has $Lysine_3$) that is not essential for signal sequence function but improves its efficiency [479], a hydrophobic core of ~10 amino acids which often ends with a turn-forming residue, and a 6-8 amino acid-long, less hydrophobic (but usually uncharged) region that includes the cleavage site information [71, 603] (Figure 3.29). KTEL sequence, on the other hand, is implicated to endoplasmic reticulum retention. It is known that variants of the KDEL motif also work to keep proteins ER resident. A large study of 24 possible variants is listed as the Prosite motif for the ER localization of soluble proteins [KRHQSA]-[DENQ]-E-L; [274] and can be found online at *www.expasy.org*. However, there are several human proteins that are ER-located and contain variants of the KDEL motif that do not fit the Prosite motif such as ERp18 and ERp27 [14, 15]. Hence, it is possible that other motifs might also work as ER-retrieval signals. Bioinformatics approach identified motifs found on soluble

human proteins that enter the secretory pathway, i.e., motifs that might function in a natural system to ER-designate human proteins [483]. Based on the initial screen of A*X*DEL, AK*X*EL, AKD*X*L, and AKDE*X* variants, the bioinformatics analysis was restricted to human proteins that contained the motif *XX*[DE][FLM] at their extreme C terminus. Proteins containing these motifs were identified using Protein Prospector [98] and their sequences were analyzed by BLAST searches, SignalP [48] which predicts the signal peptide cleavage site, and PSORT II [265] which defines features such as polarity, hydrophobicity etc, to confirm that the sequence was the full-length protein, contained an N-terminal ER signal sequence, and that it was not predicted to be a transmembrane protein. This analysis identified 113 proteins that had 63 KDEL-like variants at their C-termini. In the same study the 37 KDEL-like variants ending in L that came out of the bioinformatics screen and had not previously been analyzed were made in the reporter construct, and the subcellular localization of the transiently transfected constructs was determined by immunofluorescence microscopy. The results revealed that 15 of these motifs resulted in efficient ER localization (>80% of HeLa cells showing ER localization), whereas many others resulted in at least partial ER localization. AGR-2 was also identified in this screen as a representative KTEL-motif protein [483] and will be further analysed below.

Pilot studies involving the AGR-2 gene fused to a C-terminal Green Fluorescent Protein showed that the fusion protein is secreted from HeLa cells [364]. Moreover, the gene is found to be upregulated in many secreting organs such as oesophagus, liver, breast and placenta, not to mention the secretory epithelial cells of the prostate gland [650]. The KTEL sequence is also characteristic of many of the proteins that belong to the thierodoxin superfamily to which AGR-2 is proposed to belong [468]. In our cell system, the leader sequence combined with the KTEL motif ensured a granular distribution of the protein fused to red fluorescent marker within the cytosol and a courteous percentage of endoplasmic reticulum co-localization whereas no cell membrane staining was observed (Figures 3.16, 3.17 and 3.22). These data are totally coherent to a study by Raykhel and co-workers that identified AGR-2 in a screen of 200 proteins with KDEL-like motives [483]. In this study AGR-2 was found to be

ER-co localized in 80% of HeLa cells tested whereas Golgi co-localization was observed in 20% of cells. In our cell system no Golgi co-localization was observed (Figure 3.18). Proteins to be secreted also pass from the endoplasmic reticulum, so it is possible that the leader sequence plays a role in this staining pattern, as it leads the protein to secretion after ER-passing through, although no secretion was detected in MCF-7. In the same study the protein was found to interact with all three ERD receptors ERD21, ERD22 and ERD23 but the interaction was stronger with the ERD21 receptor which appeared to be less a specialist as it bound to most of KDEL-like motives [483]. However, as a generalization, KDEL-like motifs are conserved between human and the African clawed frog (*Xenopus laevis*), which also has three KDEL receptors, as 83% of proteins would use the same human receptor most efficiently. This is also the fact with the KTEL sequence of AGR-2, which is conserved in human mouse and frog further supporting the essentiality and importance of it. In AGR-2 null cells transfected wt protein was distributed in the cytosol and nucleus whereas traces of the protein were detected in the membrane/organelles fraction (Figure 3.26). This pattern can be explained by the fact that different cell lines show different distribution of proteins depending on which pathways are activated and where this protein is needed.

Endoplasmic reticulum entrapment was further enhanced by mutation of the last four KTEL amino acids in the extreme C-terminus of the protein to the most commonly found KDEL endoplasmic reticulum-retention sequence, typical of mammalian proteins that reside in the endoplasmic reticulum [355, 521]. This motif interacts with KDEL receptors localized in the intermediate compartment and Golgi apparatus, and especially ERD21. Such binding triggers conformational change to the receptor and leads to retrieval back to the ER via a coat protein I–dependent pathway [171]. When this KTEL to KDEL mutation was made to the full length form of AGR-2 RFP the outcome was remarkable endoplasmic reticulum retention from a percentage of 33% observed in the wt protein to 80% of this KDEL mutant, suggesting that the KDEL sequence is much stronger and determinative when it comes to endoplasmic reticulum entrapment than the KTEL one (Figure 3.25). This particular KTEL

sequence can be implicated in partial endoplasmic reticulum-retention, as suggested by studies in a viral glucoprotein that is temporarily trapped in the endoplasmic reticulum [597], so it is possible that AGR-2 remains in the endoplasmic reticulum for some time and then released to enter the secretory pathway, but when KTEL is mutated to KDEL then the protein is trapped in the endoplasmic reticulum and not being processed. Similar cases involving non-ER resident proteins have been described, such as lysozyme in which the presence of the KDEL tetrapeptide at the carboxyl-terminus ensured endoplasmic reticulum retention and prevented secretion [423]. In the AGR-2 negative cell line, presence of the KDEL tetrapeptide in the C-terminus of the protein promoted membrane/organelles distribution as expected (Figure 3.26).

Deletion of the KTEL sequence did not have tremendous effects on endoplasmic reticulum affinity and the percentage of cells having 100% ER-co-localization was similar to the wt form of the RFP-tagged protein that had this C-terminal sequence, indicating that the presence of the leader sequence is alone sufficient to ensure a certain extent of ER co-localization. The aforementioned effects were also observed by Raykhel and colleagues in HeLa and Cos cells [483]. In their study many of the proteins that had KDEL-like motives were tagged and tested my immunofluorescence either with the putative ER-retention motif present or by insertion of a stop codon right before it. Interestingly, AGR-2 was amongst the ones that did not require the presence of the KTEL sequence for endoplasmic reticulum localization, which can be explained by the fact that these studies were performed with the full length form of the protein designated to secretion due to the presence of the signal sequence. Therefore, the KTEL sequence is not essential to ER-retention and the N-terminal signal sequence is the one that targets the protein to enter the ER. On the other hand, in some cases deletion of the carboxyl-terminal retention sequence of ER-resident proteins, either viral-plant-mammalian, results in redistribution of the protein intracellularly and leads to secretion, as studies in ER-resident proteins have revealed [423, 442, 515]. This mechanism of action involves deficient binding of the protein to the KDEL receptors and therefore failure to be

recycled back to the endoplasmic reticulum via the COPI and II retrograde vesicle-mediated pathway [442, 515, 576].

Substitution of the last threonine with alanine did not alter the localization of the protein. Threonine is a slightly polar amino acid that is phosphorylated in order to facilitate signal transduction process whereas alanine is a rather neutral amino acid, non-hydrophobic, non-polar and non-reactive which does not play important roles in protein function [58]. For the aforementioned properties alanine is the most commonly used amino acid in substitutions, where the effect of another amino acid is to be determined without further affecting the protein's structure and function by selecting a polar or hydrophobic or rather reactive amino acid. In MCF-7 cells, this construct did not show significantly different localization patterns when compared to the full length wt protein (Figures 3.27and 3.28). The full length AGR-2 KAEL RFP had granular appearance distributed around the endoplasmic reticulum with some co-staining but did not reached 100% co-localization rate as the KDEL one. The distribution pattern strongly resembled the one observed in the wild type form of the protein (Figure 3.28). Further supporting these data, subcellular fractionation experiments came to verify that this mutant have analogous expression levels in the cytosolic and membrane/organelles fraction to the wt protein (Figure 3.27). On the other hand, more protein was expressed in the cytoskeleton fraction suggesting enhance mobility of the mutant. Our findings were also supported by literature, since the KAEL sequence was described to be able of maintaining endoplasmic reticulum localization after studies with methionine sulfoxide reductases [311]. Reductases that had a typical secretory signal peptide and the putative ER-retention KAEL sequence were detected in the endoplasmic reticulum while others that had no secretory signal peptide but only the KAEL tetrapeptide in their C-terminus were distributed in the cytosol. On the other hand, mutant proteins with the typical secretory peptide in their N-terminus and deletion of the KAEL sequence in their C-terminus were not localized in the endoplasmic reticulum. These data demonstrated that ER residency is partially dependent on the tetrapeptide KAEL which can act as a putative ER-

retention signal but the presence of a signal peptide is still required to define and support endoplasmic reticulum localization.

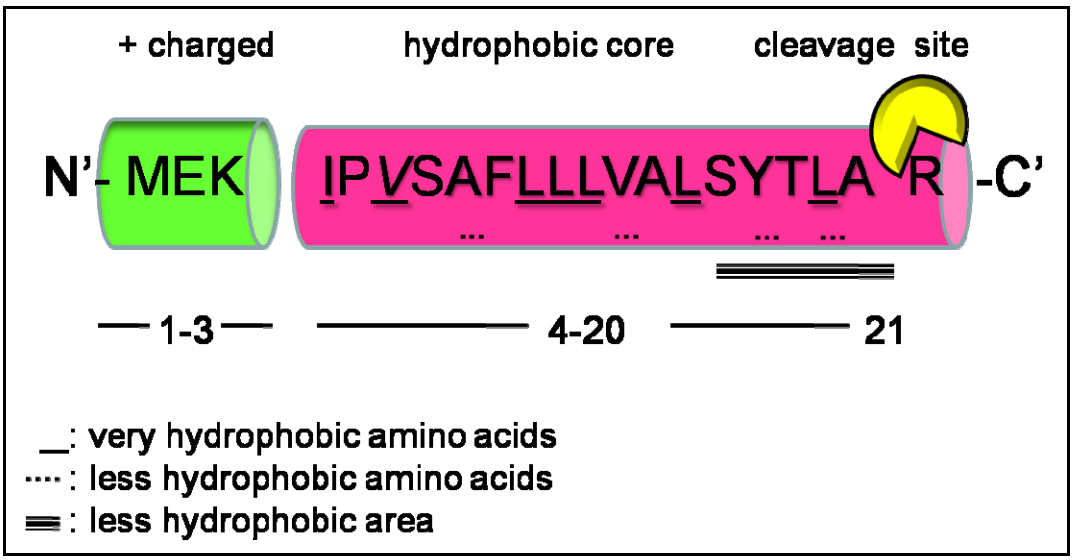

Figure 3.29: Representative diagram of hydrophobic amino acids. These amino acids have side-chains that do not like to reside in an aqueous (i.e. water) environment. For this reason, one generally finds these amino acids buried within the hydrophobic core of the protein, or within the lipid portion of the membrane (adapted after *www.russell.embl-heidelberg.de*).

It is worth mentioning that when it came to full length constructs, some nuclear expression was detected by immunoblotting whereas no nuclear staining was present in microscopic studies (Figures 3.17 and 3.24). This can be due to the close proximity of the endoplasmic reticulum with the nuclear membrane and therefore the possibility of some bleed through between these two fractions during isolation should be taken into account. Differences in expression levels in the nuclear fraction between the wt protein and the mutants can be explained by the fact that every construct shows different co-staining rate to the endoplasmic reticulum and this can lead to variable bleed through detection after fractionation. A second reason might be the presence of the protein in the nuclear membrane and therefore isolation in the

equivalent fraction. Especially the wild type and KAEL constructs show elevated nuclear distribution whereas the KDEL and Δ_{KTEL} constructs do not. Since the KTEL tetrapeptide is essential in maintaining nuclear localization of the mature form, as later described, there is no reason why this ability could be totally vanished in the full length isoform. Maybe KTEL maintains part of it nuclear retention properties but the signal peptide is the one that plays the leading role for the localization pattern of the full length isoform. Another possible reason might be the presence of the red fluorescent protein which is quite big in size, 28kDa, and can affect solubility of the constructs which is then detected after fractionation that is based on these properties and not during microscopy that does not include any solubility parameters. It is common in literature for some tags to affect solubility of the protein under study with a lot of fusion tags such as GST (Glutatheione-S-Transferase), SUMO (Small Ubiquitin MOdifier), T7PK (phage T_7 Protein Kinase) and a lot more to act in favour of it [179]. Green Fluorescent Protein is amongst the tags that affect solubility depending on which terminus the GFP is fused [162]. It has been previously shown that proteins prone to mis-folding and aggregation can arrest GFP folding when fused at the C-terminus [471, 605]. However, when the soluble protein is fused at the N-terminus, this would be translated first and perhaps increase the solubility of the downstream protein domain folding intermediates, increasing their half lives prior to irreversible aggregation. This would allow greater reversibility in the individual steps along the folding pathway and increase the probability that the protein would eventually reach the lowest free energy native conformation. Especially DsRed, which is the chromophore used in our case, is accused of poor solubility [59] when existed in wild type form whereas new variants, including the one used in our experiments, have reduced net charge near the N-terminus and thus higher solubility leading to less tendency to aggregate, although the problem is not yet fully overcome. Therefore, solubility problems may arise, affect fused protein's solubility and detected after fractionation experiments.

3.3.3 Nuclear distribution of the full length RFP isoform is controlled by the KTEL sequence in the AGR-2 negative cell line

Nuclear distribution was also observed in the AGR-2 negative cell line (Figure 3.26). Since these cells do not have endogenous AGR-2 there is a high possibility that the secretory-transportation pathway for this protein is deficient. Deficient secretory mechanism means that the leader sequence might no longer be as important as in the AGR-2 positive cell lines. As analysed below, KTEL plays a role in the nuclear maintenance of the mature wt isoform and absence of it depletes the protein from the nucleus (Figure 3.24) of MCF-7 cells. Substitution with the KDEL sequence elevated the endoplasmic reticulum retention rate but did not eliminate the protein from the nucleus in MCF-7 (Figure 3.24). It can be proposed that similar patterns are followed in the MDA-MB 231 cells; a less 'active' and deficient leader sequence combined with a KTEL sequence that might retain its ability to control nuclear distribution can lead the full length wild type isoform to be present in the nucleus. Similarly, the full length KDEL one is present in the nucleus but also elevated in the organelles fraction due to the KDEL sequence and last but not least the Δ_{KTEL} one totally absent from the nucleus since no KTEL sequence is present to control nuclear retention. What is suggested here is that the leader sequence is not totally inactive since if that was happening then the localization patterns between the mature and the full length isoform would be identical, which is not the case here (Figure 3.26). Therefore, it is recommended that the signal peptide still has some effect in orientating the protein to the membrane/organelles but it is the KTEL sequence that plays the leading role for the localization patterns and defines the expression levels in the nucleus and the membrane/organelles fraction. Of course, all the aforementioned reasons, RFP solubility problems--endoplasmic reticulum and nuclear proximity--nuclear membrane localization, explaining full length AGR-2 nuclear presence in the MCF-7 cells can also be valid for the MDA-MB 231 ones. In conclusion, the leader sequence and the KTEL sequence still play a very important role in determining the protein's

localization even in AGR-2 deficient cells and therefore the equilibrium can be easily disrupted and manipulated.

3.3.4 Nuclear retention of the mature AGR-2wt RFP is controlled by the C-terminal KTEL sequence

On the other hand, the mature form of the protein fused to red fluorescent marker, was mainly nuclear and diffuse cytoplasmic (Figures 3.19, 3.20, 3.22 and 3.24). The mature form of the protein was distributed within the whole nucleus but was excluded from the nucleoli. Absence of the signal peptide was therefore sufficient to disrupt ER-retention and shift the equilibrium towards the nucleus. Moreover, no serious endoplasmic reticulum co-staining was observed although some granules were detected in the cytoplasm but exhibited less that 10% co-localization rate (Figure 3.25). Same patterns were followed when it came to Golgi co-staining, with the protein having no signs of co-localization (Figure 3.20). All the cells tested showed nuclear distribution and variations existed only in the cytosolic staining pattern with most cells, 66% of total population, having granules but less than 10% co-localization with the endoplasmic reticulum and even less cells showing diffuse cytosolic allocation with no granules at all (Figure 3.25). In the AGR-2 negative cells, the mature wild type protein was highly expressed in the nuclear fraction and only traces in the cytosol which can be due to the absence of the signal sequence that exports the protein from the nucleus and equally distributes it to the cytosol, membrane/organelles and nuclear fraction, as shown by the full length isoform in the same cells (3.26). Interestingly, the mature form of AGR-2 is the one that acts as a p53 inhibitor [474]so the finding that this form is nuclear can explain this inhibitory action, based on the fact that both proteins have the same topology. Other proteins have also been listed as p53 inhibitors when localised in the nucleus, with the most fully characterised mdm-2 [107, 413]. Mdm-2 must localize to the nucleus to bind p53, and repress p53-mediated transactivating and apoptotic activities [477] although

the final p53 degradation happens in the cytoplasm [570]. When mdm-2 is sequestrated in the cytoplasm by an inhibitor such as PTEN, its p53 binding and inhibitory functions are repressed [393, 654]. On the other hand, p53 activation also happens in the nucleus as in the case of the PML, a nuclear phosphoprotein that acts as a tumour suppressor [201] and stimulates p53 activity by recruiting it to nuclear foci, termed as PML nuclear bodies [180, 558, 614]. Certain tumours constitutively accumulate wild-type p53, which is functionally inactive because it is sequestered in the cytoplasm [411, 449]. In addition, treatment of human primary cells with Leptomycin B, a drug that specifically blocks nuclear export, induces the relocalization of p53 into punctate subnuclear structures, reminiscent of the so-called nuclear bodies (NBs) [339] where mdm-2 and p53 co-localize and therefore interact. In conclusion, inhibition or activation of p53 is highly dependent on the localization of the proteins implicated in the interaction and so mature AGR-2, the one that inhibits p53, is mainly localized in the same compartment where the tumour suppressor acts, making the interaction possible to happen.

Mutation of the last four amino acids to KDEL, enhanced the percentage of granules detected in the cytoplasm and having more than 10% co-localization rate with the endoplasmic reticulum (Figure 3.25). ER-retention was expected since KDEL ensures efficient residency in this compartment and also reduced the protein's expression levels in the nucleus, while at the same time induced cell membrane/organelles expression levels (Figure 3.24). This reduction can be explained by the fact that more protein is exported from the nucleus, since the presence of the KDEL sequence leads the protein to the endoplasmic reticulum, but the KDEL tetrapeptide alone is not sufficient to totally deplete AGR-2 from the nucleus. In AGR-2 negative cell line, the equilibrium was shifted from nuclear localization of the wild type protein to enhanced distribution of the KDEL mutant in the cytosol and membrane/ organelles fraction, further supporting the role of the KDEL endoplasmic reticulum-retention sequence (Figure 3.26). Interestingly, nuclear expression levels remained unchanged when compared to the wild type construct.

Substitution of the last threonine to alanine reduced nuclear expression levels in MCF-7 cells, but no induction in the cytosolic and membrane/organelles fraction was observed, since the KAEL sequence is not alone sufficient to lead the protein to any other compartments as it requires the presence of a leader signal sequence, either secretory or targeting it to mitochondria and other cellular compartments [311]. Studies with methionine sulfoxide reductases revealed that absence of a signal sequence leads the protein to the cytosol, even in the presence of the KAEL sequence [311] consistent to our data. On the other hand, the cytoskeleton fraction showed elevated expression levels of the mutant, so it is possible that this sequence induces association to the cytoskeleton and promotes protein transportation, although more experiments need to be done to refine this observation.

Deletion of the last four amino acids remarkably disrupted the equilibrium and the protein could only be detected in the cytosol (Figure 3.24). No nuclear nor organellar expression was detected. In the AGR-2 negative cell line, the construct was again present in elevated levels in the cytosol and very little in the nucleus which might be a GFP artefact or maybe the GFP protein is too big to be exported from the nucleus (Figure 3.26). On supporting these data, deletion of the last ten aminoacids, including KTEL, leads to attenuation of the inhibitory action on p53 [474] which can be explained by the finding that this deletion mutant is no longer localized to the nucleus where it can interact with p53. Moreover, no endoplasmic reticulum nor Golgi co-staining was observed (Figures 3.19 and 3,20), since there is neither KTEL nor signal peptide to lead the protein these compartments as it happens with the full length form of AGR-2. What is more, GFP is accused of being unstable and sometimes folding of the fluorescent protein may interfere with the fused protein properties [286, 600]. In addition, GFP exhibits slow or incomplete fluorescence maturation which can explain why this AGR2- Δ_{KTEL} GFP is so sensitive and bleaches after a very short exposure on its excitation wavelength. Many Anthozoa GFP-like proteins also form non-specific, high molecular weight aggregates both *in vitro* and *in vivo* that are toxic to cells and this can reduce the target protein's expression levels [636] and also interfere with the fluorescent signal which can, in

our case, explain why this AGR-2 construct is detected in the nucleus along with the cytosol by microscopy and only in the cytoplasm by subcellular fractionation experiments (Figures 3.19 and 3.24, respectively). Aggregation-accumulation happens due to the presence of hydrophobic pockets within the fluorescent protein [636] and this state can be interrupted by treating with detergents or other agents, as in the case of isolation of different sub-cellular compartments. All these fluorescent proteins are being subjected to molecular engineering in order to minimize their limitations and acquire the desired properties but drawbacks still exist [405].

3.3.5 Endogenous AGR-2 is a dynamic equilibrium between the two isoforms

If the localization patterns of the two distinct forms of AGR-2, full length and mature, are combined, the result is the staining pattern supported by immunostaining with the monoclonal anti-AGR2 antibody, which showed diffuse cytoplasmic, perinuclear and nuclear distribution of the endogenous protein (Figure 3.7). Nuclear and diffuse cytoplasmic distribution is identical to the mature AGR-2wt RFP protein, whereas perinuclear staining is similar to the full length AGR-2wt RFP isoform. This distribution pattern was also supported by fractionation experiments, isolating endogenous AGR-2 in the cytosol, membrane/organelles and nuclear fraction fo MCF-7 cells (Figure 3.24). This pattern was expected, since the antibody recognizes both forms of the protein, whose only difference is the presence of the N-terminal leader sequence. Small differences in the staining pattern between the polyclonal and the monoclonal anti-AGR-2 antibodies (Figures 3.6 and 3.7) can be explained by different epitope recognition, as well as the possibility of a masked epitope recognized by any of those antibodies. Of course polyclonal antibodies also have issues when it comes to specificity of binding that therefore affects efficiency.

3.3.6 Conclusions of chapter

In conclusion, results presented in this chapter demonstrated that AGR-2 follows diverse distribution patterns in breast cancer cells that have different resistance to tamoxifen and other anti-estrogens. The exact sequences essential for each localization were defined by fluorescent-tagged AGR-2. The KTEL tetrapeptide in the C-terminal of the protein ensured nuclear retention in the absence of the N-terminal signal peptide that acts in a predominant way when present in the protein and designated the protein to the cytosol maintaining partial ER co-localization even in the absence of this KTEL tetrapeptide. This co-localization was enhanced by mutating the KTEL to KDEL. On the other hand, the minimum domain required for nuclear residency was narrowed down to KXEL, since total deletion of this tetrapeptide lead to nuclear exclusion, always in the absence of the leader peptide, whereas substitution of the KTEL with KDEL or KAEL was not sufficient to inhibit nuclear localization. Absence of the leader sequence and process to the mature form of the protein causes nuclear localization accompanied with diffuse cytosolic pattern. It is under these non-ER localizing conditions (i.e. cytosolic or nuclear localizations) which correlate with the protein's ability to inhibit p53 [474]. Deletion of the last four KTEL amino acids shifts the equilibrium to a less nuclear and more cytosolic pattern even in AGR-2 negative cells. Together, our data with previous experiments [474], provide a correlation between mature AGR-2 nuclear localization and the ability to inhibit p53-dependent transcription.

Chapter 4

Anterior Gradient 3

4.1 Introduction

4.1.1 Mitochondria and energy sufficiency

Mitochondria are the energy plants of the cells, as they produce most of the energy it needs, generate endogenous reactive oxygen species and participate in apoptosis via the mitochondrial permeability transition pore which consists of anti- and pro-apoptotic Bcl-2 and Bax family members, respectively. Mitochondria are transported to regions where ATP consumption is high and they disperse when the ratio of ADP/ATP increases [28, 29, 462]. Interestingly, in neuronal processes 1/3 of the mitochondria are in constant motion whereas the rest are stationary [202, 416] and ultrastructural studies showed the formation of cross-bridges between the mitochondria and microtubules [50, 256] or intermediate filaments [256].

These organelles play an important role in cancer, as cancer cells rely heavily on glycolysis and energy production, the so called Warburg effect, as it was firstly described by Warburg in 1930. This effect can be summarised in the observation that cancer cells even in the presence of sufficient oxygen levels undergo glycolysis to synthesize the required ATP for their metabolic activity [108]. Glycolysis consists of glucose catabolism into excessive lactic acid by consuming oxygen. During this process they upregulate glucose transporters as well as other enzymes of glycolysis [463]. A possible mechanism that contributes to the Warburg effect involves mutations in the mtDNA. mtDNA is a supercoiled, double stranded circular DNA molecule that codes for 13 of the 87 respiratory chain subunits, 12S and 16S rRNA and 22tRNAs required for mitochondrial protein synthesis [88]. Cancer cells often accumulate defects of the mitochondrial genome leading to deficient mitochondrial respiration and ATP production [72]. Mitochondrial defects fall into two categories (i) one associated with germline mutations in the mitochondrial genome that creates genetic predisposition to cancer development and (ii) one involving acquired mutations that exhibit oxidative phosphorylation, increased production of reactive

oxygen species (ROS) and thus uncontrolled cell proliferation and metastasis [72]. mtDNA often bears mutations in various types of cancer such as prostate cancer [105], breast cancer [656], gastric cancer [651], neck, bladder, head cancer [200] and leukaemia [88, 89]. Several factors contribute to the high mutation rate and vulnerability of the mitochondrial genome, such as weak DNA repair capacity, lack of protective histones, low percentage of introns in the genome, close proximity to the electron transport chain that creates superoxide radicals and therefore higher genomic instability leading to biologicaly relevant mutations and affecting the metabolic pathway of the cell, which struggles to meet its energy requirements [89]. Nevertheless the biological impact of each mutation may be variable because each cell has more than one mitochondria and therefore mutant mtDNA may coexist with wt mtDNA, a state called heteroplasmy, but the total proportion of mutant DNA is the one that determines cell fate and behaviour. Germline mutations, insertions or deletions, are more common in syndromes such as Leber's hereditary optic neuropathy, maternally inherited diabetes mellitus and Leigh's syndrome, whereas somatic mutations are more commonly linked to cancer [88]. Another mechanism contributing to Warbug effect is the adaptation of cancer cells to hypoxic environment [212]. Hypoxia is a situation that characterizes most of cancer malignacies and is associated with low percentage of oxygen in the tissue environment. If that is the case, then cancer cells are forced to use the glycolytic pathway for ATP production [212].

In the last decade of the twentieth century it was discovered that the mitochondria from cancer cells are often resistant to the induction of mitochondrial outer membrane permeabilization (MOMP) which is a process that mediates apoptosis [228, 648] through the intrinsic apoptotic pathway (thoroughly described in chapter 1.2.1.2). MOMP is a quite complicated and multifactorial phenomenon that implicates a lot of different components. Amongst them are pro-apoptotic proteins such as the Bcl-2 protein [111, 643], proteins of the permeability transition pore complex [74] whose primary role is regulate oxidative phosphorylation and utilize it for energy production [233], transcription factors such as the tumour suppressor p53

protein [409] and mitochondrial lipids as well [233]. This process leads to release of proteins that are normally localized between the inner and the outer membrane of the mitochondria, such as cytochrome c [220]. Inhibition of MOMP results in disabled apoptosis and therefore tumour progression. The mechanistic link between MOMP and aerobic glycolysis awaits further elucidation.

4.1.2 Mitochondrial and cytoskeleton

Mitochondria are not static organelles but they undergo frequent changes in their shape and position depending on the cell type, cell cycle and the organism. They can be spherical due to fusions or fragmentation of their membrane or elongated after interaction with cytoskeletal filaments. Interactions between mitochondria and the cytoskeleton are essential to their normal function as well as for localization of the organelles to their sites of action within the cell when required. Cytoskeleton participates in mitochondrial respiratory activity, fusion, fission and inheritance as well as ensuring localization of mitochondria into the right position in cells, such as where energy requirements are higher, where reactive oxygen species are generated, where calcium homeostasis takes place and of course where apoptosis is happening. On the other hand, mitochondria in turn, utilize cytoskeleton to be assembled correctly, to control their movement and anchorage within a cell. High energy demanding cells, such as neurons, are characterized by rapid mitochondrial movement towards their axons by interaction of the mitochondria with the dynamic +end of microtubules [630] towards the axons and retrograde movement towards the opposite direction [257]. Moreover, during mitosis in yeast, mitochondria appear to attach to the spindle pole bodies and move to the cellular ends during spindle elongation [630]. Chada and Hollenbeck recently found that placing a nerve growth factor, NGF, coated bead on the axon of a chick neuron, results in TrkA-mediated accumulation of mitochondria in this site and that agents that inhibit actin polymerization halt this accumulation [97].

Mitochondria co-localize with intermediate filaments, IFs, which are part of the cytoskeletal system of the cell. Several evidence that associate mitochondria to IFs exist in various cell types and organisms [156, 165, 419]. Treatments with drugs that disrupt microtubules or intermediate filaments cause redistribution of mitochondria [564] and change the organization of the cellular organelles as well [165]. Interestingly, in muscle cells, silencing of desmin, IF protein, leads to disassembly of the mitochondria as well as respiratory dysfunction [402]. The same observations were made by knock-out mice that had no intermediate filament desmin and showed no mitochondria motility [363, 402]. On the other hand, overproduction of Bcl-2 when combined with total deletion of desmin, restores mitochondrial function and capacity and corrects cardiomyopathy in $des^{-/-}$ mice suggesting a potential mechanism through which cells deficient in cytoskeleton components may overcome this problem, restore mitochondrial function and escape cell death [618].

When it comes to microtubules, another component of the cytoskeleton, it is noteworthy that mitochondria can use cytoskeleton-based mechanisms for movement that are distinct from the mechanism for force generation by kinesins and dyneins along cytoskeletal tracks [630]. Studies in fission yeast showed that mitochondrial movement is microtubule-dependent and destabilization of the last causes mitochondrial disassembly and other morphological defects [629, 630]. In the same model organism, polymerization and depolymerization of microtubules plays a key role in mitochondrial localization and behaviour during interphase and a protein called Mmd1p links mitochondria to microtubules and stabilizes the last in yeast [616], but no evidence for such protein exist in mammalian cells so far. It is noteworthy that spindle aster microtubules have also been implicated with mitochondria as well as other structures such as ER, microbodies, lipids, vacuoles movement during mitosis in yeast and *Drosophila* [11, 465] ensuring equal distribution of the mitochondria and other structures to the daughter cells. Attachment of cellular organelles to the growing ends of microtubules has also been observed in mammalian cells, sometimes associated with the ER [575] and others associated with phagosomes [61, 219, 469] and of course chromosomal movement

during cell division. Interestingly, in different phases of their movement, phagosomes exhibit altered preference for microtubules, with the early phagosomes attached to the plus end of the microtubules whereas the late did not [61]. It is noteworthy that cells deficient in microtubules or actin filaments fail to maintain mitochondrial mobility and correct docking [416].

As far as the actin is concerned, experiments in plants [528, 595], neurons [322] and budding yeast shed light to the interaction between mitochondria and actin and of course implications in the apoptotic pathway. In these cells, mitochondria exhibit track-dependent short-distance movement along F-actin, polymerized actin, and immobilization of the organelle to the cell cortex. In yeast, mitochondria bind to actin bundles and undergo both anterograde and retrograde movement [189]. During cell division, this interaction requires the presence of several proteins, called Mmms or Mdms in yeast that affect the maintenance of mitochondrial morphology or mitochondrial distribution and morphology, that organize the complex and deletion of any of these proteins result in mitochondrial mislocalization and malfunction [251, 394]. Experiments in Jurkat cells revealed that gelsolin, a Ca^{2+} actin regulatory protein and a substrate for caspase-3 that is mainly localized in the cytosol [321], is also present in the mitochondria and inhibit apoptosis by blocking cytochrome c release [322]. The mechanism of inhibition resembles the one observed by anti-apoptotic Bcl-2 family members in terms of a product cleaved by caspase-3 and capable of stimulating cell death [109, 534]. Gelsolin acts through blocking cytochrome c release and also regulates the mitochondrial permeability transition pore [322] along with the voltage dependent Ca^{2+} ion channel [208]. Surprisingly, there is no evidence for a direct role of myosin in actin-based mitochondrial movement in any animal cells or fungi [189, 257].

All the above suggest a dynamic system that plays a role in mitochondria localization and distribution and is under the strong influence of different components of the cytoskeleton which can act synergistically or substitunionally in the presence of drug-induced inhibition. The factors and conditions regulating these interactions are difficult to be determined and examined in *in vivo* systems.

4.1.3 Mitochondria and cell death

During apoptosis mitochondria undergo two major alterations. The first one refers to the permeabilization of the outer mitochondrial membrane due to huge accumulation of Ca^{+2} and is highly regulated by pro-apoptotic Bcl-2 family members. The second refers to the loss of the electrochemical gradient, normally present across the inner mitochondrial membrane, an effect called 'membrane depolarization', sometimes mediated by the permeability transition pore. The whole process is known as the intrinsic apoptotic pathway or mitochondrial pathway or Bcl-regulated pathway. Bcl-2 family members interact with mitochondria either constitutively or on induction of apoptosis and have a impact on the outer mitochondrial membrane (OMM) [643].

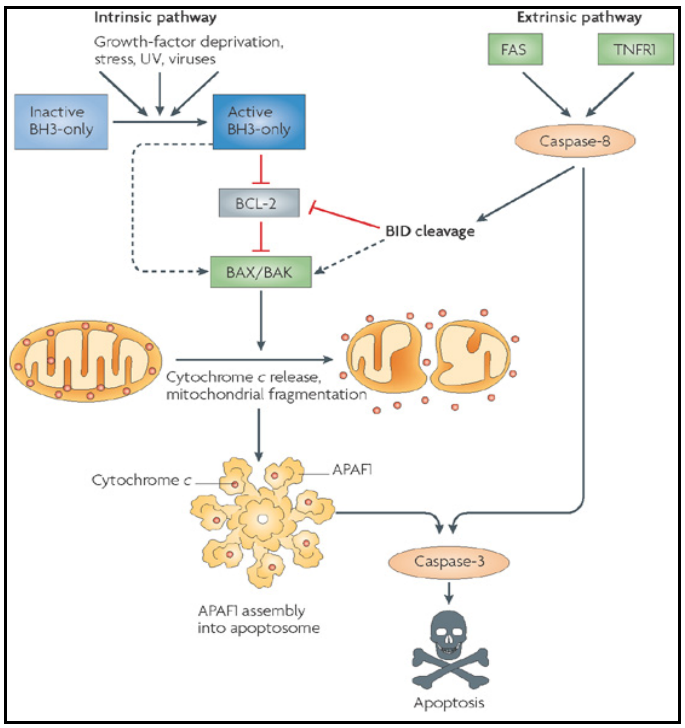

Figure 4.1: Diagram depicting intrinsic and extrinsic pathways of apoptosis. Details on both pathways can be found in sections 1.2.1/1.2.1.2/4.1.3. The Bcl-2 family regulates the intrinsic pathway and can modulate the extrinsic pathway when cleavage of BID communicates between the two pathways. FAS/TNFR3: cell surface death receptors, BH3-only proteins: Bim/Puma, APAF1: apoptosis protease-activating factor 1, dotted line shows activation whereas red T line indicates inhibition. (Adapted from [643])

The number and shape of mitochondria is tightly regulated by a dynamic equilibrium between mitochondrial fission and fusion process, which in turns is regulated by several mitochondrial proteins [291]. These mammalian mitochondria-shaping proteins include the large nuclearly-encoding mitochondrial transmembrane GTPases mitofusins Mfn1 and Mfn2 [104, 494], the optic atrophy protein Opa1 [514] of the inner mitochondrial membrane, dynamin-related protein Drp1 [204, 545] of the outer mitochondrial membrane and hFis 1 which regulates mitochondrial fission [641]. Mitochondrial shape is a result of dynamic alterations between fusion and fission events that lead from rod-globular to tubular shape and vice versa [252]. Both processes are necessary to ensure appropriate distribution of the mitochondria during mitosis and have distinct roles in apoptosis. Disturbance of the equilibrium leads to abnormally-shaped mitochondria such as elongated, clustered [545] or fragmented ones (summarised in Figure 4.2) [291]. As already mentioned previously (Chapter 1.2.1.2), mitochondria are the main component of the intrinsic apoptotic pathway and Bcl-2 family of pro-apoptotic and anti-apoptotic proteins is a key player in this process as they regulate the outer mitochondria membrane integrity and function [234, 310, 444] (summarised in Figure 4.1). In this chapter the relation of AGR-3 with mitochondrial proteins will be investigated and for that reason each family member should be analysed in more detail here. The Bcl-2 family can be divided into three different groups based on Bcl-2 homology (BH) domains and function [6, 306], (i)The anti-apoptotic members, such as Bcl-2 and Bcl-xL, that typically have BH1 through BH4 domains, [337]: (ii) the pro-apoptotic family members with BH1, BH2 and BH3 domains, such as Bax and Bak, and those (iii) pro-apoptotic family members with only BH3 domains, such as Bad, Bid, Puma and Bim [6, 589]. Briefly, the mitochondrial apoptotic cascade includes the membrane-permeability transition pore, which is regulated by all the above Bcl-2 family members through the composition of the voltage-dependent anion cells (VDAC, also called mitochondrial porin channel) [534] and adenine nucleotide translocator (ATN). The last two proteins are components of the permeability transition pore in the outer and inner side of the pore respectively. Studies by Narita and co-workers supported that pro-

apoptotic Bax and Bak accelerated the opening of the VDAC which is then permeable to cytochrome c, whereas anti-apoptotic Bcl-x_L closes the pore by binding directly to VDAC [427, 534], and also that Bax and VDAC form a large pore [534]. BH3-only proteins can directly activate pro-apoptotic Bax/Bax or act indirectly via binding and neutralising of pro-apoptotic Bcl-2 which prevents mitochondria permeabilization through Bax/Bak inhibition (Figure 4.1). Once activated, Bax and Bak, promote cytochrome c release and mitochondrial fission, which leads to the activation of APAF1 into an apoptosome and activates caspase-9 to activate caspase-3. Caspases in turn cleave a series of substrates, activate DNases and orchestrate the destruction of the cell. The extrinsic pathway can detour the mitochondrial step and activate caspase-8 directly, which leads to caspase-3 activation and cell death [643]. Recent data also support that Bcl-2 inhibition is not sufficient to induce apoptosis and that Bid/Bim-mediated activation of Bax/Bak is required.

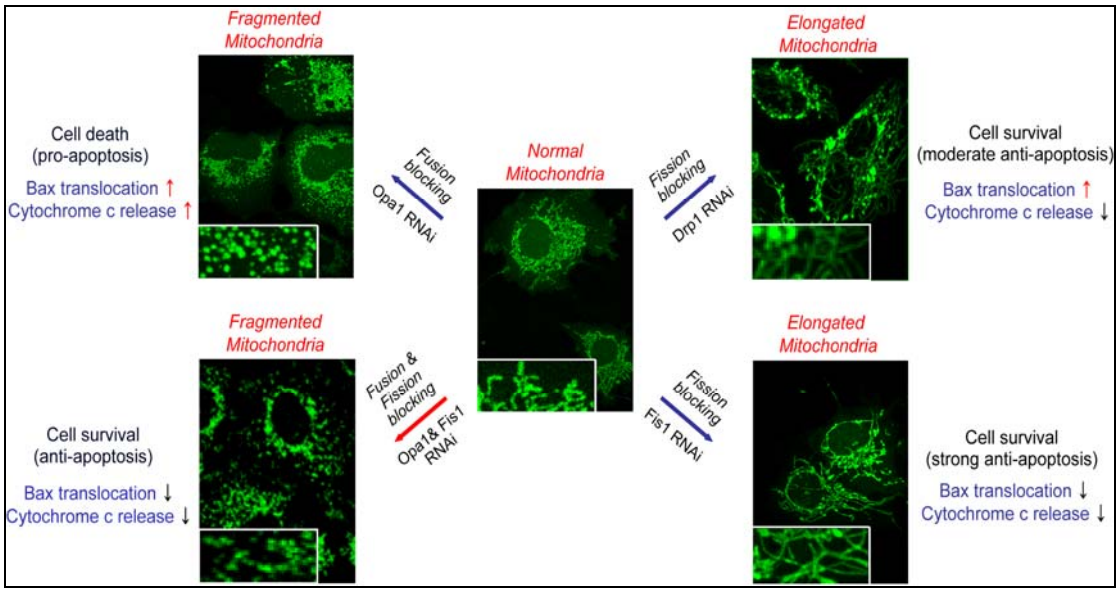

Figure 4.2: Correlation between mitochondrial morphology and apoptotic sensibility. Blocking of mitochondrial fission by knockdown (RNAi) of Fis1 or Drp1 expression induces mitochondrial fusion. HeLa cells with the elongated and interconnected mitochondria show apoptosis resistance. Fis1 RNAi cells show stronger anti-apoptotic phenotype than Drp1 RNAi cells. Elongated mitochondria in the Fis1 RNAi cells inhibit both Bax translocation to

mitochondria and cytochrome *c* release from mitochondria. Elongated mitochondria, however, in the cells depleted of Drp1 inhibit cytochrome *c* release but not Bax translocation. In contrast to hFis1 and Drp1 RNAi cells, Opa1 RNAi cells having fragmented mitochondria are more sensitive to apoptosis induced by various stimuli compared to the control cells. Fragmented mitochondria in the cells promote both Bax translocation and cytochrome *c* release. In the cells depleted of both hFis1 and Opa1, despite of mitochondria are extensively fragmented, the cells show apoptosis resistance (adapted from [291]).

4.1.4 Mitochondria and p53

p53 mediates apoptosis primarily via the mitochondrial pathway by stimulating transcription of various mitochondria-anchored pro-apoptotic genes like Puma, Bax, Bid, that participate in mitochondrial cell death, in response to various exogenous or endogenous stimuli. p53 can also mediate trans-repression of anti-apoptotic genes such as Bcl-2. Various stimuli such as DNA damaging agents, UV irradiation, γ-irradiation, hypoxia, chemotherapeutics, ROS agents, RNA interference and growth factor deprivation can cause p53 mitochondrial translocation [401, 511, 651]. This translocation is rapid and happens in less that 1h, preceding early dysfunctional changes in the mitochondrial membrane potential. Mitochondrial p53 stimulates a series of events including cytochrome c release, change in the membrane potential and pro-caspase-3 activation. The majority of p53 is localized to the membranous mitochondrial compartment whereas a fraction is found in complex with the mitochondrial import motor mtHsp70 [383]. Anti-apoptotic regulators such as Bcl-2 and Bcl-x_L specifically block stress-induced p53 translocation and therefore apoptosis, but interestingly do not halt nuclear p53 induction and cell cycle arrest suggesting a regulatory feedback loop in the organellar level [383]. p53 directly forms inhibitory complexes with the Bcl-x_L/2 via its DNA-binding domain [401] and these interactions terminate in the permeabilization of the outer mitochondrial membrane and therefore cytochrome c release and activation of effector caspases. The ability of Bcl-x_L/2 to block p53-mediated cytochrome c release parallels that

seen with Bax and Bid from isolated mitochondria [140]. In p53 null cells, total mitochondrial p53 expression was capable of triggering post-mitochondrial caspase cascade and lead to apoptosis in comparable levels as with the nuclear p53 [383].The above data are consistent with the observation by Ding and co-workers, who showed that p53 protein from cell-free post-nuclear extracts directly activates caspase-3 through an unknown mechanism, provided that cell-free extracts are derived from irradiated tumours [142]. This result is a clear biochemical evidence of an inducible, transcription-independent pro-apoptotic function of p53. Of note, these extracts contained mitochondria and therefore could have been the source of the p53-dependent effect [142]. Interestingly, it was also found that mitochondrial p53 translocation apart from triggering caspase-3 activation cascade, it also triggers a second slower transcription-dependent p53 death wave that includes p53-target gene induction and a further increase in active caspase-3 levels [177]. p53 mitochondrial translocation has been observed in various tissues such as testis, thymus [401], spleen *in vivo* [177] which are also radiosensitive organs and in primary cells cultures including human mammary epithelial [65], dermal fibroblasts and skin keratinocytes. On the other hand, p53 mitochondrial translocation does not occur in p53-independent apoptotic pathway nor p53-mediated cell cycle arrest [383].

The precise signal on p53 for its mitochondrial translocation is yet undefined. A translocation motif within the p53 amino-acid sequence has not been found and phosphorylation/acetylation modifications of p53 are not determinants for mitochondria translocation [428]. Studies on the Arg/Pro codon 72 variants proposed that mdm-2-mediated polyubiquitylation of p53 mediates nuclear export and mitochondrial translocation, but this area is has not been fully characterised yet [157].

4.1.5 Objectives of chapter

AGR-3 is the second member of the AGR family studied in terms of localization and function. Not much evidence exists regarding the distribution and the exact role of the protein in cancer although few data suggest the endosomal residency of the protein [5]. As far as the function is concerned, AGR-3 was found to enhance colony survival, but not much is known regarding the exact mechanism of action [270]. Characterization of newly-generated antibodies along with immunofluorescent microscopy and chemical fractionation in the cellular level will aid in studying the localization of the endogenous protein in MCF-7 cells. Small interference RNA technology will elucidate the role of the protein and also a series of other proteins will be tested for any quantative expression differences after AGR-3 depletion.

4.2 Results

4.2.1 Evaluation of AGR-3 antibodies

Anti-AGR-3 mouse monoclonal antibodies (Moravian Biotechnologies) were tested by ELISA for epitope recognition. Peptides representing the full length AGR-3 and AGR-2 proteins (Figure 4.3, kindly provided by Dr. Murray) were bound to an ELISA 96-well plate and incubated overnight with each of the four antibodies, termed as 1.2, 2.2, 3.1, 4.1 (Figure 4.4).

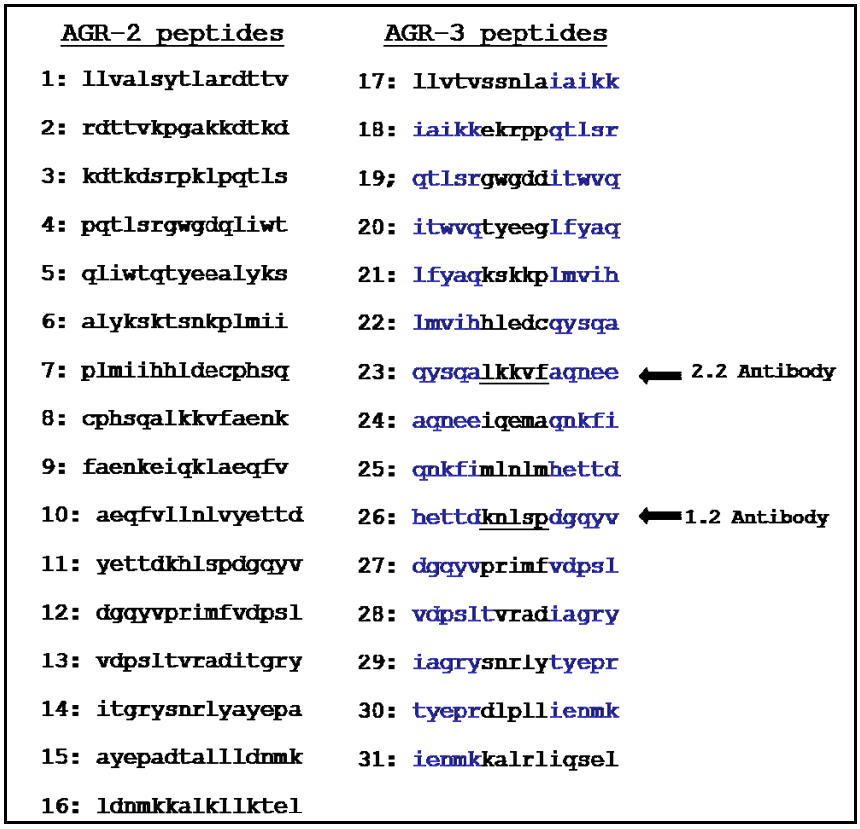

Figure 4.3: Diagram of peptides used in epitope mapping of anti-AGR3 antibodies. Peptides 1-16 represent AGR-2 a.a composition whereas peptides 17-31 correspond to AGR-3. Black arrows indicate the peptide recognised by the two AGR3-specific antibodies, 1.2 and 2.2. Underlined sequences are the exact epitope recognised when the overlapping sequences of adjacent peptides are excluded (shown in blue).

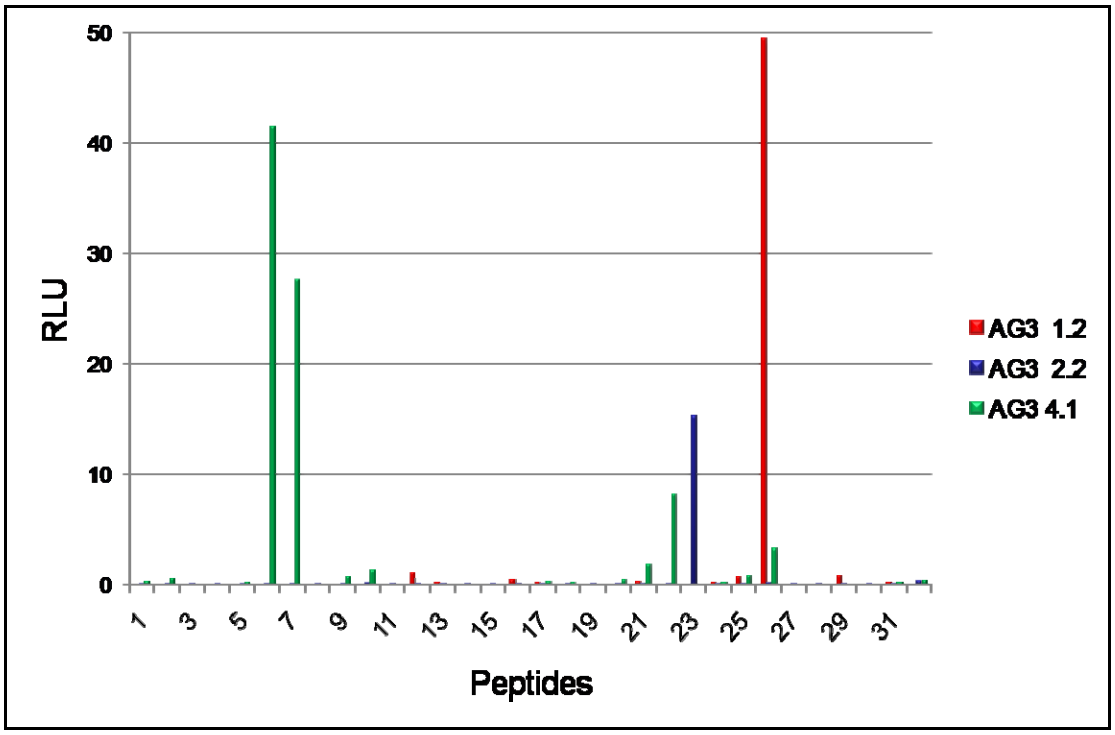

Figure 4.4: Representative ELISA diagram of epitope mapping. Anti-AGR3 antibodies , termed 1.2, 2.2 and 4.1, were tested by ELISA for efficient binding to peptides representing AGR-2 and AGR-3 full length proteins.

The 1.2 antibody bound strongly and repetitively to peptide 26 (Figure 4.4, red label) but not to peptide number 27 nor 25 which have some overlapping peptides with 26 (Figure 4.3 indicated in blue letters, Figure 4.4,), further narrowing down epitope mapping for this antibody to: knlsp (Figure 4.3, underlined). The second antibody tested, 2.2, strongly recognised epitope 23 of the AGR-3 peptides (Figure 4.4, blue label). Again no strong binding was observed with partially overlapping peptides 24 and 22, further defying the exact sequence of recognition to: lkkvf (Figure 4.3, underlined). The 3.1 antibody showed no specific binding as this antibody recognised a lot of epitopes without overlapping sequences and totally different to each other as well as giving contradictory and non-repetitive results throughout multiple experiments (Figure 4.4) and for that reason was not included in the study. The last

antibody tested, 4.1, was consistent in identifying peptides 2, 6, 7, 9 and 10 which represent AGR-2 sequence as well as to AGR-3 peptides number 21, 22, 25 and 26, behaving like a polyclonal antibody, although RLU were much lower to the 1.2 and 2.2 antibodies (up to 30x more than 4.1, Figure 4.4, green label). Since the two proteins share high homology, this antibody cannot be used for accurate experiments. To further characterize their binding affinity and specificity to AGR-3 and not be restricted to only one evaluation method, the same four antibodies were tested for *in vivo* recognition of endogenous AGR-3 (Figure 4.5) in MCF-7 cells that have endogenous AGR-2 and AGR-3. Lysates were pulled down with each of the antibodies and then immunoblotted against AGR-3 (antibodies 1.2, 2.2 and 4.1 depicted in Figure 4.5 A, C and D, respectively) and AGR-2 (Figure 4.5 B). The antibodies used for pulling down endogenous protein included a monoclonal anti-AGR-2 antibody (Figure 4.5 lanes A2, B2, C3 and D2), antibodies 1.2, 2.2, 3.1 and 4.1 anti-AGR-3 ones (Figure 4.5). The anti-AGR-3 ones were not able of pulling down endogenous AGR-3 from MCF-7 cells. The 1.2 antibody recognised the protein in total lysate before immunoprecipitation but after pulling down with the same antibody, no AGR-3 signal was detected (Figure 4.5 A lane 1 and 3 respectively). The other two antibodies, 2.2 and 3.1 were unable to recognise endogenous AGR-3 neither in crude lysate nor after precipitation with themselves. Only the 4.1 antibody pulled down a protein of 20kDa, which was positive when tested by the AGR-2 antibody (Figure 4.5 D lanes 1 and 3). As verified before, by ELISA, this antibody is able to recognize AGR-2 epitopes as well as AGR-3 ones (Figure 4.4, green label), which explains why after immunoprecipitation with the monoclonal anti AGR-2 antibody, the 4.1 detects the right 20kDa size band of AGR-2 (Figure 4.5 D lanes 1 and 2). Control co-immunoprecipitation experiments with the anti-AGR-2 monoclonal antibody, ensured efficient experiment conditions regarding solutions, temperature and beads' concentration. The monoclonal anti-AGR-2 detected AGR-2 in lysate before and after co-immunoprecipitation by the same antibody, as expected (Figure 4.5 B lanes 1 and 2). Negative-lysate control pull downs were performed to test for unspecific binding of the antibodies to the beads

and potential interference with the results (Figure 4.5 A lane 7 and C lane 1). Light chain and heavy chain of the antibodies was detected at ~54 and ~305kDa, respectively (Figure 4.5 A, B, C and D).

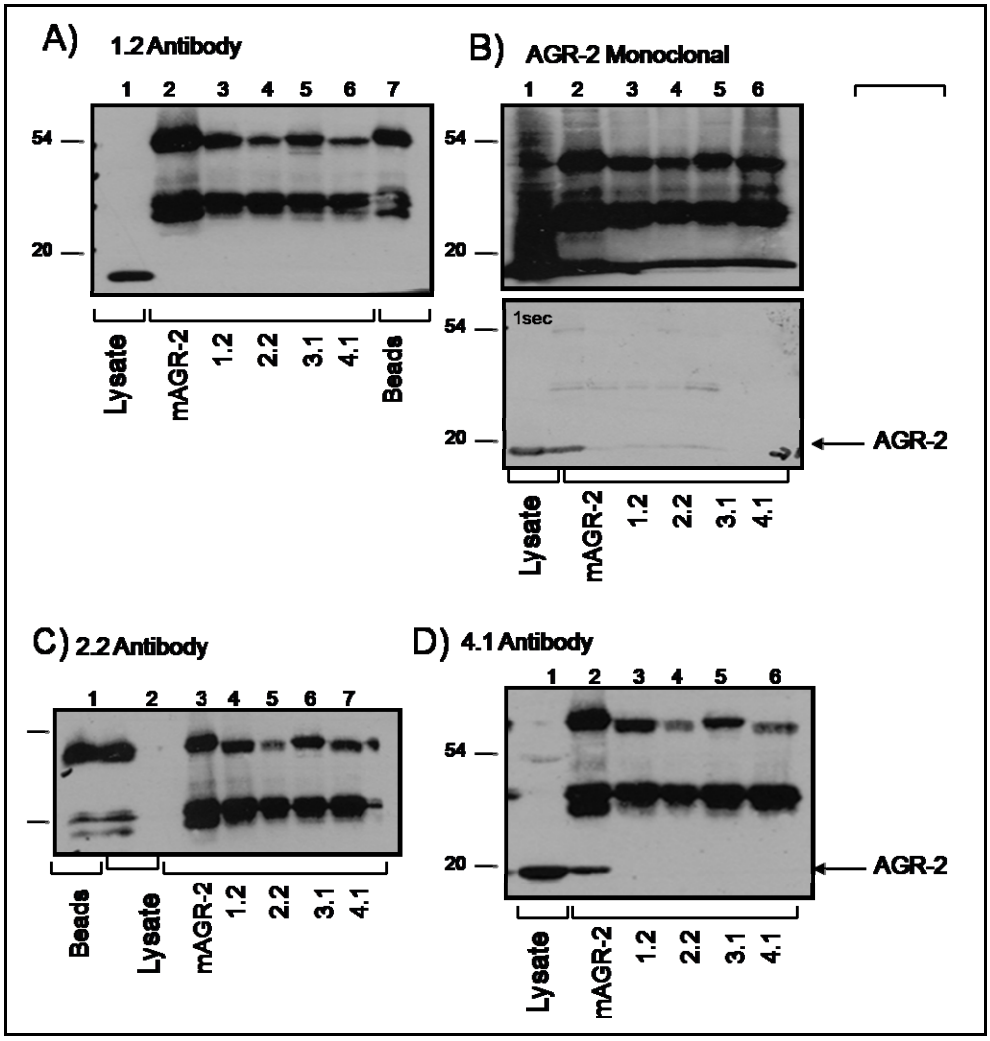

Figure 4.5: Anti-AGR3 antibodies do not IP endogenous AGR-3. Endogenous AGR-3 protein from MCF-7 cells was pulled-down with a series of antibodies including monoclonal anti-AGR-2 (Lanes A2/B2/C3/D2), 1.2 anti-AGR3 (lanes A3/B3/C4/D3), 2.2 anti-AGR3 (lanes A4/B4/C5/D4), 3.1 anti-AGR3 (lanes A5/B5/C6/D5) and 4.1 anti-AGR2 (lanes A6/ B6/C7/D6). Lysates were immunoblotted with a monoclonal anti-AGR-2 antibody (panel B1-B6) and AGR-3 with the same 1.2 (lanes A1-A6), 2.2 (lanes C1-C7), and 4.1antibodies (lanes D1-D6) against AGR-3. Beads only and total cell lysate pre-IP were used as controls.

The last step of evaluation involved immunofluorescence testing for endogenous AGR-3 in MCF-7 cells. The first antibody tested was 1.2 and it gave a string-like pattern around the nucleus resembling the endoplasmic reticulum but with thicker and more extensive structures within the cytoplasm and not strictly around the nucleus (Figure 4.6 panels A-C and Figure 4.8 panels D-F). Comparing these string-like structures with MCF-7 fluorescent images presented in the literature, resulted in the conclusion that this pattern strongly resembled mitochondrial staining. Apart from this reticulum-like staining, this antibody also showed signs of low diffused cytoplasmic AGR-3 expression (Figures 4.6 panels A-C and 4.8 panels D-F). This observation concerning mitochondrial detection was further characterised in Chapter 4.2.2. The second antibody, termed as 2.2, gave a totally different pattern resembling cell membrane staining, with signal detected in the boundaries of the cells and (Figure 4.6 panels D-F), which was also separately determined by brightfield microscopy in a confocal Leica microscope and (Figure 4.7 panels A-I). The third antibody, 3.1, gave no positive results at all which was totally expected as the antibody does not recognise any AGR-3 epitopes, as determined by ELISA and co-immunoprecipitation (data not shown). Last but not least, the 4.1 antibody, gave a rather peculiar model which resembled the 1.2 string-like staining (Figures 4.6 panels A-C and 4.8 panels D-F) and the monoclonal anti-AGR2 antibody diffused staining within the cytoplasm (Figure 4.8 panels A-C). This staining pattern was thought to be a combination between diffused cytoplasmic and string-like reticulum accompanied by small granules within the cytoplasm (Figures 4.6 panels G-I and 4.8 panels G-I) consistent with to the ELISA data which characterised the 4.1 antibody as a polyclonal-like one, due to its multi-epitope recognition (Figure 4.4, green label).

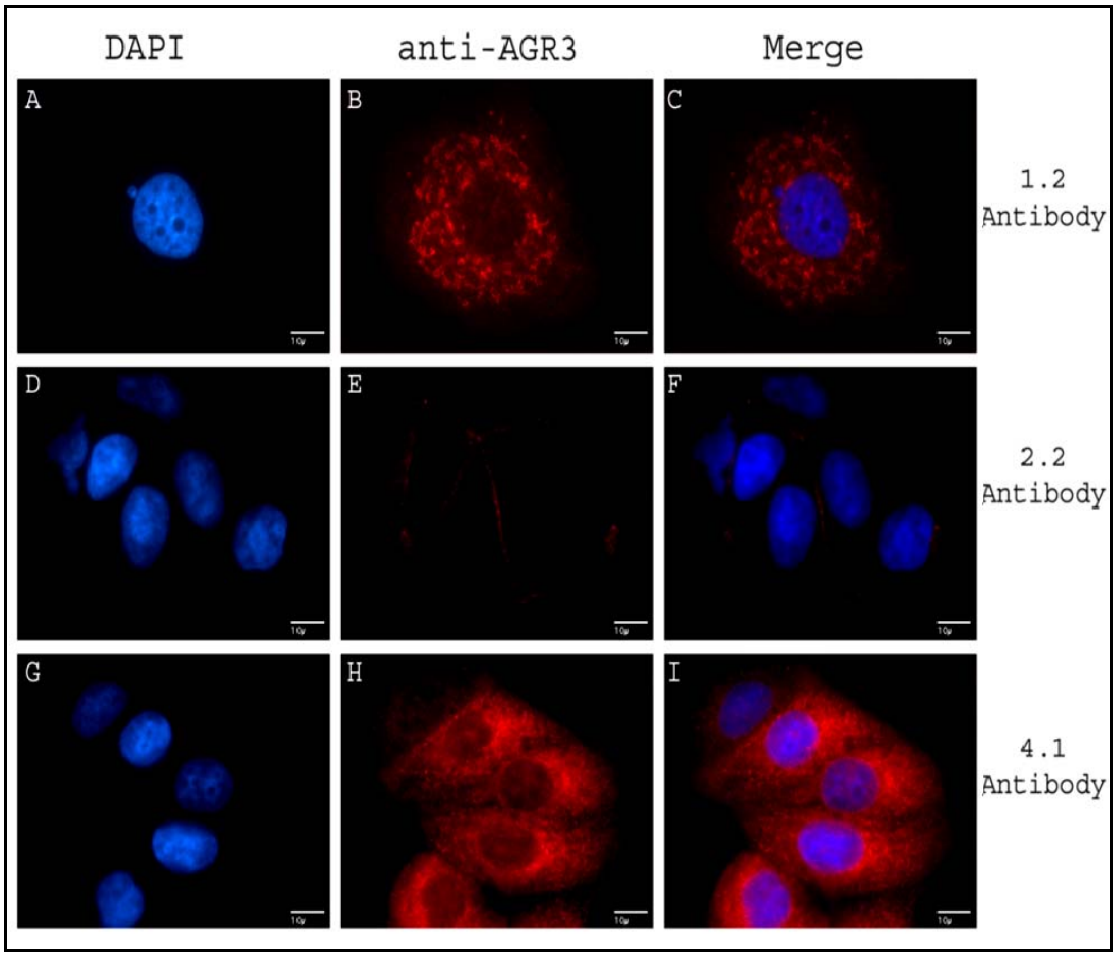

Figure 4.6: Intracellular localization of endogenous AGR-3 in MCF-7 using fluorescent microscopy. After fixation the protein was visualized using 1.2 (panels A-C) 2.2 (panels D-F) and 4.1 anti-AGR3 (panels G-I) antibodies and Alexa-conjugated secondary antibody was applied (Alexa-549, Molecular Probes). Nuclei were visualized by DAPI. Images captured by Sony Cool Snap 3.2 (Anti-AGR3: panels B, E and H, DAPI: A, D and G, merge: C, F and I) by Zeiss Axionplan microscope. Same exposure times used for all images. Figure showing representative of at least 4 independent experiments. Scalebar represents 10μm.

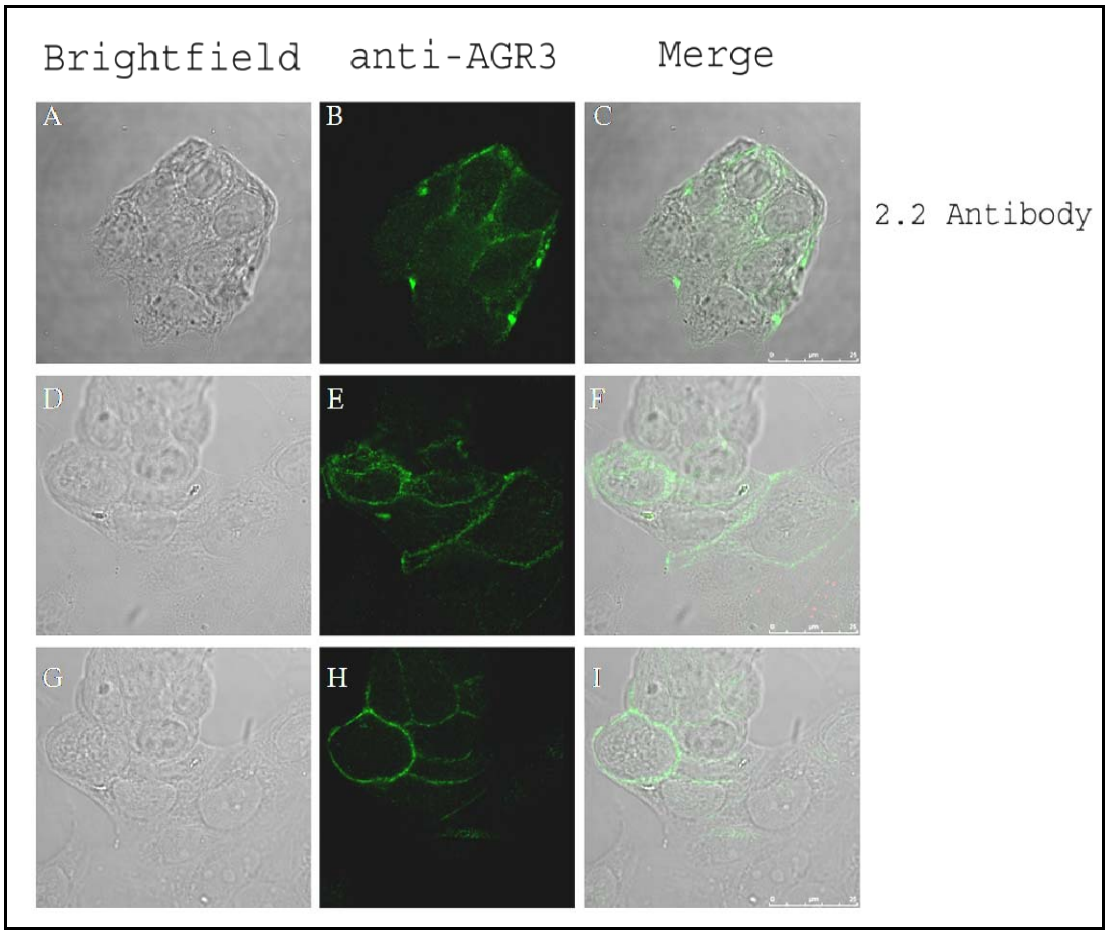

Figure 4.7: Membrane staining of endogenous AGR-3 in MCF-7 using fluorescent microscopy. After fixation the protein was visualized using 2.2 anti-AGR3 (panels A-I) antibody and Alexa-conjugated secondary antibody was applied (Alexa-488, Molecular Probes). Nuclei were visualized by DAPI. Images visualised by concfocal Leica SP5 microscope (Anti-AGR3: panels B, E and H, Brightfield: A, D and G, merge: C, F and I) . Same exposure times used for all images excited under the 488nm laser. Brightfield was each time adjusted to achieve high resolution of cells' boundaries. Figure showing representative of at least 4 independent experiments

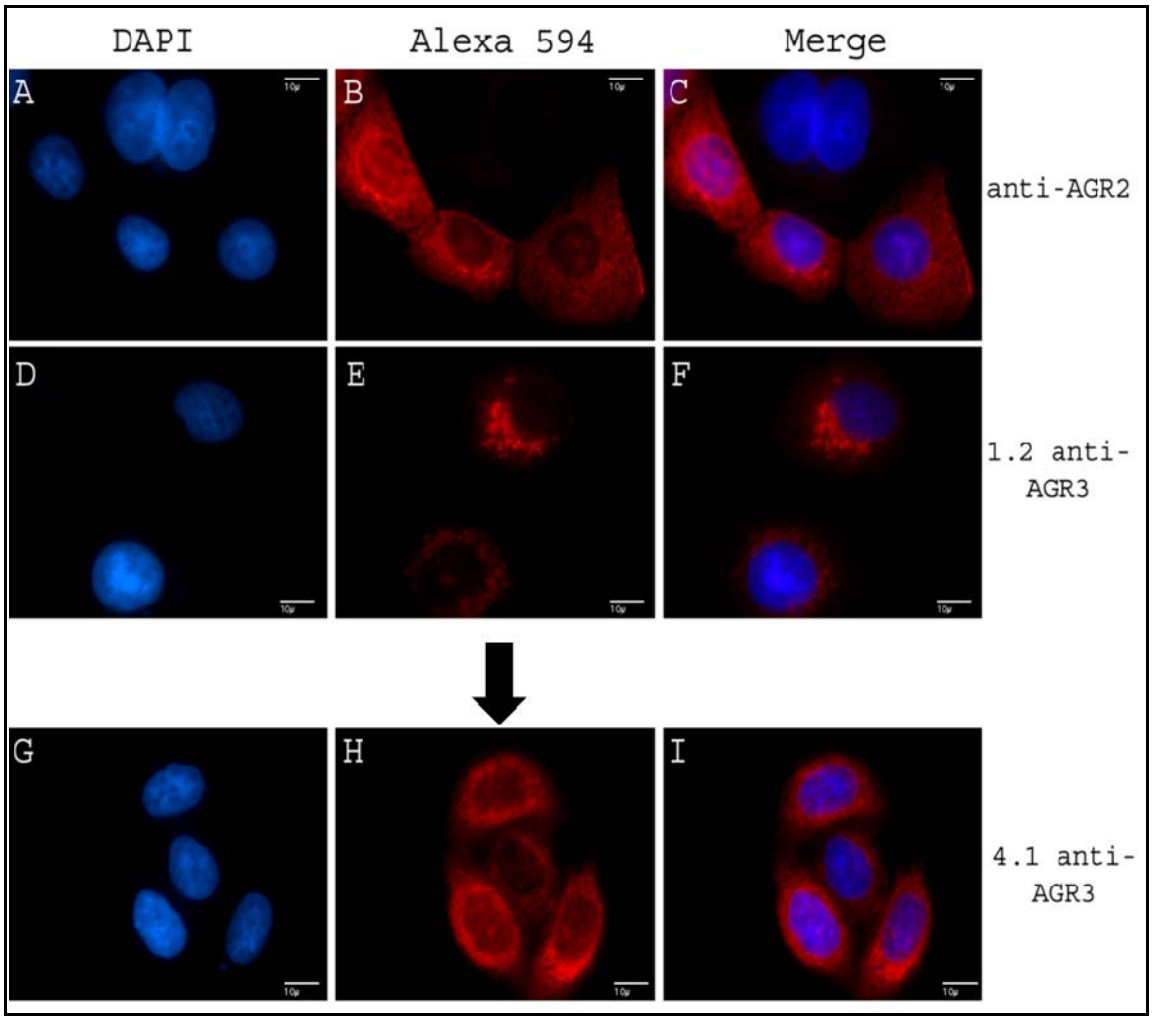

Figure 4.8: Comparison between AGR-2 and AGR-3 localization by microscopy. After fixation the protein was visualized using anti-AGR2 monoclonal antibody (panels A-C) 1.2 anti-AGR3 (panels D-F) and 4.1 anti-AGR3 (panels G-I) antibodies. Alexa-conjugated secondary antibody was applied (Alexa-549, Molecular Probes). Nuclei were visualized by DAPI. Images captured by Sony Cool Snap 3.2 camera (Anti-AGR3: panels B, E and H, DAPI: A, D and G, merge: C, F and I) by Zeiss Axionplan microscope . Same exposure times used for all images. Figure showing representative of at least 4 independent experiments (scalebar:10μm).

To sum up, of all four antibodies tested, only 1.2 and 2.2 antibodies can be used for further applications. Immunoblotting experiments favoured the 1.2 antibody against all the others when it comes to AGR-3 recognition in cell lysates (Figure 4.5 A lane 1) but before immunoprecipitation, as well as in immunofluorescence. The 2.2 antibody failed to detect endogenous AGR-3 protein from cell lysate (Figure 4.5 C lanes 1 and 5) and was only efficient in immunofluorescent experiments, where it recognized cell-membrane AGR-3 (Figures 4.6 panels D-F and 4.7 panels A-I). Interestingly, the recognition epitope for this antibody is not the leader sequence of the protein, as it would be expected for this staining pattern (Figure 4.3). The third antibody, 3.1, was totally inadequate for either immunoblotting or immunofluorescent experiments, and therefore its used was discontinued. The last antibody, 4.1, was behaving as a polyclonal one and recognised AGR-2 along with AGR-3 epitopes (Figure 4.4 green label), whereas in IF experiments it gave a combined pattern of monoclonal anti-AGR2 and 1.2 anti-AGR3 antibodies (Figures 4.6 panels G-I and 4.8 panels G-I) patetrns. This antibody's recognition epitopes shared some identical peptide sequences, which explains these multi-binding properties of the antibody but will not be further analysed in this thesis.

4.2.2 Localization of endogenous AGR-3 in MCF-7 breast cancer cell lines

4.2.2.1. Endogenous AGR-3 under normal conditions

Endogenous AGR-3 expression was tested in the MCF- cell line, since this is the one used throughout the whole project. MCF-7 cells were found positive for AGR-3 and were used to study the localization of the protein. To elucidate the exact position of the protein within the cell, subcellular fractionation experiments along with fluorescent microscopy studies were performed. Four different fractions were

isolated, representing proteins of the cytoplasm, cell membrane and organelles, nucleus and cytoskeleton, respectively. Interestingly, AGR-3 was detected in the F_1 cytoplasmic and F_2 cell membrane and organelles fraction, in the MCF-7 cell line (Figure 4.9 A). No nuclear nor cytoskeleton localization was observed. MDA-MB 231 breast cancer cells which are ER-negative were tested for AGR-3 expression and found negative. In immunofluorescence experiments the 1.2 antibody gave a repetitive string-like pattern along with some diffused cytoplasmic staining on the same MCF-7 cells (Figure 4.9 B). The 1.2 antibody is therefore consistent in detecting cytoplasmic and organellar AGR-3.

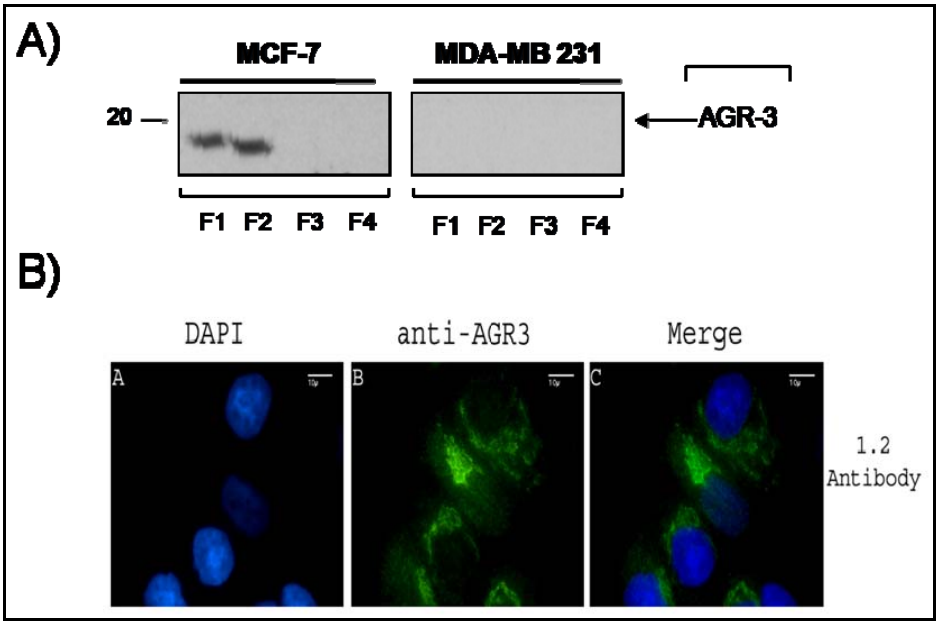

Figure 4.9: Intracellular localization of endogenous AGR-3 by chemical fraction and immunofluorescence. A) MCF-7 and MDA-MB 231 negative control cells were tested for endogenous AGR-3 and analysed by fractionation methodologies into F_1 (cytosolic), F_2 (membrane/organelles), F_3 (nuclear), and F_4 (cytoskeletal) as indicated. The distribution of endogenous AGR-3 (~ 19 kDa) was determined by immunoblotting with the 1.2 anti-AGR3-specific antibody. B) Immunofluorescence of the same cells with the same anti-AGR3-specific antibody and Alexa 488 secondary antibody. Images visualised by Zeiss Axionplan and captured by Sony CoolSnap HQ camera. A:DAPI, B:anti-AGR3, C:Merge. Figures A and B are representative of at least 3 independent experiments (scalebar:10μm).

4.2.2.2 Endogenous AGR-3 after irradiation

Since AGR-2 was found to be induced by UV and act as a p53 inhibitor [474] and also AGR-2 and AGR-3 were both found to be upregulated in breast cancer [199] and belong to the same family [199, 468] , the effects of UV in AGR-3 expression levels were tested (Figure 4.10 A). MCF-7 cells were irradiated and analysed by IF after six hours. In order to define the right dose that would allow visible results in AGR-3 localization patterns, three different doses were used, 10, 50 and 150 J/m^2 (Figure 4.10 B). No translocation of the protein was observed in neither of these doses although in the highest dose applied the fluorescent signal aggregated in some cells. AGR-3 was still detected in this string-like cytosolic reticulum and also distributed in a diffused pattern within the cytoplasm of the cells, but this reticulum was not as extended as in the non-UV control and looked rather disrupted and condensed, due to UV damage (Figure 4.10 B, panels B, E, H, and K). The presence of condensed apoptotic nuclei was enhanced as irradiation doses were increased, as expected. In order to ensure that the expression levels of the protein remained the same, immunoblotting analysis followed after chemical fractionation (Figure 4.10 A). Interestingly, AGR-3 was detected in the cytoplasm and cell membrane/organelles fractions in untreated cells as well as cells treated with $50J/m^2$, an intermediate dose applied, causing not too much cell death but sufficient to induce cellular response. No nuclear, nor cytoskeleton localization shift was observed, after UV damage. The ratio between cytoplasmic and cell membrane/organelles AGR-3 was unchanged, with cytoplasmic AGR-3 being expressed in higher levels compared to the membrane/organellar expression levels (Figure 4.10 A).

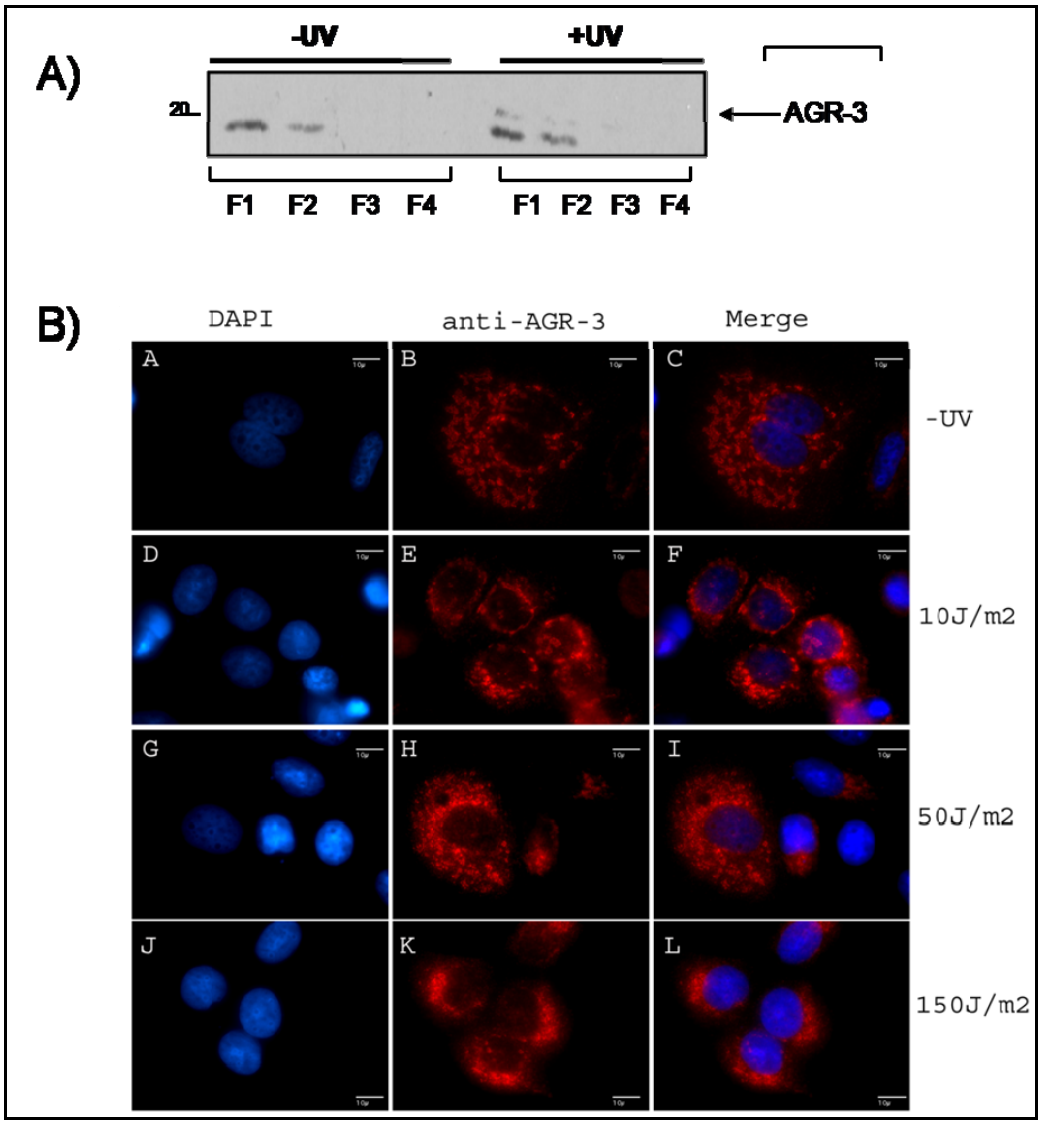

Figure 4.10: UV irradiation does not alter endogenous AGR-3 localization in MCF-7 cells. A) MCF-7 were irradiated at 50J/ m2 and 6h post-UV analysed by using chemical fractionation methodologies into F1 (cytosolic), F2 (membrane/organelles), F3 (nuclear), and F4 (cytoskeletal) as indicated. The distribution of endogenous AGR-3 (~ 19 kDa) was determined by the 1.2 anti-AGR3-specific antibody. B) Immunofluorescence of the same cells irradiated with different doses of UV starting from 10J/m^2 (panels D-F), 50J/m^2 (panels G-I and 150J/m^2 (panels J-L) and incubated with the same 1.2 anti-AGR3-specific antibody and Alexa-488 secondary antibody. Images visualised by Zeiss Axionplan and captured by Sony CoolSnap HQ camera. A, D, G, and J:DAPI, B, E, H and K:anti-AGR3, C, F, I and L:Merge. Figures A and B are representative of 3 independent experiments (scalebar:10µm).

4.2.3 Mitochondrial co-localization of AGR-3 in MCF-7 cells

The first observations for AGR-3 localization regarding the 1.2 antibody resulted in a string-like pattern around the nucleus (Figure 4.6 panels A-C). This specific pattern resembled the mitochondria pattern within a cell, so further studies were performed to determine co-localization of AGR-3 and mitochondria. Mitotracker Red (Molecular Probes, Invitrogen) was used as a mitochondrial marker along with anti-Golgin and anti-PDI antibodies staining the Golgi compartment and ER, respectively. As expected, AGR-3 was strongly co-localized with the mitochondria (Figure 4.11 A) and the co-localization rate, as determined by Leica software Leica Application Suite, LAS AF, varied between 85-100% (data not shown). AGR-3 covers most of Mitotracker's signal with only a few red-only (indicated by white arrows) or green-only areas that represent non-colocalization areas. Brightfield microscopy determined the boundaries of the nucleus and the cell. Minus primary/+secondary antibody controls were used in all the experiments to determine unspecific binding (data not shown). As far as the ER and Golgi are concerned, AGR-3 did not co-localize with any of those markers (data not shown). After confirming co-localization of AGR-3 with the mitochondrial by microscopy, chemical extraction of mitochondria versus cytoplasm was applied (Figure 4.11 B). As expected, endogenous AGR-3 was detected in high levels in the mitochondrial fraction as well as in the cytoplasmic fraction (Figure 4.11 B upper panel) consistent with the microscopy data. Efficient mitochondria isolation was tested by an anti-cytochrome c antibody (Figure 4.11 B lower panel) which is mitochondrial under non-stress conditions. MCF-7 cells have an extended cytoplasm, representing 80% of total cell volume. Therefore, the cytoplasmic fraction should contain a lot of protein and equal μg of cytoplasm and mitochondria, where AGR-3 mainly resides, both contain high levels of the protein.

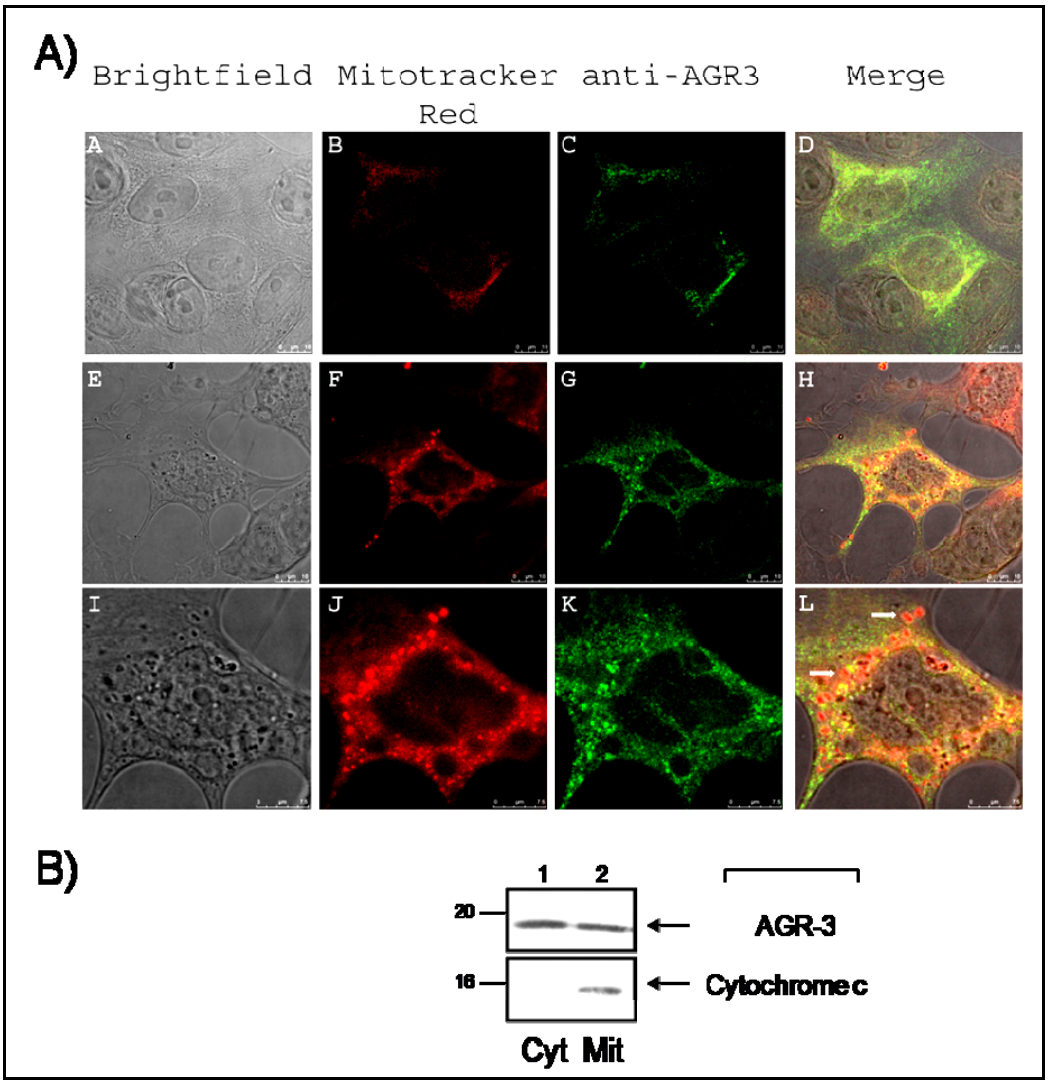

Figure 4.11: Endogenous AGR-3 co-localizes with the mitochondria. A) MCF-7 cells were incubated with Mitotracker Red and after fixation blotted against AGR-3 with the 1.2 anti-AGR3-specific antibody. Alexa488 secondary was used to visualize the protein. Brightfields are shown in panels A , E and I; AGR-3 localization is highlighted in panels C, G and K, mitochondria are depicted in panels B, F and J and the extent of co-localization of AGR-3 and Mitotracker Red was determined by merging the respective images (D, H and L) using a Leica SP5 confocal microscope. Panel I-L is a higher magnification of panel E-H. Figure is representative of at least 5 independent experiments. B) Cytosolic and mitochondrial distribution of endogenous AGR-3 (lane 1-2, upper panel) in MCF-7 using the 1.2 anti-AGR3-specific antibody. Anti-cytochrome c (16kDa) was used a mitochondrial fraction marker (lane 2, bottom panel). L: White arrows indicate non-colocalization areas.

4.2.4 Anterior Gradient 2 and Anterior Gradient 3 co-localization

Co-staining for endogenous AGR-2 and AGR-3 simultaneously was beyond reach as both antibodies derived from immunized mice. As shown in Figure 4.12 I, the two proteins exhibit quite distinct localization patterns and the possibility of them being in the same compartment is not high. To further characterize the localization of AGR-3 as well as compare it to that of AGR-2, MCF-7 cells were transfected with either full length or mature AGR-2 RFP (Figure 4.12 II panels B and F respectively) and co-staining for endogenous AGR-3 was applied by the 2.2 or 1.2 antibody (Figure 4.12 II panels E-H and A-D) respectively. When it came to studying full length AGR-2wt RFP and endogenous AGR-3, the 2.2 antibody was used (Figure 4.12 II panels A-D). As already mentioned, this antibody recognised cell membrane AGR-3 and it was considered as more adequate since full length AGR-2wt is the one that supposed to be secreted although AGR-2wt RFP did not show any signs of secretion so far. No co-localization between the two proteins was observed (Figure 4.12 II panel D). Full length AGR-2wt RFP showed the same granular appearance within the cytoplasm, as several times before, and AGR-3 was detected in the cell membrane of the cell. When it came to mature AGR-2wt RFP and endogenous AGR-3 the 1.2 antibody was used because it is the one that recognises mitochondrial and cytoplasmic AGR-3 and mature AGR-2wt RFP is the one distributed in a diffused way within the cytoplasm apart from the nucleus. Mature AGR-2wt RFP was nuclear and diffused cytoplasmic, whereas AGR-3 was detected in this string-like reticulum, that represents the mitochondria, and in the cytoplasm where it was not distributed in a diffused way, like AGR-2wt RFP does, but followed a granular pattern (Figure 4.12 II panels E-H). Therefore, no colocalization of the proteins was observed (Figure 4.12 II panel H) in either case.

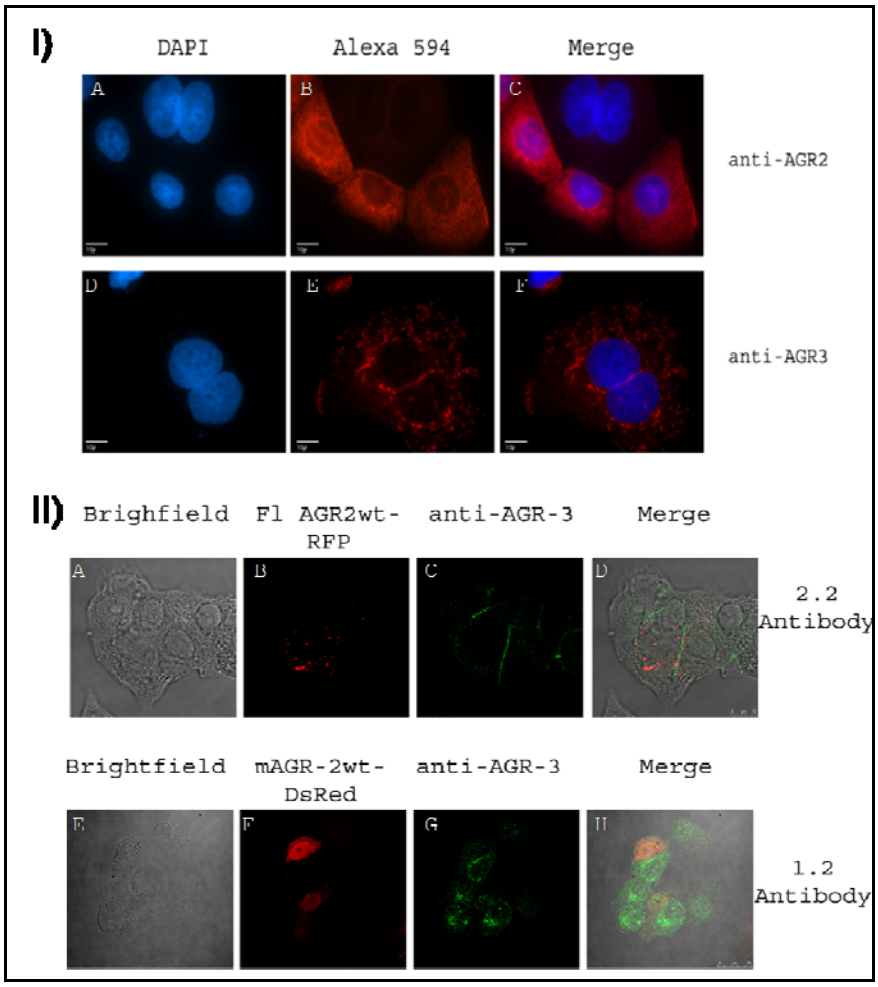

Figure 4.12: Endogenous AGR-3 do not co-localize with AGR-2. I) Endogenous AGR-2 (panels A-C) and AGR-3 (panels D-F) in MCF-7 cells. Anti-AGR-2 monoclonal and anti-AGR-3 1.2 antibodies were used. Alexa 594 secondary was used to visualize the protein. Images visualised by Zeiss Axionplan and captured by Sony CoolSnap HQ camera. DAPI: panels A and D, anti-AGR2: panel B, anti-AGR3:panel E and Merge: panels C and F (scalebar:10μm). II) MCF-7 cells were transfected with the indicated vector expressing full-length AGR-2wt RFP (panels A-D) or mature AGR-2wt RFP. Endogenous AGR-3 was detected by the 1.2 or 2.2 anti-AGR3-specific antibody (panels E-H and A-D respectively). Brightfields are shown in panels A and E, AGR-3 localization is highlighted in panels C and G, full length AGR-2wt RFP is depicted in panels B, mature AGR-2wt RFP in panel F and the extent of co-localization of AGR-3 and AGR-2 RFP constructs was determined by merging the respective images (panels D and H) using a Leica SP5 confocal microscope. Figures are representative of at least 3 independent experiments.

4.2.5 AGR-3 silencing and implications of mitochondria

In order to study the role of AGR-3, siRNA to the protein was applied and the expression levels of a series of proteins were tested. MCF-7 cells were transfected with siRNA unspecific control and siRNA specific to a unique AGR-3 sequence. Untransfected controls were also included in the experiment (Figures 4.13 and 4.14). siRNA was applied and the cells were harvested every day, at the same time, during a five-day time course. Since AGR-3 was found to be a mitochondria-localized protein in MCF-7 cells, a series of mitochondrial apoptotic or survival markers were tested. anti-Bax, anti-Bax6A7 and anti-Beclin1 anti-antibodies were used (as indicated on the right-hand margin of figures 4.13-4.14). AGR-3 expression levels are depicted in the first from top panel of each figure. Interestingly, when AGR-3 was silenced no alterations in Bcl-2 and Bid expression levels were detected (data not shown). On the other hand, after 48h and 72h of AGR-3 silencing, total Bax levels were particularly increased but returned to normal levels after 96h of AGR-3 depletion (Figure 4.13 second panel from bottom). In this case, 'normal' is defined as the expression levels observed at t_0. What is more, after 48h of AGR-3 silencing, a decrease in Beclin-1 autophagy-marker protein was detected in cells that had the protein depleted but not in the untransfected and si-control transfected cells. Same reduction was detected at 72h and 96h post-depletion (Figure 4.13 third panel from bottom). Untransfected cells and cells transfected with control siRNA had significantly higher expression levels of Beclin-1 after 48h, indicating the induction of autophagy. At t_0, no Beclin-1 protein was detected in neither of the samples, due to low levels of autophagy in a newly-split cell population (data not shown). Interestingly, Bax6A7 conformational change, characteristic of apoptosis, was observed when AGR-3 was depleted (Figure 4.14 A second panel from bottom). When mitochondria are undergoing apoptosis, then Bax changes conformation and the 6A7 epitope is exposed in the outer mitochondrial membrane, enabling the antibody to detect it. Twenty-four hours after AGR-3 silencing Bax conformational change is slightly detected and this effect is further induced after 48h and even more

after 72h. Interestingly, after 72h untransfected and siRNA control transfected cells also show elevated levels of Bax conformational change, but this is expected due to normal levels of apoptotic death occurring in cells growing in the same media and being overconfluent for long. Moreover, apoptotic cells are released in the media and toxic substances can further affect the remaining cells viability. In that case again AGR-3 siRNA shows the strongest band when compared to the other two untransfected and transfected with sicontrol cells which can be explained by the synergistic effect of AGR-3 depletion and the above stress conditions. It is worth mentioning that siRNA for AGR-3 is pretty effective and total depletion of the protein is observed after 48h, although in 24h most of the protein is silenced.

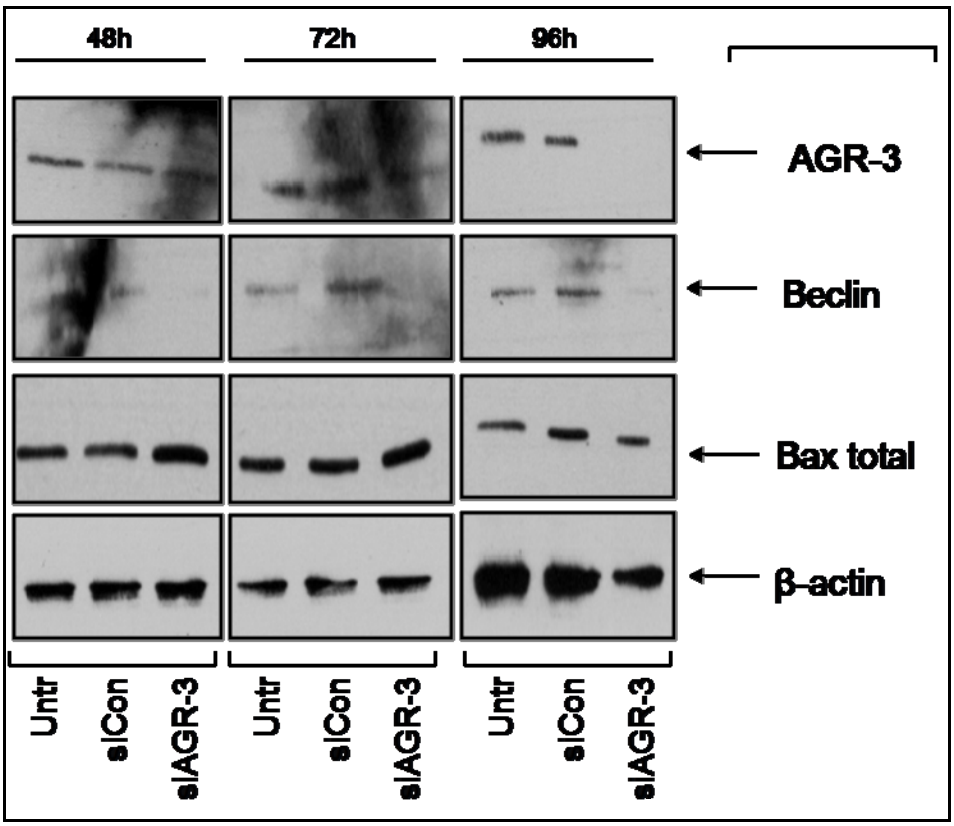

Figure 4.13: AGR-3 silencing is followed by Beclin-1 depletion. MCF-7 cells untreated or treated with siRNA against AGR-3 or control siRNA for 48-72 and 96 hours. Lysates were immunoblotted to determine changes in AGR-3/ Beclin-1/ Bax levels. β-actin was used as a loading control. Figure is representative of 2 independent experiments.

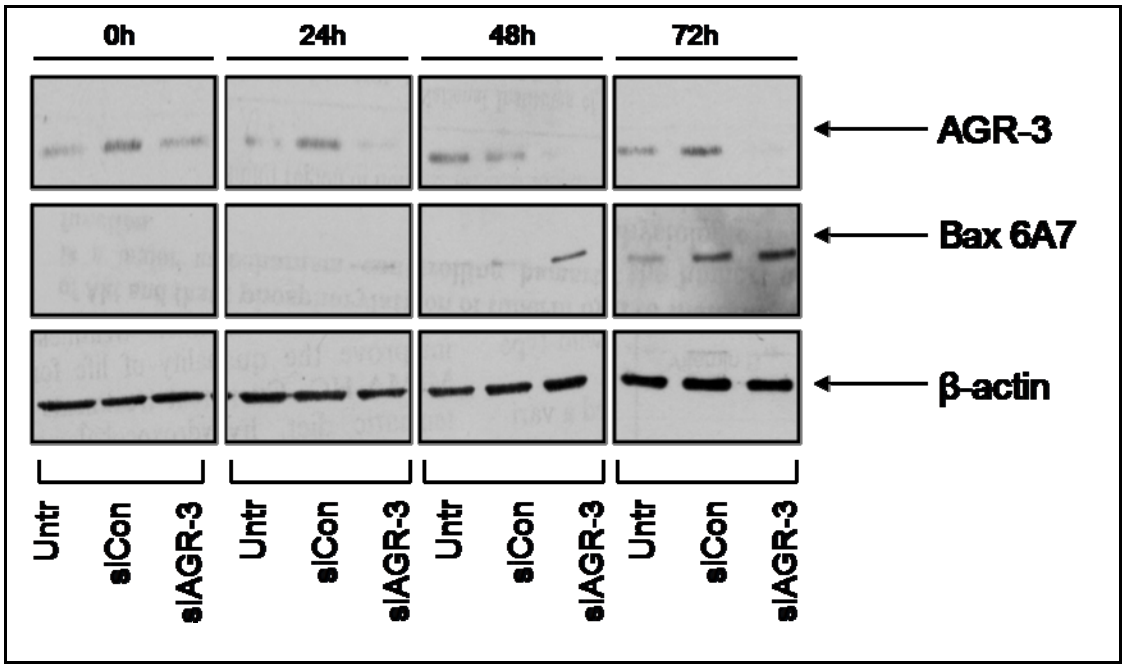

Figure 4.14: AGR-3 silencing is followed by Bax conformational change. MCF-7 cells were left untreated or treated with siRNA against AGR-3 or control siRNA, siCon, for 0-24-48-72 and 96 hours. Lysates were immunoblotted to determine changes in AGR-3 levels (A and B), conformationally changed Bax levels, Bax 6A7, (A and B). β-actin was used as a loading control for total protein levels. Figure showing is representative of 2 independent experiments.

It is worth mentioning that differences in the timepoints where siRNA efficiently depleted the AGR-3 protein were observed and this can be due to cell 'age'. siRNA applied in cells of early passages was more efficient in shorter timepoints (Figure 4.14 first panel from top) whereas cells grown for longer needed more time to totaly deplete the protein from their pool (Figure 4.13 first panel from top).

4.3 Discussion

4.3.1 Monoclonal antibodies vary in ability detecting AGR-3

After characterising a series of mouse antibodies (Moravian Biotechnologies, Czech Republic) generated to identify the AGR-3 protein a lot of interesting data were obtained. The 1.2 antibody when used in immunoblotting identified cytoplasmic and cell membrane/organelles fraction AGR-3 (Figure 4.9) and when used in immunofluoresence experiment gave a string-like pattern which was totally co-localized with the mitochondria in MCF-7 cells (Figure 4.11). On the other hand, the 2.2 antibody which recognizes a different epitope to the 1.2 antibody, is totally inappropriate for immunoblotting, as no detection of AGR-3 was observed (Figure 4.5) whereas in immunofluorescence experiments gives a cell membrane-specific staining pattern (Figures 4.6 and 4.7). The 3.1 antibody is totally inefficient in immunoblotting as well as immunofluorescence applications. Last but not least, the 4.1 antibody is the one that recognises both AGR-2 and AGR-3 epitopes and gives a mixed pattern of mitochondria-like, due to AGR-3 epitopes, and cytoplasmic, due to AGR-2 epitopes, staining when applied in immunofluorescence, acting as a polyclonal instead of a monoclonal one (Figures 4.4 and 4.8). A possible reason explaining the finding that two monoclonal antibodies, 1.2 and 2.2, give such different patterns when applied in immunofluoresence experiments might be the presence of a hidden epitope when the protein is in its native form, such as in microscopy studies where no denaturating step is involved, whereas this epitope is exposed after heating at 95°C for western analysis and co-immunoprecipitation experiments. It is worth mentioning that the different staining of the two antibodies, 1.2 and 2.2, could have been explained if the 2.2 antibody recognised an epitope in the leader sequence of AGR-3 which is supposed to be secreted and therefore detected in the cell membrane, but this is not the case here. Moreover, a possible reason might be the phosphorylation of the 2.2 recognition epitope when the protein

is in its native form and therefore the detection of a cell membrane-specific localization after microscopic observation.

4.3.2 AGR-3 is a mitochondrial protein implicated in cell death

4.3.2.1 AGR-3 depletion promotes Bax conformational change

In HeLa and Cos cells AGR-3 was found to be retained in the endoplasmic reticulum when the putative KDEL-like motif is present whereas this equilibrium was shifted to the Golgi compartment after deleting these last four aminoacids [483]. The same study also revealed that AGR-3 was ER-localized in 60% of cells tested, Golgi and ER mixed in 30% of cells and Golgi-only in 10% of cells tested. After the discovery that AGR-3 co-localizes with the mitochondria in MCF-7 cells, we next wondered whether AGR-3 silencing affects the pro-apoptotic or anti-apoptotic mitochondrial proteins. AGR-3 inhibition had no effect on the expression levels of Bid, Bcl-2, but changed the conformation of Bax and led to the N-terminal 6A7 epitope exposure, as detected by the anti-Bax 6A7 conformation-specific antibody [271, 272] (Figure 4.14). Bax is an apoptosis-promoting protein that normally resides in the cytoplasm of healthy cells but under specific apoptotic stimuli it translocates to the mitochondrial membrane [221, 565], where it oligomerizes and forms pores that enable cytochrome c and other pro-apoptotic factors release [176]. Coincident with activation and translocation to the outer mitochondrial membrane, Bax undergoes a conformation change that exposes the 6A7 epitope and induces oligomerization [271, 272, 473]. When AGR-3 is totally depleted, then total Bax levels are increased and this epitope, indicative of apoptosis, is being exposed (Figure 4.14). Interestingly, no Bid induction is observed after AGR-3 silencing (data not shown). Bid is a pro-apoptotic Bcl-2 family member that is processed after proteolytic cleavage and triggers Bax conformational change [140, 178]. When tBid (truncated Bid) activates

Bax, then Bax translocates to the outer mitochondrial membrane where it oligomerizes and the apoptotic cascade is initiated [639]. Since there is no alteration on Bid levels but only on Bax, it is suggested that AGR-3 acts downstream Bid and upstream Bax in the apoptotic cascade. Studies have suggested that tBid alone is not sufficient to induce Bax translocation and that Bax-lipid interactions are sometimes essential to promote activation [639], so maybe something similar applies to AGR-3 and Bid with AGR-3 inhibiting Bid to activate Bax and so when AGR-3 is absent Bid is free to interact with Bax. Goping and co-workers have previously dissected how changes at the Bax N- and C- termini affect the ability of the protein to target to intracellular membranes [221]. They concluded that the C-terminal Bax α-helix is a signal-anchor required for membrane targeting and insertion but elements at the N-terminus are key-players to regulating this process. Deletion of the N-terminal 20 amino acids of Bax (encompassing the 6A7 epitope) stimulated Bax targeting to mitochondrial membranes *in vitro* and increased its pro-apoptotic activity *in vivo* [221]. In the same study it was suggested that exposure of the 6A7 epitope occurs when the N-terminus is released from some inhibitory interaction with the rest of the protein that may mask the C-terminal targeting sequence or a site of interaction with another protein. Bax activation happens in a series of steps including Bax-lipid interaction, 6A7 epitope exposure that is not essential for Bax membrane insertion [639] and tBid as a potential triggering factor for Bax membrane insertion, indicating the multiple levels of regulation and control for this procedure. A possible candidate for Bax regulation might be AGR-3 which can act by a different pathway from the Bid one, promoting epitope exposure but not affecting Bid levels. Apoptosis and its characteristic pathways are very complex and allow multiple crosstalk and control mechanisms amongst them, so further experiments need to be performed in order to establish the exact AGR-3 function. Our data showing activation of apoptotic Bax when AGR-3 is silenced are consistent to its ability to enhance colony formation and induce cell survival in breast cancer panels [270], suggesting an anti-apoptotic role for the protein.

4.3.2.2 AGR-3 silencing induces an autophagy-marker's expression levels

Another interesting but puzzling finding was that AGR-3 silencing negatively affects Beclin-1 expression (Figure 4.13). Beclin-1, a mammalian ortholog of Apg6, was first identified as a Bcl-2 interacting protein [360] and was the first mammalian autophagy gene discovered [359]. MCF-7 cells are devoid of caspase-3 activity and a lot of studies have revealed that autophagy plays an important role when it comes to cell death in this particular cell line [634, 635]. Beclin-1 along with Atg 7 protein are key player in this cell death process [2, 13]. Akar and coworkers discovered that silencing of Bcl-2 induces autophagic cell death in MCF-7 cells as proven by GFP-LC3 II induction and lead to Atg5 and Beclin-1 increase [13]. A possible explanation can be that AGR-3 acts in an opposite way of that of Bcl-2 and act in favour of autophagy, therefore when silenced caspase-dependent cell death is being induced as it can also happen with other molecules that favour one type of cell death instead of another [516]. No LC-3 cleavage was observed in our experiments (data not shown) but this can be due to difficulty detecting native LC3 in cells. For that reason the generation of an MCF-7 LC3-GFP stable cell line would be really useful. Another interesting explanation that can be taken into account is that some molecules, such as fenretinide, do not strictly stimulate an apoptotic response but are capable of inducing autophagy when the apoptotic pathway is deregulated [187]. Caspase deficiency is a form of deregulated apoptotic pathway, so there is the possibility that AGR-3 under these conditions only, can promote autophagy but more cell lines should be tested to further characterize this observation. Another possible explanation might be that AGR-3 is not alone sufficient to totally inhibit apoptosis in favour of autophagy in caspase-3 deficient cells, and that can explain why when silenced neither apoptosis is being highly induced nor autophagy is totally reduced. Moreover, studies have revealed that reduction or total loss of Beclin-1 expression abrogates the autophagic response of MCF-7 cells to DNA damage, allowing cells to die by apoptosis [2]. Although DNA damage was not the case here, maybe AGR-3 loss leads to Beclin-1 reduction and this cascade triggers mitochondrial apoptosis

that is detected by Bax conformational change. Or perhaps and opposite mechanism involving AGR-3 inhibition of Bax translocation and increase of autophagosomes formation is valid here, as in the case of cathepsins and Bid inhibition by drugs [341, 626], so when AGR-3 is present no Bax translocation occurs. Calpain, a calcium-dependent cysteine protease, is another example of a molecule that disrupts the equilibrium between autophagy and apoptosis and favours one type of cell death of the other. Indeed, when calpain is inhibited it induces Bax activation, cytochrome c release, PARP cleavage and reduces Beclin-1 expression in oridonin-induced L929 cells [112]. The above studies suggested that inhibition of autophagy increased the apoptotic response and vice versa, indicating a rather antagonistic relationship, which can also be the case in our studies and suggesting AGR-3 as a molecular switch between the two processes. Paradoxically, later studies revealed that Beclin-1 contains a conserved BH3 domain and interacts with Bcl-2/Bcl-x_L suggesting a role in initiating apoptosis [438, 533] or even helps loading mitochondria to autophagosomes [166, 333, 438]. All the above observations reveal a multi-tasking Beclin-1 molecule which is involved in autophagy as well as apoptosis depending on the stress conditions or cell type and therefore a similar role for AGR-3, which upregulates Beclin-1, can be proposed. Also one has to consider that in some cases autophagy act as a means of delaying apoptosis or prolonging survival in non-invasive breast tumour cells [2], so absence of AGR-3/ Beclin-1 weakens autophagy and no apoptosis delay happens which therefore leads to Bax translocation and initiation of apoptosis. The boundaries between Type I and II cell death have never been completely clear and perhaps do not exist due to intrinsic factors among different cell types and the crosstalk among organelles within each type. Apoptosis can begin with autophagy, autophagy can end with apoptosis, and blockage of caspase activity can cause a cell to default to Type II cell death from Type I [367]. Experiments are underway to verify the exact mechanism of AGR-3 function in terms of cell death.

4.3.3 Conclusions of chapter

The results in this chapter demonstrated the significance of monoclonal antibodies into detecting variable epitopes that can give totally different staining patterns. Indeed, the protein was detected in the mitochondria and cell membrane by two different antibodies. Mitochondrial AGR-3 was the one targeted with siRNA and depleted from cells in an attempt to detect differences in other mitochondrial proteins. Interestingly, AGR-3 silencing was followed by reduction in Beclin-1 expression levels and increase in conformationaly-changed Bax expression levels, suggesting a role in autophagy and apoptosis equilibrium. This is distinct from the localization of AGR-2 and highlights the distinct roles of AGR-2 and AGR-3 in reducing the activity of pro-apoptotic pathways. These data also suggest that the AGR-2 and AGR-3 proteins (+ associated pathway) might represent anti-cancer drug targets for re-activating pro-apoptotic pathways in cancers.

Chapter 5

AGR-2 as Potential Anti-Cancer Drug Target

5.1 Introduction

5.1.1 Combinatorial application of nucleic acid-based agents

Cancer development is a multi-step processes which at its core involves clonal evolution under natural selection resulting in the survival of cells with an enhanced capacity to evade normal growth control. The core genetic outline of the cancer cell is being developed and involves universal perturbation in sets of signal transduction pathways regulated by well-studied proteins such as RAS, WNT, ARF, BRCA, Bcl-2, TGF-β, p16, and p53 as well as small signalling molecules such as TGF-B, TNF, and interferons [245]. This had led to drug-discovery programmes in each of these areas concerning molecular-targeted smart cancer drugs.

The progress made in cancer biology, genetics and biotechnology has led to a major evolution in cancer drug design and development, from non-specific, cytotoxic agents to specific, molecular-targeted smart cancer drugs [283]. These agents are characterised by improved selectivity for cancer versus normal cells and are associated with better anti-tumor effectiveness and lower toxicity [551]. The new generation of anti-cancer drugs requires low concentrations and minimizes unwanted side effects. The strategy behind antisense therapy is the development of specific therapeutic agents that aim to correct the mutations and abnormal expression of oncogenes by decreasing gene expression, inducing degradation of target mRNA and causing premature termination of transcription [283]. A fascinating class of anti-cancer drugs include antisense oligonucleotides (ASOs) or small interfering RNAs (siRNAs) which are able to specifically down-regulate the expression of the target genes. These small molecules are specific for a range of proteins including inhibitors of apoptosis, cell cycle and growth promoting protein kinases, de-acetylases that modify the transcription programme of a cell, and enzyme machines that regulate protein degradation like the proteasome. The combination of nucleic acid-based

agents with conventional chemotherapeutic drugs have shown synergistic inhibitory effects in terms of cell proliferation, tumour growth, induction of cell cycle arrest and apoptosis [632]. These two strategies (ASOs and siRNAs) will help to improve current therapeutic regimens. In addition, the combination of targeted drugs with common chemotherapeutic agents might be able to make resistant cells again sensitive towards a chemotherapeutic agent. Another rapidly emerging field of research concerning the development of highly specific anti-cancer drugs is focused on small peptides that bind to the target and affect its activity, in a negative or a positive way.

5.1.2 Aptamers as novel anti-cancer drugs

In 1990, Robertson and Joyce invented new techniques on the mutation, amplification and selection of *Tetrahymena* RNA enzymes *in vitro* that cleaved DNA or RNA with high efficiency in an attempt to discover RNAs with novel catalytic function [492]. At the same time, Tuerk and Gold isolated high affinity nucleic acid ligands by a procedure based on multiple cycles of ligand selection from a pool of variants and then amplification of the ones that bound to the T_4 DNA polymerase [592]. Multiple round of selection exponentially enriched the pool and the strongest candidates that bound to the DNA polymerase were further characterised. Amongst them was the wt sequence of the bacteriophage mRNA and a similar sequence differed at four positions. The technique used could yield high-affinity ligands for any protein that binds nucleic acids as part of its function and then these ligands could be developed and modified for any other target [592]. Independently, a third group identified small RNA molecules that bound to specific targets at the same time and they were the ones that termed these molecules as aptamers [172]. They used small RNA molecules that interacted with targets that mimicked metabolic cofactors and after iterative rounds of selection, mutated the final candidates to map the exact region of interaction. In the early 90s was therefore, the initiation of the systematic

evolution of ligands by exponential enrichment (SELEX) or *in vitro* selection for production of oligonucleotide aptamers with high affinity toward target molecules (Figure 5.1).

Aptamers, from the latin word “aptus”=bind and the Greek word “meros”=particles, posses highly selective molecular recognition properties and can target specific key molecules inside or outside a diseased cell [172]. They were first described in viruses and particularly in pathways that regulate HIV-1 replication [129]. Aptamers can be RNA or DNA ligands [172, 186, 492, 592]. Aptamers can be fused to several molecules useful for upstream application such as microscopy, chromatography, electrophoresis, without affecting their affinity to the target [305]. The susceptibility of the aptamers to various modifications makes them a valuable tool for biotechnology, drug therapy, diagnostics, target validation, genetic screening and purification processes [478]. Their functional asset that distinguishes them from the widely used antibodies is the fact that aptamers distinct between closely related but non-identical members of a protein family, or between different functional or conformational states of the same protein [44]. They also present a highly stable 3-dimensional structure that ensures efficient and tight binding to their targets along with resistance to nuclease degradation [283]. They are characterised by high stability despite of the environment, lack of immunogenicity [181] and a smaller size which makes them more efficient to penetrating tumors and then removed by circulating blood (Table 5.1).

The first approved aptamer with therapeutic function was the anti-human VEGF aptamer (VEGF: vascular endothelial grow factor) first tested in rhesus monkeys [591]. The PEGylated form of this aptamer was called Pegaptanib and used as the medicinal active component of the newly developed drug for the treatment of wet age related macular degeneration. The pharmaceutical product Macugen1 (pegaptanib sodium injection) from Pfizer Inc./OSI Pharmaceuticals was approved in December 2004 (USA) and January 2006 (Europe) [101, 371]. Other examples of applied aptamers in clinical field are summarized in Table 5.2.

Antibodies	Aptamers
Antibodies often suffer variations from batch to batch	Smaller size and chemically synthesized without batch variation
Production requires the use of animals	In vitro production, rapidly, reproducibly and accurately with no animals or cell lines involved
Labelling can cause reduction or loss in affinity	Can be labelled without affecting their affinity
Cross-reactivity in other species	High specificity within species
Manipulation only under physiological conditions	Selection conditions can be manipulated, temperature, pH, buffer, etc.
Limited to molecules that produce an immunoresponse	Able to bind with drugs or toxic substances or targets with low immunogenicity
No live cell applicability	Highly efficient for live cell applications and study of interactions [186]
Sensitive to temperature and humidity changes	Storage and transport can be done at room temperature
Limited applicability only as detection probes	Can be used as detection probes, inhibitors or regulators of protein function or even competitors [79]

Table 5.1: Advantages of aptamers over antibodies [172, 375, 560]

Target	*Aptamer/assay*	*Field of application*	*Reference*
VEGF	RNA aptamer	Therapy, wet age related macula degeneration	[44, 371]
Thrombin	DNA aptamer (thrombin inhibitor ARC-138)	Therapy, anticoagulant	[434]
Factor IXa	RNA aptamer (factor IXa inhibitor) and its antidote REG1	Therapy, anticoagulant	[161, 434]
Abrin toxin	DNA aptamer	Medicine	[569]

Table 5.2:Examples of applied aptamers (adapted after [560]).

The identification of active compounds is succeeded through specialized and highly sophisticated cycles of selection and amplification which require encoding strategies for the resolution of the molecules. Approaches thoroughly used are based in displaying peptides, proteins or antibody fragments on phage or cell surfaces, which convert the amino acids sequence into genetic information that can be amplified in vivo. Most aptamers are capable of regulating the biological function of the compound molecules, are excellent candidates for drugs or drug leads. Two general types of experimental procedures have been applied, one designed to find peptide-based ligands in vitro (phage display), the other tailored to identify protein to protein interaction in vivo (two hybrid analysis).

5.1.2.1 SELEX isolation of aptamers

SELEX stands for Systematic Evolution of Ligands by EXponential enrichment. First described in 1990 [172, 592], this method refers to isolation of nucleic acid ligands by exponential enrichment of a potential target pool.

The SELEX procedure conscists of iterative cycles of in vitro selection and enzymatic amplification of nucleic acids that drives the selection towards relatively few, but optimized structural motifs for binding [224]. By these iterative cycles of selection and purification the initial random olignucleotide pool is narrowed down to a minimum group of ligand oligonucleotides that show high specificity and affinity for the target. The binding complexes are the partitioned from unbound and weakly bound oligonucleotides. This is one of the crucial steps towards the selection of highly specific and efficient aptamers. Target bounds are amplified by PCR (in the case of DNA) or RT-PCR (in case of RNA). This ds DNA is then transformed to a new oligonucleotide enriched pool that is used for binding to the target in a new SELEX round. After the last round the selected oligonucleotides are cloned and sequenced and then tested for their affinity and specificity in binding assays. The region required for binding can be reduced by mutation and truncation experiments [560]. Several techniques were evolved from SELEX and can be used in the generation of aptamers such as photoSELEX, capillary electrophoresis SELEX, blended SELEX, genomic SELEX that vary in applicability but they all offer high specificity and quality aptamers .

Various molecules can be used as targets for an aptamer selection. The smallest molecular target so far used for an aptamer selection is ethanolamine, a simple structured molecule (C_2 chain) with two functional groups (–OH, $–NH_2$) [381] widely used in cosmetic industry but also associated with Schizophrenia [264] and Alzheimer disease as well as characterised as a carcinogenic substance. Other targets can be Neomycin [606], T_4 DNA polymerase [592], ATP [513], cAMP [317], African trypanosomes [259], amino acids [376], Zn^{+2} [117], NAD/FAD [79], Shephadex [556], coA [512], interferon$_\gamma$ [329] and a lot more.

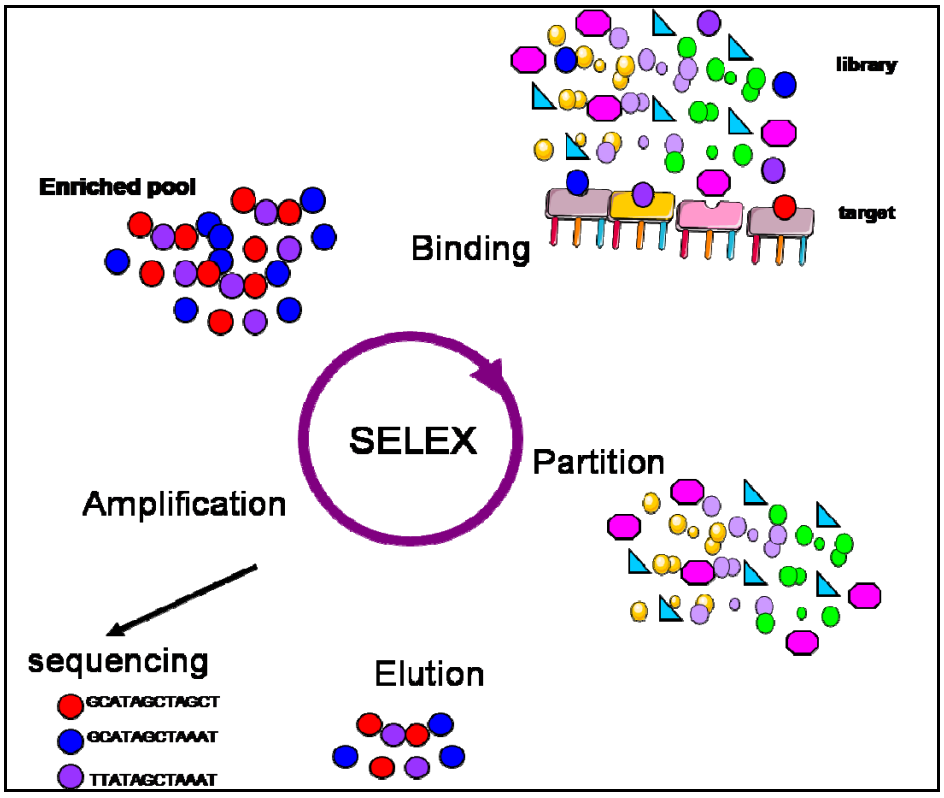

Figure 5.1: SELEX technique for aptamer isolation. For details of this technique refer to text 5.1.2.

5.1.3 Peptide aptamers

Peptide aptamers were developed after nucleic acid aptamers and are combinatorial protein reagents that bind to target proteins with high specificity and strong affinity. Aptamers can interfere with the function of their associated intracellular targets and also probe for regulatory networks within cells [32, 68, 123, 127, 283]. The design of peptide aptamers is inspired directly from the structure of immunoglobulins or T cell receptors, where variable peptidic loops are displayed by constant framework regions [32] (Figure 5.2). Peptide aptamers are most commonly used as disrupters of protein interactions due to their ability to bind to a region of the target protein and disrupt the scaffold that would otherwise mediate protein-protein interaction [127]. They also

aid to validating therapeutic targets at the intracellular level but also have therapeutic potential, both as lead structures for drug design and also as a basis for the development of protein drugs [263]. The most widely used expression system for combinatorial protein libraries has been the filamentous bacteriophage M13. Briefly, a phage library is added to a plastic dish coated with a protein target and unbound phages are washed away. Binding particles are eluted, amplified and added back to the dish. Significant enrichment of binding molecules is achieved by multiple rounds of this experimental sequence [123].

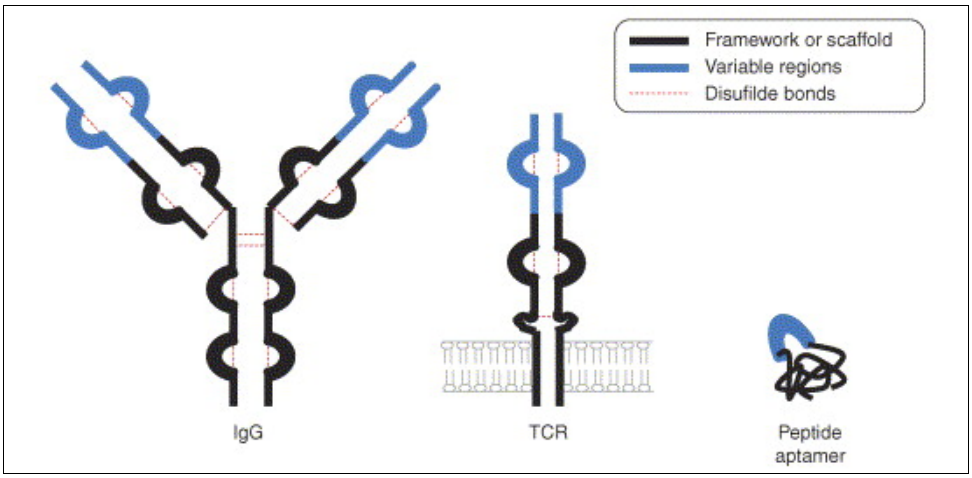

Figure 5.2: Recognition protein molecules. Three major classes of constrained recognition protein molecules are depicted: immunoglobulin G (IgG), T cell receptor (TCR) and peptide aptamer. Black lines represent constant framework or scaffold residues. Blue lines represent variable peptidic regions. Red dotted lines represent disulfide bonds. Major distinguishing features of peptide aptamers include the much smaller size and the absence of requirement of disulfide bonds to ensure structural constraint of the variable region, as opposed to IgG and TCR molecules (image adapted from [32])

Peptide aptamers belong to the most popular methods used to validate targets as they act upon protein expression levels in cellular or animal models. Aptamers along with other specific ligands such as chemical or biotherapeutic molecules, do not affect

protein expression levels but aim at inhibiting protein function unlike gene knockouts that abolish expression, antisense or RNA interference methods that reduce expression to various extents and also overexpression of target proteins either constitutively or in an inducible fashion [32]. For example, a range of peptide aptamers have been generated to CDK [35, 191], p300 [147] and a lot of other proteins.

5.1.4 Aptamers to Anterior Gradient 2

Two sets of peptide-aptamers were identified from a 12-mer peptide combinatorial library that can interact with the AGR-2 protein [424]. One of them was chosen and passed through four rounds of selection and alanine scan, substitution mutagenesis of every single aminoacid to alanine to identify the minimum number of aminoacids required for efficient binding to AGR-2, narrowed it down to six in number consisting a bioactive hexapeptide PTTIYY core consensus site [424]. Given the likelihood that AGR-2 contains a peptide-binding groove, Murray and colleagues further evaluated whether a mutant derivative of the hexapeptide (PTTIYY) consensus sequence with altered binding to AGR-2 could be generated. Substitution scan mutagenesis at each position (1-6) of the hexapeptide core identified the class of amino acid residues that were tolerated as AGR2-binding peptides. Especially notable from the mutagenesis scan is that the double hydrophobic residues YY are required for AGR2-binding [424]. Accordingly, AGR-2 binding directly to a series of peptides containing the core PTTIYY sequence was attenuated when the C-terminal Y was mutated to an alanine [424]. Such peptides containing the PTTIYY motif can be used to affinity purify the AGR-2 protein from crude lysates [52].
Based on this data, a bioactive AGR2-binding peptide containing the PTTIYY core was cloned into AcGFP expression vector for creating an AcGFP fusion scaffold to analyze effects of the peptide on the AGR-2 pathway in cells, analysed in this thesis. GFP scaffolds have been utilized in monitoring localization of the binding

interaction, detecting functional activity, expression levels and quality of the aptamer by analysing fluorescent signals of different intensity [1, 458].

5.1.5 Objectives of chapter

As described above, novel technologies for identifying potential anti-cancer drugs have utilised the generation of small molecules interfering with the function of target genes. AGR-2 is now known to reside in the nucleus and behave as a p53 inhibitor, attenuating p53 phosphorylation at Ser^{15}. In this chapter siRNA molecules and novel peptide-aptamers against AGR-2 were evaluated to determine whether inhibition of AGR-2 has any effect on stimulation of the p53 pathway. If so, this would hold promise for targeting AGR-2 as a drug target for stimulating the p53 pathway in cancers.

5.2 Results

5.2 .1 Cloning of Peptide Aptamers

5.2.1.1 Conventional cloning

Three peptides, 60bp in length, identified to bind AGR-2 by phage display library [424], were cloned in order to define their role in the AGR-2 pathway. The wt aptamer has high affinity to AGR-2 whereas the Y-A substitution aptamer less and the premature stop aptamer even less when compared to the other two (data confirmed by ELISA, Dr. Murray). These peptides can serve as potential inhibitors or activators of AGR-2 and therefore affect p53 or other genes of the tumour suppression pathway. 60bp oligos were cloned into a GFP or RFP vector and co-localization along with co-immunoprecipitation experiments determined their binding affinity to AGR-2. The first vector tested was the EGFP-C_3 vector (4.2kb, Clontech).

Forward and reverse oligo were annealed to form a double-strand oligo which was inserted into the appropriate EGFP-C_3 vector, by conventional cloning techniques including digestion-ligation-bacterial expression. Due to the small size of the oligos compared to the EGFP-C_3 vector (70-fold smaller) certain problems appeared during the cloning process. PCR product formation was optimized by adjusting the cycling parameters, including the cycle number and primer annealing temperature but no positive results were obtained. A different strategy was then chosen˙ Different restriction sites were integrated at the end of the oligos and different vectors were used for cloning. Each step of the cloning procedure (annealing, restriction digest, dephosphorylation, ligation) was tested for its effectiveness, by electrophoresis, and different molar ratios of vector: insert were tried each time, varying from 1:1 to 1:10. Again, no positive clones were found after sequencing analysis. A major problem faced throughout the whole process was the high amount of colonies, present in the

digested and dephosphorylated vector, either in the presence or absence of T_4 DNA ligase, indicating insufficient digestion of the vector. The vector was gel purified (Qiagen) to eliminate traces of uncut plasmid, but the problem persisted.

5.2.1.2 Sequential cloning

Since neither of the above mentioned strategies was fruitful, a third method was adopted. The whole GFP gene was amplified with the oligo sequence on its C-terminus as a tag. After the amplification, the whole gene was cloned into a AcGFP-vector, which was previously digested to exclude the GFP gene (613-1329). This method was adopted because of the size of the insert (750bp) compared to the vector. The AcGFP-C_1 vector was PCR amplified with a first set of primers that annealed to the N-terminus of the GFP gene and included the *AgeI* restriction site, unique and at the very start of the GFP gene, and the reverse primer annealed to the 18-first base pairs of the MCS region and included the first 21 base pairs of the aptamer wt (PTTIYY core). The 750bp DNA fragment amplified included the GFP gene along with the first 18 bases of the MCS and the first 21 bases of the aptamer sequence which were integrated as an extra sequence, as a tag. This fragment was PCR-purified (Qiagen) and a second round of PCR followed with the same forward primer, *AgeI* site and GFP sequence, but a different reverse one. This time the reverse primer included the rest of the aptamer wt sequence, including 12bp of the already amplified aptamer sequence which served as a recognition site for annealing, and an *EcoRI* restriction site for the MCS. The AcGFP-C_1 vector was cut with *AgeI* and *EcoRI*. *AgeI* cuts in the beginning of the GFP gene and *EcoRI* in the MCS. After amplification the GFP-aptamer wt fragment and the AcGFP-C_1 vector were digested with the two restriction endonucleases, purified (Qiagen Gel Purification kit) and ligated to the GFP-aptamer as described in Materials and Methods. Positive clones were isolated from *E.coli* cells and sequence analysis verified the correct ones used for further experiments.

5.2.1.3 Site-directed mutagenesis of the GFP-Aptamer wt

In order to test the effect of the GFP-Aptamer wt, containing the PTTIYY core, to the AGR-2 activity and the specificity of the interaction, negative controls were essential to the studies. For that reason, GFP-Aptamer mutants were created by site-directed mutagenesis, following the manufacturer's protocol (Stratagene). The first Y-A mutation was selected because ELISA experiments had shown that a single mutation from Lysine to Alanine at position 22 of the aptamer had significantly less binding affinity to AGR-2 (Dr Euan Murray). The premature stop aptamer mutant did not contain the whole core and had even less binding affinity to AGR-2. Therefore, the three negative controls included (i) GFP alone with no fusion peptide cloned; (ii) GFP vector containing the bioactive PTTIYY sequence but containing a stop codon before the PTTIYY peptide start which produces a GFP control protein (termed as GFP-aptamer premature stop), and (iii) GFP containing the bioactive AGR2-binding peptide but with the single attenuating point mutation, PTTIYA (termed as GFP-aptamer Y-A)

5.2.2 Localization of the Aptamers in MCF-7 cells.

In order to study the localization of the AcGFP-C_1 Aptamer wt/Y-A/stop mutants, the aptamers were transfected in MCF-7 cells and subcellular fractionation experiments were performed. Monoclonal anti-GFP antibody was used to detect the aptamer. All the aptamers were detected in the cytoplasmic fraction (Figure 5.3 A) although expression levels were not similar between the aptamers. The GFP-Apt stop had the lowest expression levels (Figure 5.3). The AcGFP-C_1 vector was also detected in the aforementioned fractions. Coomassie Blue stain verified the fractionation efficiency and equal loading of each fraction (Figure 5.3 B).
Fluorescent microscopy showed the GFP-Aptamers (wt/stop/22Y-A) in the cytoplasm (Figure 5.1 I-III) and no co-localization with ER and Golgi markers was

observed (data not shown). Interestingly, a lot of nuclei transfected with the wt or the mutants, showed a distinguished pyknotic shape. GFP-artificial nuclear staining was observed in all the aptamer-transfected cells along with the GFP-control transfected ones (Figure 5.5), although no GFP was detected in the nucleus after chemical fractionation. The reason for characterising it as artificial is discussed thouroughly in section 5.3.1.

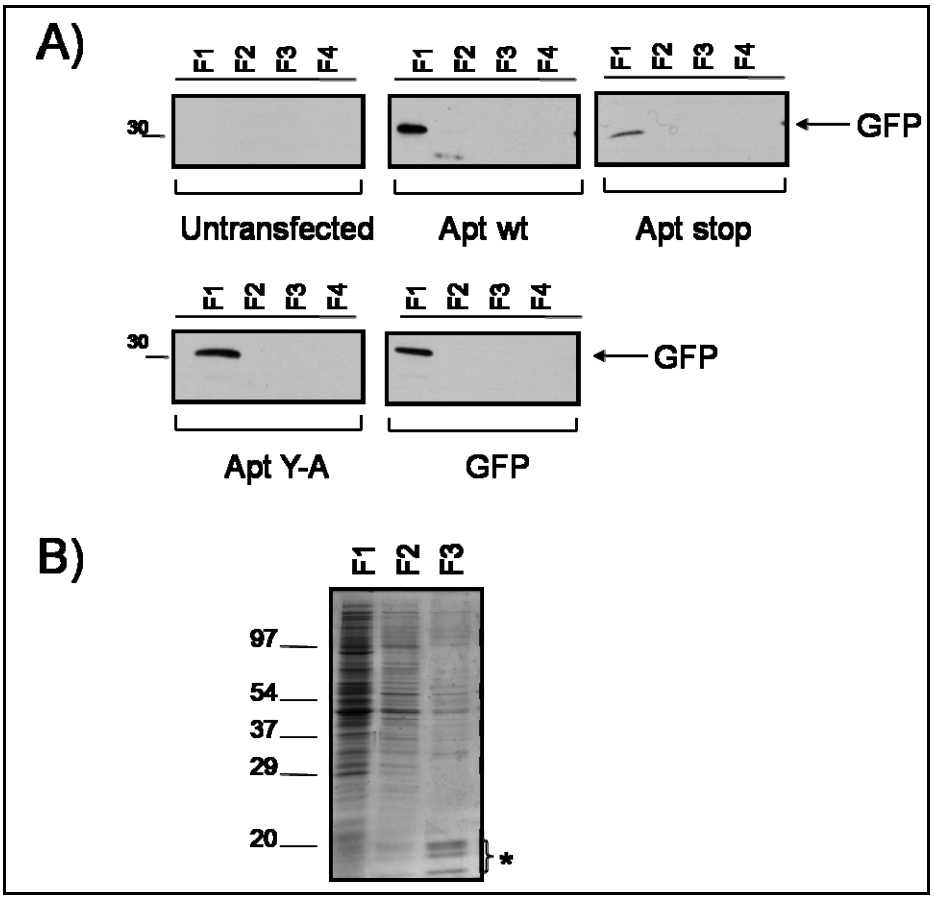

Figure 5.3: GFP-Aptamers are localized in the cytoplasm of MCF-7 cells. A) MCF-7 cells transfected with each of the GFP-Aptamers, wt/premature stop mutant/ 22Y-A. Untransfected and GFP-vector controls were included. The cells were processed using fractionation methodologies into F_1 (cytosolic), F_2 (membrane/organelles), F_3 (nuclear), and F_4 (cytoskeletal) as indicated. The distribution of the GFP-tagged aptamers (~ 30 kDa) was determined by immunoblotting. B) Representative Coomassie blue stain as fractionation control *: histones as defined by MS. Figure is representative of 3 independent experiments.

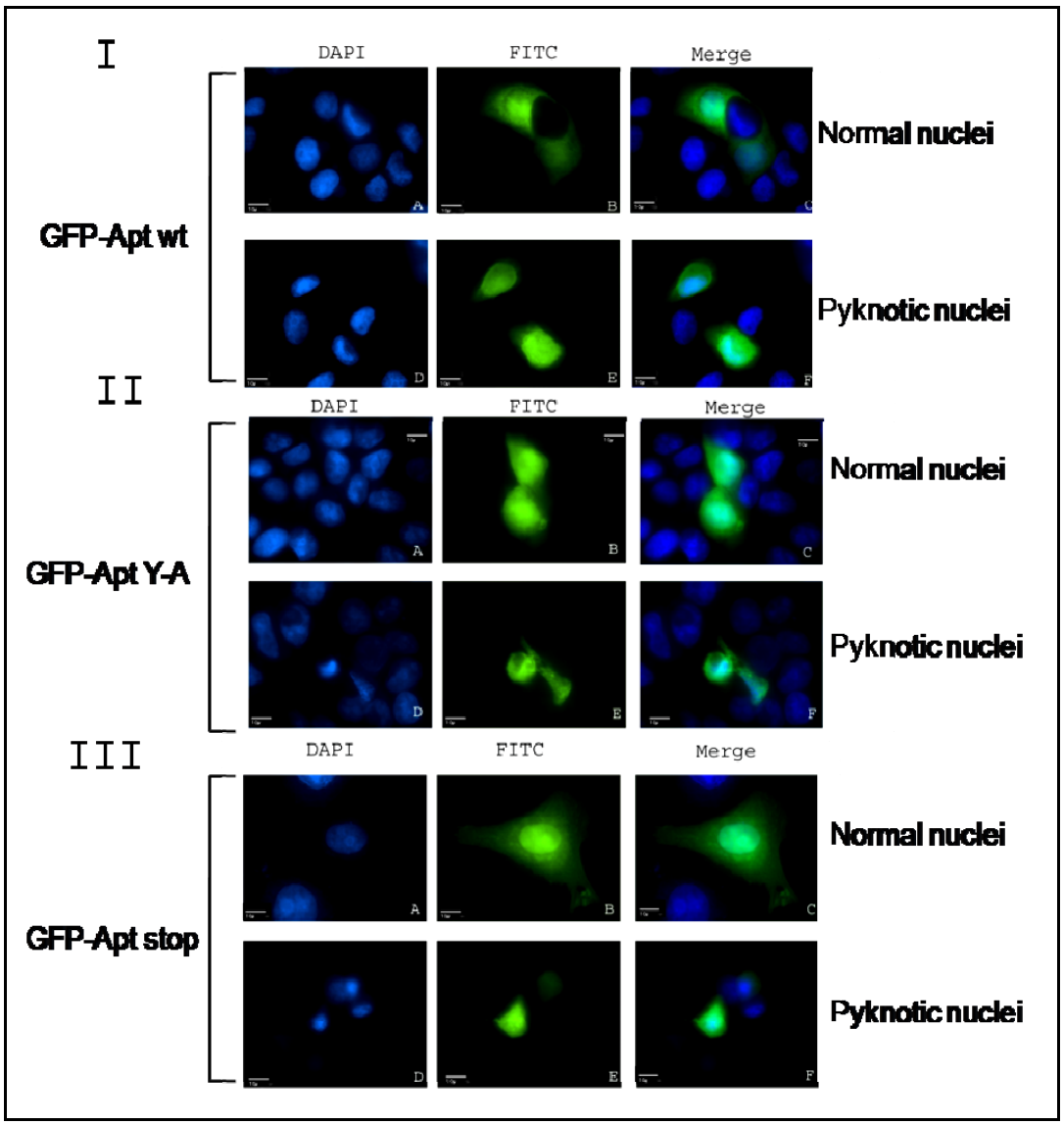

Figure 5.4: Intracellular localization GFP-Aptamers in MCF-7 cells by fluorescent microscopy. MCF-7 cells were transfected with the indicated vector expressing GFP-Aptamer wt (panels IA-IF)/Y-A (panels IIA-IIF)/stop(panels IIIA-IIIF). DAPI staining shows the location of the nucleus (panels I,II,III A and I, II, III D), FITC depicts the localization of each aptamer (I, II, III B and I, II, III E) and merge images are shown in panels I, II, III C and I, II, IIIF. Images visualized by Zeiss Axionplan microscope and captured with the photometric CoolSnap HQ camera. Same exposure times applied for all images. Figure is representative of at least 3 independent experiments (scalebar:10μm).

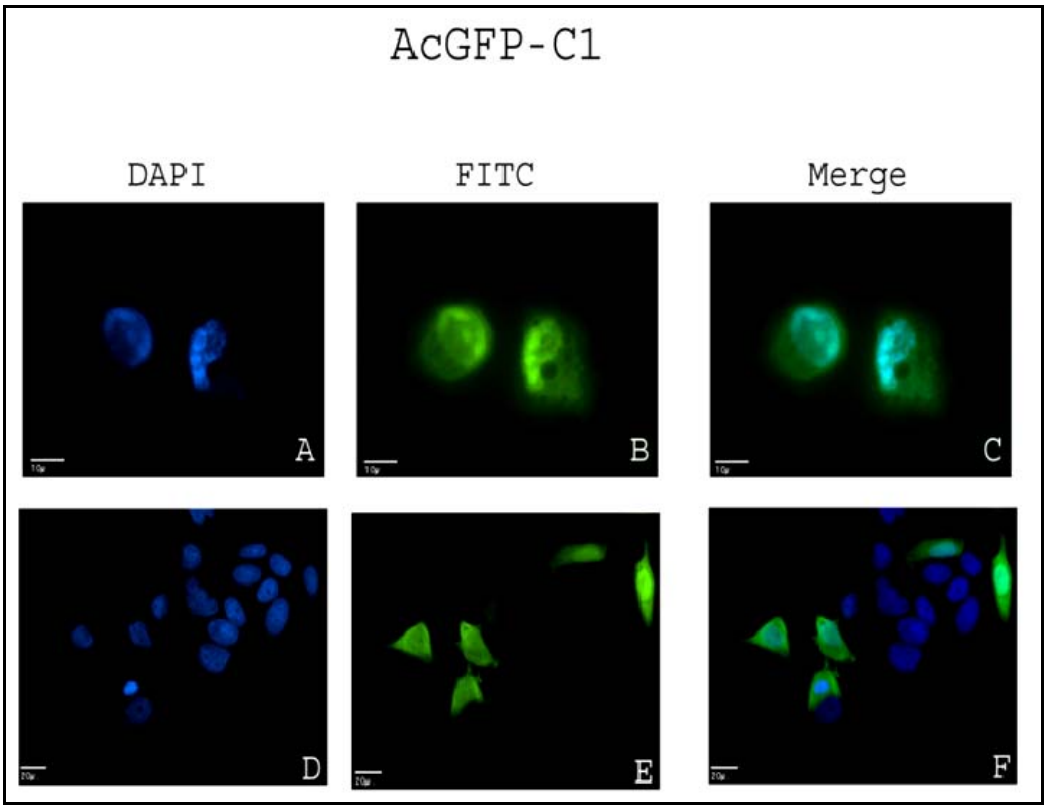

Figure 5.5: Intracellular localization of GFP-vector control in MCF-7 cells by fluorescent microscopy MCF-7 cells were transfected with the indicated vector expressing GFP (panels A-F). DAPI staining shows the location of the nucleus (panels A and D), FITC depicts the localization of each aptamer (B and E) and merge images are shown in panels C and F. Images visualized by Zeiss Axionplan microscope and captured with the photometric CoolSnap HQ camera. Same exposure times applied for all images. Figure is representative of at least 3 independent experiments

5.2.3 Aptamers induce the formation of pyknotic nuclei

Quantative studies, counting the number of aptamer-transfected pyknotic nuclei (Figure 5.6) against the total number of transfected cells revealed that the GFP-aptamer$_{wt}$ stimulated the formation of pyknotic nuclei the most. A total of 1000 nuclei per chamber in randomly chosen fields were counted under a Zeiss

epifluorescent microscope (Figure 5.7). The GFP-Aptamer wt had very high levels of pyknotic nuclei, reaching a percentage of 75% of total cell population (Figure 5.7 B, blue label). The GFP-Aptamer$_{stop}$ and the GFP-Aptamer Y-A had less pyknotic nuclei percentage when compared to the GFP-Aptamer wt, (Figure 5.7 B, orange and purple labels respectively). The GFP-Aptamer stop was shown to be a little less drastic than the GFP-Aptamer Y-A and 55% of abnormal nuclei against 58%, respectively. Interestingly, the AcGFP-C_1 vector only samples had also high levels of pyknotic nuclei, indicating the toxicity of the GFP (Figure 5.7 B, green label). Nevertheless, the pyknotic nuclei observed in the GFP control were lower than the GFP-Aptamer$_{wt}$ ones and of equal levels to the GFP-aptamer Y-A/stop which were used as an unspecific binding control, as expected.

Moreover, live cell imaging further supported the initial observations made in fixed cells. MCF-7 GFP-Aptamer wt -transfected cells were monitored for V days at a 10-minutes interval base (data not shown). The m-cherry vector was used as a nuclear marker (kindly provided by Dr David Lierres, Dundee). Several fields were screened. In most occasions, cells transfected with the GFP-Aptamer wt started to show signs of condensed nuclei after day I and cell death occurred on day II-III.

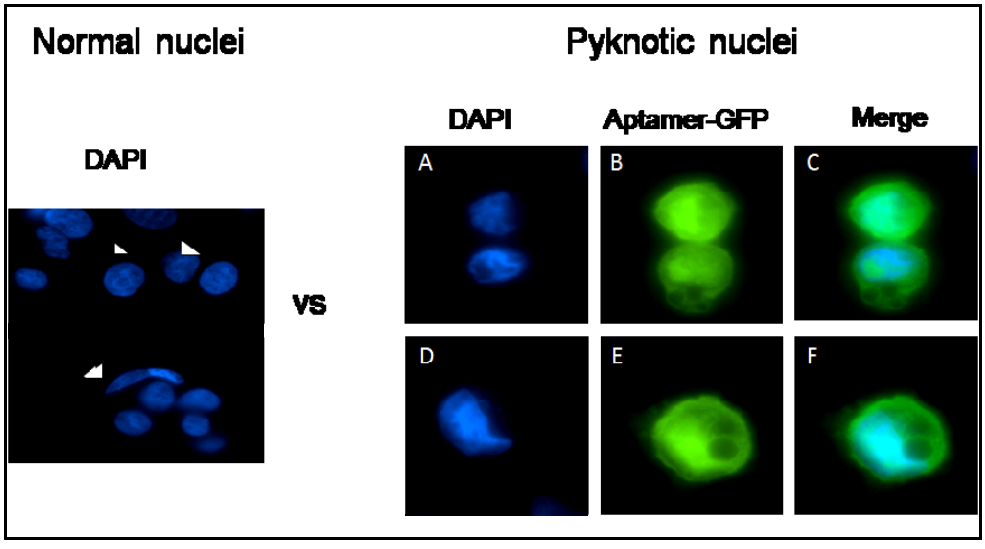

Figure 5.6: Aptamers induce the formation of pyknotic nuclei in MCF-7. Representative figure of pyknotic nuclei induced by GFP-Aptamer compared to normal ones, white

arrowhead, is shown. DAPI staining shows the location of the nucleus (panels A and D), FITC depicts the localization of each aptamer (panels B and E) and merge images are shown in panels C and F. Images visualized by Zeiss Axionplan microscope and captured with the photometric CoolSnap HQ camera. Same exposure times applied for all images. Figure is representative of at least 3 independent experiments

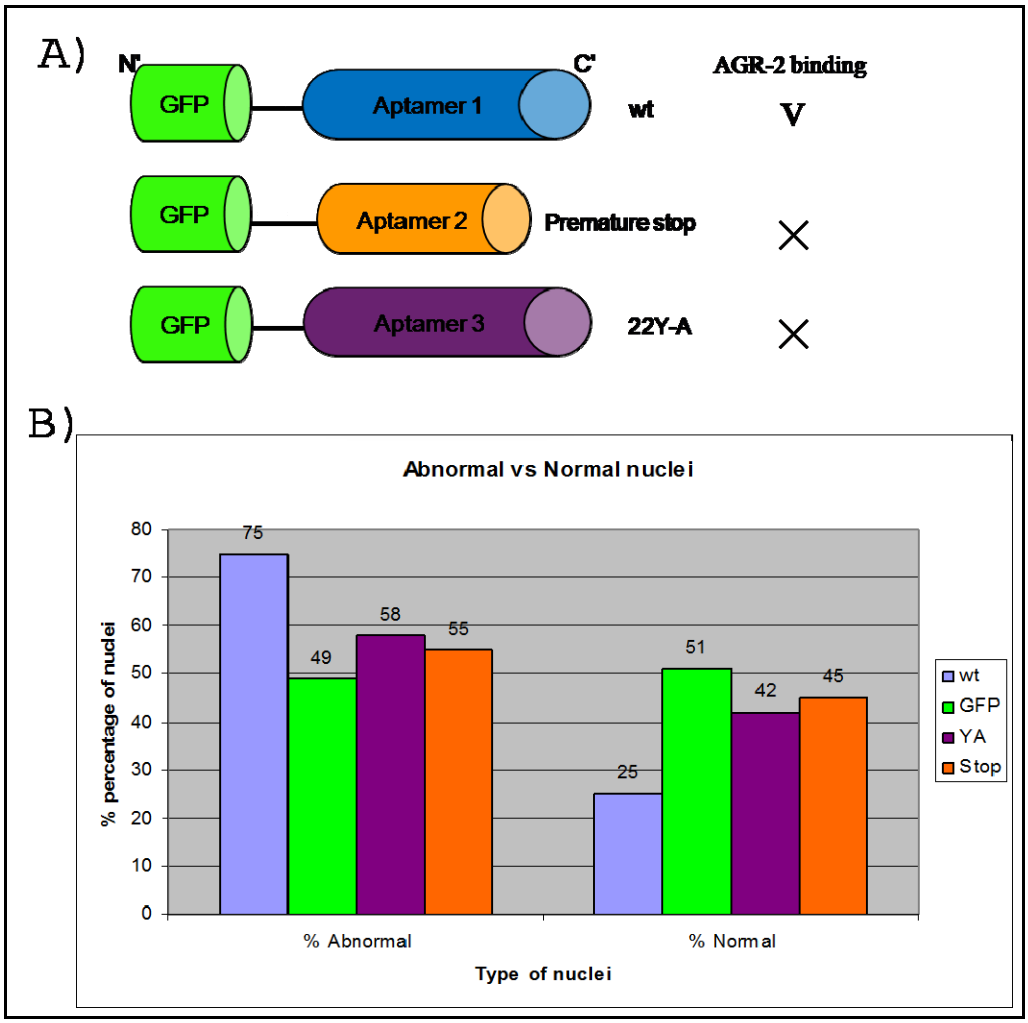

Figure 5.7: Quantative studies on pyknotic nuclei induction after GFP-Aptamer expression. A) Cartoon of GFP-Aptamers wt/truncated and 22 Y-A mutants and their affinity to AGR-2. B) Quantative analysis of pyknotic nuclei in MCF-7 cells after each aptamer's transfection. The percentage of abnormal versus normal nuclei is presented. Blue label :GFP-Aptamer wt Purple label: GFP-Aptamer Y-A Orange label: GFP-Aptamer stop and Green label: GFP control vector. A total of 1500 nuclei per aptamer were counted.

5.2.4 Aptamers induced p53 translocation before and after UV irradiation

Upon initial characterization of the GFP-Aptamer wt (GFP-PTTIYY) fusion protein, it was noticed that upon transfection of vectors encoding GFP-PTTIYY, wt, and GFP control, there was significant stabilization of p53 protein (Figure 5.8 upper panel). This correlated with a striking stabilization of AGR-2 protein presumably due to perturbation of the AGR-2 protein degradation pathway (Figure 5.8 second from top panel). Correlating with this, the GFP-Aptamer wt is also expressed at higher steady-state levels which presumably correlates with the enhanced stability of the AGR-2 protein (Figure 5.8 third panel from top).

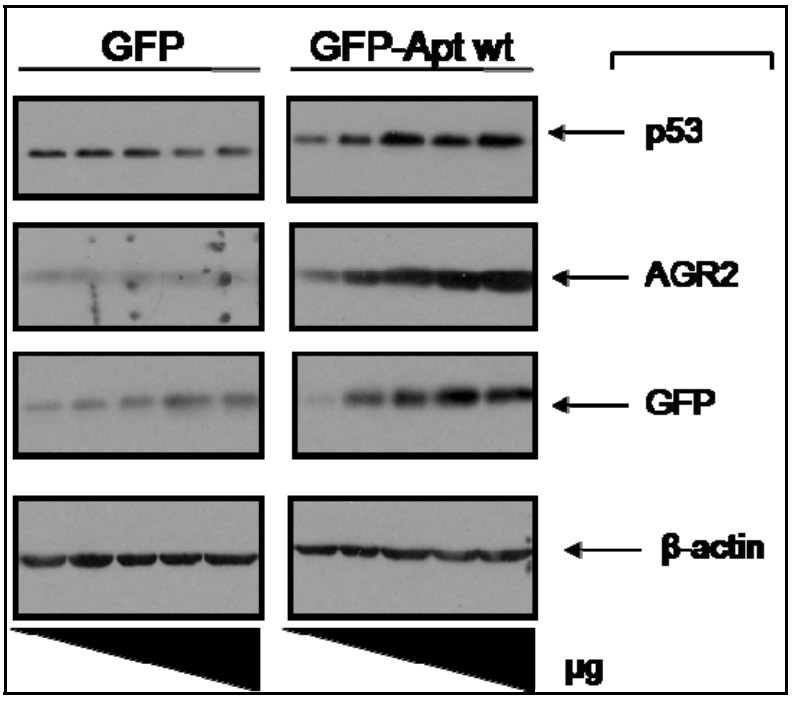

Figure 5.8: GFP-Aptamer wt titration stabilised p53 and AGR-2. Increasing concentration of GFP-Aptamer wt was added to MCF-7 cells and p53/AGR-2 expression levels were tested by immunoblotting. Stabilization of p53 and AGR-2 was observed in the GFP-Aptamer wt–transfected cells. β-actin was used as a loading control. Figure showing representative of 2 experiments.

In order to define the less lethal but most effective dose of UV that will be applied to MCF-7 cells for Aptamer transfection, a series of different doses and lysis buffers was tested. Doses starting from 1J/m^2 and reaching 100J/m^2 energy were tested (Figure 5.9 A:high dose titration and B:low dose titration), but all indicated 10J/m^2 as the ideal dose for irradiated MCF-7 cells, since in that scale p53 phosphorylation at Ser^{15} was induced and therefore measurements on p53 activation could be made (Figure 5.9 A and B, third from bottom panel). Total AGR-2 expression levels were increased between 1-10J/m^2 independent of lyses buffers used (Figure 5.9 A but not B due to overexposed signal). Total levels of p53 were also increased between the same 1-10J/m^2 doses, following the same pattern as phosphorylated p53 which is the active one. Therefore, 10J/m^2 was the adequate dose to test for any effects of the aptamers on AGR-2 and p53 expression levels.

Presence of the GFP-Aptamer wt did not induce nor reduce AGR-2 expression levels in the cytosol and membrane/organelles but significantly reduced AGR-2 in the nuclear fraction (Figure 5.10 A). As far as the control GFP-$Aptamer_{Y\text{-}A}$ is concerned, no alteraction in AGR-2 localization was observed in any of the three fractions. Interestingly, GFP-Aptamer wt altered the localization of the p53 protein as well (Figure 5.10 A). Before irradiation and in the presence of the GFP-Aptamer wt, p53 was mislocalized from the cytosolic fraction where it is normally detected in MCF-7 cells, and distributed in the membrane/organelles and nuclear fraction as well. Irradiation further induced this effect and especially when it came to the membrane/organelles and nuclear fraction. Interestingly, the localization of the aptamer was not affected by UV. The effect of UV in p53 distribution patterns was minimised in the case of the GFP-$Aptamer_{Y\text{-}A}$. Indeed, before UV no change in p53 cytosolic localization was detected, whereas after irradiation p53 was mislocalised to the membrane/organelles and nuclear fraction. Same observations were made in the case of untransfected samples as expected, since the GFP-Aptamer Y-A was used as a control due to deficient binding to AGR-2. Quantification of p53 in the first three fraction verified the above observation, that the GFP-$Aptamer_{wt}$ (YY in Figure 5.10 B) induced p53 nuclear translocation in non-irradiated cells after UV damage to a

much higher degree compared to the GFP-Aptamer Y-A and GFP-control treansfected cells. p53 nuclear levels before UV in the GFP-Aptamer wt transfected cells were undetectable by the programme although immunoblotting showed clear redistribution of the protein to the nucleus. Coommasie staining was used as a loading and fractionation control. GFP-Aptamer Y-A also acted synergistically to UV for p53 nuclear translocation but to a much lesser extent than the Aptamer wt.

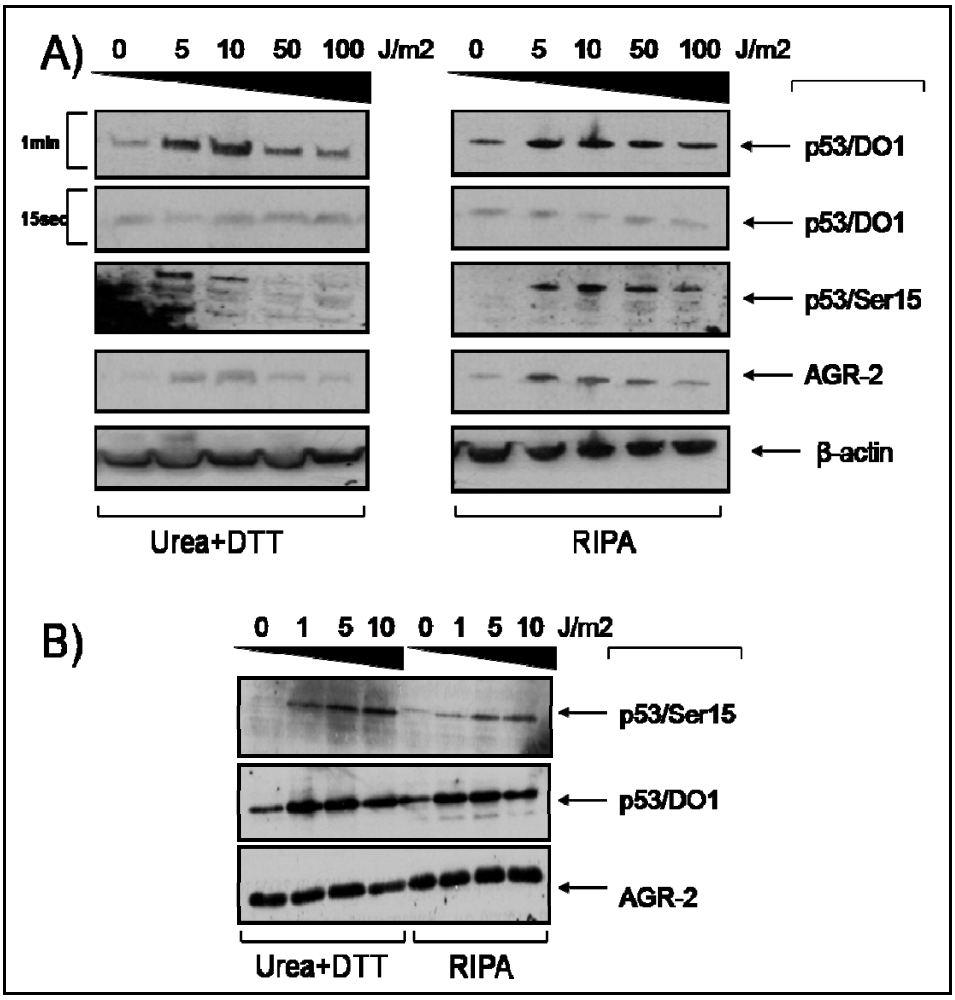

Figure 5.9: UV titration and p53 levels. A) MCF-7 cells were UV-irradiated with high doses of UV and expression levels of AGR-2 (row A4 and B3), p53 (row A1, row A2 represents shorter exposure and B2) and phosphorylated p53 at Serine[15] (row A3 and B1) were determined by immunoblotting. A) High dose UV titration. B) Low dose UV titration. β-actin was used as a loading control.

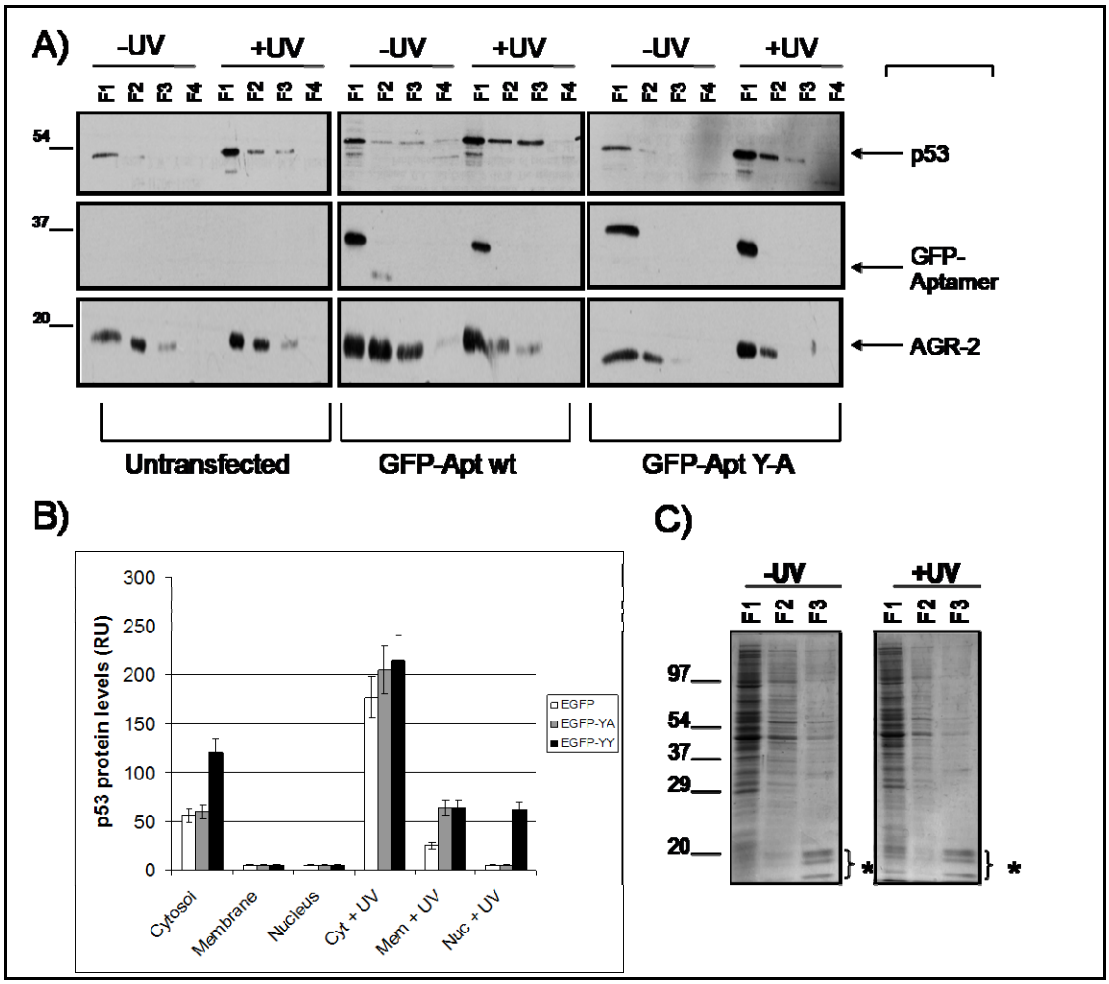

Figure 5.10. Effects of GFP-Aptamer wt/YA expression on p53 subcellular localization after UV damage. A) Changes in p53 localization induced by the GFP-Aptamer wt protein. MCF-7 cells were transfected with GFP-Aptamer wt/ GFP-Aptamer Y-A and also left untreated as a control, for 24h. The cells were harvested 6 hours post-irradiation and fractionated to determine changes in the subcellular distribution of p53 protein. Changes in AGR-2 localization induced by the EGFP-PTTIYY (Aptamer wt) protein. B: Quantitation of p53 protein levels in F_1, F_2, and F_3 before and after UV verified p53 elevated levels C) Loading controls for total protein in fractions F_1, F_2, and F_3 were developed by coomassie blue staining of protein after denaturing gel electrophoresis, *: Histones protein as identified by MS. RU:relative units.

5.2.5 Silencing of AGR-2 also induced p53 translocation before and after UV irradiation

Since AGR-2 was found to act as a p53 inhibitor [474], we analyzed whether AGR-2 protein depletion using siRNA had any effect on p53 protein subcellular localization. AGR-2 protein can be depleted to differing degrees using four distinct siRNA hybrids (Figure 5.11) at different timepoints. siRNA #5 and #6 were the ones that resulted in attenuation in AGR-2 protein levels (Figure 5.11) after 24-48h when compared to the untransfected and $si_{control}$-transfected cells. p53 total protein expression levels remained unchanged even though AGR-2 was totally depleted from the cells (Figure 5.11). Therefore, siRNA #5 and #6 were the ones used during the UV radiation experiments that followed (Figure 5.12 A, B and C).

Since AGR-2 can inhibit p53 only after UV irradiation in H1299 cells [474], MCF-7 cells were subjected to siRNA, irradiated with $10J/m^2$ and different subcellular fractions were analysed for p53 and AGR-2 protein expression levels. In control siRNA-transfected cells, UV induced relocalization of p53 from the cytosol to membrane/organelles and nuclear fraction as expected (Figure 5.12 A top panel and B black label). Slight induction in AGR-2's protein levels in all the fractions was observed, coherent to the UV titration data that showed elevated levels of total AGR-2 after irradiation (Figure 5.9). Surprisingly, AGR-2 depletion was most notably detected in the F_3 nuclear fraction (Figure 5.12 A bottom panel) and was accompanied by redistribution of p53 protein into the membrane/organelles and nuclear F_2 and F_3 fractions, irrespective to irradiation and the type of siRNA specific to AGR-2 (siRNA#6 or #5 Figure 5.12 A). UV slightly induced these redistribution patterns of p53 but had no effect on AGR-2 protein levels in the cytosolic and membrane/organelles fraction of the AGR-2 siRNA-transfected samples. Representative loading controls after control or AGR-2 siRNA using coomassie blue staining of total protein in each fraction, F_1-F_4, is depicted in Figure 5.12 C.

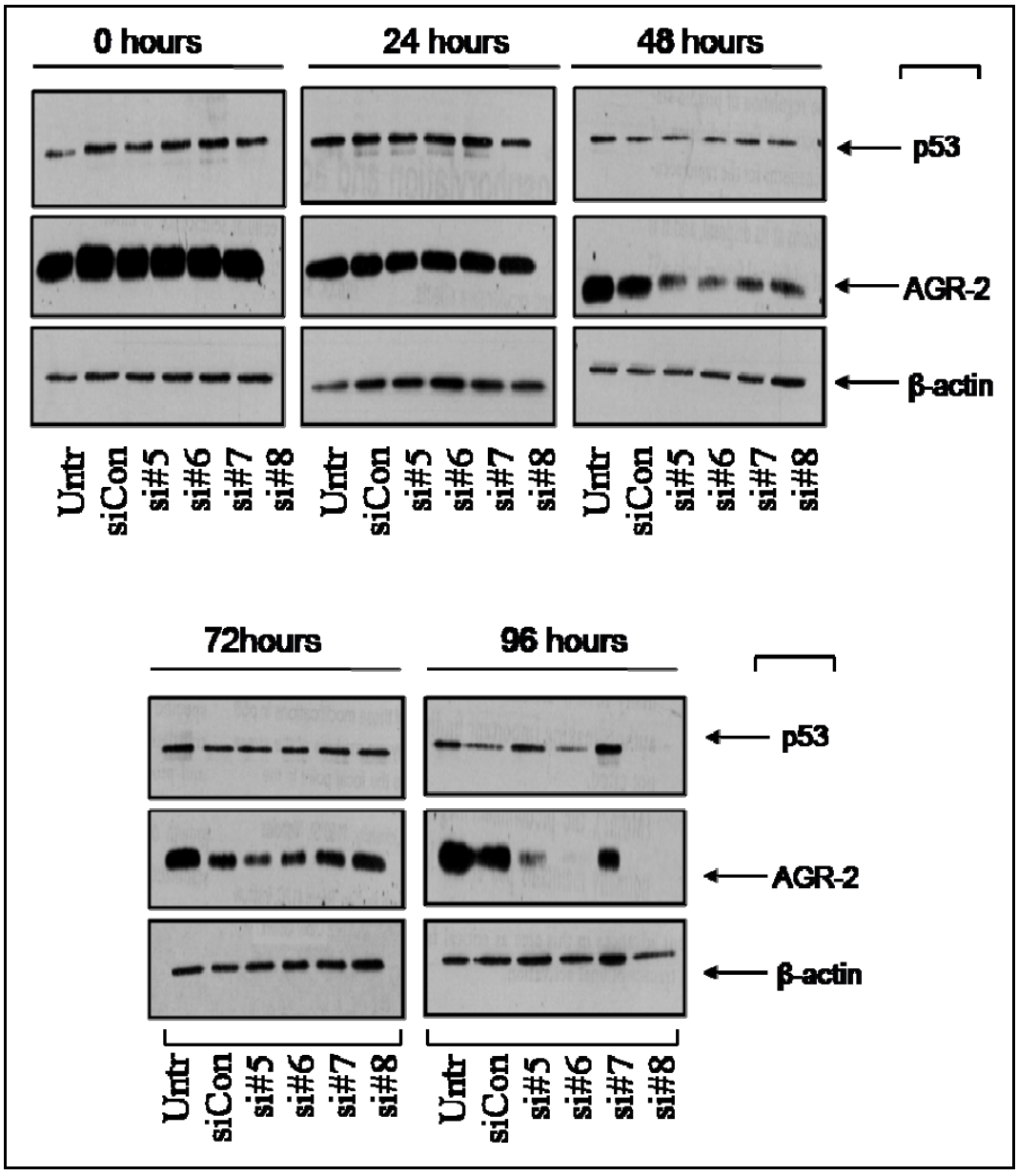

Figure 5.11: AGR-2 depletion after four different siRNA pools. MCF-7 cells were treated with a range of four distinct siRNA oligonucleotides (#5-8) targeting AGR-2 and the protein's expression levels were determined by immunoblotting in different timepoints at a four-day timecourse. siRNA #5 and #6 were the most efficient ones in terms of AGR-2 depletion after 48h.

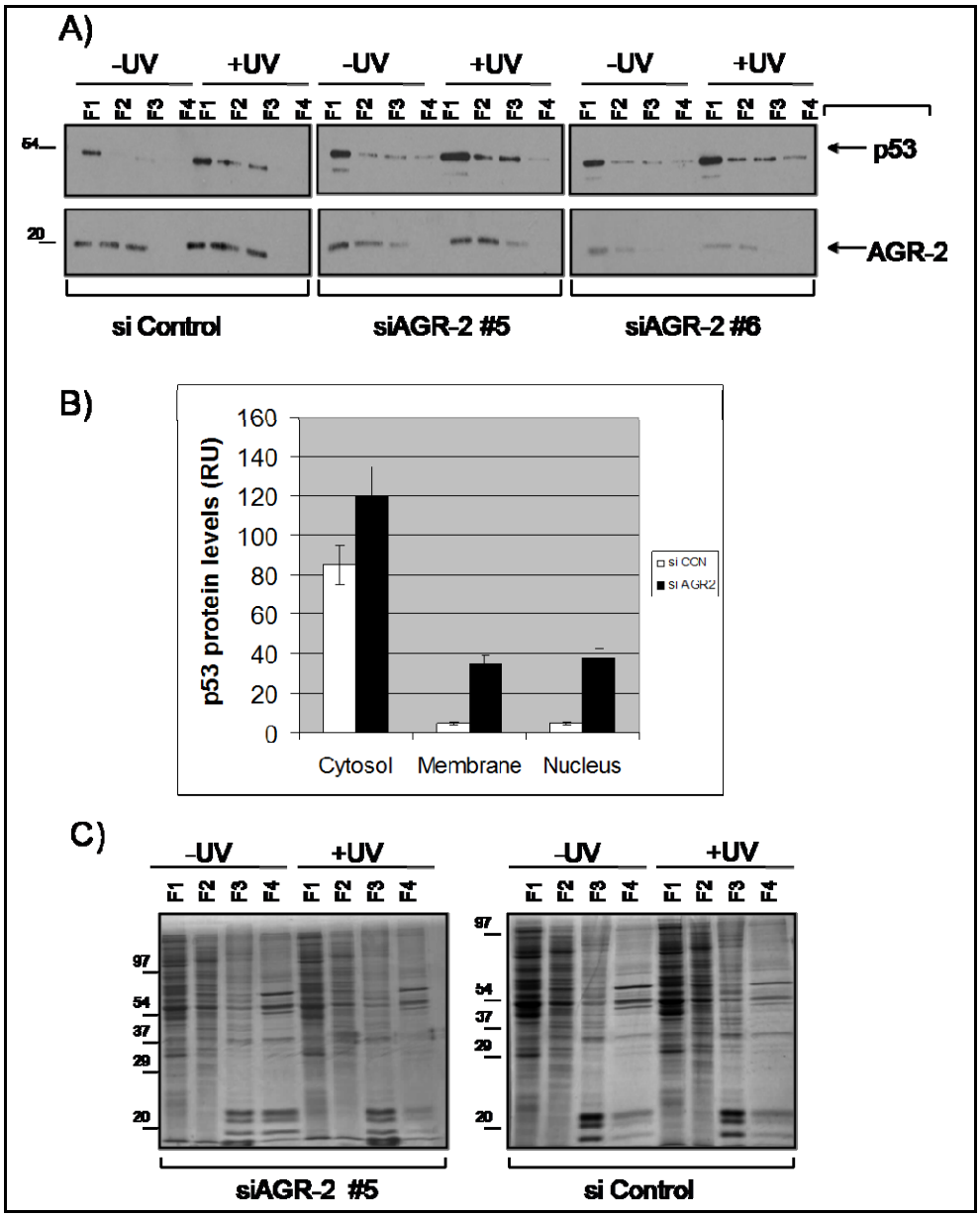

Figure 5.12: AGR-2 depletion alters the localization of p53. A) MCF-7 cells were treated with siRNA#5, or #6 or control siRNA and after fractionation into the F_1, F_2, F_3 and F_4 fractions, lysates were immunoblotted to determine changes in p53 levels and AGR-2 levels B) Quantitation of p53 protein levels in the cytosol/membrane-organelles/nuclear fraction after siRNA control or AGR2-specific #5 before UV. C) Loading controls for total protein in fractions F_1, F_2, F_3 and F_4 in control and #5 siRNA-AGR2 treatments were developed by Coomassie blue staining of protein after denaturing gel electrophoresis. RU:relativeunits.

5.3 Discussion

5.3.1 Aptamers to AGR-2 induce the formation of pyknotic nuclei but cells do not show signs of apoptosis or autophagy

A high level of pyknotic nuclei in cells expressing the GFP-PTTIYY fusion (GFP-Aptamer$_{wt}$) peptide was detected. Quantitation revealed that approximately 75% of transfected cells had altered nuclear morphology with another 25% exhibiting normal nuclear morphology (Figure 5.7). Using GFP control, GFP-STOP-PTTIYY (GFP-Aptamer stop), or GFP-PTTIYA (GFP-Aptamer Y-A) as a series of negative controls, a similar ~50% background of normal/abnormal nuclei were observed (Figure 5.7). Since MCF-7 cells are caspase-3 deficient and also follow autophagy as their main pathway of cell death under specific condition such as Tamoxifen or other anti-estrogen treatment, paclitaxel, starvation and UV [2, 80, 128, 225, 289, 452, 453, 516], we tested both types of cell death, apoptosis and autophagy. When it came to apoptosis since no caspase-3 cleaved products could be used as an apoptotic marker and since literature suggests that although caspase-3 deficient MCF-7 cells can undergo apoptosis through caspase-8 activation that leads to PARP cleavage [7, 144, 288, 373], we investigated the PARP pathway. No PARP cleaved products were detected after aptamers transfection (data not shown). Moreover, Annexin-V staining was negative (data not shown). Annexin-V is a Ca^{+2} -dependent, phospholipid binding protein with a high affinity for phospholipid phosphatidylserine that translocates from the inner to the outer leaflet of the plasma membrane during early apoptosis.

The next step was to investigate whether autophagy was the main pathway induced by aptamers transfection. MCF-7 cells utilize autophagy as their predominant type of cell death under certain conditions previously mentioned [80, 225, 452, 453] although contradictory views also exist in the field. LC-3 is a strong marker of autophagic cell death, as it is being cleaved in LC-3 I and LC-3 II when autophagy

takes place [346, 453]. Aptamer transfection in MCF-7 cells and western blot analysis with an anti-LC3 II antibody did not reveal any signs of autophagy (data not shown). Microscopic analysis of transfected with the aptamers cells had no signs of large autophagic vacuoles or other hallmarks of autophagy in the majority of the cells (data not shown). It is commonly accepted that determination between types of cell death is difficult to achieve, as there are no clear signs that enable strict classification in one type and also cell death types often overlap or switch between each other. The formation of pyknotic nuclei was a clear characteristic of the cells that were transfected with the aptamer but no other features of apoptosis or autophagy were detected. Further studies need to be performed in order to elucidate the pathway leading to pyknotic nuclei formation. Moreover, different cell lines that are caspase-3- and AGR-2-positive should be tested to further support the aforementioned data.

5.3.2 Aptamers to AGR-2 stabilize AGR-2 and promote nuclear accumulation of p53

The transfection of EGFP-PTTIYY fusion peptide followed by subcellular fraction, demonstrated that p53 protein is indeed stabilized relative to the EGFP-PTTIYA control and EGFP-control (Figure 5.8). This also correlates with enhanced AGR-2 protein stabilization. The fact that no in vivo binding was observed between AGR-2 and the aptamers after co-immunoprecipitation and FRET co-localization experiments (data not shown), might indicate the spontaneous and dynamic nature of the interaction. Moreover, there is always the possibility that this delicate *in vivo* binding of the protein and the aptamer is easily disrupted after chemical manipulation following immunoprecipitation and fixation methods.

Given that AGR-2 acts as a p53 inhibitor after UV damage we examined whether the EGFP-PTTIYY, wt, peptide fusion exhibited greater stimulation of p53 nuclear entry in irradiated MCF-7 cells (Figure5.10). UV damage induces p53 response and disrupts the balance of gene expression leading to growth arrest, DNA repair or

apoptosis, thus preventing the proliferation of genetically damaged cells [602, 604]. p53 stability and DNA binding activity are modulated by post-translational modifications such as acetylation and phosphorylation. Phosphorylation at several different serines or threonines residues in p53 has been shown to occur after UV or other DNA damage [507]. Five serines in the C-terminal portion and seven serines and one threonine within the N-terminal 46 amino acids are known to be inducibly phosphorylated [290]. UV damage and ionizing radiation specifically induces phosphorylation at the N-terminus of p53 at residues Ser^{15}, Ser^{20} and Ser^{37} [539]. Rapid nuclear localization of p38 kinase as well as p53 stabilization is also observed after UV damage [77]. The data presented here showed enhanced p53 phosphorylation at Ser^{15} after UV dose titration with the highest phosphorylation happening at $10J/m^2$, which was the dose chosen for all the experiments that followed.

UV stimulates p53 abundance in MCF-7 cells that have wild type p53 [241]. Transfection of GFP-$Aptamer_{wt}$ fusion in the irradiated cells resulted in accumulation of p53 in the membrane and nuclear fractions relative to GFP controls and depletion of AGR-2 from the nuclear fraction. Enhanced exposure of the immunoblot demonstrated that this peptide stimulated a shift in p53 protein localization into membrane, nuclear, and cytosolic F_1-F_3 fractions, relative to the GFP-Aptamer Y-A and GFP control (Figure 5.10). The stimulation in p53 protein presence in the cytoskeletal fraction is presumably due to the dynein-mediated microtubule transport pathway that promotes nuclear entry of p53 protein after stress [214]. Abnormal p53 cellular localization has been considered to be one of the mechanisms that could inactivate p53 function. In breast cancers p53 is mainly localized in the cytoplasm [412] suggesting that the inactivation of wild-type p53 in cancer cells could partly result from a defect in the regulation of p53 subcellular localization [70, 358, 410, 412].

Moreover, the GFP-Aptamer wt and AGR-2 siRNA both deplete AGR-2 from the nuclear fraction while on the other hand accumulate p53 in the nucleus. Therefore, the GFP-Aptamer wt acts as an AGR-2 inhibitor, having effects in p53 nuclear

translocation as well. After AGR-2 inhibition, p53 is free to enter the nucleus and act as a transcription factor. The Y-A substitution GFP-Aptamer has no affinity to AGR-2 and therefore no signs of p53 nuclear translocation were observed, further supporting the specificity of the interaction-inhibition between the GFP-Aptamer wt and the AGR-2 protein.

5.3.3 p53 nuclear import is promoted by AGR-2 depletion

Previous data showed that AGR-2 inhibition of p53 and related clonogenic survival is mediated by the "mature" isoform which has an intact C-terminus and UV irradiation triggers the maximal inhibition of p53 by this form of AGR-2 [474]. Our data supported that this mature isoform of AGR-2 protein has a relatively specific nuclear and cytoplasmic expression. We analyzed whether this active isoform of AGR-2 co-localized with p53 protein and/or altered the p53 subcellular localization. In many tumour cell lines, p53 protein accumulates in the nucleus after irradiation to initiate transcription. To study the effects of AGR-2 in p53 after DNA damage we depleted AGR-2 from MCF-7 cells and irradiate them before isolating different subcellular fractions. Surprisingly, AGR-2 silencing was only happened in the F_3 nuclear fraction while at the same time resulted in p53 relocalization and accumulation to the same nuclear fraction (Figure 5.12). UV further stimulated this effect and more p53 was translocated to the nucleus compared to non-irradiated and control siRNA-transfected cells (Figure 5.12). A possible mechanism of p53 inhibition by AGR-2 is summarised below. When AGR-2 is active and present in the nucleus, then p53 can no longer enter the nucleus and stimulate transcription. Abnormal p53 cellular localization and especially nuclear export has been considered to be one of the mechanisms that could inactivate p53 function [358]. It has been shown that the p53 protein has both an NLS (nuclear localization signal) and NES (nuclear export signal) sequence [431, 617] that is recognised by certain receptors, named 'importins' and 'exportins', and so is subject to both nuclear import and

export via a fast, energy-dependent pathway [400]. Since a defect in p53 nuclear translocation would impair its biological function, the cellular trafficking of p53 must be tightly regulated to ensure normal and optimal function [409, 502]. It is therefore proposed that AGR-2 functions as Bcl-2 and c-myc do, which alter the subcellular trafficking of p53 during the cell cycle and accumulate it in the cytoplasm of p53 co-transfected cells during a critical period in G_1. By this mechanism they are able to overcome p53-induced apoptosis and cell cycle arrest [502]. It is suggested that AGR-2 does not allow p53 to enter the nucleus and when the first is depleted p53 is free to act. The exact mechanism of this nuclear export, e.g. interaction with other proteins, awaits further elucidation.

The significance of AGR-2 in drug therapy as a prognostic factor and also as a drug target is supported by studies with aromatase inhibitors [374] and tamoxifen [270]. Anastrozole and letrozole are highly specific and efficient inhibitors of the aromatase enzyme, leading to profound estrogen deprivation in postmenopausal women. Mackay and coworkers identified genes that respond to estrogen withdrawal in primary breast tumours *in vivo*, and may be used to understand and predict the response of patients to AI treatment [374]. AGR-2 was amongst the ones downregulated after AIs treatments. Recent data form a clinical collaborative study (including T.Hupp group) indicated that AGR-2 and AGR-3 expression can serve as a negative prognostic factor in ERα positive breast cancers treated with tamoxifen [270]. Moreover, the same study showed that AGR-2 overexpression was correlated with that of cyclin D_1 which is a known negative predictive factor for tamoxifen response [557]. The previously identified suppression of AGR-2 expression by letrozole suggests a potential diagnostic-linked strategy for the treatment of AGR-2 positive tumours in tamoxifen resistant patients using aromatase inhibitors [374]. On the other hand AGR-2 has been associated with a poor response to hormonal therapy and therefore survival [282] although a contradictory study suggested that AGR-2 is a marker of differentiation linked with significantly longer overall survival times [207]. More research should be focused on the connection between AGR-2 and breast cancer treatment. Our data on p53 inhibition combined with AGR-2

upregulation by tamoxifen [270] could explain why AGR-2 positive patients show resistance to tamoxifen and have lower survival [282] due to AGR-2 induced p53 inactivation. These data along with downregulation of the protein by aromatase inhibitors [374], suggest a selectively resistance function of AGR-2 to different drugs and can be used to treating Tamoxifen-resistant patients that have high AGR-2 levels and positively affect response to endocrine therapy. Peptide aptamers that inhibit AGR-2 function and activate p53 can be used as excellent drug leads towards targeted breast cancer therapy, through reconstitution of a functional p53 protein able to induce cell cycle arrest and apoptosis of cancer cells.

5.3.4 Conclusions of chapter

Aptamers against AGR-2 were capable of inducing nuclear import of p53 consistent with effects of AGR2-specific siRNA that depleted the protein from the nucleus and promoted p53 nuclear import. The aforementioned data combined with studies supporting the mature form of AGR-2 as the one being active as a p53 inhibitor and as shown here the one that is localized to the nucleus, set the basis for defining the mechanism of p53 inhibition. Since this mechanism is defined, novel anti-cancer drugs could be generated and focus on inactivating AGR-2 and promoting p53 activation.

Chapter 6

Conclusions and Future Work

6.1 Conclusions and future work

The work presented here investigated the role of AGR-2 as a protein unregulated in breast cancer. AGR-2 is now known to be over-produced in a range of human cancers including breast, oesophagus, lung, prostate, and pancreas [207, 374, 403, 611]. In order to elucidate the exact mechanism of AGR-2 function we had to define the localization of the protein. Fluorescent tags were used to monitor the protein's localization within the cell. Since AGR-2 is present in two isoforms, (i) the full length with an N-terminal signal sequence and (ii) the mature which derives from the first after proteolytic cleavage of the leader sequence [3] we fused both isoforms to fluorescent proteins and investigate any differences in the distribution patterns. Interestingly the presence of the leader sequence determines endoplasmic reticulum-retention which was further enhanced by mutating the putative C-terminal ER-retention KTEL sequence to KDEL, which is characteristic of ER resident proteins, leading to a dramatic change in co-localization rate from 33% to 80%. Deletion or substitutional changes of the C-terminal KTEL tetrapeptide did not significantly alter ER co-staining compared to the wild type protein, totally consistent with data in HeLa cells supporting that the putative ER-retention KTEL motif is not required to ensure endoplasmic reticulum withholding [483]. No secretion of the protein was observed in MCF-7 cells.

On the other hand, deletion of the N-terminal leader sequence totally altered the protein's distribution pattern and led to predominant nuclear retention with only a few signs of endoplasmic reticulum co-localization. Neither KDEL nor KAEL substitutions were capable of enormous changes in the nuclear distribution of this isoform, although the rate of ER co-staining changed. Interestingly, deletion of this tetrapeptide resulted in total loss of the protein from the nucleus and resulted in a peculiar diffuse cytosolic pattern, suggesting that the presence of a minimum KXEL peptide at the C-terminus of the protein is essential to maintain its nuclear position. It would be of interest to test mutations in the remaining amino acids of the KTEL

tetrapeptide apart from this Threonine and further define the minimum amino acid composition required for nuclear localization.

Very recent data published, identified a novel member of the PDI superfamily, named Erp16, as an ER-resident protein [292]. The protein has a cleavable signal peptide and a putative ER-retention EDEL tetrapeptide, and it resides in the luminal compartment of the endoplasmic reticulum of HeLa cells. In the same study, the EDEL-deletion mutant was present in the supernatant apart from the cell lysate, supporting the secretory potential of the protein when the EDEL ER-retention sequence is absent. It was also found that when the wt protein was overexpressed and Brefeldin A/or Tunicamicyn/ or dithiothreitol treatment followed, neither PARP nor pro-caspase-3 cleavage were observed, which was not the case with the EDEL-truncated mutant which was not able to completely inhibit apoptosis. These results thus indicated that endogenous ERp16 suppresses apoptosis induced by ER stress. ERp16 share some common features with AGR-2 in terms of structure, localization and function. Both proteins have cleavable N-terminal signal sequences, both reside in the ER although in the case of AGR-2 this retention is partial, both inhibit cell death by different mechanisms each (Erp16 attenuates the induction of apoptosis by brefeldin A, tunicamycin, or dithiothreitol, whereas AGR-2 inhibits p53 nuclear translocation) and in both deletion of the extreme C-terminal putative ER-retention tetrapeptide attenuates their function. Our hypothesis suggest that AGR-2 have evolved from the strict role of PDIs and released from the endoplasmic reticulum to the cytosol and nucleus where it was able to develop new functions such as p53 inhibition. AGR-3 falls into the same category and re-localized to the mitochondria where it developed its new function regarding cell death.

It is worth mentioning that recently a newly identified protein named CAP10-like was cloned and characterised [574]. This protein had a hydrophobic leader sequence at its N-terminus and an endoplasmic reticulum retention KTEL motif at the C-terminus just like AGR-2. The protein was characterised as and ER-resident protein as it strongly co-localized with endoplasmic reticulum markers. Moreover, it was present in two transcripts, one of 1.9kb and one of 3.5 kb, with the second isoform

being more plentiful in tissues such as liver, spleen, heart and kidney whereas the short isoform was less abundant in all the tissues tested [574]. This protein affects U937 cells growth rate by promoting cell proliferation just like AGR-2 [474] does in H1299. The above data suggest that the presence of a leader sequence do not guarantee secretion of the protein and that when this signal sequence is combined with putative ER-retention tetrapeptides, ER-residency can be achieved although in different extents, since AGR-2 is not totally co-localized to the ER and CAP10-like is an ER-resident protein.

Combining the observation that the mature form is the nuclear one with the already published data that this form is the active one that inhibits p53 and that deletion of the last ten amino acids, including KTEL sequence, is sufficient to disrupt this interaction [474] and also exclude the protein from the nucleus as supported here by RFP deletion mutant, it is suggested that the nucleus is the area that p53 inhibition takes place through the mechanism of nuclear exclusion. Our hypothesis was further strengthened after depleting the protein from the nuclear fraction, by small interference RNA technologies, and observing nuclear accumulation of p53. UV irradiation that activates p53 to enter the nucleus and start transcription of certain genes acted synergistically with AGR-2 depletion and further induced this import. Two models emerge from these findings. The first one involves *in situ* inhibition of active p53 from AGR-2 when both are present in the nucleus whereas the second refers to inhibition of the p53 protein from entering the nucleus and becoming transcriptionally active. The use of Leptomycin to block nuclear entry would be a potential experimental strategy to further characterise these models.

The use of concepts in the peptide therapeutics field has also led us to develop bioactive peptide aptamers that bind to AGR-2 and which can stimulate nuclear accumulation of p53. In our research we have used these AGR2-binding consensus site peptides to begin to determine whether p53 pathway responses can be altered and we show that the ability of AGR-2 to mediate nuclear exclusion of p53 can be attenuated using the bioactive peptide with the PTTIYY core consensus sequence. AGR-2 attenuation using siRNA gave rise to qualitatively similar results. These data

provide proof of principle that the AGR-2 pathway might prove to be a target whose inhibition would stimulate the p53 response to DNA damage and provide a peptide lead for drug design aimed at blocking the pro-oncogenic function of AGR-2. Ongoing research in microarrays has revealed that the PTTIYY aptamer, wt, is capable of inducing expression of p53-upregulated genes (Dr Murray, unpublished data), further supporting the aptamer's stabilization and activation effect on the tumour suppressor gene as well as the inhibitory effect on AGR-2.

As a final approach to evaluate whether the AGR2-hexapeptide could perturb subcellular localization of p53 protein, the bioactive PTTIYY and attenuated PTTIYA peptides were introduced into cells by fusion with an optimized heptapeptide cell membrane permeabilizing peptide derived from the antennapedia protein named penetratin [198, 579]. The incubation of PTTIYY- and PTTIYA–penetratin peptides at a concentration of 50μM stimulated relocalization of p53 protein to the F_3 nuclear fractions, with the wild-type peptide inducing more p53 relocalization than the attenuated point mutant peptide (Dr. Murray, unpublished data) as it was the case with the GFP-aptamers analysed in this thesis. The PTTIYA mutant peptide retained some bioactivity in promoting the nuclear import of p53 which is similar to the intermediate activity of the GFP-fusion PTTIYA peptide. A titration of lower amounts of PTTIYY and PTTIYA peptide indicated that PTTIYY peptide was more active at lower concentrations (Dr. Murray, unpublished data). This data are consistent with the relative bioactivities of the GFP-fusion PTTIYY/A peptide constructs of results presented here, showing induction of p53 nuclear import in the GFP-Aptamer$_{wt}$ (PTTIYY) compared to the GFP-Aptamer $_{Y\text{-}A}$ one. The same AcGFP scaffold was validated previously to identify fusion peptides that inhibit p300, inhibit MDM2, and mimic IRF-1 protein effects on p53-dependent activity [148, 149].

It was also shown that another member of the AGR family, AGR-3 is primarily mitochondrial. No AGR-2 co-localization was observed, neither with the mature nor the full length form of the protein, although both AGR-2 and AGR-3 are candidate members of the same thierodoxin family [468]. This can be explained by the

observation that many protein members of this family do not necessarily share the same compartment and are localized in separate areas of the cell, such as ER, Golgi nucleus and mitochondria [14, 15, 125, 232, 354, 451]. AGR-3 is not the only PDI family member that resides in the mitochondria, as other characterised members including ERp57 [451] and P5 [314] are also mitochondrial. In 1995 Rigobello and co-workers observed that rat liver mitochondria show a marked disulphide reductase activity in the presence of low-molecular-mass disulphides and later refined these observations and proposed that PDI along with thierodoxin reductase enzymes are localized in different mitochondrial compartments and are probably involved in the redox regulation of mitochondrial functions and might co-operate in the maintenance of thiol homoeostasis [488]. The presence of a PDI protein in the mitochondria could contribute to some extent to the assembly and functioning of enzyme systems involving pore-forming proteins, receptors responsible for protein import, as well as pathways involved in the mitochondrial-dependent control of cell death such as pro-apoptotic members of the Bcl-2 family [486]. Evidence presented here proposed AGR-3 to belong to this last category of PDI proteins that have a role in mitochondrial-dependent cell death. Indeed, depletion of AGR-3 leads to Bax conformational change and Beclin-1 decrease. Both proteins have a role in apoptosis and autophagy, respectively. Since there is no alteration in Bid levels, which is the one that activates Bax, but only in Bax levels, it is suggested that AGR-3 acts downstream Bid and upstream Bax in the apoptotic cascade [639]. Reduced Beclin-1 expression levels were observed in the absence of AGR-3, suggesting a positive role of the protein in favour of autophagy and negative against apoptosis, as it was also observed with other molecules that support one death pathway against the other [187, 516]. However, AGR-3 alone was not sufficient to totally shift the equilibrium from apoptosis to autophagy, since these pathways are highly sophisticated, inter-connected to each other and require a whole cascade of molecules to function correctly [367]. More experiments are underway to further characterize the type of cell death induced by AGR-3 and also define the role of membrane-localized AGR-3.

Data obtained from Y2H interactions of AGR-3 and potential binding partners in breast cancer libraries (Hybrigenics, France) are being investigated to further elucidate the role of the novel gene. A lot of interesting genes have emerged including proliferation and cell growth enhancers (BAIAP3, HUWE1, IXL1, LRBA), cytoskeleton-associated proteins (CKAP2, HIP1R, MAST1, SPTBN1/4, TLN1), tumour suppressors (DLG1), migration stimulators (GIT1), drug resistance-associated genes (GSTM4), apoptosis involved genes (KIBRA), proteosome activators (PSME1) and a lot more. Further research is underway into characterizing the above interactions in different cancers and shedding light towards the mechanism of AGR-3 function through protein complexes.

Protein	**Function**
BAT3	multiple levels of interaction with apoptogenic mitochondrial intermembrane protein AIF (apop inducing factor)
DLG1	Tumor suppressor,functions as a scaffolding protein that facilitates transmission of diverse downstrea signals. In Drosophila hDLG inter with the mitochondrial ribosomal protein S-34 (MRP-S34).present i mammary ductal carcinoma
MYBBP1A	Enhanced mitochondrial biogenes during neuronal differentiation

Table 6.1: Mitochondrial binding partners of AGR-3 after Y2H analysis (Hybrigenics).

It is worth mentioning, that although cell lines are a powerful tool for analysing the molecular AGR-2 or AGR-3 networks, they do not always mirror the complex biology of cells within a multicellular organism. To characterize the *in vivo* function and regulation of the genes, novel animal models need to be generated. Both genes are highly conserved from fish to humans [532], therefore these organisms can be utilised for studying the genes' function in vertebrates. Zebrafish is an ideal model and also it has recently been shown that the molecular networks involved in tumour progression are conserved between humans and zebrafish [340]. Moreover, zebrafish is easy to study due to rapid external development which makes it perfect for developmental studies coupled with the ability to modify gene expression through silencing and analyse the derived symptoms directly [344]. What is more, generation of zebrafish lines defective in certain genes, such as p53, makes it easier to evaluate the role of the gene of interest [345]. Pilot experiments underway have shown that AGR-2 expression affects goblet cells of the gut and oesophagus (data kindly provided by Dr. Patton). AGR-2 morpholinos that are deficient in AGR-2 exhibit reduced formation of epithelial invaginations in the intestinal bulb, accompanied with absence of goblet cells and under-expanded anterior intestine compared to the control ones (data kindly provided by Dr. Patton). More research towards these models should be conducted to have the whole picture of AGR-2 and AGR-3 mechanism of function.

6.2 Preliminary data

Apart from its function as a p53 inhibitor, subsequent studies have shown a significant role for AGR-2 in a range of biological pathways including cell migration [364], cellular transformation, metastasis [611], and limb regeneration in vertebrates [331]. Clinical studies have also implicated the protein in inflammatory bowel disease [652], hormone-dependent breast cancers [374, 662], and in predicting poor prognosis in prostate cancers [650]. The molecular mechanisms underlying these wide-ranging biological pathways trigged by AGR-2 are not defined and as the AGR-2 gene is confined to vertebrates, the AGR-2 gene pathway cannot be analyzed and solved directly in genetic systems like yeast. To characterize potential interaction with other protein and therefore start defining the role of the protein in many pathways, we conducted Y2H analysis to identify potential binding partners [40, 158, 284, 653]. Surprisingly a lot of positive hits came out in breast and placenta prey libraries (Hybrigenics, France) (Chosen candidates to be tested in breast cancer cells are summarized in table 6.2).

Gene	Role	Tested
Ruvb-L 2	Bacterial RuvB prctein is a DNA helicase essential for homologous recombination and DNA double-strand break repair. ATPase and DNA helicase activities	√
KCT-3	member of the cell membrane-associated mucin family, mediates oncosis-ike cell death	x
RIP140	nuclear protein that specifically interacts with the hormone-dependent activation domain AF2 of nuclear receptors,modulates transcriptional activity of the estrogen receptor.	√
CHD6	cell proliferation	NT
Ckap2	cyclin-dependent kinase inhibitor, and has been shown to interact with, and dephosphorylate CDK2 kinase, thus prevent the activation of CDK2 kinase. Deleted, mutated, or overexpressed in several kinds of cancers	x
HECD1	HEC is one of several proteins involved in spindle checkpoint signaling. This surveillance mechanism assures correct segregation of chromosomes during cell division by detecting unaligned chromosomes and causing prometaphase arrest until the proper bipolar attachment of chromosomes is achieved.[	NT
LGN	Heterotrimeric G proteins transduce extracellular signals received by cell surface receptors into integrated cellular responses. Belongs to a group of proteins that modulate activation of G proteins	√

Table 6.2: AGR- binding partners. Potential AGR-2 binding protein identified by Y2H through a breast cancer library. Right column shows which were found to bind AGR-2 in MCF-7 cells. (NT:not tested, x:no binding, √: positive binding).

In order to confirm the interaction between AGR-2 and the positive hits from the Y2H, co-immunoprecipitations assays were performed. Plasmid DNA containing the gene of interest with an HA or FLAG sequence (LGN, C-KAP, RuvBL-2 plasmids kindly provided by Dr. E. Pohler,University of Dundee, Rip140 plasmids: by Dr. E. Kiskinis, Imperial College, London) was transfected into MCF-7, from the European and the American collection as well.

The first protein tested was the RuvBL2 protein (also known as Tip49, Reptin32); a DNA helicase essential for homologous recombination and DNA double-strand break repair [536, 619]. Functional analysis showed that this gene product has both ATPase and DNA helicase activities [281, 294, 302, 538] as it promotes DNA, RNA and DNA-RNA duplex unwinding. In particular, Ruvbl-2 is a protein implicated in chromatin acetylation and remodelling as a component of the NuA4 histone acetyltransferase complex [529] and also in nucleolar organization and trafficking in human cells. Ruvbl-2 was found to interact with centrosomes which harbour with several important cell cycle genes such as p33, BRCA1, Chk1, Chk2 etc [538] and also interacts with c-myc and β-catenin [42, 115, 398, 624] controlling their oncogenic activity. Moreover, the protein is a member of a twelve polypeptide chromatin remodelling complex (INO80), that has a role in DNA damage [304, 440, 529] and also a novel component of the ATF2 trenscription factor which is implicated in the transcriptional control of several stress-response genes [115]. The protein is overexpressed in human hepatocellular carcinoma (HCC) where it is correlated to poor prognosis and weak differentiated tumours [498], in ovarian cancer [501], prostate cancer [313] and cervical cancer where it translocates depending on mitotic phases [538]. In the same study, it was found that Ruvbl-2 silencing increased apoptosis and reduced cell growth in HCC cells, by elevated expression of pro-apoptotic genes, DNA fragmentation and caspase 3 activity[498]. Our data revealed that Ruvbl-2 is overexpressed in the cytoplasm, cell membrane and nucleus of MCF-7 (Figure 6.1 B and C) as also supported by literature for other cancerous cell lines [218, 498, 538, 624] and co-immunoprecipitated with AGR-2 in both cell lines tested, MCF-7 from the American and European collection (Figure 6.1

A). It was also shown that in the same MCF-7 cells, Ruvbl-2 and AGR-2 form a complex which is stabilized by p53 (unpublished data kindly provided by Magdalena Maslon, T.Hupp group). It would be of interest to further analyse this interaction which may shed light into new mechanisms of AGR-2 function in mitosis, cell growth or other oncogenic features.

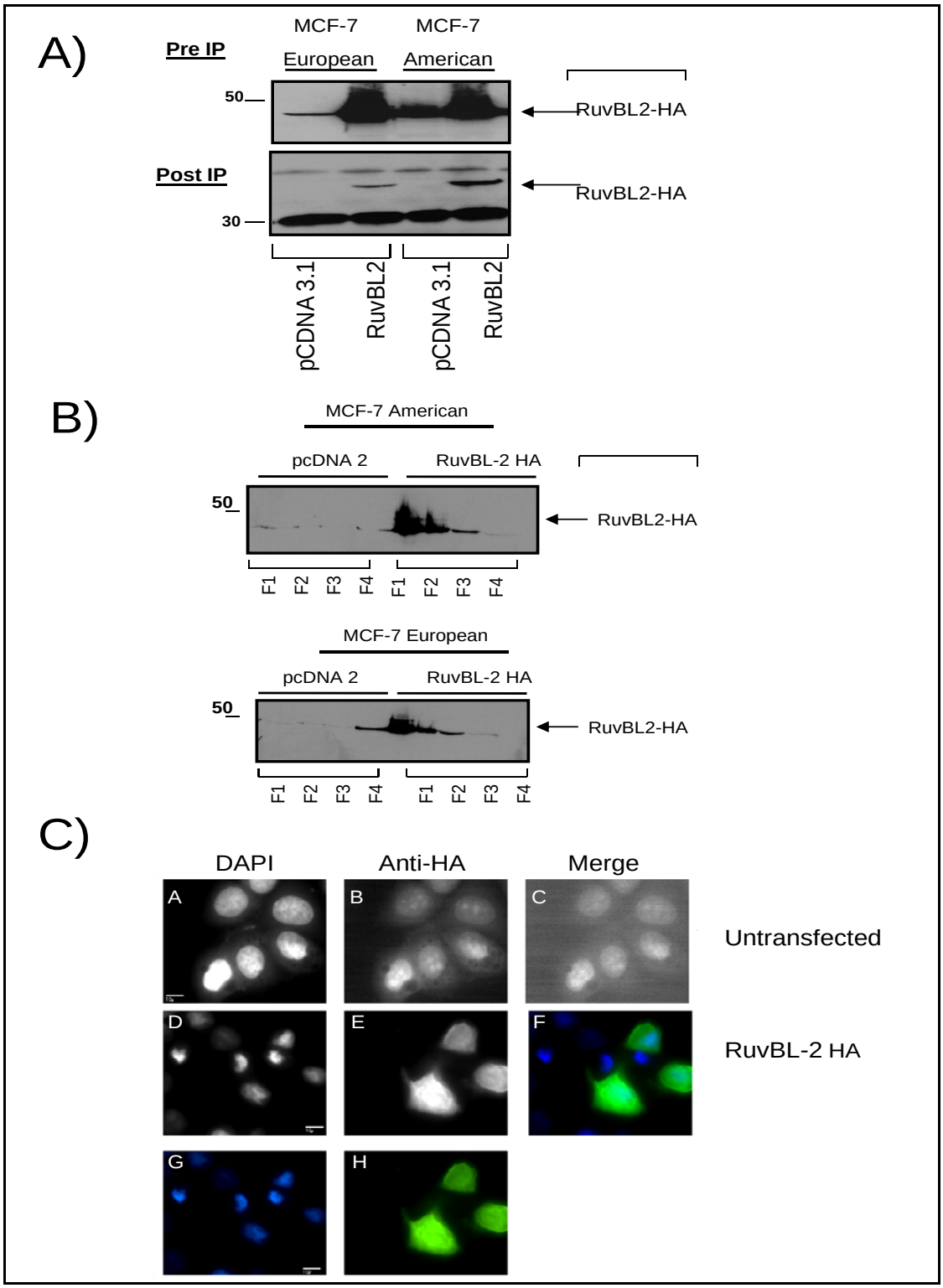

Figure 6.1: Ruvbl-2 binds AGR-2 in MCF-7 cells. The first potential binding partner tested was a DNA-helicase RuvBL-2. A) AGR-2 binds to RuvBL-2 after IP lysates from

RuvBL-2 HA-tagged and empty pcDNA3.1 control vector –transfected cells (American and European collection). B) Chemical fractionation identified RuvBL-2 in F_1 cytoplasm/F_2 membrane-organelles and F_3 nucleus fraction. C) IF of RuvBL-2 detected the protein in the nucleus and cytoplasm of cells. Untransfected control showed high autofluorescence when tested against the anti-HA antibody (panels A-C: B&W aquisition). RuvBL-2 HA tagged: panels D-E: B&W, panels F-H: RGB aquisition. Observed under a Zeiss Axionplan microscope equipped with Sony CoolSnap camera. Scalebar represents 10μm.

The second binding partner identified and tested was LGN. LGN is a heterotrimeric G-protein family member (whose name derived from its amino acid motif, containing 10 Leu-Gly-Asn motifs [63, 407] and mediates transduction of extracellular signals received by cell surface receptors into integrated cellular responses as well as contributing to the functional activity of G_α proteins by regulating metabolism of molecules in response to hormonal signals [63]. LGN belongs to a group of other proteins also known as GPSM2 or Pins. In Drosophila, PINS are required for spindle polarity, orientation, asymmetric division of neuroblasts, diverse polarity [266, 517] and for regulating planar polarity of sensory organs precursor cells [47, 457, 517, 644]. Localization of the protein is dynamic and changes during mitosis and interphase [63]. In mitosis the protein is concentrated at the midbody, which serves as a focal point for adhesion of proteins and leads to the abscission of the dividing cell [216]. It binds to a protein called NuMA [154, 155] which is a protein of the nuclear mitotic apparatus, and Lgl-2 [638] and together they organise the mitotic spindle [155, 210, 222, 247]. AGR-2 was found to co-immunoprecipitate LGN (Figure 6.2 A) which was distributed in the nucleus and the cytoplasm in a diffused manner with cytosolic speckles, during interphase (Figure 6.2 B). These localization patterns resembled the distribution of the protein in other cell types such as COS7 [63, 153, 216, 638]. In *Xenopus* egg extracts, LGN is a major negative regulator of aster formation and addition of exogenous LGN can block this process [154]. Overexpression of LGN in *Xenopus* causes disorientated

MTs formation, disruption of spindle organization and unequal chromosome segregation [154, 155]. AGR-2 on the other hand, plays a vital role in the anterior-dorsal orientation of the *Xenopus* embryo and is also connected to mitotic events [3]. Possibly, LGN and AGR-2 are evolutionary-conserved members of a protein complex from *Xenopus* to human but further research should be conducted into that area. It is worth mentioning that MCF-7 cells had high levels of autofluorescence (Figure 6.2 B panels F-H) in the absence of the anti-HA antibody or even when transfected with pcDNA 3.1 control vector (Figure 6.2 panels I-K). LGN-HA transfected cells showed much stronger and specific signal (Figure 6.2 B panels A-E). B&W images are shown for comparison purposes (Figure 6.2 B A, B, F-K).

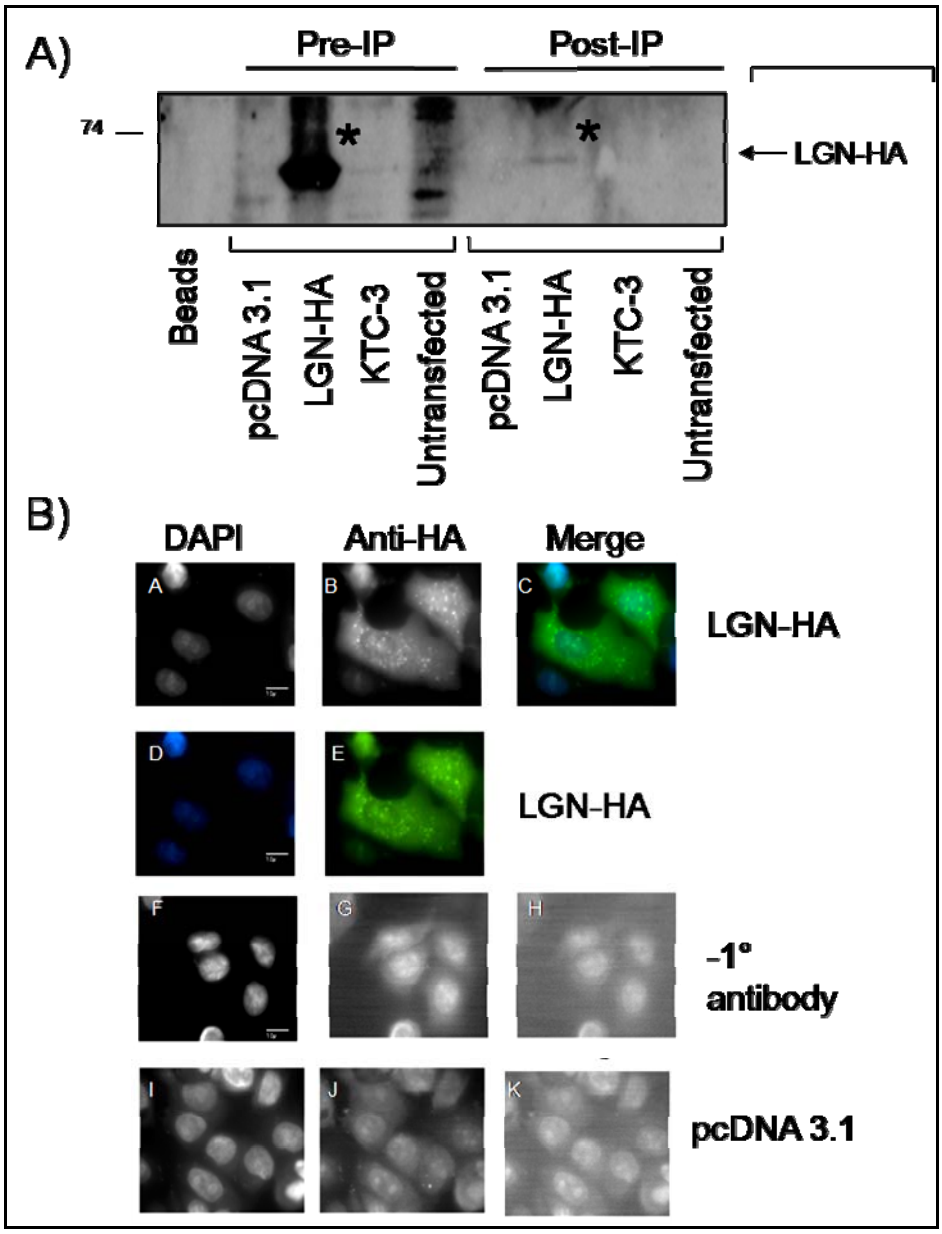

Figure 6.2: LGN binds AGR-2 in MCF-7 cells. A) AGR-2 binds to LGN after IP lysates from LGN HA-tagged and empty pcDNA3.1 control vector –transfected cells. B) LGN was detected in the nucleus and cytoplasm of MCF-7 cells (panels A-E). pcDNA 3.1 control transfected cells showed high autofluorescence when tested against the anti-HA antibody (panels I-K: B&W aquisition) and untransfected cells without primary antibody also autofluoresced (F-H B&W aquisition). LGN HA tagged: panels A-B: B&W, panels C-E: RGB aquisition. Observed under a Zeiss Axionplan microscope equipped with a Sony CoolSnap camera. *: LGN-HA. Scalebar represents 10µm.

The last binding partner tested was Rip 140, also known as Nuclear receptor interacting protein 1 (NRIP1) [95], is a transcription factors that activate or suppress gene transcription, after interacting with ligand-activated receptors [332, 347, 572] by binding their hormone response elemens (HREs) [496]. The protein modulates transcriptional activity of the estrogen receptor [94, 95] represses receptor activity, including AR [87], GR [563, 572] and RAR [347, 613], by competing with coactivators for binding to receptors [563, 588]. As defined by Y2H and co-immunoprecipitation experiments Rip140 binds AGR-2 (Figure 6.3 A) and immunofluorecent experiments detected the Rip140-FLAG protein (concstruct kindly provided by Dr. Kiskinis, Imperial College) in the nucleus in discrete foci as also supported by literature [572] (Figure 6.3 B panels A-F). pci-control vector showed totally unspecific fluorescent signal detected everywhere within the cell in a diffused manner (Figure 6.3 B panels G-I) while MCF-7 cells witoun primary antibody also showed enhanced fluorescence which was also unspecific (Figure 6.3 B panesl J-L). Tazawa and colleagues also supported that Rip140 redistributes to larger nuclear domains upon binding to a nuclear receptor [572]. It would be of interest to define the exact mechanism of AGR-2 and Rip140 interaction which might implicate the estrogen receptor as well. The reason underlying this hypothesis is that AGR-2 is selectively co-expressed with the estrogen receptor and bears ERα -response elements on its promoter whereas Rip140 on the other hand modulates the receptor's transcriptional activity [94, 299]. Since the only form of AGR-2 that localizes to the nucleus is the mature one, it is rational to consider that this form is the one that interacts with Rip140 which is also in the nucleus.

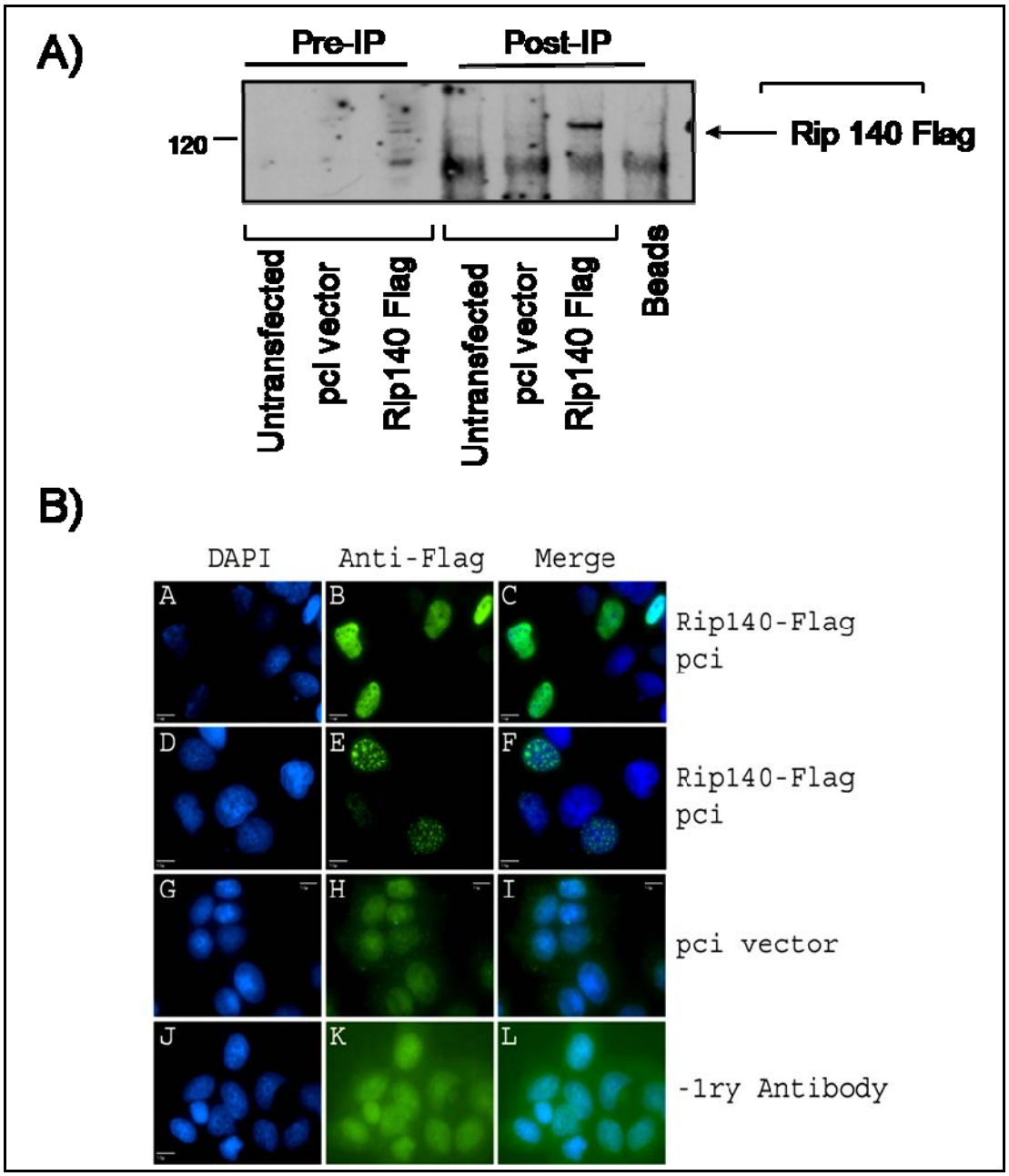

Figure 6.3: Rip140 binds AGR-2 in MCF-7 cells. A) AGR-2 binds to LGN after IP lysates from Rip140-FLAG-tagged and empty pcI control vector –transfected cells. B) Rip140-FLAG was detected in discrete foci in the nucleus of MCF-7 cells. (panels A-F). pci control transfected cells emitted green fluorescence when tested against the anti-FLAG antibody (panels G-I) and untransfected cells without primary antibody also autofluoresced (panels J-L). (ALexa 488 secondary B, E, H and K). Images observed under a Zeiss Axionplan microscope equipped with a Sony CoolSnap camera. Scalebar represents 10μm.

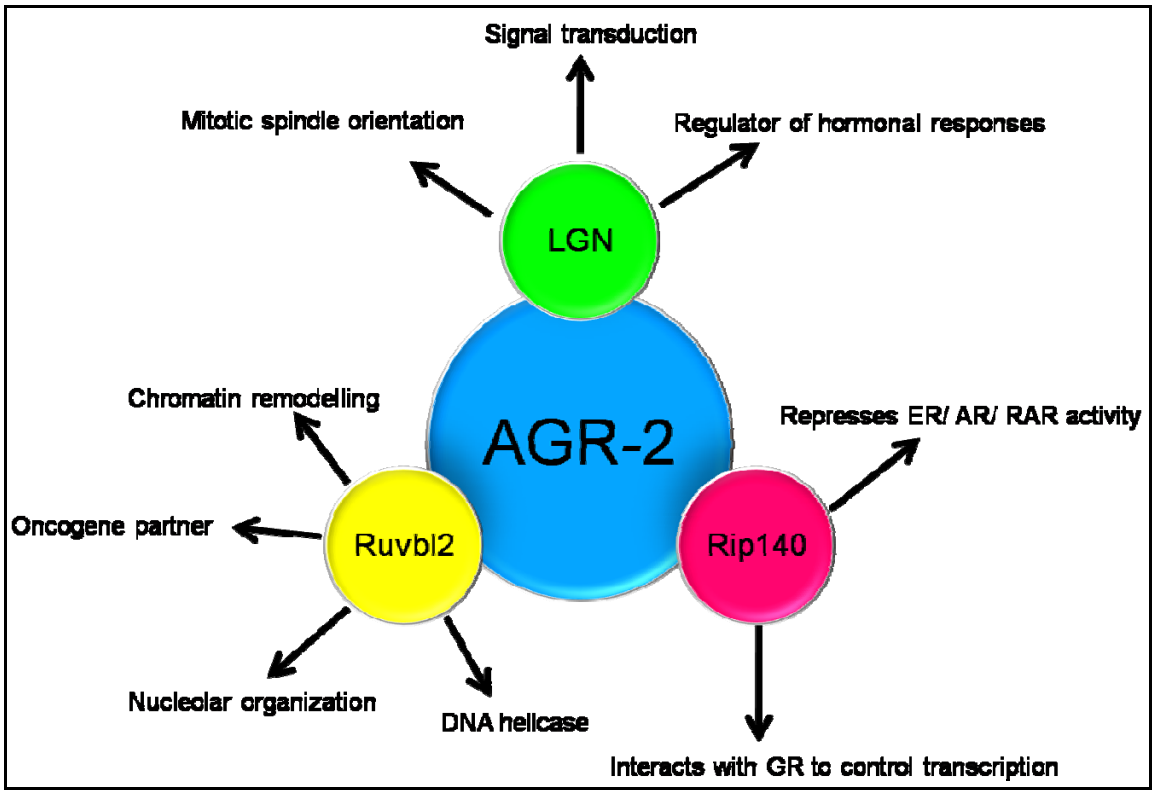

Figure 6.4: Overview of AGR-2 and binding partners in MCF-7 cells.

Final Conclusion

Data presented in this thesis confirmed AGR-2 gene product as a potential drug target for reactivating the p53 pathway in cancer cells. Inhibition of AGR-2 can follow the steps of another nuclear p53 inhibitor, iASPP and therefore provide an important new strategy for treating tumours expressing wild-type p53 [51]. In this report, we defined the subcellular localization of AGR-2 and how this relates to its ability to inhibit the p53 tumour suppressor protein setting the basis for further manipulation of the mechanism of this inhibition and therefore cancer. Our data indicate that AGR-2 attenuates p53 transcriptional response through its localization and two models emerged supporting this inhibition by either inducing nuclear exclusion of p53 protein (Figure 6.5A/I) or by *in situ* inhibiting the tumour suppressor protein in irradiated or non cells (Figure 6.5A/II). These data provide a proof-of-principle that the AGR-2 pathway forms a novel type of pro-oncogenic drug target in cancers and highlights the utility of combining clinical proteomics with peptide combinatorial chemistry to discover and validate novel anti-cancer drug targets. The mechanism that regulates AGR-2 and mediates its effects in cancer growth in these various biological systems is yet not entirely defined. However, given the possibility that AGR-2 might prove to be a novel and wide-spread anti-cancer drug target whose inhibition activates the p53 tumour suppressor, we further characterised and manipulated this mechanism by using peptide leads as therapeutic agents. Our analysis has shown that (i) AGR-2 can mediate a change in nuclear-cytoplasmic localization of p53 protein which is consistent with the link between p53 nuclear localization and its function as a transcription factor and (ii) that aptamers can disrupt this exclusion by eliminating nuclear AGR-2 and therefore inducing p53 activation. On the other hand, the other AGR- family protein member, AGR-3 inhibits apoptosis through Bax inactivation, conferring resistance of cells to cell death and enhancing survival. Two member of the same family have evolved to function by two totally distinct mechanisms of promoting cancer cell grown and resistance to death.

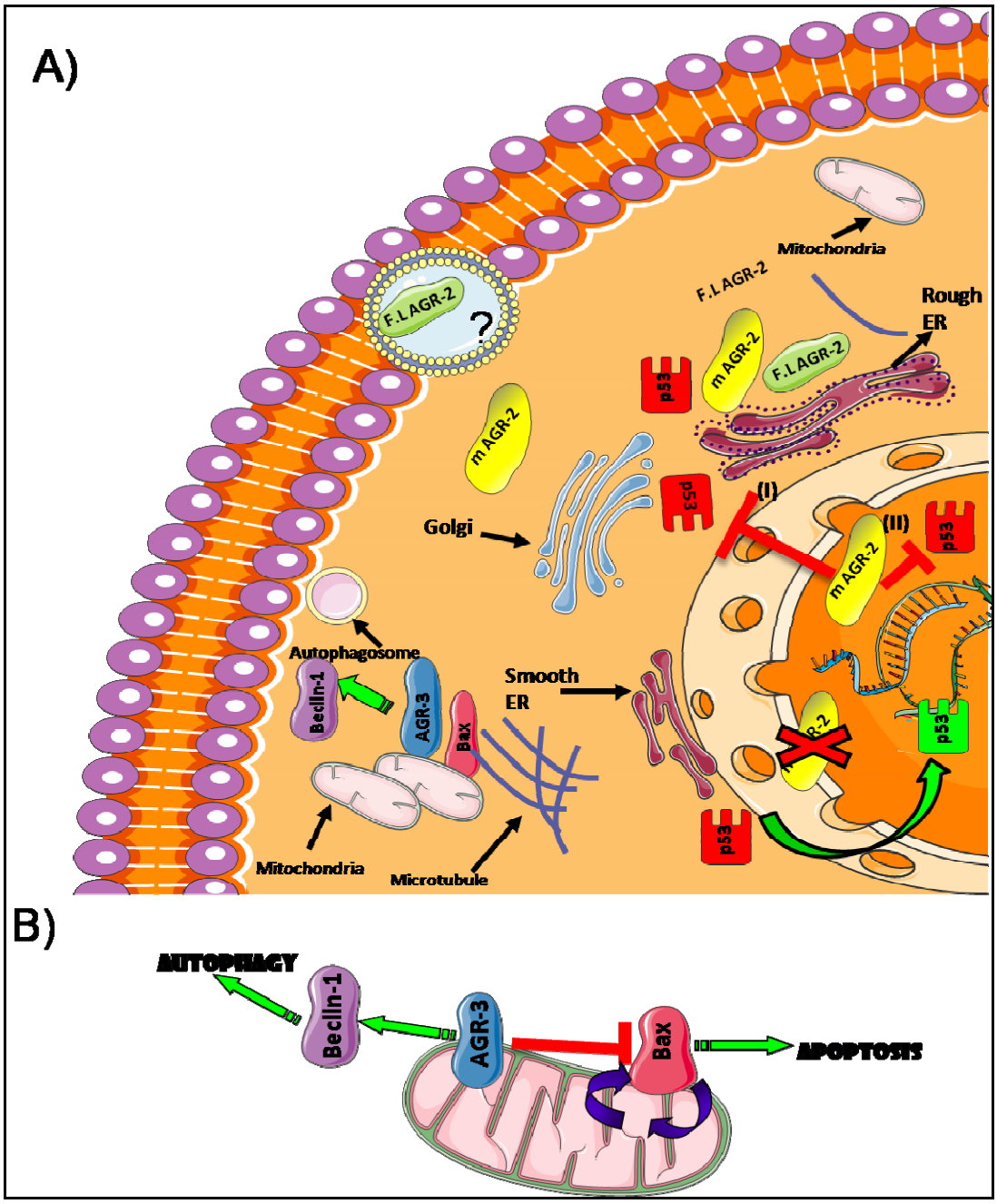

Figure 6.5. Schematic model of AGR-2 and AGR-3 function. A) Nuclear mature AGR-2 inhibits p53 translocation into the nucleus and when depleted, p53 enters the nucleus to transcripionally-activate target genes. Full length is localized in the ER but secretory designation is still pending (?) (I) and (II) represent the two different models on p53 inhibition. B) Mitochondrial AGR-3 activates autophagy protein Beclin-1and inhibits pro-apoptotic Bax, acting as a molecular switch towards autophagy (Designed by Servier Medical Art Tools software).

1. Abedi, M., Caponigro, G. and Kamb, A. 1998 "Green fluorescent protein as a scaffold for intracellular presentation of peptides". *Nucleic Acids Res*, *26* (2). 623-630.
2. Abedin, M.J., Wang, D., McDonnell, M.A., Lehmann, U. and Kelekar, A. 2006 "Autophagy delays apoptotic death in breast cancer cells following DNA damage". *Cell Death Differ*, *14* (3). 500-510.
3. Aberger, F., Weidinger, G., Grunz, H. and Richter, K. 1998 "Anterior specification of embryonic ectoderm: the role of the Xenopus cement gland-specific gene XAG-2". *Mech Dev*, *72* (1-2). 115.
4. Adam, P.J., Boyd, R., Tyson, K.L., Fletcher, G.C., Stamps, A., Hudson, L., Poyser, H.R., Redpath, N., Griffiths, M., Steers, G., Harris, A.L., Patel, S., Berry, J., Loader, J.A., Townsend, R.R., Daviet, L., Legrain, P., Parekh, R. and Terrett, J.A. 2003 "Comprehensive proteomic analysis of breast cancer cell membranes reveals unique proteins with potential roles in clinical cancer". *J Biol Chem*, *278* (8). 6482-6489.
5. Adam, P.J., Boyd, R., Tyson, K.L., Fletcher, G.C., Stamps, A., Hudson, L., Poyser, H.R., Redpath, N., Griffiths, M., Steers, G., Harris, A.L., Patel, S., Berry, J., Loader, J.A., Townsend, R.R., Daviet, L., Legrain, P., Parekh, R. and Terrett, J.A. 2003 "Comprehensive Proteomic Analysis of Breast Cancer Cell Membranes Reveals Unique Proteins with Potential Roles in Clinical Cancer". *J Biol Chem*, *278* (8). 6482-6489.
6. Adams, J.M. and Cory, S. 1998 "The Bcl-2 Protein Family: Arbiters of Cell Survival". *Science*, *281* (5381). 1322-1326.
7. Affar, E.B., Germain, M., Winstall, E., Vodenicharov, M., Shah, R.G., Salvesen, G.S. and Poirier, G.G. 2001 "Caspase-3-mediated Processing of Poly(ADP-ribose) Glycohydrolase during Apoptosis". *J Biol Chem*, *276* (4). 2935-2942.
8. Agarwal, M., Agarwal, A., Taylor, W. and Stark, G. 1995 "p53 controls both the G2/M and the G1 cell cycle checkpoints and mediates reversible growth arrest in human fibroblasts". *Proc Natl Acad Sci U S A*, *92* (18). 8493-8497.
9. Aggarwal, B., Sethi, G., Baladandayuthapani, V., Krishnan, S. and Shishodia, S. 2007 "Targeting cell signaling pathways for drug discovery: an old lock needs a new key". *J Cell Biochem*, *102* (3). 580-592.
10. Ahn, J. and Prives, C. 2001 "The C-terminus of p53: the more you learn the less you know". *Nat Struct Mol Biol*, *8* (9). 730-732.
11. Aist, J. and Bayles, C. 1991 "Organelle motility within mitotic asters of the fungus Nectria haematococca". *Eur J Cell Biol*, *56* (2). 358-363.
12. Aita, V.M., Liang, X.H., Murty, V.V.V.S., Pincus, D.L., Yu, W., Cayanis, E., Kalachikov, S., Gilliam, T.C. and Levine, B. 1999 "Cloning and Genomic Organization of Beclin 1, a Candidate Tumor Suppressor Gene on Chromosome 17q21". *Genomics*, *59* (1). 59-65.
13. Akar, U., Chaves Reyez, A., Barria, M., Tari, A., Sanguino, A., Kondo, Y., Kondo, S., Arun, B., Lopez Berestein, G. and Ozpolat, B. 2008 "Silencing of

Bcl-2 expression by small Interfering RNA induces autophagic cell death in MCF-7 breast cancer cells". *Autophagy*, *4* (5). 669-679.

14. Alanen, H.I., Williamson, R.A., Howard, M.J., Hatahet, F.S., Salo, K.E.H., Kauppila, A., Kellokumpu, S. and Ruddock, L.W. 2006 "ERp27, a New Non-catalytic Endoplasmic Reticulum-located Human Protein Disulfide Isomerase Family Member, Interacts with ERp57". *J Biol Chem*, *281* (44). 33727-33738.
15. Alanen, H.I., Williamson, R.A., Howard, M.J., Lappi, A.-K., Jantti, H.P., Rautio, S.M., Kellokumpu, S. and Ruddock, L.W. 2003 "Functional Characterization of ERp18, a New Endoplasmic Reticulum-located Thioredoxin Superfamily Member". *J Biol Chem*, *278* (31). 28912-28920.
16. Allen, T.M., Williamson, P. and Schlegel, R.A. 1988 "Phosphatidylserine as a Determinant of Reticuloendothelial Recognition of Liposome Models of the Erythrocyte Surface". *PNAS*, *85* (21). 8067-8071.
17. Alnemri, E.S., Livingston, D.J., Nicholson, D.W., Salvesen, G., Thornberry, N.A., Wong, W.W. and Yuan, J. 1996 "Human ICE/CED-3 Protease Nomenclature". *Cell*, *87* (2). 171-171.
18. Altmeyer, A., Maki, R., Feldweg, A., Heike, M., Protopopov, V., Masur, S. and Srivastava, P. 1996 "Tumor-specific cell surface expression of the-KDEL containing, endoplasmic reticular heat shock protein gp96". *Int J Cancer*, *69* (4). 340-349.
19. Ambrosini, G., Sambol, E., Carvajal, D., Vassilev, L., Singer, S. and Schwartz, G. 2007 "Mouse double minute antagonist Nutlin-3a enhances chemotherapy-induced apoptosis in cancer cells with mutant p53 by activating E2F1". *Oncogene*, *26* (24). 3473-3481.
20. An, W.G., Kanekal, M., Simon, M.C., Maltepe, E., Blagosklonny, M.V. and Neckers, L.M. 1998 "Stabilization of wild-type p53 by hypoxia-inducible factor 1[alpha]". *Nature*, *392* (6674). 405-408.
21. Anderson, W.F., Chatterjee, N., Ershler, W.B. and Brawley, O.W. 2002 "Estrogen Receptor Breast Cancer Phenotypes in the Surveillance, Epidemiology, and End Results Database". *Breast Cancer Research and Treatment*, *76* (1). 27-36.
22. Anelli, T., Alessio, M., Mezghrani, A., Simmen, T., Talamo, F., Bachi, A. and Sitia, R. 2002 "ERp44, a novel endoplasmic reticulum folding assistant of the thioredoxin family". *Embo J*, *21* (4). 835-844.
23. Angeloni, S.V., Martin, M.B., Garcia-Morales, P., Castro-Galache, M.D., Ferragut, J.A. and Saceda, M. 2004 "Regulation of estrogen receptor-alpha expression by the tumor suppressor gene p53 in MCF-7 cells". *J Endocrinol*, *180* (3). 497-504.
24. Arafah, B., Finegan, H., Roe, J., Manni, A. and Pearson, O. 1982 "Hormone dependency in N-nitrosomethylurea-induced rat mammary tumors." *Endocrinology*, *111* (2). 584-588.
25. Archer, S., Eliopoulos, A., Spandidos, D., Barnes, D., Ellis, I., Blamey, R., Nicholson, R. and Robertson, J. 1995 "Expression of ras p21, p53 and c-

erbB-2 in advanced breast cancer and response to first line hormonal therapy". *Br J Cancer*, *72* (5). 1259-1266.

26. Arthur, C., Gupton, J., Kellogg, G., Yeudall, W., Cabot, M., Newsham, I. and Gewirtz, D. 2007 "Autophagic cell death, polyploidy and senescence induced in breast tumor cells by the substituted pyrrole JG-03-14, a novel microtubule poison". *Biochem Pharmacol*, *74* (7). 981-991.
27. Ashkenazi, A. and Dixit, V.M. 1998 "Death Receptors: Signaling and Modulation". *Science*, *281* (5381). 1305-1308.
28. Aw, T. and Jones, D. 1985 "ATP concentration gradients in cytosol of liver cells during hypoxia". *Am J Physiol Renal Physiol*, *249* (5 Pt 1).
29. Aw, T. and Jones, D. 1989 "Nutrient supply and mitochondrial function". *Annu Rev Nutr*, *23* (9). 229-251.
30. Azim, H. and Azim Jr, H.A. 2008 "Targeting Her-2/neu in Breast Cancer: As Easy as This!" *Oncology*, *74* (3-4). 150-157.
31. Baehrecke, E.H. 2003 "Autophagic programmed cell death in Drosophila". *Cell Death Differ*, *10* (9). 940-945.
32. Baines, I.C. and Colas, P. 2006 "Peptide aptamers as guides for small-molecule drug discovery". *Drug Discov Today*, *11* (7-8). 334-341.
33. Baird, G.S., Zacharias, D.A. and Tsien, R.Y. 2000 "Biochemistry, mutagenesis, and oligomerization of DsRed, a red fluorescent protein from coral". *PNAS*, *97* (22). 11984-11989.
34. Baker, S., Markowitz, S., Fearon, E., Willson, J. and Vogelstein, B. 1990 "Suppression of human colorectal carcinoma cell growth by wild-type p53". *Science*, *249* (4971). 912-915.
35. Ball, K., Lain, S., Fåhraeus, R., Smythe, C. and Lane, D. 1997 "Cell-cycle arrest and inhibition of Cdk4 activity by small peptides based on the carboxy-terminal domain of p21WAF1". *Curr Biol*, *7* (1). 71-80.
36. Banin, S., Moyal, L., Shieh, S.Y., Taya, Y., Anderson, C.W., Chessa, L., Smorodinsky, N.I., Prives, C., Reiss, Y., Shiloh, Y. and Ziv, Y. 1998 "Enhanced Phosphorylation of p53 by ATM in Response to DNA Damage". *Science*, *281* (5383). 1674-1677.
37. Barak, Y. and Oren, M. 1992 " Enhanced binding of a 95 kDa protein to p53 in cells undergoing p53-mediated growth arrest." *EMBO J*, *11* (6). 2115-2121.
38. Bardou, V.-J., Arpino, G., Elledge, R.M., Osborne, C.K. and Clark, G.M. 2003 "Progesterone Receptor Status Significantly Improves Outcome Prediction Over Estrogen Receptor Status Alone for Adjuvant Endocrine Therapy in Two Large Breast Cancer Databases". *J Clin Oncol*, *21* (10). 1973-1979.
39. Barkla, D. and Gibson, P. 1999 "The fate of epithelial cells in the human large intestine." *Pathology*, *31* (3). 230-238.
40. Bartel, P.L., Roecklein, J.A., SenGupta, D. and Fields, S. 1996 "A protein linkage map of Escherichia coli bacteriophage T7". *Nat Genet*, *12* (1). 72-77.
41. Basanez, G., Nechushtan, A., Drozhinin, O., Chanturiya, A., Choe, E., Tutt, S., Wood, K.A., Hsu, Y.T., Zimmerberg, J. and Youle, R.J. 1999 "Bax, but

not Bcl-xL, decreases the lifetime of planar phospholipid bilayer membranes at subnanomolar concentrations". *PNAS*, *96* (10). 5492-5497.

42. Bauer, A., Chauvet, S., Huber, O., Usseglio, F., Rothbacher, U., Aragnol, D., Kemler, R. and Pradel, J. 2000 "Pontin52 and reptin52 function as antagonistic regulators of beta-catenin signalling activity". *Embo J*, *19* (22). 6121-6130.
43. Baumann, D., Cook, M., Ma, L., Mushegian, A., Sanders, E., Schwartz, J. and Yu, C. 2008 " A family of GFP-like proteins with different spectral properties in lancelet Branchiostoma floridae". *Biol Direct*, *3* (28).
44. Becker, K.C. and Becker, R.C. 2006 "Nucleic acid aptamers as adjuncts to vaccine development". *Curr Opin Mol Ther*, *8* (2). 122-129.
45. Beham, A., Marin, M., Fernandez, A., Herrmann, J., Brisbay, S., Tari, A., Lopez-Berestein, G., Lozano, G., Sarkiss, M. and McDonnell, T. 1997 "Bcl-2 inhibits p53 nuclear import following DNA damage". *Oncogene*, *15* (23). 2767-2772.
46. Bell, H.S. and Ryan, K.M. 2008 "iASPP Inhibition: Increased Options in Targeting the p53 Family for Cancer Therapy". *Cancer Res*, *68* (13). 4959-4962.
47. Bellaiche, Y., Radovic, A., Woods, D.F., Hough, C.D., Parmentier, M.L., O'Kane, C.J., Bryant, P.J. and Schweisguth, F. 2001 "The Partner of Inscuteable/Discs-Large Complex Is Required to Establish Planar Polarity during Asymmetric Cell Division in Drosophila". *Cell*, *106* (3). 355-366.
48. Bendtsen, J., Nielsen, H., Von Heijne, G. and Brunak, S. 2004 "Improved prediction of signal peptides: SignalP 3.0". *J Mol Biol*, *340* (4). 783-795.
49. Bennett, M.R., Gibson, D.F., Schwartz, S.M. and Tait, J.F. 1995 "Binding and Phagocytosis of Apoptotic Vascular Smooth Muscle Cells Is Mediated in Part by Exposure of Phosphatidylserine". *Circ Res*, *77* (6). 1136-1142.
50. Benshalom, G. and Reese, T. 1985 "Ultrastructural observations on the cytoarchitecture of axons processed by rapid-freezing and freeze-substitution". *J Neurocytol*, *14* (6). 943-960.
51. Bergamaschi, D., Samuels, Y., O'Neil, N.J., Trigiante, G., Crook, T., Hsieh, J.-K., O'Connor, D.J., Zhong, S., Campargue, I., Tomlinson, M.L., Kuwabara, P.E. and Lu, X. 2003 "iASPP oncoprotein is a key inhibitor of p53 conserved from worm to human". *Nat Genet*, *33* (2). 162-167.
52. Bergh, J. 1999 "Clinical studies of p53 in treatment and benefit of breast cancer patients". *Endocr Relat Cancer*, *6* (1). 51-59.
53. Bergmann, A. 2007 "Autophagy and Cell Death: No Longer at Odds". *Cell*, *131* (6). 1032-1034.
54. Berns, E.M., Klijn, J.G., van Putten, W.L., de Witte, H.H., Look, M.P., Meijer-van Gelder, M.E., Willman, K., Portengen, H., Benraad, T.J. and Foekens, J.A. 1998 "p53 protein accumulation predicts poor response to tamoxifen therapy of patients with recurrent breast cancer". *J Clin Oncol*, *16* (1). 121-127.
55. Berns, E.M.J.J., Foekens, J.A., Vossen, R., Look, M.P., Devilee, P., Henzen-Logmans, S.C., van Staveren, I.L., van Putten, W.L.J., Inganas, M., Gelder,

M.E.M.-v., Cornelisse, C., Claassen, C.J.C., Portengen, H., Bakker, B. and Klijn, J.G.M. 2000 "Complete Sequencing of TP53 Predicts Poor Response to Systemic Therapy of Advanced Breast Cancer". *Cancer Res*, *60* (8). 2155-2162.

56. Bertucci, F. and Birnbaum, D. 2008 "Reasons for breast cancer heterogeneity". *J. Biol.*, *7* (2). 6.
57. Béthune, J., Wieland, F. and Moelleken, J. 2006 "COPI-mediated transport". *J Membr Biol*, *211* (2). 65-79.
58. Betts, M.J., Russell, R.B., Barnes, M.R. and Gray, C. (eds.). *Amino acid properties and consequences of substitutions. In Bioinformatics for Geneticists*. Wiley, 2003.
59. Bevis, B.J. and Glick, B.S. 2002 "Rapidly maturing variants of the Discosoma red fluorescent protein (DsRed)". *Nat Biotech*, *20* (1). 83-87.
60. Blanc, C., Deveraux, Q.L., Krajewski, S., Janicke, R.U., Porter, A.G., Reed, J.C., Jaggi, R. and Marti, A. 2000 "Caspase-3 Is Essential for Procaspase-9 Processing and Cisplatin-induced Apoptosis of MCF-7 Breast Cancer Cells". *Cancer Res*, *60* (16). 4386-4390.
61. Blocker, A., Griffiths, G., Olivo, J., Hyman, A. and Severin, F. 1998 " A role for microtubule dynamics in phagosome movement". *J Cell Sci*, *111* (Pt 3). 303-312.
62. Blommaart, E., Luiken, J. and Meijer, A. 1997 "Autophagic proteolysis: control and specificity". *J Mol Histol*, *29* (5). 365-385.
63. Blumer, J.B., Chandler, L.J. and Lanier, S.M. 2002 "Expression Analysis and Subcellular Distribution of the Two G-protein Regulators AGS3 and LGN Indicate Distinct Functionality.Localization of LGN to the midbody during cytokinesis ". *J Biol Chem*, *277* (18). 15897-15903.
64. Boatright, K.M., Renatus, M., Scott, F.L., Sperandio, S., Shin, H., Pedersen, I.M., Ricci, J.-E., Edris, W.A., Sutherlin, D.P., Green, D.R. and Salvesen, G.S. 2003 "A Unified Model for Apical Caspase Activation". *Mol Cell*, *11* (2). 529-541.
65. Bonafé, M., Salvioli, S., Barbi, C., Trapassi, C., Tocco, F., Storci, G., Invidia, L., Vannini, I., Rossi, M., Marzi, E., Mishto, M., Capri, M., Olivieri, F., Antonicelli, R., Memo, M., Uberti, D., Nacmias, B., Sorbi, S., Monti, D. and Franceschi, C. 2004 "The different apoptotic potential of the p53 codon 72 alleles increases with age and modulates in vivo ischaemia-induced cell death". *Cell Death Differ*, *11* (9). 962-973.
66. Bonifacino, J. and Weissman, A. 1998 "Ubiquitin and the control of protein fate in the secretory and endocytic pathways". *Annu Rev Cell Dev Biol*, *14*. 19-57.
67. Borg, A., Baldetorp, B., Fernö, M., Killander, D., Olsson, H., Rydén, S. and Sigurdsson, H. 1994 " ERBB2 amplification is associated with tamoxifen resistance in steroid-receptor positive breast cancer". *Cancer Lett*, *81* (2). 137-144.
68. Borghouts, C., Kunz, C. and Groner, B. 2005 "Peptide aptamers: recent developments for cancer therapy". *Expert Opinion 5*(6). 783-797.

69. Borgna, J.L. and Rochefort, H. 1981 "Hydroxylated metabolites of tamoxifen are formed in vivo and bound to estrogen receptor in target tissues". *J Biol Chem.*, *256* (2). 859-868.
70. Bosari, S., Viale, G., Roncalli, M., Graziani, D., Borsani, G., Lee, A.K. and Coggi, G. 1995 "p53 gene mutations, p53 protein accumulation and compartmentalization in colorectal adenocarcinoma". *Am J Pathol*, *147* (3). 790-798.
71. Boyd, D. and Beckwith, J. 1990 "The role of charged amino acids in the localization of secreted and membrane proteins". *Cell*, *62* (6). 1031-1033.
72. Brandon, M., Baldi, P. and Wallace, D. 2006 "Mitochondrial mutations in cancer". *Oncogene*, *25* (34). 4647-4662.
73. Breedlove, G. and Busenhart, C. 2005 "Screening and detection of ovarian cancer". *J of Midwifery & Women's Health*, *50* (1). 51-54.
74. Brenner, C. and Grimm, S. 2006 "The permeability transition pore complex in cancer cell death". *Oncogene*, *25* (34). 4744-4756.
75. Brunner, N., Boysen, B., Jirus, S., Skaar, T.C., Holst-Hansen, C., Lippman, J., Frandsen, T., Spang-Thomsen, M., Fuqua, S.A.W. and Clarke, R. 1997 "MCF7/LCC9: An Antiestrogen-resistant MCF-7 Variant in Which Acquired Resistance to the Steroidal Antiestrogen ICI 182,780 Confers an Early Cross-Resistance to the Nonsteroidal Antiestrogen Tamoxifen". *Cancer Res*, *57* (16). 3486-3493.
76. Bueso Ramos, C.E., Yang, Y., deLeon, E., McCown, P., Stass, S.A. and Albitar, M. 1993 "The human MDM-2 oncogene is overexpressed in leukemias". *Blood*, *82* (9). 2617-2623.
77. Bulavin, D.V., Saito, S., Hollander, M.C., Sakaguchi, K., Anderson, C.W., Appella, E. and Fornace, A.J., Jr. 1999 "Phosphorylation of human p53 by p38 kinase coordinates N-terminal phosphorylation and apoptosis in response to UV radiation". *Embo J*, *18* (23). 6845-6854.
78. Bunone, G., Briand, P., Miksicek, R. and Picard, D. 1996 "Activation of the unliganded estrogen receptor by EGF involves the MAP kinase pathway and direct phosphorylation". *EMBO J*, *15* (9). 2174-2183.
79. Burgstaller, P., Girod, A. and Blind, M. 2002 "Aptamers as tools for target prioritization and lead identification". *Drug Discov Today*, *7* (24). 1221-1228.
80. Bursch, W., Ellinger, A., Kienzl, H., Torok, L., Pandey, S., Sikorska, M., Walker, R. and Hermann, R.S. 1996 "Active cell death induced by the anti-estrogens tamoxifen and ICI 164 384 in human mammary carcinoma cells (MCF-7) in culture: the role of autophagy". *Carcinogenesis*, *17* (8). 1595-1607.
81. Butt, A., Caldon, C., McNeil, C., Swarbrick, A., Musgrove, E. and Sutherland, R. 2008 " Cell cycle machinery: links with genesis and treatment of breast cancer". *Adv Exp Med Biol*, *20* (630). 189-205.
82. Buzdar, A., Plourde, P. and Hortobagyi, G. 1996 "Aromatase inhibitors in metastatic breast cancer." *Semin Oncol.*, *4* (9). 28-32.

83. Cabrera, M., Muñiz, M., Hidalgo, J., Vega, L., Martín, M. and Velasco, A. 2003 " The retrieval function of the KDEL receptor requires PKA phosphorylation of its C-terminus". *Mol Biol Cell*, *14* (10). 4114-4125.
84. Cahilly Snyder L., Yang-Feng, T., Francke, U. and George, D. 1987 "Molecular analysis and chromosomal mapping of amplified genes isolated from a transformed mouse 3T3 cell line." *Somat Cell Mol Genet*, *13* (3). 235-244.
85. Campbell, R.E., Tour, O., Palmer, A.E., Steinbach, P.A., Baird, G.S., Zacharias, D.A. and Tsien, R.Y. 2002 "A monomeric red fluorescent protein". *PNAS*, *99* (12). 7877-7882.
86. Cande, C., Cecconi, F., Dessen, P. and Kroemer, G. 2002 "Apoptosis-inducing factor (AIF): key to the conserved caspase-independent pathways of cell death?" *J Cell Sci*, *115* (24). 4727-4734.
87. Carascossa, S., Gobinet, J., Georget, V., Lucas, A., Badia, E., Castet, A., White, R., Nicolas, J.C., Cavailles, V. and Jalaguier, S. 2006 "Receptor-Interacting Protein 140 Is a Repressor of the Androgen Receptor Activity". *Mol Endocrinol*, *20* (7). 1506-1518.
88. Carew, J. and Huang, P. 2002 " Mitochondrial defects in cancer". *Mol Cancer Res* (9). 1-9.
89. Carew, J., Zhou, Y., M., A., JD., C., Keating, M. and Huang, P. 2003 "Mitochondrial DNA mutations in primary leukemia cells after chemotherapy: clinical significance and therapeutic implications". *Leukemia*, *17* (8). 1437-1447.
90. Carmeliet, P., Dor, Y., Herbert, J.-M., Fukumura, D., Brusselmans, K., Dewerchin, M., Neeman, M., Bono, F., Abramovitch, R., Maxwell, P., Koch, C.J., Ratcliffe, P., Moons, L., Jain, R.K., Collen, D. and Keshet, E. 1998 "Role of HIF-1[alpha] in hypoxia-mediated apoptosis, cell proliferation and tumour angiogenesis". *Nature*, *394* (6692). 485-490.
91. Caron de Fromentel, C. and Soussi, T. 1992 "TP53 tumor suppressor gene: a model for investigating human mutagenesis". *Genes Chromosomes Cancer*, *4* (1). 1-15.
92. Carrick, S., Ghersi, D., Wilcken, N. and Simes, J. 2004 " Platinum containing regimens for metastatic breast cancer". *Cochrane Database Syst Rev* (3).
93. Casciola-Rosen, L., Nicholson, D.W., Chong, T., Rowan, K.R., Thornberry, N.A., Miller, D.K. and Rosen, A. 1996 "Apopain/CPP32 cleaves proteins that are essential for cellular repair: a fundamental principle of apoptotic death". *J Exp Med*, *183* (5). 1957-1964.
94. Castet, A., Herledan, A., Bonnet, S., Jalaguier, S., Vanacker, J. and Cavaillès, V. 2006 "Receptor-interacting protein 140 differentially regulates estrogen receptor-related receptor transactivation depending on target genes". *Mol Endocrinol*, *20* (5). 1035-1047.
95. Cavailles, V., Dauvois, S., L'Horset, F., Lopez, G., Hoare, S., Kushner, P.J. and Parker, M.G. 1995 "Nuclear factor RIP140 modulates transcriptional activation by the estrogen receptor". *Embo J*, *14* (15). 3741-3751.

96. Cecconi, F., Alvarez-Bolado, G., Meyer, B.I., Roth, K.A. and Gruss, P. 1998 "Apaf1 (CED-4 Homolog) Regulates Programmed Cell Death in Mammalian Development". *Cell*, *94* (6). 727-737.
97. Chada, S. and Hollenbeck, P. 2004 "Nerve growth factor signaling regulates motility and docking of axonal mitochondria". *Curr Biol*, *14* (14). 1272-1276.
98. Chalkley, R., Baker, P., Huang, L., Hansen, K., Allen, N., Rexach, M. and Burlingame, A. 2005 "Comprehensive analysis of a multidimensional liquid chromatography mass spectrometry dataset acquired on a quadrupole selecting, quadrupole collision cell, time-of-flight mass spectrometer: II. New developments in Protein Prospector allow for reliable and comprehensive automatic analysis of large datasets". *Mol Cell Proteomics*, *4* (8). 1194-1204.
99. Chandel, N., Vander Heiden, M., Thompson, C. and Schumacker, P. 2000 "Redox regulation of p53 during hypoxia." *Oncogene*, *19* (34). 3840-3848.
100. Chandra, D., Liu, J.W. and Tang, D.G. 2002 "Early Mitochondrial Activation and Cytochrome c Up-regulation during Apoptosis". *J Biol Chem*, *277* (52). 50842-50854.
101. Chapman, J.A. and Beckey, C. 2006 "Pegaptanib: A Novel Approach to Ocular Neovascularization". *Ann Pharmacother*, *40* (7). 1322-1326.
102. Chautan, M., Chazal, G., Cecconi, F., Gruss, P. and Golstein, P. 1999 "Interdigital cell death can occur through a necrotic and caspase-independent pathway". *Curr Biol*, *9* (17). 967-970.
103. Chehab, N.H., Malikzay, A., Stavridi, E.S. and Halazonetis, T.D. 1999 "Phosphorylation of Ser-20 mediates stabilization of human p53 in response to DNA damage". *PNAS*, *96* (24). 13777-13782.
104. Chen, H., Detmer, S.A., Ewald, A.J., Griffin, E.E., Fraser, S.E. and Chan, D.C. 2003 "Mitofusins Mfn1 and Mfn2 coordinately regulate mitochondrial fusion and are essential for embryonic development". *J Cell Sci*, *160* (2). 189-200.
105. Chen, J. and Kadlubar, F. 2004 "Mitochondrial mutagenesis and oxidative stress in human prostate cancer". *J Environ Sci Health C Environ Carcinog Ecotoxicol Rev*, *22* (1). 1-12.
106. Chen, J., Marechal, V. and Levine, A.J. 1993 "Mapping of the p53 and mdm-2 interaction domains". *Mol Cell Biol*, *13* (7). 4107-4114.
107. Chen, J., Wu, X., Lin, J. and Levine, A.J. 1996 "mdm-2 inhibits the G1 arrest and apoptosis functions of the p53 tumor suppressor protein". *Mol Cell Biol*, *16* (5). 2445-2452.
108. Chen, Z., Lu, W., Garcia Prieto, C. and Huang, P. 2007 "The Warburg effect and its cancer therapeutic implications". *J Bioenerg Biomembr*, *39* (3). 267-274.
109. Cheng, E., Kirsch, D., Clem, R., Ravi, R., Kastan, M., Bedi, A., Ueno, K. and Hardwick, J. 1997 "Conversion of Bcl-2 to a Bax-like death effector by caspases". *Science*, *278* (5345). 1966-1968.
110. Cheng, J., Moyer, B.D., Milewski, M., Loffing, J., Ikeda, M., Mickle, J.E., Cutting, G.R., Li, M., Stanton, B.A. and Guggino, W.B. 2002 "A Golgi-

associated PDZ Domain Protein Modulates Cystic Fibrosis Transmembrane Regulator Plasma Membrane Expression". *J Biol Chem*, *277* (5). 3520-3529.

111. Cheng, W., Berman, S., Ivanovska, I., Jonas, E., Lee, S., Chen, Y., Kaczmarek, L., Pineda, F. and Hardwick, J. 2006 " Mitochondrial factors with dual roles in death and survival". *Oncogene*, *25* (34). 4697-4705.
112. Cheng, Y., Qiu, F., Huang, J., Tashiro, S., Onodera, S. and Ikejima, T. 2008 "Apoptosis-suppressing and autophagy-promoting effects of calpain on oridonin-induced L929 cell death". *Arch Biochem Biophys*, *475* (2). 148-155.
113. Cheson, B. and Leonard, J. 2008 "Monoclonal antibody therapy for B-cell non-Hodgkin's lymphoma". *N Engl J Med*, *359* (6). 613-626.
114. Chicheportiche, Y., Bourdon, P.R., Xu, H., Hsu, Y.-M., Scott, H., Hession, C., Garcia, I. and Browning, J.L. 1997 "TWEAK, a New Secreted Ligand in the Tumor Necrosis Factor Family That Weakly Induces Apoptosis". *J Biol Chem.*, *272* (51). 32401-32410.
115. Cho, S.-G., Bhoumik, A., Broday, L., Ivanov, V., Rosenstein, B. and Ronai, Z.e. 2001 "TIP49b, a Regulator of Activating Transcription Factor 2 Response to Stress and DNA Damage". *Mol Cell Biol*, *21* (24). 8398-8413.
116. Choi, J.H., Wong, A.S.T., Huang, H.F. and Leung, P.C. 2007 "Gonadotropins and Ovarian Cancer". *Endocr Rev*, *28* (4). 440-461.
117. Ciesiolka, J., Gorski, J. and Yarus, M. 1995 "Selection of an RNA domain that binds Zn2+". *RNA*, *1* (5). 538-550.
118. Cleator, S., Heller, W. and Coombes, R.C. 2007 "Triple-negative breast cancer: therapeutic options". *Lancet Oncol.*, *8*. 235 - 244.
119. Clérico, E., Maki, J. and Gierasch, L. 2008 "Use of synthetic signal sequences to explore the protein export machinery". *Biopolymers*, *90* (3). 307-319.
120. Clive, D.R. and Greene, J.J. 1996 "Cooperation of protein disulfide isomerase and redox environment in the regulation of NF-kappaB and AP1 binding to DNA". *Cell Biochem Funct*, *14* (1). 49-55.
121. Clore, G., Omichinski, J., Sakaguchi, K., Zambrano, N., Sakamoto, H., Appella, E. and Gronenborn, A. 1994 "High-resolution structure of the oligomerization domain of p53 by multidimensional NMR". *Science*, *265* (5170). 386-391.
122. Coezy, E., Borgna, J.-L. and Rochefort, H. 1982 "Tamoxifen and Metabolites in MCF7 Cells: Correlation between Binding to Estrogen Receptor and Inhibition of Cell Growth". *Cancer Res*, *42* (1). 317-323.
123. Colas, P. 2000 "Combinatorial protein reagents to manipulate protein function". *Curr Opin Chem Biol*, *4* (1). 54-59.
124. Coppari, S., Altieri, F., Ferraro, A., Chichiarelli, S., Eufemi, M. and Turano, C. 2002 "Nuclear localization and DNA interaction of protein disulfide isomerase ERp57 in mammalian cells". *J Cell Biochem*, *85* (2). 325-333.
125. Coppari, S., Altieri, F., Ferraro, A., Chichiarelli, S., Eufemi, M. and Turano, C. 2002 "Nuclear localization and DNA interaction of protein disulfide isomerase ERp57 in mammalian cells". *J Cell Biochem*, *85* (2). 325-333.

126. Cortez, D. 2005 "Unwind and slow down: checkpoint activation by helicase and polymerase uncoupling". *Genes Dev*, *19* (9). 1007-1012.
127. Crawford, M., Woodman, R. and Ferrigno, P.K. 2003 "Peptide aptamers: Tools for biology and drug discovery". *Brief Funct Genomic Proteomic*, *2* (1). 72-79.
128. Cui, Q., Tashiro, S., Onodera, S., Minam, i.M. and Ikejima, T. 2007 "Autophagy preceded apoptosis in oridonin-treated human breast cancer MCF-7 cells". *Biol Pharm Bull*, *30* (5). 859-864.
129. Cullen, B.R. and Greene, W.C. 1989 "Regulatory pathways governing HIV-1 replication". *Cell*, *58* (3). 423-426.
130. D'Assoro, A., Busby, R., Acu, I., Quatraro, C., Reinholz, M., Farrugia, D., Schroeder, M., Allen, C., Stivala, F., Galanis , E. and Salisbury, J. 2008 "Impaired p53 function leads to centrosome amplification, acquired ERalpha phenotypic heterogeneity and distant metastases in breast cancer MCF-7 xenografts". *Oncogene*, *27* (28). 3901-3911.
131. Dai, J., Liu, B., Caudill, M., Zheng, H., Qiao, Y., Podack, E. and Li, Z. 2003 "Cell surface expression of heat shock protein gp96 enhances cross-presentation of cellular antigens and the generation of tumor-specific T cell memory". *Cancer Immun*, *3* (1). 1-2.
132. Damber, J. and Aus, G. 2008 "Prostate cancer". *The Lancet*, *371* (9625). 1710-1721.
133. Dauvois, S., White, R. and Parker, M.G. 1993 "The antiestrogen ICI 182780 disrupts estrogen receptor nucleocytoplasmic shuttling". *J Cell Sci*, *106* (4). 1377-1388.
134. David, H., Ellermann, J. and Uerlings, I. 1992 "Primary phase of hepatocytic autophagocytosis under ischaemic conditions." *Exp Toxicol Pathol*, *44* (2). 74-80.
135. Davidoff, A.M., Kerns, B.-J.M., Dirk Iglehart, J. and Marks, J.R. 1991 "Maintenance of p53 Alterations throughout Breast Cancer Progression". *Cancer Res*, *51* (10). 2605-2610.
136. Dawson, R., Muller, L., Dehner, A., Klein, C., Kessler, H. and Buchner, J. 2003 "The N-terminal Domain of p53 is Natively Unfolded". *J Mol Biol*, *332* (5). 1131-1141.
137. De Duve, C. and Wattiaux, R. 1966 "Functions of Lysosomes". *Annu Rev Physiol*, *28* (1). 435-492.
138. Denecke, J., De Rycke, R. and Botterman, J. 1992 "Plant and mammalian sorting signals for protein retention in the endoplasmic reticulum contain a conserved epitope". *EMBO J*, *11* (6). 2345-2355.
139. Denzer, A., Nabholz, C. and Spiess, M. 1995 "Transmembrane orientation of signal-anchor proteins is affected by the folding state but not the size of the N-terminal domain". *EMBO J.*, *14* (24). 6311-6317.
140. Desagher, S., Osen-Sand, A., Nichols, A., Eskes, R., Montessuit, S., Lauper, S., Maundrell, K., Antonsson, B. and Martinou, J.-C. 1999 "Bid-induced Conformational Change of Bax Is Responsible for Mitochondrial Cytochrome c Release during Apoptosis". *J Cell Biol*, *144* (5). 891-901.

141. Desta, Z., Ward, B.A., Soukhova, N.V. and Flockhart, D.A. 2004 "Comprehensive Evaluation of Tamoxifen Sequential Biotransformation by the Human Cytochrome P450 System in Vitro: Prominent Roles for CYP3A and CYP2D6". *J Pharmacol Exp Ther*, *310* (3). 1062-1075.
142. Ding, H., McGill, G., Rowan, S., Schmaltz, C., Shimamura, A. and Fisher, D. 1998 "Oncogene-dependent regulation of caspase activation by p53 protein in a cell-free system". *J Biol Chem*, *273* (43). 28378-28383.
143. Doelling, J.H., Walker, J.M., Friedman, E.M., Thompson, A.R. and Vierstra, R.D. 2002 "The APG8/12-activating Enzyme APG7 Is Required for Proper Nutrient Recycling and Senescence in Arabidopsis thaliana". *J Biol Chem*, *277* (36). 33105-33114.
144. Doman, R.K., Perez, M. and Donato, N.J. 1999 "JNK and p53 Stress Signaling Cascades Are Altered in MCF-7 Cells Resistant to Tumor Necrosis Factor-Mediated Apoptosis". *J Interferon Cytokine Res*, *19* (3). 261-269.
145. Donehower, L.A., Harvey, M., Slagle, B.L., McArthur, M.J., Montgomery, C.A., Butel, J.S. and Allan, B. 1992 "Mice deficient for p53 are developmentally normal but susceptible to spontaneous tumours". *Nature*, *356* (6366). 215-221.
146. Donepudi, M., Sweeney, A.M., Briand, C. and Grütter, M.G. 2003 "Insights into the Regulatory Mechanism for Caspase-8 Activation". *Mol Cell*, *11* (2). 543-549.
147. Dornan, D., Eckert, M., Wallace, M., Shimizu, H., Ramsay, E., Hupp, T. and Ball, K. 2004 "Interferon regulatory factor 1 binding to p300 stimulates DNA-dependent acetylation of p53". *Mol Cell Biol*, *24* (22). 10083-10098.
148. Dornan, D., Eckert, M., Wallace, M., Shimizu, H., Ramsay, E., Hupp, T. and KL., B. 2004 "Interferon regulatory factor 1 binding to p300 stimulates DNA-dependent acetylation of p53". *Mol Cell Biol*, *24* (22). 10083-10098.
149. Dornan, D. and Hupp, T. 2001 " Inhibition of p53-dependent transcription by BOX-I phospho-peptide mimetics that bind to p300". *EMBO Rep*, *2* (2). 139-144.
150. Dos Santos, N.M.S., Taverne Thiele, J.J., Barnes, A.C., Van Muiswinkel, W.B., Ellis, A.E. and Rombout, J.H.W.M. 2001 "The gill is a major organ for antibody secreting cell production following direct immersion of sea bass (Dicentrarchus labrax, L.) in a Photobacterium damselae ssp. piscicida bacterin: an ontogenetic study". *Fish Shellfish Immunol*, *11* (1). 65-74.
151. Doyle, D.M. and Miller, K.D. 2008 "Development of new targeted therapies for breast cancer". *Breast Cancer*, *15* (1). 49-56.
152. Drummond, I.A., Lee, A.S., Resendez, E., Jr. and Steinhardt, R.A. 1987 "Depletion of intracellular calcium stores by calcium ionophore A23187 induces the genes for glucose-regulated proteins in hamster fibroblasts". *J Biol Chem*, *262* (26). 12801-12805.
153. Du, Q. and Macara, I.G. 2004 "Mammalian Pins Is a Conformational Switch that Links NuMA to Heterotrimeric G Proteins". *Cell*, *119* (4). 503-516.

154. Du, Q., Stukenberg, P.T. and Macara, I.G. 2001 "A mammalian Partner of inscuteable binds NuMA and regulates mitotic spindle organization". *Nat Cell Biol*, *3* (12). 1069-1075.
155. Du, Q., Taylor, L., Compton, D.A. and Macara, I.G. 2002 "LGN Blocks the Ability of NuMA to Bind and Stabilize Microtubules: A Mechanism for Mitotic Spindle Assembly Regulation". *Curr Biol*, *12* (22). 1928-1933.
156. Dudani, A., Austin, R., Venner, T. and Gupta, R. 1990 " Effects of antimitotic and antimitochondrial agents on the cellular distribution of microtubules and mitochondria". *Cytobios*, *63* (253). 95-108.
157. Dumont, P., Leu, J., Della Pietra, A., George, D. and Murphy, M. 2003 "The codon 72 polymorphic variants of p53 have markedly different apoptotic potential". *Nat Genet*, *33* (3). 357-365.
158. Dunn, J.J. and Studier, F.W. 1983 "Complete nucleotide sequence of bacteriophage T7 DNA and the locations of T7 genetic elements". *J Mol Biol*, *166* (4). 477-535.
159. Dunn, W.A., Jr. 1990 "Studies on the mechanisms of autophagy: formation of the autophagic vacuole". *J Biol Chem*, *110* (6). 1923-1933.
160. Duong, V., Boulle, N., Daujat, S., Chauvet, J., Bonnet, S., Neel, H. and Cavaillès, V. 2007 " Differential regulation of estrogen receptor alpha turnover and transactivation by Mdm2 and stress-inducing agents". *Cancer Res*, *67* (11). 5513-5521.
161. Dyke, C.K., Steinhubl, S.R., Kleiman, N.S., Cannon, R.O., Aberle, L.G., Lin, M., Myles, S.K., Melloni, C., Harrington, R.A., Alexander, J.H., Becker, R.C. and Rusconi, C.P. 2006 "First-in-Human Experience of an Antidote-Controlled Anticoagulant Using RNA Aptamer Technology: A Phase 1a Pharmacodynamic Evaluation of a Drug-Antidote Pair for the Controlled Regulation of Factor IXa Activity". *Circulation*, *114* (23). 2490-2497.
162. Dyson, M., Shadbolt, S., Vincent, K., Perera, R. and McCafferty, J. 2004 "Production of soluble mammalian proteins in Escherichia coli: identification of protein features that correlate with successful expression." *BMC Biotechnol.*, *4* (32).
163. Early Breast Cancer Trialists' Collaborative Group. 2005 "Effects of chemotherapy and hormonal therapy for early breast cancer on recurrence and 15-year survival: an overview of the randomised trials". *Lancet*, *365* (9472). 1687 - 1717.
164. Eccles, D., Russell, S., Haites, N., Atkinson, R., Bell, D., Gruber, L., Hickey, I., Kelly, K., Kitchener, H. and Leonard, R. 1992 " Early loss of heterozygosity on 17q in ovarian cancer. The Abe Ovarian Cancer Genetics Group." *Oncogene*, *7* (10). 2069-2072.
165. Eckert, B. 1986 "Alteration of the distribution of intermediate filaments in PtK1 cells by acrylamide. II: Effect on the organization of cytoplasmic organelles". *Cell Motil Cytoskeleton*, *6* (1). 15-24.
166. Edinger, A.L. and Thompson, C.B. 2003 "Defective autophagy leads to cancer". *Cancer Cell*, *4* (6). 422-424.

167. El-Aneed, A. 2004 "Current strategies in cancer gene therapy". *European Journal of Pharmacology*, *498* (1-3). 1-8.
168. El-Deiry, W., Tokino, T., Velculescu, V., Levy, D., Parsons, R., Trent, J., Lin, D., Mercer, W., Kinzler, K. and Vogelstein, B. 1993 "WAF1, a potential mediator of p53 tumor suppression". *Cell*, *75* (4). 817-825.
169. Elledge, R. and Allred, D.C. 1998 "Prognostic and predictive value of p53 and p21 in breast cancer". *Breast Cancer Res Treat*, *52* (1). 79-98.
170. Elledge, R.M., Green, S., Howes, L., Clark, G.M., Berardo, M., Allred, D.C., Pugh, R., Ciocca, D., Ravdin, P., O'Sullivan, J., Rivkin, S., Martino, S. and Osborne, C.K. 1997 "bcl-2, p53, and response to tamoxifen in estrogen receptor-positive metastatic breast cancer: a Southwest Oncology Group study". *J Clin Oncol*, *15* (5). 1916-1922.
171. Ellgaard, L., Molinari, M. and Helenius, A. 1999 "Setting the Standards: Quality Control in the Secretory Pathway". *Science*, *286* (5446). 1882-1888.
172. Ellington, A.D. and Szostak, J.W. 1990 "In vitro selection of RNA molecules that bind specific ligands". *Nature*, *346* (6287). 818-822.
173. Elston, C. and Ellis, I. 2002 "Pathological prognostic factors in breast cancer. I. The value of histological grade in breast cancer: experience from a large study with long-term follow-up." *Histopathology*, *41* (3A). 154-161.
174. Elston CW, E.I. 2002 "Pathological prognostic factors in breast cancer. I. The value of histological grade in breast cancer: experience from a large study with long-term follow-up." *Histopathology*, *41* (3A). 154-161.
175. Emptage, N. 2001 "Fluorescent imaging in living systems". *Curr Opin Pharmacol*, *1* (5). 521-525.
176. Epand, R.F., Martinou, J.-C., Montessuit, S., Epand, R.M. and Yip, C.M. 2002 "Direct evidence for membrane pore formation by the apoptotic protein Bax". *Biochem Biophys Res Commun*, *298* (5). 744-749.
177. Erster, S., Mihara, M., Kim, R., Petrenko, O. and Moll, U. 2004 " In vivo mitochondrial p53 translocation triggers a rapid first wave of cell death in response to DNA damage that can precede p53 target gene activation". *Mol Cell Biol*, *24* (15). 6728-6741.
178. Eskes, R., Desagher, S., Antonsson, B. and Martinou, J.-C. 2000 "Bid Induces the Oligomerization and Insertion of Bax into the Outer Mitochondrial Membrane". *Mol Cell Biol*, *20* (3). 929-935.
179. Esposito, D. and Chatterjee, D.K. 2006 "Enhancement of soluble protein expression through the use of fusion tags". *Curr Opin Biotechnol*, *17* (4). 353-358.
180. Everett, R.D., Lomonte, P., Sternsdorf, T., Van Driel, R. and Orr, A. 1999 "Cell cycle regulation of PML modification and ND10 composition". *J Cell Sci*, *112* (24). 4581-4588.
181. Eytech Study Group 2002 "Preclinical and phase 1A clinical evaluation of an anti-VEGF pegylated aptamer (EYE001) for the treatment of exudative age-related macular degeneration". *Retina*, *22* (2). 143-152.
182. Fabian, C. 2001 "Breast cancer chemoprevention: beyond tamoxifen". *Breast Cancer Res*, *3* (2). 99-103.

183. Fadok, V.A., Savill, J.S., Haslett, C., Bratton, D.L., Doherty, D.E., Campbell, P.A. and Henson, P.M. 1992 "Different populations of macrophages use either the vitronectin receptor or the phosphatidylserine receptor to recognize and remove apoptotic cells". *J Immunol*, *149* (12). 4029-4035.
184. Fadok, V.A., Voelker, D.R., Campbell, P.A., Cohen, J.J., Bratton, D.L. and Henson, P.M. 1992 "Exposure of phosphatidylserine on the surface of apoptotic lymphocytes triggers specific recognition and removal by macrophages". *J Immunol*, *148* (7). 2207-2216.
185. Falck, J., Coates, J. and Jackson, S.P. 2005 "Conserved modes of recruitment of ATM, ATR and DNA-PKcs to sites of DNA damage". *Nature*, *434* (7033). 605-611.
186. Famulok, M., Blind, M. and Mayer, G. 2001 "Intramers as promising new tools in functional proteomics". *Chem Biol*, *8* (10). 931-939.
187. Fazi, B., Bursch, W., Fimia, G., Nardacci, R., Piacentini, M., Di Sano, F. and Piredda, L. 2008 " Fenretinide induces autophagic cell death in caspase-defective breast cancer cells". *Autophagy*, *4* (4). 435-441.
188. Fearon, E.R. 1997 "Human Cancer Syndromes: Clues to the Origin and Nature of Cancer". *Science*, *278* (5340). 1043-1050.
189. Fehrenbacher, K., Yang, H., Gay, A., Huckaba, T. and Pon, L. 2004 "Live cell imaging of mitochondrial movement along actin cables in budding yeast". *Curr Biol*, *14* (22). 1996-2004.
190. Ferguson, H.A., Marietta, P.M. and Van Den Berg, C.L. 2003 "UV-induced Apoptosis Is Mediated Independent of Caspase-9 in MCF-7 Cells:". *J Biol Chem*, *278* (46). 45793-45800.
191. Ferguson, M., Luciani, M., Finlan, L., Rankin, E., Ibbotson, S., Fersht, A. and Hupp, T. 2004 "The development of a CDK2-docking site peptide that inhibits p53 and sensitizes cells to death". *Cell Cycle*, *3* (1). 80-89.
192. Fernandes-Alnemri, T., Armstrong, R.C., Krebs, J., Srinivasula, S.M., Wang, L., Bullrich, F., Fritz, L.C., Trapani, J.A., Tomaselli, K.J., Litwack, G. and Alnemri, E.S. 1996 "In vitro activation of CPP32 and Mch3 by Mch4, a novel human apoptotic cysteine protease containing two FADD-like domains". *PNAS*, *93* (15). 7464-7469.
193. Ferrari, D. and Söling, H. 1999 "The protein disulphide-isomerase family: unravelling a string of folds." *Biochem J*, *1* (339). 1-10.
194. Ferrari, D.M. and Soling, H.D. 1999 "The protein disulphide-isomerase family: unravelling a string of folds". *Biochem J*, *339 (Pt 1)*. 1-10.
195. Fidler, I.J., Raz, A., Fogler, W.E., Kirsh, R., Bugelski, P. and Poste, G. 1980 "Design of Liposomes to Improve Delivery of Macrophage-augmenting Agents to Alveolar Macrophages". *Cancer Res*, *40* (12). 4460-4466.
196. Finlay, C.A. 1993 "The mdm-2 oncogene can overcome wild-type p53 suppression of transformed cell growth". *Mol Cell Biol*, *13* (1). 301-306.
197. Finley, R.L., Zhang, H., Zhong, J. and Stanyon, C.A. 2002 "Regulated expression of proteins in yeast using the MAL61-62 promoter and a mating scheme to increase dynamic range". *Gene*, *285* (1-2). 49-57.

198. Fischer, P., Zhelev, N., Wang, S., Melville, J., Fåhraeus, R. and Lane, D. 2000 "Structure-activity relationship of truncated and substituted analogues of the intracellular delivery vector Penetratin". *J Pept Res*, *55* (2). 163-172.
199. Fletcher, G.C., Patel, S., Tyson, K., Adam, P.J., Schenker, M., Loader, J.A., Daviet, L., Legrain, P., Parekh, R., Harris, A.L. and Terrett, J.A. 2003 "hAG-2 and hAG-3, human homologues of genes involved in differentiation, are associated with oestrogen receptor-positive breast tumours and interact with metastasis gene C4.4a and dystroglycan". *Br J Cancer*, *88* (4). 579-585.
200. Fliss, M., Usadel, H., Caballero, O., Wu, L., Buta, M., Eleff, S., Jen, J. and Sidransky, D. 2000 " Facile detection of mitochondrial DNA mutations in tumors and bodily fluids". *Science*, *287* (5460). 2017-2019.
201. Fogal, V., Gostissa, M., Sandy, P., Zacchi, P., Sternsdorf, T., Jensen, K., Pandolfi, P., Will, H., Schneider, C. and Del Sal, G. 2000 "Regulation of p53 activity in nuclear bodies by a specific PML isoform". *EMBO J*, *19* (22). 6185-6195.
202. Forman, D., Lynch, K. and Smith, R. 1987 " Organelle dynamics in lobster axons: anterograde, retrograde and stationary mitochondria". *Brain Res*, *412* (1). 96-106.
203. Foulkes, W.D., Stefansson, I.M., Chappuis, P.O., Begin, L.R., Goffin, J.R., Wong, N., Trudel, M. and Akslen, L.A. 2003 "Germline BRCA1 Mutations and a Basal Epithelial Phenotype in Breast Cancer". *J Natl Cancer Inst.*, *95* (19). 1482-1485.
204. Frank, S., Gaume, B., Bergmann-Leitner, E.S., Leitner, W.W., Robert, E.G., Catez, F., Smith, C.L. and Youle, R.J. 2001 "The Role of Dynamin-Related Protein 1, a Mediator of Mitochondrial Fission, in Apoptosis". *Dev Cell*, *1* (4). 515-525.
205. Freedman, D., Epstein, C., Roth, J. and Levine, A. 1997 "A genetic approach to mapping the p53 binding site in the MDM2 protein." *Mol Med*, *3* (4). 248-259.
206. Freedman, R.B., Hirst, T.R. and Tuite, M.F. 1994 "Protein disulphide isomerase: building bridges in protein folding." *Trends Biochem Sci*, *19* (8). 331-336.
207. Fritzsche, F.R., Dahl, E., Pahl, S., Burkhardt, M., Luo, J., Mayordomo, E., Gansukh, T., Dankof, A., Knuechel, R., Denkert, C., Winzer, K.-J., Dietel, M. and Kristiansen, G. 2006 "Prognostic Relevance of AGR2 Expression in Breast Cancer". *Clin Cancer Res*, *12* (6). 1728-1734.
208. Furukawa, K., Fu, W., Li, Y., Witke, W., Kwiatkowski, D. and Mattson, M. 1997 "The actin-severing protein gelsolin modulates calcium channel and NMDA receptor activities and vulnerability to excitotoxicity in hippocampal neurons". *J Neurosci*, *17* (21). 8178-8186.
209. Futreal, P., Söderkvist, P., Marks, J., Iglehart , J., Cochran, C., Barrett, J. and Wiseman, R. 1992 "Detection of frequent allelic loss on proximal chromosome 17q in sporadic breast carcinoma using microsatellite length polymorphisms." *Cancer Res*, *52* (9). 2624-2627.

210. Gaglio, T., Saredi, A. and Compton, D.A. 1995 "NuMA is required for the organization of microtubules into aster-like mitotic arrays". *J Cell Biol*, *131* (3). 693-708.
211. Gao, X., Zacharek, A., Salkowski, A., Grignon, D.J., Sakr, W., Porter, A.T. and Honn, K.V. 1995 "Loss of Heterozygosity of the BRCA1 and Other Loci on Chromosome 17q in Human Prostate Cancer". *Cancer Res*, *55* (5). 1002-1005.
212. Gatenby, R. and Gillies, R. 2004 "Why do cancers have high aerobic glycolysis?" *Nat Rev Cancer*, *4* (11). 891-899.
213. Gerner, C., Holzmann, K., M., M., Gotzmann, J., Grimm, R. and Sauermann, G. 1999 "Reassembling proteins and chaperones in human nuclear matrix protein fractions". *J Cell Biochem*, *74* (2). 145-151.
214. Giannakakou, P., Sackett, D., Ward, Y., Webster, K., Blagosklonny, M. and Fojo, T. 2000 "p53 is associated with cellular microtubules and is transported to the nucleus by dynein". *Nat Cell Biol*, *2* (10). 709-717.
215. Giuseppe, C. 2007 "Estrogen and prostate cancer: An eclipsed truth in an androgen-dominated scenario". *J Cell Biochem*, *102* (4). 899-911.
216. Glotzer, M. 2001 "Animal cell cytokinesis". *Annu Rev Cell Dev Biol*, *17* (1). 351-386.
217. Goder, V. and Spiess, M. 2003 "Molecular mechanism of signal sequence orientation in the endoplasmic reticulum". *EMBO J*, *22* (14). 3645-3653.
218. Gohshi, T., Shimada, M., Kawahire, S., Imai, N., Ichimura, T., Omata, S. and Horigome, T. 1999 "Molecular cloning of mouse p47, a second group mammalian RuvB DNA helicase-like protein: homology with those from human and Saccharomyces cerevisiae". *J Biochem*, *125* (5). 939-946.
219. Goldstein, I., Hoffstein, S., Gallin and Weissmann, G. 1973 "Mechanisms of lysosomal enzyme release from human leukocytes: microtubule assembly and membrane fusion induced by a component of complement". *Proc Natl Acad Sci U S A*, *70* (10). 2916-2920.
220. Goldstein, J., Waterhouse, N., Juin, P., Evan, G. and Green, D. 2000 "The coordinate release of cytochrome c during apoptosis is rapid, complete and kinetically invariant". *Nat Cell Biol*, *3* (3). 156-162.
221. Goping, I.S., Gross, A., Lavoie, J.N., Nguyen, M., Jemmerson, R., Roth, K., Korsmeyer, S.J. and Shore, G.C. 1998 "Regulated Targeting of BAX to Mitochondria". *J Biol Chem*, *143* (1). 207-215.
222. Gordon, M.B., Howard, L. and Compton, D.A. 2001 "Chromosome Movement in Mitosis Requires Microtubule Anchorage at Spindle Poles". *J Cell Biol*, *152* (3). 425-434.
223. Gordon, P.B., Kovacs, A.L. and Seglen, P.O. 1987 "Temperature dependence of protein degradation, autophagic sequestration and mitochondrial sugar uptake in rat hepatocytes". *Biochim Biophys Acta*, *929* (2). 128-133.
224. Göringer, H., Homann, M. and Lorger, M. 2003 " In vitro selection of high-affinity nucleic acid ligands to parasite target molecules". *Int J Parasitol*, *33* (12). 1309-1317.

225. Górka, M., Daniewski, W., Gajkowska, B., Lusakowska, E., Godlewski, M. and Motyl, T. 2005 "Autophagy is the dominant type of programmed cell death in breast cancer MCF-7 cells exposed to AGS 115 and EFDAC, new sesquiterpene analogs of paclitaxel." *Anticancer Drugs*, *16* (7). 777-788.
226. Goss, P. 2008 "Addressing the future: combination with targeted therapies, adjuvant setting and beyond". *Anticancer Drugs*, *19* (2). S3-5.
227. Graeber, T.G., Peterson, J.F., Tsai, M., Monica, K., Fornace, A.J., Jr. and Giaccia, A.J. 1994 "Hypoxia induces accumulation of p53 protein, but activation of a G1-phase checkpoint by low-oxygen conditions is independent of p53 status". *Mol Cell Biol*, *14* (9). 6264-6277.
228. Green, D.R. and Kroemer, G. 2004 "The Pathophysiology of Mitochondrial Cell Death". *Science*, *305* (5684). 626-629.
229. Griffin, F.M., Jr., Griffin, J.A., Leider, J.E. and Silverstein, S.C. 1975 "Studies on the mechanism of phagocytosis. I. Requirements for circumferential attachment of particle-bound ligands to specific receptors on the macrophage plasma membrane". *J Exp Med*, *142* (5). 1263-1282.
230. Griffin, F.M., Jr., Griffin, J.A. and Silverstein, S.C. 1976 "Studies on the mechanism of phagocytosis. II. The interaction of macrophages with anti-immunoglobulin IgG-coated bone marrow-derived lymphocytes". *J Exp Med*, *144* (3). 788-809.
231. Griffiths, G., Ericsson, M., Krijnse Locker, J., Nilsson, T., Goud, B., Söling, H., Tang, B., Wong, S. and Hong, W. 1994 "Localization of the Lys, Asp, Glu, Leu tetrapeptide receptor to the Golgi complex and the intermediate compartment in mammalian cells". *J Cell Biol*, *127* (6 Pt 1). 1557-1574.
232. Grillo, C., D'Ambrosio, C., Consalvi, V., Chiaraluce, R., Scaloni, A., Maceroni, M., Eufemi, M. and Altieri, F. 2007 "DNA-binding Activity of the ERp57 C-terminal Domain Is Related to a Redox-dependent Conformational Change". *J Biol Chem*, *282* (14). 10299-10310.
233. Grimm , S. and Brdiczka, D. 2007 " The permeability transition pore in cell death". *Apoptosis*, *12* (5). 841-855.
234. Gross, A., McDonnell, J.M. and Korsmeyer, S.J. 1999 "BCL-2 family members and the mitochondria in apoptosis". *Genes Dev*, *13* (15). 1899-1911.
235. Grossman, S., Perez, M., Kung, A., Joseph, M., Mansur, C., Xiao, Z., Kumar, S., Howley, P. and Livingston, D. 1998 "p300/MDM2 complexes participate in MDM2-mediated p53 degradation". *Mol Cell*, *2* (4). 405-415.
236. Gruss, H.J. and Dower, S.K. 1995 "Tumor necrosis factor ligand superfamily: involvement in the pathology of malignant lymphomas". *Blood*, *85* (12). 3378-3404.
237. Gu, Y., Kuida, K., Tsutsui, H., Ku, G., Hsiao, K., Fleming, M.A., Hayashi, N., Higashino, K., Okamura, H., Nakanishi, K., Kurimoto, M., Tanimoto, T., Flavell, R.A., Sato, V., Harding, M.W., Livingston, D.J. and Su, M.S.S. 1997 "Activation of Interferon-gamma Inducing Factor Mediated by Interleukin-1beta Converting Enzyme". *Science*, *275* (5297). 206-209.
238. Gudjonsson, T., Rønnov Jessen, L., Villadsen, R., Rank, F., Bissell, M. and Petersen, O. 2002 "Normal and tumor-derived myoepithelial cells differ in

their ability to interact with luminal breast epithelial cells for polarity and basement membrane deposition". *J Cell Sci*, *115* (Pt 1). 39-50.

239. Gupta, K., Kshirsagar, S., Li, W., Gui, L., Ramakrishnan, S., Gupta, P., Law, P.Y. and Hebbel, R.P. 1999 "VEGF Prevents Apoptosis of Human Microvascular Endothelial Cells via Opposing Effects on MAPK/ERK and SAPK/JNK Signaling". *Exp Cell Res*, *247* (2). 495-504.
240. Haes, A.J., Giordano, B.C. and Collins, G.E. 2006 "Aptamer-Based Detection and Quantitative Analysis of Ricin Using Affinity Probe Capillary Electrophoresis". *Anal Chem*, *78* (11). 3758-3764.
241. Hain, J., Weller, E., Jung, T. and Burkart, W. 1996 "Effects of ionizing- and UV B-radiation on proteins controlling cell cycle progression in human cells: comparison of the MCF-7 adenocarcinoma and the SCL-2 squamous cell carcinoma cell line." *Int J Radiat Biol*, *70* (3). 261-271.
242. Hakem, R., Hakem, A., Duncan, G.S., Henderson, J.T., Woo, M., Soengas, M.S., Elia, A., de la Pompa, J.L., Kagi, D., Khoo, W., Potter, J., Yoshida, R., Kaufman, S.A., Lowe, S.W., Penninger, J.M. and Mak, T.W. 1998 "Differential Requirement for Caspase 9 in Apoptotic Pathways In Vivo". *Cell*, *94* (3). 339-352.
243. Hanaoka, H., Noda, T., Shirano, Y., Kato, T., Hayashi, H., Shibata, D., Tabata, S. and Ohsumi, Y. 2002 "Leaf Senescence and Starvation-Induced Chlorosis Are Accelerated by the Disruption of an Arabidopsis Autophagy Gene". *Plant Physiol*, *129* (3). 1181-1193.
244. Hanein, D., Matlack, K., Jungnickel, B., Plath, K., Kalies, K., Miller, K., Rapoport, T. and Akey, C. 1996 "Oligomeric rings of the Sec61p complex induced by ligands required for protein translocation". *Cell*, *87* (4). 721-732.
245. Hannahan, D. and Weinberg, R.A. 2000 "The Hallmarks of Cancer". *Cell*, *100* (1). 57-70.
246. Hardt, B., Kalz Fuller, B., Aparicio, R., Volker, C. and Bause, E. 2003 "(Arg)3 within the N-terminal domain of glucosidase I contains ER targeting information but is not required absolutely for ER localization". *Glycobiology*, *13* (3). 159-168.
247. Haren, L. and Merdes, A. 2002 "Direct binding of NuMA to tubulin is mediated by a novel sequence motif in the tail domain that bundles and stabilizes microtubules". *J Cell Sci*, *115* (9). 1815-1824.
248. Harris, A., Nicholson, S., Sainsbury, J., Farndon, J. and Wright, C. 1989 "Epidermal growth factor receptors in breast cancer: association with early relapse and death, poor response to hormones and interactions with neu". *J Steroid Biochem*, *34* (1-6). 123-131.
249. Harris, S.L. and Levine, A.J. 2005 "The p53 pathway: positive and negative feedback loops". *Oncogene*, *24* (17). 2899-2908.
250. Hartmann, E., Rapoport, T. and Lodish, H. 1989 "Predicting the orientation of eukaryotic membrane-spanning proteins". *Proc Natl Acad Sci U S A*, *15* (15). 5786-5790.

251. Hermann, G., King, E. and Shaw, J. 1997 "The yeast gene, MDM20, is necessary for mitochondrial inheritance and organization of the actin cytoskeleton". *J Cell Biol*, *137* (1). 141-153.
252. Hermann, G.J. and Shaw, J.M. 1998 "Mitochondrial dynamics in yeast". *Annu Rev Cell Dev Biol*, *14* (1). 265-303.
253. Higashimoto, Y., Saito, S.i., Tong, X.-H., Hong, A., Sakaguchi, K., Appella, E. and Anderson, C.W. 2000 "Human p53 Is Phosphorylated on Serines 6 and 9 in Response to DNA Damage-inducing Agents". *J Biol Chem*, *275* (30). 23199-23203.
254. Hinds, P., Finlay, C., Quartin, R., Baker, S., Fearon, E., Vogelstein, B. and Levine, A. 1990 "Mutant p53 DNA clones from human colon carcinomas cooperate with ras in transforming primary rat cells: a comparison of the "hot spot" mutant phenotypes". *Cell Growth Differ*, *1* (12). 571-580.
255. Hirao, A., Kong, Y.Y., Matsuoka, S., Wakeham, A., Ruland, J., Yoshida, H., Liu, D., Elledge, S.J. and Mak, T.W. 2000 "DNA Damage-Induced Activation of p53 by the Checkpoint Kinase Chk2". *Science*, *287* (5459). 1824-1827.
256. Hirokawa, N. 1982 "Cross-linker system between neurofilaments, microtubules, and membranous organelles in frog axons revealed by the quick-freeze, deep-etching method". *J Cell Biol*, *94* (1). 129-142.
257. Hollenbeck, P. and Saxton, W. 2005 "The axonal transport of mitochondria". *J Cell Sci*, *118* (Pt 23). 5411-5419.
258. Hollstein, M., Rice, K., Greenblatt, M., Soussi, T., Fuchs, R., Sørlie, T., Hovig, E., Smith-Sørensen, B., Montesano, R. and Harris, C. 1994 "Database of p53 gene somatic mutations in human tumors and cell lines". *Nucleic Acids Res*, *22* (17). 3551-3555.
259. Homann, M. and Goringer, H.U. 1999 "Combinatorial selection of high affinity RNA ligands to live African trypanosomes". *Nucl Acids Res*, *27* (9). 2006-2014.
260. Homburg, C.H., de Haas, M., von dem Borne, A.E., Verhoeven, A.J., Reutelingsperger, C.P. and Roos, D. 1995 "Human neutrophils lose their surface Fc gamma RIII and acquire Annexin V binding sites during apoptosis in vitro". *Blood*, *85* (2). 532-540.
261. Honda, R., Tanaka, H. and Yasuda, H. 1997 "Oncoprotein MDM2 is a ubiquitin ligase E3 for tumor suppressor p53". *FEBS Letters*, *420* (1). 25-27.
262. Hope, I.A. and Struhl, K. 1986 "Functional dissection of a eukaryotic transcriptional activator protein, GCN4 of Yeast". *Cell*, *46* (6). 885-894.
263. Hoppe Seyler, F., Crnkovic Mertens, Tomai, E. and Butz, K. 2004 "Peptide aptamers: specific inhibitors of protein function". *Curr Mol Med*, *4* (5). 529-538.
264. Horrobin, D.F. 1998 "The membrane phospholipid hypothesis as a biochemical basis for the neurodevelopmental concept of schizophrenia". *Schizophr Res*, *30* (3). 193-208.

265. Horton, P. and Nakai, K. 1997 "Better prediction of protein cellular localization sites with the k nearest neighbors classifier". *Proc Int Conf Intell Syst Mol Biol*, *5*. 147-152.
266. Horvitz, H.R. and Herskowitz, I. 1992 "Mechanisms of asymmetric cell division: Two Bs or not two Bs, that is the question". *Cell*, *68* (2). 237-255.
267. Hotchkiss, K.A., Matthias, L.J. and Hogg, P.J. 1998 "Exposure of the cryptic Arg-Gly-Asp sequence in thrombospondin-1 by protein disulfide isomerase". *Biochim Biophys Acta*, *1388* (2). 478-488.
268. Houston, S., Plunkett, T., Barnes, D., Smith, P., Rubens, R. and Miles, D. 1999 "Overexpression of c-erbB2 is an independent marker of resistance to endocrine therapy in advanced breast cancer". *Br J Cancer*, *79* (7-8). 1220-1226.
269. Howard, A.D., Kostura, M.J., Thornberry, N., Ding, G.J., Limjuco, G., Weidner, J., Salley, J.P., Hogquist, K.A., Chaplin, D.D. and Mumford, R.A. 1991 "IL-1-converting enzyme requires aspartic acid residues for processing of the IL-1 beta precursor at two distinct sites and does not cleave 31- kDa IL-1 alpha". *J Immunol*, *147* (9). 2964-2969.
270. Hrstka, R., Nenutil, R., Fourtouna, A., Howie, J., Naughton, C., Macleod, K., Larionov, A., Dixon, M., Langdon, S., Murray, E., Knoflickova, D., Petrakova, K., Holcakova, J., Hayward, R., Hupp, T.R. and Vojtesek, B. 2008 "Elevated Expression of AGR2 and AGR3 in Response to Tamoxifen Treatment in Breast Cancers". *In press*.
271. Hsu, Y.-T. and Youle, R.J. 1998 "Bax in Murine Thymus Is a Soluble Monomeric Protein That Displays Differential Detergent-induced Conformations". *J Biol Chem*, *273* (17). 10777-10783.
272. Hsu, Y.-T. and Youle, R.J. 1997 "Nonionic Detergents Induce Dimerization among Members of the Bcl-2 Family". *J Biol Chem*, *272* (21). 13829-13834.
273. Huber, M., Bahr, I., Kratzschmar, J.R., Becker, A., Muller, E.C., Donner, P., Pohlenz, H.D., Schneider, M.R. and Sommer, A. 2004 "Comparison of proteomic and genomic analyses of the human breast cancer cell line T47D and the antiestrogen-resistant derivative T47D-r". *Mol Cell Proteomics*, *3* (1). 43-55.
274. Hulo, N., Bairoch, A., Bulliard, V., Cerutti, L., De Castro, E., Langendijk-Genevaux, P.S., Pagni, M. and Sigrist, C.J.A. 2006 "The PROSITE database". *Nucleic Acids Res*, *34* (suppl.1). 227-230.
275. Hupp, T., Meek, D., Midgley, C. and Lane, D. 1992 "Regulation of the specific DNA binding function of p53". *Cell*, *71* (5). 875-886.
276. Hupp, T.R. and Lane, D.P. 1994 "Allosteric activation of latent p53 tetramers". *Current Biology*, *4* (10). 865-875.
277. Hurd, C., Khattree, N., Dinda, S., Alban, P. and Moudgil, V. 1997 "Regulation of tumor suppressor proteins, p53 and retinoblastoma, by estrogen and antiestrogens in breast cancer cells". *Oncogene*, *15* (8). 991-995.
278. Hwang, H. and Clurman, B. 2005 "Cyclin E in normal and neoplastic cell cycles". *Oncogene*, *24* (17). 2776-2786.

279. Ichikawa, A., Ando, J. and Suda, K. 2008 "G1 arrest and expression of cyclin-dependent kinase inhibitors in tamoxifen-treated MCF-7 human breast cancer cells". *Hum Cell*, *21* (2). 28-37.
280. Ignatiadis, M. and Sotiriou, C. 2008 "Understanding the Molecular Basis of Histologic Grade". *Pathobiology*, *75* (2). 104-111.
281. Ikura, T., Ogryzko, V.V., Grigoriev, M., Groisman, R., Wang, J., Horikoshi, M., Scully, R., Qin, J. and Nakatani, Y. 2000 "Involvement of the TIP60 Histone Acetylase Complex in DNA Repair and Apoptosis". *Cell*, *102* (4). 463-473.
282. Innes, H.E., Liu, D., Barraclough, R., Davies, M.P., O'Neill, P.A., Platt-Higgins, A., de Silva Rudland, S., Sibson, D.R. and Rudland, P.S. 2006 "Significance of the metastasis-inducing protein AGR2 for outcome in hormonally treated breast cancer patients". *Br J Cancer*, *94* (7). 1057 - 1065.
283. Ireson, C. and Kelland, L. 2006 "Discovery and development of anticancer aptamers". *Mol Cancer Ther*, *5* (12). 2957-2962.
284. Ito, T., Chiba, T., Ozawa, R., Yoshida, M., Hattori, M. and Sakaki, Y. 2001 "A comprehensive two-hybrid analysis to explore the yeast protein interactome". *Proc Natl Acad Sci U S A*, *98* (8). 4569-4574.
285. Itoh, N. and Nagata, S. 1993 "A novel protein domain required for apoptosis. Mutational analysis of human Fas antigen". *J Biol Chem.*, *268* (15). 10932-10937.
286. Jackson, S.E., Craggs, T.D. and Huang, J.-r. 2006 "Understanding the folding of GFP using biophysical techniques". *Expert Rev Proteomics*, *3* (5). 545-559.
287. Jackson, T.A., Richer, J.K., Bain, D.L., Takimoto, G., S. , Tung, L. and Horwitz, K.B. 1997 "The Partial Agonist Activity of Antagonist-Occupied Steroid Receptors Is Controlled by a Novel Hinge Domain-Binding Coactivator L7/SPA and the Corepressors N-CoR or SMRT". *Mol Endocrinol*, *11* (6). 693-705.
288. Janicke, R.U., Ng, P., Sprengart, M.L. and Porter, A.G. 1998 "Caspase-3 Is Required for alpha -Fodrin Cleavage but Dispensable for Cleavage of Other Death Substrates in Apoptosis". *J Biol Chem*, *273* (25). 15540-15545.
289. Janicke, R.U., Sprengart, M.L., Wati, M.R. and Porter, A.G. 1998 "Caspase-3 Is Required for DNA Fragmentation and Morphological Changes Associated with Apoptosis". *J Biol Chem*, *273* (16). 9357-9360.
290. Jay, G., Khoury, G., DeLeo, A.B., Dippold, W.G. and Old, L.J. 1981 "p53 transformation-related protein: detection of an associated phosphotransferase activity". *Proc Natl Acad Sci U S A*, *78* (5). 2932-2936.
291. Jeong, S. and Seol, D. 2008 "The role of mitochondria in apoptosis". *BMB Rep*, *41* (1). 11-22.
292. Jeong, W., Lee, D.Y., Park, S. and Rhee, S.G. 2008 "ERp16, an Endoplasmic Reticulum-resident Thiol-disulfide Oxidoreductase:Biochemical properties abd role in apoptosis induced by Endoplasmic reticulum stress ". *J Biol Chem*, *283* (37). 25557-25566.

293. Jiang, G. and Sancar, A. 2006 "Recruitment of DNA Damage Checkpoint Proteins to Damage in Transcribed and Nontranscribed Sequences". *Mol Cell Biol*, *26* (1). 39-49.
294. Jin, J., Cai, Y., Yao, T., Gottschalk, A.J., Florens, L., Swanson, S.K., Gutierrez, J.L., Coleman, M.K., Workman, J.L., Mushegian, A., Washburn, M.P., Conaway, R.C. and Conaway, J.W. 2005 "A Mammalian Chromatin Remodeling Complex with Similarities to the Yeast INO80 Complex". *J Biol Chem*, *280* (50). 41207-41212.
295. Johnson, N., Speirs, V., Curtin, N. and Hall, A. 2008 "A comparative study of genome-wide SNP, CGH microarray and protein expression analysis to explore genotypic and phenotypic mechanisms of acquired antiestrogen resistance in breast cancer". *Breast Cancer Res Treat*, *111* (1). 55-63.
296. Jones, S.N., Roe, A.E., Donehower, L.A. and Bradley, A. 1995 "Rescue of embryonic lethality in Mdm2-deficient mice by absence of p53". *Nature*, *378* (6553). 206-208.
297. Jordan, V. 1982 "Metabolites of tamoxifen in animals and man: identification, pharmacology and significance". *Breast Cancer Res Treat*, *2* (2). 123-138.
298. Jordan, V., Collins, M., Rowsby, L. and Prestwich, G. 1977 "A monohydroxylated metabolite of tamoxifen with potent antioestrogenic activity." *J Endocrinol.*, *75* (2). 305-316.
299. Joyeux, A., Cavailles, V., Balaguer, P. and Nicolas, J.C. 1997 "RIP 140 Enhances Nuclear Receptor-Dependent Transcription in Vivo in Yeast". *Mol Endocrinol*, *11* (2). 193-202.
300. Kabeya, Y., Mizushima, N., Ueno, T., Yamamoto, A., Kirisako, T., Noda, T., Kominami, E., Ohsumi, Y. and Yoshimori, T. 2000 "LC3, a mammalian homologue of yeast Apg8p, is localized in autophagosome membranes after processing". *Embo J*, *19* (21). 5720-5728.
301. Kahana, J. and Silver, P. 2001 "Use of the A. victoria green fluorescent protein to study protein dynamics in vivo". *Curr Protoc Neurosci*, *5* (5). 15.
302. Kanemaki, M., Makino, Y., Yoshida, T., Kishimoto, T., Koga, A., Yamamoto, K., Yamamoto, M., Moncollin, V., Egly, J.-M., Muramatsu, M. and Tamura, T.-a. 1997 "Molecular Cloning of a Rat 49-kDa TBP-Interacting Protein (TIP49) That Is Highly Homologous to the Bacterial RuvB". *Biochem Biophys Res Commun*, *235* (1). 64-68.
303. Kastan, M., Onyekwere, O., Sidransky, D., Vogelstein, B. and Craig, R. 1991 "Participation of p53 protein in the cellular response to DNA damage". *Cancer Res*, *51* (23 Pt 1). 6304-6311.
304. Kawashima, S., Ogiwara, H., Tada, S., Harata, M., Wintersberger, U., Enomoto, T. and Seki, M. 2007 "The INO80 complex is required for damage-induced recombination". *Biochem Biophys Res Commun*, *355* (3). 835-841.
305. Kawazoe, N., Ito, Y. and Imanishi, Y. 1997 "Bioassay Using a Labeled Oligonucleotide Obtained by in Vitro Selection". *Biotechnol Prog*, *13* (6). 873-874.

306. Kelekar, A. and Thompson, C.B. 1998 "Bcl-2-family proteins: the role of the BH3 domain in apoptosis". *Trends Cell Biol*, *8* (8). 324-330.
307. Kellen, E., Vansant, G., Christiaens, M., Neven, P. and Van Limbergen, E. 2008 "Lifestyle changes and breast cancer prognosis: a review". *Breast Cancer Res Treat*, *Epub ahead of print*.
308. Kern, S., Kinzler, K., Bruskin, A., Jarosz, D., Friedman, P., Prives, C. and Vogelstein, B. 1991 " Identification of p53 as a sequence-specific DNA-binding protein". *Science*, *252* (5013). 1708-1711.
309. Kerr JF, W.A., Currie AR 1972 "Apoptosis: a basic biological phenomenon with wide-ranging implications in tissue kinetics." *Br J Cancer*, *26* (4). 239-257.
310. Kim, H., Rafiuddin-Shah, M., Tu, H.-C., Jeffers, J.R., Zambetti, G.P., Hsieh, J.J.D. and Cheng, E.H.Y. 2006 "Hierarchical regulation of mitochondrion-dependent apoptosis by BCL-2 subfamilies". *Nat Cell Biol*, *8* (12). 1348-1358.
311. Kim, H.Y. and Gladyshev, V.N. 2004 "Methionine Sulfoxide Reduction in Mammals: Characterization of Methionine-R-Sulfoxide Reductases". *Mol Biol Cell*, *15* (3). 1055-1064.
312. Kim, J., Huang, W.-P., Stromhaug, P.E. and Klionsky, D.J. 2002 "Convergence of Multiple Autophagy and Cytoplasm to Vacuole Targeting Components to a Perivacuolar Membrane Compartment Prior to de Novo Vesicle Formation". *J Biol Chem*, *277* (1). 763-773.
313. Kim, J.H., Choi, H.J., Kim, B., Kim, M.H., Lee, J.M., Kim, I.S., Lee, M.H., Choi, S.J., Kim, K.I., Kim, S.I., Chung, C.H. and Baek, S.H. 2006 "Roles of sumoylation of a reptin chromatin-remodelling complex in cancer metastasis". *Nat Cell Biol*, *8* (6). 631-639.
314. Kimura, T., Horibe, T., Sakamoto, C., Shitara, Y., Fujiwara, F., Komiya, T., Yamamoto, A., Hayano, T., Takahashi, N. and Kikuchi, M. 2008 "Evidence for Mitochondrial Localization of P5, a Member of the Protein Disulphide Isomerase Family". *J Biochem*, *144* (2). 187-196.
315. Klein, C. and Vassilev, L. 2004 "Targeting the p53-MDM2 interaction to treat cancer". *Br J Cancer*, *91* (8). 1415-1419.
316. Klionsky, D.J., Cregg, J.M., Dunn, W.A., Emr, S.D., Sakai, Y., Sandoval, I.V., Sibirny, A., Subramani, S., Thumm, M., Veenhuis, M. and Ohsumi, Y. 2003 "A Unified Nomenclature for Yeast Autophagy-Related Genes". *Dev Cell*, *5* (4). 539-545.
317. Koizumi, M. and Breaker, R.R. 2000 "Molecular Recognition of cAMP by an RNA Aptamer". *Biochemistry*, *39* (30). 8983-8992.
318. Komiya, T., Tanigawa, Y. and Hirohashi, S. 1999 "Cloning of the gene gob-4, which is expressed in intestinal goblet cells in mice". *Biochim Biophys Acta*, *1444* (3). 434-438.
319. Konishi, N., Shimada, K., Ishida, E. and Nakamura, M. 2005 "Molecular pathology of prostate cancer". *Pathol Int*, *55* (9). 531-539.
320. Kosta, A., Roisin-Bouffay, C., Luciani, M.-F., Otto, G.P., Kessin, R.H. and Golstein, P. 2004 "Autophagy Gene Disruption Reveals a Non-vacuolar Cell Death Pathway in Dictyostelium". *J Biol Chem*, *279* (46). 48404-48409.

321. Kothakota, S., Azuma, T., Reinhard, C., Klippel, A., Tang, J., Chu, K., McGarry, T.J., Kirschner, M.W., Koths, K., Kwiatkowski, D.J. and Williams, L.T. 1997 "Caspase-3-Generated Fragment of Gelsolin: Effector of Morphological Change in Apoptosis". *Science*, *278* (5336). 294-298.
322. Koya, R., Fujita, H., Shimizu, S., Ohtsu, M., Takimoto, M., Tsujimoto, Y. and Kuzumaki, N. 2000 "Gelsolin inhibits apoptosis by blocking mitochondrial membrane potential loss and cytochrome c release". *J Biol Chem*, *275* (20). 15343-15349.
323. Kozutsumi, Y., Segal, M., Normington, K., Gething, M.-J. and Sambrook, J. 1988 "The presence of malfolded proteins in the endoplasmic reticulum signals the induction of glucose-regulated proteins". *Nature*, *332* (6163). 462-464.
324. Kraiss, S., Quaiser, A., Oren, M. and Montenarh, M. 1988 "Oligomerization of oncoprotein p53". *J Virol*, *62* (12). 4737-4744.
325. Kroemer G, Z.N., Susin SA. 1997 "Mitochondrial control of apoptosis." *Immunol Today*, *18* (1). 44-51.
326. Krysko, D.V., Denecker, G., Festjens, N., Gabriels, S., Parthoens, E., D'Herde, K. and Vandenabeele, P. 2006 "Macrophages use different internalization mechanisms to clear apoptotic and necrotic cells". *Cell Death Differ*, *13* (12). 2011-2022.
327. Krysko, D.V., Vanden Berghe, T., D'Herde, K. and Vandenabeele, P. 2008 "Apoptosis and necrosis: Detection, discrimination and phagocytosis". *Methods*, *44* (3). 205-221.
328. Kubbutat, M.H.G., Jones, S.N. and Vousden, K.H. 1997 "Regulation of p53 stability by Mdm2". *Nature*, *387* (6630). 299-303.
329. Kubik, M.F., Bell, C., Fitzwater, T., Watson, S.R. and Tasset, D.M. 1997 "Isolation and characterization of 2'-fluoro-, 2'-amino-, and 2'-fluoro- /amino-modified RNA ligands to human IFN-gamma that inhibit receptor binding". *J Immunol*, *159* (1). 259-267.
330. Kuida, K., Zheng, T.S., Na, S., Kuan, C.-Y., Yang, D., Karasuyama, H., Rakic, P. and Flavell, R.A. 1996 "Decreased apoptosis in the brain and premature lethality in CPP32-deficient mice". *Nature*, *384* (6607). 368-372.
331. Kumar, A., Godwin, J.W., Gates, P.B., Garza-Garcia, A.A. and Brockes, J.P. 2007 "Molecular Basis for the Nerve Dependence of Limb Regeneration in an Adult Vertebrate". *Science* (5). 772-777.
332. Kumar, M.B., Tarpey, R.W. and Perdew, G.H. 1999 "Differential Recruitment of Coactivator RIP140 by Ah and Estrogen Receptors.Absense of a role for LXXLL motifs". *J Biol Chem*, *274* (32). 22155-22164.
333. Kundu, M. and Thompson, C.B. 2005 "Macroautophagy versus mitochondrial autophagy: a question of fate?" *Cell Death Differ*, *12* (S2). 1484-1489.
334. Kuperwasser, C., Pinkas, J., Hurlbut, G.D., Naber, S.P. and Jerry, D.J. 2000 "Cytoplasmic Sequestration and Functional Repression of p53 in the Mammary Epithelium Is Reversed by Hormonal Treatment". *Cancer Res*, *60* (10). 2723-2729.

335. Kurokawa, H., Lenferink, A., Simpson, J., Pisacane, P., Sliwkowski, M., Forbes, J. and Arteaga, C. 2000 "Inhibition of HER2/neu (erbB-2) and mitogen-activated protein kinases enhances tamoxifen action against HER2-overexpressing, tamoxifen-resistant breast cancer cells". *Cancer Res*, *60* (20). 5887-5894.
336. Kussie, P.H., Gorina, S., Marechal, V., Elenbaas, B., Moreau, J., Levine, A.J. and Pavletich, N.P. 1996 "Structure of the MDM2 Oncoprotein Bound to the p53 Tumor Suppressor Transactivation Domain". *Science*, *274* (5289). 948-953.
337. Kuwana, T., Bouchier-Hayes, L., Chipuk, J.E., Bonzon, C., Sullivan, B.A., Green, D.R. and Newmeyer, D.D. 2005 "BH3 Domains of BH3-Only Proteins Differentially Regulate Bax-Mediated Mitochondrial Membrane Permeabilization Both Directly and Indirectly". *Mol Cell*, *17* (4). 525-535.
338. Lahav, G., Rosenfeld, N., Sigal, A., Geva-Zatorsky, N., Levine, A.J., Elowitz, M.B. and Alon, U. 2004 "Dynamics of the p53-Mdm2 feedback loop in individual cells". *Nat Genet*, *36* (2). 147-150.
339. Laín, S., Midgley, C., Sparks, A., Lane, E.B. and Lane, D.P. 1999 "An Inhibitor of Nuclear Export Activates the p53 Response and Induces the Localization of HDM2 and p53 to U1A-Positive Nuclear Bodies Associated with the PODs". *Exp Cell Res*, *248* (2). 457-472.
340. Lam, S. and Gong, Z. 2006 "Modeling liver cancer using zebrafish: a comparative oncogenomics approach". *Cell Cycle*, *5* (6). 573-577.
341. Lamparska Przybysz, M., Gajkowska, B. and Motyl, T. 2005 "Cathepsins and BID are involved in the molecular switch between apoptosis and autophagy in breast cancer MCF-7 cells exposed to camptothecin". *J Physiol Pharmacol*, *56* (3). 159-179.
342. Lamprakos, P. (ed.), *Helios Greek Encyclopaedia*. Athens Press, 1998.
343. Land, H., Parada, L. and Weinberg, R. 1983 "Tumorigenic conversion of primary embryo fibroblasts requires at least two cooperating oncogenes". *Nature*, *304* (5927). 596-602.
344. Langheinrich, U. 2003 "Zebrafish: a new model on the pharmaceutical catwalk". *Bioessays*, *25* (9). 904-912.
345. Langheinrich, U., Hennen, E., Stott, G. and Vacun, G. 2002 "Zebrafish as a model organism for the identification and characterization of drugs and genes affecting p53 signaling". *Curr Biol*, *10* (23). 2023-2028.
346. Lavieu, G., Scarlatti, F., Sala, G., Carpentier, S., Levade, T., Ghidoni, R., Botti, J. and Codogno, P. 2006 "Regulation of Autophagy by Sphingosine Kinase 1 and Its Role in Cell Survival during Nutrient Starvation". *J Biol Chem*, *281* (13). 8518-8527.
347. Lee, C.-H., Chinpaisal, C. and Wei, L.-N. 1998 "Cloning and Characterization of Mouse RIP140, a Corepressor for Nuclear Orphan Receptor TR2". *Mol Cell Biol*, *18* (11). 6745-6755.
348. Lee, C.Y. and Baehrecke, E.H. 2001 "Steroid regulation of autophagic programmed cell death during development". *Development 128* (8). 1443-1455.

349. Leist, M., Single, B., Castoldi, A.F., Kuhnle, S. and Nicotera, P. 1997 "Intracellular Adenosine Triphosphate (ATP) Concentration: A Switch in the Decision Between Apoptosis and Necrosis". *J Exp Med*, *185* (8). 1481-1486.
350. Lemasters, J.J., Nieminen, A.-L., Qian, T., Trost, L.C., Elmore, S.P., Nishimura, Y., Crowe, R.A., Cascio, W.E., Bradham, C.A., Brenner, D.A. and Herman, B. 1998 "The mitochondrial permeability transition in cell death: a common mechanism in necrosis, apoptosis and autophagy". *Biochim Biophys Acta*, *1366* (1-2). 177-196.
351. Lewandowski, S.A., Thiery, J., Jalil, A., Leclercq, G., Szczylik, C. and Chouaib, S. 2005 "Opposite effects of estrogen receptors alpha and beta on MCF-7 sensitivity to the cytotoxic action of TNF and p53 activity". *Oncogene*, *24* (30). 4789.
352. Lewis, J., Vijayanathan, V., Thomas, T., Pestell, R., Albanese, C., Gallo, M. and Thomas, T. 2005 " Activation of cyclin D1 by estradiol and spermine in MCF-7 breast cancer cells: a mechanism involving the p38 MAP kinase and phosphorylation of ATF-2". *Oncol Res*, *15* (3). 113-128.
353. Lewis, M. and Pelham, H. 1992 "Ligand-induced redistribution of a human KDEL receptor from the Golgi complex to the endoplasmic reticulum". *Cell*, *68* (2). 353-364.
354. Lewis, M.J., Mazzarella, R.A. and Green, M. 1986 "Structure and assembly of the endoplasmic reticulum: biosynthesis and intracellular sorting of ERp61, ERp59, and ERp49, three protein components of murine endoplasmic reticulum". *Arch Biochem Biophys*, *245* (2). 389-403.
355. Lewis, M.J., Sweet, D.J. and Pelham, H.R.B. 1990 "The ERD2 gene determines the specificity of the luminal ER protein retention system". *Cell*, *61* (7). 1359-1363.
356. Li, P., Nijhawan, D., Budihardjo, I., Srinivasula, S.M., Ahmad, M., Alnemri, E.S. and Wang, X. 1997 "Cytochrome c and dATP-Dependent Formation of Apaf-1/Caspase-9 Complex Initiates an Apoptotic Protease Cascade". *Cell*, *91* (4). 479-489.
357. Li, W.W., Alexandre, S., Cao, X. and Lee, A.S. 1993 "Transactivation of the grp78 promoter by Ca2+ depletion. A comparative analysis with A23187 and the endoplasmic reticulum Ca(2+)-ATPase inhibitor thapsigargin". *J Biol Chem*, *268* (16). 12003-12009.
358. Liang, S.H. and Clarke, M.F. 1999 "A Bipartite Nuclear Localization Signal Is Required for p53 Nuclear Import Regulated by a Carboxyl-terminal Domain". *J Biol Chem*, *274* (46). 32699-32703.
359. Liang, X.H., Jackson, S., Seaman, M., Brown, K., Kempkes, B., Hibshoosh, H. and Levine, B. 1999 "Induction of autophagy and inhibition of tumorigenesis by beclin 1". *Nature*, *402* (6762). 672-676.
360. Liang, X.H., Kleeman, L.K., Jiang, H.H., Gordon, G., Goldman, J.E., Berry, G., Herman, B. and Levine, B. 1998 "Protection against Fatal Sindbis Virus Encephalitis by Beclin, a Novel Bcl-2-Interacting Protein". *J Virol*, *72* (11). 8586-8596.

361. Lin, J., Chen, J., Elenbaas, B. and Levine, A.J. 1994 "Several hydrophobic amino acids in the p53 amino-terminal domain are required for transcriptional activation, binding to mdm-2 and the adenovirus 5 E1B 55-kD protein". *Genes Dev*, *8* (10). 1235-1246.
362. Lin, Y.C., Lin, J.H., Chou, C.W., Chang, Y.F., Yeh, S.H. and Chen, C.C. 2008 "Statins Increase p21 through Inhibition of Histone Deacetylase Activity and Release of Promoter-Associated HDAC1/2". *Cancer Res*, *68* (7). 2375-2383.
363. Lindén, M., Li, Z., Paulin, D., Gotow, T. and Leterrier, J. 2001 " Effects of desmin gene knockout on mice heart mitochondria". *J Bioenerg Biomembr*, *33* (4). 333-341.
364. Liu, D., Rudland, P., Sibson, D., Platt Higgins, A. and Barraclough, R. 2005 "Human homologue of cement gland protein, a novel metastasis inducer associated with breast carcinomas". *Cancer Res*, *65* (9). 3796-3805.
365. Liu, E.S., Ou, J.H. and Lee, A.S. 1992 "Brefeldin A as a regulator of grp78 gene expression in mammalian cells". *J Biol Chem*, *267* (10). 7128-7133.
366. Liu, X., Kim, C.N., Yang, J., Jemmerson, R. and Wang, X. 1996 "Induction of Apoptotic Program in Cell-Free Extracts: Requirement for dATP and Cytochrome c". *Cell*, *86* (1). 147-157.
367. Lockshin, R. and Zakeri, Z. 2004 "Apoptosis, autophagy, and more". *Int J Biochem Cell Biol*, *36* (12).
368. Lombardi, M., Castoria, G., Migliaccio, A., Barone, M.V., Di Stasio, R., Ciociola, A., Bottero, D., Yamaguchi, H., Appella, E. and Auricchio, F. 2008 "Hormone-dependent nuclear export of estradiol receptor and DNA synthesis in breast cancer cells". *J Cell Biol*, *182* (2). 327-340.
369. Lønning, P. 2007 "Breast cancer prognostication and prediction: are we making progress?" *Ann Oncol*, *18* (8). 3-7.
370. Lyons, S.K. and Clarke, A.R. 1997 "Apoptosis and carcinogenesis". *Br Med Bull*, *53* (3). 554-569.
371. Maberley, D. 2005 "Pegaptanib for neovascular age-related macular degeneration". *Issues Emerg Health Technol* (76). 1-4.
372. MacFarlane, M., Ahmad, M., Srinivasula, S.M., Fernandes-Alnemri, T., Cohen, G.M. and Alnemri, E.S. 1997 "Identification and Molecular Cloning of Two Novel Receptors for the Cytotoxic Ligand TRAIL". *J Biol Chem.*, *272* (41). 25417-25420.
373. MacFarlane, M., Merrison, W., Dinsdale, D. and Cohen, G.M. 2000 "Active Caspases and Cleaved Cytokeratins Are Sequestered into Cytoplasmic Inclusions in TRAIL-induced Apoptosis". *J Cell Biol*, *148* (6). 1239-1254.
374. Mackay, A., Urruticoechea, A., Dixon, J.M., Dexter, T., Fenwick, K., Ashworth, A., Drury, S., Larionov, A., Young, O., White, S., Miller, W., Evans, D. and Dowsett, M. 2007 "Molecular response to aromatase inhibitor treatment in primary breast cancer". *Breast Cancer Res*, *9* (3). R37.
375. Mairal, T., Cengiz Özalp, V., Lozano Sánchez, P., Mir, M., Katakis, I. and O'Sullivan, C. 2008 "Aptamers: molecular tools for analytical applications". *Anal Bioanal Chem*, *390* (4). 989-1007.

376. Majerfeld, I. and Yarus, M. 1994 "An RNA pocket for an aliphatic hydrophobe". *Nat Struct Biol*, *1* (5). 287-292.
377. Majno, G. and Joris, I. 1995 "Apoptosis, oncosis, and necrosis. An overview of cell death." *Am J Pathol*, *146* (1). 3-15.
378. Malayeri, R., Pirker, R. and Huber, H. 2001 "New drugs in the palliative chemotherapy of advanced non-small-cell lung cancer". *Onkologie*, *24* (5). 416-421.
379. Malkin, D., Li, F.P., Strong, L.C., Fraumeni, J.F., Jr., Nelson, C.E., Kim, D.H., Kassel, J., Gryka, M.A., Bischoff, F.Z., Tainsky, M.A. and et al. 1990 "Germ line p53 mutations in a familial syndrome of breast cancer, sarcomas, and other neoplasms". *Science*, *250* (4985). 1233-1238.
380. Maltzman, W. and Czyzy, L. 1984 "UV irradiation stimulates levels of p53 cellular tumor antigen in nontransformed mouse cells." *Mol Cell Biol*, *4* (9). 1689–1694.
381. Mann, D., Reinemann, C., Stoltenburg, R. and Strehlitz, B. 2005 "In vitro selection of DNA aptamers binding ethanolamine". *Biochem Biophys Res Commun*, *338* (4). 1928-1934.
382. Marchant, J., Stutzmann, G., Leissring, M., LaFerla, F. and Parker, I. 2001 "Multiphoton-evoked color change of DsRed as an optical highlighter for cellular and subcellular labeling". *Nat Biotechnol*, *19* (7). 645-649.
383. Marchenko, N., Zaika, A. and Moll, U. 2000 "Death signal-induced localization of p53 protein to mitochondria. A potential role in apoptotic signaling". *J Biol Chem*, *275* (21). 16202-16212.
384. Marchetti, P., Castedo, M., Susin, S., Zamzami, N., Hirsch, T., Macho, A., Haeffner, A., Hirsch, F., Geuskens, M. and Kroemer, G. 1996 "Mitochondrial permeability transition is a central coordinating event of apoptosis". *J Exp Med*, *184* (3). 1155-1160.
385. Mariathasan, S., Newton, K., Monack, D.M., Vucic, D., French, D.M., Lee, W.P., Roose-Girma, M., Erickson, S. and Dixit, V.M. 2004 "Differential activation of the inflammasome by caspase-1 adaptors ASC and Ipaf". *Nature*, *430* (6996). 213-218.
386. Martin, S.A.M., Blaney, S.C., Houlihan, D.F. and Secombes, C.J. 2006 "Transcriptome response following administration of a live bacterial vaccine in Atlantic salmon (Salmo salar)". *Mol Immunol*, *43* (11). 1900-1911.
387. Martinez, J., Georgoff, I., Martinez, J. and Levine, A.J. 1991 "Cellular localization and cell cycle regulation by a temperature-sensitive p53 protein". *Genes Dev*, *5* (2). 151-159.
388. Marzo I. , Brenner, C., Zamzami, N., Jürgensmeier, J.M., Susin, S.A., Vieira, H.L.A., Prévost, M.-C., Xie, Z., Matsuyama, S., Reed, J.C. and Kroemer, G. 1998 "Bax and Adenine Nucleotide Translocator Cooperate in the Mitochondrial Control of Apoptosis". *Science*, *281* (5385). 2027-2031.
389. Massarweh, S. and Schiff, R. 2006 "Resistance to endocrine therapy in breast cancer: exploiting estrogen receptor/growth factor signaling crosstalk". *Endocr Relat Cancer*, *13* (1). S15-24.

390. Matsuura-Tokita, K., Takeuchi, M., Ichihara, A., Mikuriya, K. and Nakano, A. 2006 "Live imaging of yeast Golgi cisternal maturation". *Nature*, *441* (7096). 1007.
391. Matz, M.V., Fradkov, A.F., Labas, Y.A., Savitsky, A.P., Zaraisky, A.G., Markelov, M.L. and Lukyanov, S.A. 1999 "Fluorescent proteins from nonbioluminescent Anthozoa species". *Nat Biotech*, *17* (10). 969-973.
392. May, P. and May, E. 1999 "Twenty years of p53 research: structural and functional aspects of the p53 protein". *Oncogene*, *18* (53). 7621-7636.
393. Mayo, L.D., Dixon, J.E., Durden, D.L., Tonks, N.K. and Donner, D.B. 2002 "PTEN Protects p53 from Mdm2 and Sensitizes Cancer Cells to Chemotherapy". *J Biol Chem*, *277* (7). 5484-5489.
394. McConnell, S., Stewart, L., Talin, A. and Yaffe, M. 1990 "Temperature-sensitive yeast mutants defective in mitochondrial inheritance". *J Cell Biol*, *111* (3). 967-976.
395. McMillan, D.R., Gething, M.-J. and Sambrook, J. 1994 "The cellular response to unfolded proteins: intercompartmental signaling". *Curr Opin Biotechnol*, *5* (5). 540-545.
396. Medina, D., Kittrell, F., Shepard, A., Contreras, A., Rosen, J. and Lydon, J. 2003 "Hormone dependence in premalignant mammary progression". *Cancer Res*, *63* (5). 1067-1072.
397. Meijer, A.H., Verbeek, F.J., Salas-Vidal, E., Corredor-Adámez, M., Bussman, J., van der Sar, A.M., Otto, G.W., Geisler, R. and Spaink, H.P. 2005 "Transcriptome profiling of adult zebrafish at the late stage of chronic tuberculosis due to Mycobacterium marinum infection". *Mol Immunol*, *42* (10). 1185-1203.
398. Menssen, A. and Hermeking, H. 2002 "From the Cover: Characterization of the c-MYC-regulated transcriptome by SAGE: Identification and analysis of c-MYC target genes". *Proc Natl Acad Sci U S A*, *99* (9). 6274-6279.
399. Mevorach, D., Mascarenhas, J.O., Gershov, D. and Elkon, K.B. 1998 "Complement-dependent Clearance of Apoptotic Cells by Human Macrophages". *J Exp Med*, *188* (12). 2313-2320.
400. Middeler, G., Zerf, K., Jenovai, S., Thulig, A., Tschödrich Rotter, M., Kubitscheck, U. and Peters, R. 1997 "The tumor suppressor p53 is subject to both nuclear import and export, and both are fast, energy-dependent and lectin-inhibited". *Oncogene*, *14* (12). 1407-1417.
401. Mihara, M., Erster, S., Zaika, A., Petrenko, O., Chittenden, T., Pancoska, P. and Moll, U. 2003 " p53 has a direct apoptogenic role at the mitochondria". *Mol Cell*, *11* (3). 577-590.
402. Milner, D., Mavroidis, M., Weisleder, N. and Capetanaki, Y. 2000 "Desmin cytoskeleton linked to muscle mitochondrial distribution and respiratory function". *J Cell Biol*, *150* (6). 1283-1298.
403. Missiaglia, E., Blaveri, E., Terris, B., Wang, Y., Costello, E., Neoptolemos, J., Crnogorac, J.T. and Lemoine, N. 2004 "Analysis of gene expression in cancer cell lines identifies candidate markers for pancreatic tumorigenesis and metastasis". *Int J Cancer*, *112* (1). 100-112.

404. Miura, M., Zhu, H., Rotello, R., Hartwieg, E.A. and Yuan, J. 1993 "Induction of apoptosis in fibroblasts by IL-1[beta]-converting enzyme, a mammalian homolog of the C. elegans cell death gene ced-3". *Cell*, *75* (4). 653-660.
405. Miyawaki, A., Nagai, T. and Mizuno, H. 2005 "Engineering fluorescent proteins". *Adv Biochem Eng Biotechnol*, *8* (95). 1-15.
406. Mizuno, H., Sawano, A., Eli, P., Hama, H. and Miyawaki, A. 2001 "Red Fluorescent Protein from Discosoma as a Fusion Tag and a Partner for Fluorescence Resonance Energy Transfer". *Biochemistry*, *40* (8). 2502-2510.
407. Mochizuki, N., Cho, G., Wen, B. and Insel, P.A. 1996 "Identification and cDNA cloning of a novel human mosaic protein, LGN, based on interaction with G alpha i2". *Gene*, *181* (1-2). 39-43.
408. Molinari, A., Bontempo, P., Schiavone, E., Verdicchio, M., Napolitano, M., Nola, E., Moncharmont, B., Medici, N., Nigro, V., Armetta, I., Abbondanza, C. and Puca, G. 2000 "Estradiol induces functional inactivation of p53 by intracellular redistribution". *Cancer Res*, *60* (10). 2594-2597.
409. Moll, U., Marchenko, N. and Zhang, X. 2006 "p53 and Nur77/TR3 - transcription factors that directly target mitochondria for cell death induction". *Oncogene*, *25* (34). 4725-4743.
410. Moll, U.M., LaQuaglia, M., Bénard, J. and Riou, G. 1995 "Wild-type p53 protein undergoes cytoplasmic sequestration in undifferentiated neuroblastomas but not in differentiated tumors". *PNAS*, *92* (10). 4407-4411.
411. Moll, U.M., Ostermeyer, A.G., Haladay, R., Winkfield, B., Frazier, M. and Zambetti, G. 1996 "Cytoplasmic sequestration of wild-type p53 protein impairs the G1 checkpoint after DNA damage". *Mol Cell Biol*, *16* (3). 1126-1137.
412. Moll, U.M., Riou, G. and Levine, A.J. 1992 "Two distinct mechanisms alter p53 in breast cancer: mutation and nuclear exclusion". *PNAS*, *89* (15). 7262-7266.
413. Momand, J., Zambetti, G.P., Olson, D.C., George, D. and Levine, A.J. 1992 "The mdm-2 oncogene product forms a complex with the p53 protein and inhibits p53-mediated transactivation". *Cell*, *69* (7). 1237-1245.
414. Montes de Oca Luna, R., Wagner, D. and Lozano, G. 1995 "Rescue of early embryonic lethality in mdm2-deficient mice by deletion of p53". *Nature*, *378* (6553). 203-206.
415. Morais da Silva, S., Gates, P.B. and Brockes, J.P. 2002 "The Newt Ortholog of CD59 Is Implicated in Proximodistal Identity during Amphibian Limb Regeneration". *Dev Cell*, *3* (4). 547-555.
416. Morris, R. and Hollenbeck, P. 1995 "Axonal transport of mitochondria along microtubules and F-actin in living vertebrate neurons". *J Cell Biol*, *131* (5). 1315-1326.
417. Morris, S. and Carey, L. 2006 "Trastuzumab and beyond: New possibilities for the treatment of HER2-positive breast cancer". *Oncology*, *20* (14). 1763-1771.

418. Morrison, R.N., Cooper, G.A., Koop, B.F., Rise, M.L., Bridle, A.R., Adams, M.B. and Nowak, B.F. 2006 "Transcriptome profiling the gills of amoebic gill disease (AGD)-affected Atlantic salmon (Salmo salar L.): a role for tumor suppressor p53 in AGD pathogenesis?" *Physiol Genomics*, *26* (1). 15-34.
419. Mose Larsen, P., Bravo, R., Fey, S., Small, J. and Celis, J. 1982 "Putative association of mitochondria with a subpopulation of intermediate-sized filaments in cultured human skin fibroblasts". *Cell*, *31* (3 Pt 2). 681-692.
420. Moudgil, V.K., Dinda, S., Khattree, N., Jhanwar, S., Alban, P. and Hurd, C. 2001 "Hormonal regulation of tumor suppressor proteins in breast cancer cells". *J Steroid Biochem Mol Biol*, *76* (1-5). 105.
421. Moulder, S. and Hortobagyi, G.N. 2007 "Advances in the Treatment of Breast Cancer". *Clin Pharmacol Ther*, *83* (1). 26-36.
422. Mower, D.A., Jr., Peckham, D.W., Illera, V.A., Fishbaugh, J.K., Stunz, L.L. and Ashman, R.F. 1994 "Decreased membrane phospholipid packing and decreased cell size precede DNA cleavage in mature mouse B cell apoptosis". *J Immunol*, *152* (10). 4832-4842.
423. Munro, S. and Pelham, H.R.B. 1987 "A C-terminal signal prevents secretion of luminal ER proteins". *Cell*, *48* (5). 899-907.
424. Murray, E., McKenna, E.O., Burch, L.R., Dillon, J., Langridge Smith, P., Kolch, W., Pitt, A. and Hupp, T.R. 2007 "Microarray-Formatted Clinical Biomarker Assay Development Using Peptide Aptamers to Anterior Gradient-2". *Biochemistry*, *46* (48). 13742-13751.
425. Muzio, M., Salvesen, G.S. and Dixit, V. 1997 "FLICE Induced Apoptosis in a Cell-free System. Cleavage of caspase zymogens". *J Biol Chem*, *272* (5). 2952-2956.
426. Na, S., Chuang, T.-H., Cunningham, A., Turi, T.G., Hanke, J.H., Bokoch, G.M. and Danley, D.E. 1996 "D4-GDI, a Substrate of CPP32, Is Proteolyzed during Fas-induced Apoptosis". *J Biol Chem*, *271* (19). 11209-11213.
427. Narita, M., Shimizu, S., Ito, T., Chittenden, T., Lutz, R., Matsuda, H. and Tsujimoto, Y. 1998 "Bax interacts with the permeability transition pore to induce permeability transition and cytochrome c release in isolated mitochondria". *Proc Natl Acad Sci U S A.*, *95* (25). 14681-14686.
428. Nemajerova, A., Erster, S. and Moll, U. 2005 "The post-translational phosphorylation and acetylation modification profile is not the determining factor in targeting endogenous stress-induced p53 to mitochondria". *Cell Death Differ*, *12* (2). 197-200.
429. Newton, H. 2007 "Small-molecule and antibody approaches to molecular chemotherapy of primary brain tumors". *Curr Opin Investig Drugs*, *8* (12). 1009-1021.
430. Nielsen, T.O., Hsu, F.D., Jensen, K., Cheang, M., Karaca, G., Hu, Z., Hernandez-Boussard, T., Livasy, C., Cowan, D., Dressler, L., Akslen, L.A., Ragaz, J., Gown, A.M., Gilks, C.B., van de Rijn, M. and Perou, C.M. 2004 "Immunohistochemical and Clinical Characterization of the Basal-Like Subtype of Invasive Breast Carcinoma". *Clin Cancer Res*, *10* (16). 5367-5374.

431. Nigg, E.A. 1997 "Nucleocytoplasmic transport: signals, mechanisms and regulation". *Nature*, *386* (6627). 779-787.
432. Nigro, J., Baker, S., Preisinger, A., Jessup, J., Hostetter, R., Cleary, K., Bigner, S., Davidson, N., Baylin, S. and Devilee, P. 1989 "Mutations in the p53 gene occur in diverse human tumour types". *Nature*, *342* (6250). 705-708.
433. Nilsson, T. and Warren, G. 1994 "Retention and retrieval in the endoplasmic reticulum and the Golgi apparatus". *Curr Opin Cell Biol*, *6* (4). 517-521.
434. Nimjee, S.M., Rusconi, C.P., Harrington, R.A. and Sullenger, B.A. 2005 "The potential of aptamers as anticoagulants". *Trends Cardiovasc Med*, *15* (1). 41-45.
435. Nopanitaya, W. and Misch, D.W. 1974 "Developmental cytology of the midgut in the flesh-fly, Sarcophaga bullata (Parker)". *Tissue Cell*, *6* (3). 487-502.
436. Novoselov, V.V., Alexandrova, E.M., Ermakova, G.V. and Zaraisky, A.G. 2003 "Expression zones of three novel genes abut the developing anterior neural plate of Xenopus embryo". *Gene Expr Patterns*, *3* (2). 225-230.
437. Nutt, L.K., Pataer, A., Pahler, J., Fang, B., Roth, J., McConkey, D.J. and Swisher, S.G. 2002 "Bax and Bak Promote Apoptosis by Modulating Endoplasmic Reticular and Mitochondrial Ca2+ Stores". *J Biol Chem*, *277* (11). 9219-9225.
438. Oberstein, A., Jeffrey, P.D. and Shi, Y. 2007 "Crystal Structure of the Bcl-XL-Beclin 1 Peptide Complex: Beclin 1 is a novel BH3-only protein". *J Biol Chem*, *282* (17). 13123-13132.
439. Ocker, M. and Schneider Stock, R. 2007 "Histone deacetylase inhibitors: Signalling towards p21cip1/waf1". *Int J Biochem Cell Biol*, *39* (7-8). 1367-1374.
440. Ogiwara, H., Ui, A., Kawashima, S., Kugou, K., Onoda, F., Iwahashi, H., Harata, M., Ohta, K., Enomoto, T. and Seki, M. 2007 "Actin-related protein Arp4 functions in kinetochore assembly". *Nucl Acids Res*, *35* (9). 3109-3117.
441. Okamoto, T., Minamikawa, T., Edward, G., V., V. and Herman, E. 1999 "Posttranslational removal of the carboxyl-terminal KDEL of the cysteine protease SH-EP occurs prior to maturation of the enzyme". *J Biol Chem*, *274* (16). 11390-11398.
442. Okamoto, T., Shimada, T., Hara-Nishimura, I., Nishimura, M. and Minamikawa, T. 2003 "C-Terminal KDEL Sequence of A KDEL-Tailed Cysteine Proteinase (Sulfhydryl-Endopeptidase) Is Involved in Formation of KDEL Vesicle and in Efficient Vacuolar Transport of Sulfhydryl-Endopeptidase". *Plant Physiol*, *132* (4). 1892-1900.
443. Oliner, J.D., Kinzler, K.W., Meltzer, P.S., George, D.L. and Vogelstein, B. 1992 "Amplification of a gene encoding a p53-associated protein in human sarcomas". *Nature*, *358* (6381). 80-83.
444. Oltval, Z.N., Milliman, C.L. and Korsmeyer, S.J. 1993 "Bcl-2 heterodimerizes in vivo with a conserved homolog, Bax, that accelerates programed cell death". *Cell*, *74* (4). 609-619.

445. Opalka, B., Dickopp, A. and Kirch, H.C. 2002 "Apoptotic Genes in Cancer Therapy". *Cells Tissues Organs*, *172* (2). 126-132.
446. Opat, A., Houghton, F. and Gleeson, P. 2000 "Medial Golgi but not late Golgi glycosyltransferases exist as high molecular weight complexes. Role of luminal domain in complex formation and localization". *J Biol Chem*, *275* (16). 11836-11845.
447. Oren, M. and Levine, A.J. 1983 "Molecular cloning of a cDNA specific for the murine p53 cellular tumor antigen". *Proc Natl Acad Sci U S A*, *80* (1). 56-59.
448. Ormö, M., Cubitt, A., Kallio, K., Gross, L., Tsien, R. and Remington, S. 1996 "Crystal structure of the Aequorea victoria green fluorescent protein". *Science*, *273* (5280). 1392-1395.
449. Ostermeyer, A., Runko, E., Winkfield, B., Ahn, B. and Moll, U. 1996 "Cytoplasmically sequestered wild-type p53 protein in neuroblastoma is relocated to the nucleus by a C-terminal peptide". *PNAS*, *93* (26). 15190-15194.
450. Otto, G.P., Wu, M.Y., Kazgan, N., Anderson, O.R. and Kessin, R.H. 2003 "Macroautophagy Is Required for Multicellular Development of the Social Amoeba Dictyostelium discoideum". *J Biol Chem*, *278* (20). 17636-17645.
451. Ozaki, T., Yamashita, T. and Ishiguro, S.-i. 2008 "ERp57-associated mitochondrial [mu]-calpain truncates apoptosis-inducing factor". *Biochim Biophys Acta*, *1783* (10). 1955-1963.
452. Paglin, S., Hollister, T., Delohery, T., Hackett, N., McMahill, M., Sphicas, E., Domingo, D. and Yahalom, J. 2001 "A Novel Response of Cancer Cells to Radiation Involves Autophagy and Formation of Acidic Vesicles". *Cancer Res*, *61* (2). 439-444.
453. Paglin, S., Lee, N.-Y., Nakar, C., Fitzgerald, M., Plotkin, J., Deuel, B., Hackett, N., McMahill, M., Sphicas, E., Lampen, N. and Yahalom, J. 2005 "Rapamycin-Sensitive Pathway Regulates Mitochondrial Membrane Potential, Autophagy, and Survival in Irradiated MCF-7 Cells". *Cancer Res*, *65* (23). 11061-11070.
454. Pan, G., Ni, J., Wei, Y.-F., Yu, G.-l., Gentz, R. and Dixit, V.M. 1997 "An Antagonist Decoy Receptor and a Death Domain-Containing Receptor for TRAIL". *Science*, *277* (5327). 815-818.
455. Pan, G., O'Rourke, K., Chinnaiyan, A.M., Gentz, R., Ebner, R., Ni, J. and Dixit, V.M. 1997 "The Receptor for the Cytotoxic Ligand TRAIL". *Science*, *276* (5309). 111-113.
456. Parks, G. and Lamb, R. 1991 "Topology of eukaryotic type II membrane proteins: importance of N-terminal positively charged residues flanking the hydrophobic domain". *Cell*, *64* (4). 777-787.
457. Parmentier, M.-L., Woods, D., Greig, S., Phan, P.G., Radovic, A., Bryant, P. and O'Kane, C.J. 2000 "Rapsynoid/Partner of Inscuteable Controls Asymmetric Division of Larval Neuroblasts in Drosophila". *J Neurosci*, *20* (14). 84RC-.

458. Paschke, M., Tiede, C. and Höhne, W. 2007 "Engineering a circularly permuted GFP scaffold for peptide presentation". *J Mol Recognit*, *20* (5). 367-378.
459. Pastorino, J.G., Chen, S.-T., Tafani, M., Snyder, J.W. and Farber, J.L. 1998 "The Overexpression of Bax Produces Cell Death upon Induction of the Mitochondrial Permeability Transition". *J Biol Chem*, *273* (13). 7770-7775.
460. Pecorino, A.L. (ed.), *Molecular Biology of Cancer*. Oxford Press, 2002.
461. Pecorino, A.L. (ed.), *Molecular Biology of Cancer*. Oxford Press, 2005.
462. Pedersen, P. 2007 "The cancer cell's "power plants" as promising therapeutic targets: an overview". *J Bioenerg Biomembr*, *39* (1). 1-12.
463. Pelicano, H., Xu, R., M., D., Feng, L., Sasaki, R., Carew, J., Hu, Y., Ramdas, L., Hu, L., Keating, M., Zhang, W., Plunkett, W. and Huang, P. 2006 "Mitochondrial respiration defects in cancer cells cause activation of Akt survival pathway through a redox-mediated mechanism". *J Cell Biol*, *175* (6). 913-923.
464. Pellegata, N.S., Cajot, J.F. and Stanbridge, E.J. 1995 "The basic carboxy-terminal domain of human p53 is dispensable for both transcriptional regulation and inhibition of tumor cell growth". *Oncogene*, *11* (2). 337-349.
465. Pereira, A., Dalby, B., Stewart, R., Doxsey, S. and Goldstein, L. 1997 " Mitochondrial association of a plus end-directed microtubule motor expressed during mitosis in Drosophila". *J Cell Biol*, *136* (5). 1081-1090.
466. Perou, C.M., Sorlie, T., Eisen, M.B., van de Rijn, M., Jeffrey, S.S., Rees, C.A., Pollack, J.R., Ross, D.T., Johnsen, H., Akslen, L.A., Fluge, O., Pergamenschikov, A., Williams, C., Zhu, S.X., Lonning, P.E., Borresen-Dale, A.-L., Brown, P.O. and Botstein, D. 2000 "Molecular portraits of human breast tumours". *Nature*, *406* (6797). 747-752.
467. Persson, S., Rosenquist, M., Knoblach, B., Khosravi-Far, R., Sommarin, M. and Michalak, M. 2005 "Diversity of the protein disulfide isomerase family: identification of breast tumor induced Hag2 and Hag3 as novel members of the protein family". *Mol Phylogenet Evol*, *36* (3). 734-740.
468. Persson, S., Rosenquist, M., Knoblach, B., Khosravi-Far, R., Sommarin, M. and Michalak, M. 2005 "Diversity of the protein disulfide isomerase family: Identification of breast tumor induced Hag2 and Hag3 as novel members of the protein family". *Mol Phylogenet Evol*, *36* (3). 734-740.
469. Pesanti, E. and Axline, S. 1975 "Phagolysosome formation in normal and colchicine-treated macrophages". *J Exp Med*, *142* (4). 903-913.
470. Petek, E., Windpassinger, C., Egger, H., Kroisel, P.M. and Wagner, K. 2000 "Localization 1 of the human anterior gradient-2 gene (AGR2) to chromosome band 7p21.3 by radiation hybrid mapping and fluorescencein situ hybridisation". *Cytogenet Genome Res*, *89* (3-4). 141-142.
471. Peters, R. and Sikorski, R. 1999 "Protein Expression:Folding to Green". *Science*, *285* (5431). 1229-.
472. Peto, R., Boreham, J., Clarke, M., Davies, C. and Beral, V. 2000 "UK and USA breast cancer deaths down 25% in year 2000 at ages 20-69 years". *The Lancet*, *355* (9217). 1822-1822.

473. Peyerl, F.W., Dai, S., Murphy, G.A., Crawford, F., White, J., Marrack, P. and Kappler, J.W. 2006 "Elucidation of some Bax conformational changes through crystallization of an antibody-peptide complex". *Cell Death Differ*, *14* (3). 447-452.
474. Pohler, E., Craig, A.L., Cotton, J., Lawrie, L., Dillon, J.F., Ross, P., Kernohan, N. and Hupp, T.R. 2004 "The Barrett's Antigen Anterior Gradient-2 Silences the p53 Transcriptional Response to DNA Damage". *Mol Cell Proteomics*, *3* (6). 534-547.
475. Prasher, D., Eckenrode, V., Ward, W., Prendergast, F. and Cormier, M. 1992 "Primary structure of the Aequorea victoria green-fluorescent protein". *Gene*, *111* (2). 229-233.
476. Presley, J.F. 2005 "Imaging the secretory pathway: The past and future impact of live cell optical techniques". *Biochim Biophys Acta*, *1744* (3). 259.
477. Prives, C. 1998 "Signaling to p53: Breaking the MDM2-p53 Circuit". *Cell*, *95* (1). 5-8.
478. Proske, D., Blank, M., Buhmann, R. and Resch, A. 2005 "Aptamers--basic research, drug development, and clinical applications". *Appl Microbiol Biotechnol*, *69* (4). 367-374.
479. Puziss, J.W., Fikes, J.D. and Bassford, P.J. 1989 "Analysis of mutational alterations in the hydrophilic segment of the maltose-binding protein signal peptide". *J Bacteriol*, *171* (5). 2303-2311.
480. Qu, X., Yu, J., Bhagat, G., Furuya, N., Hibshoosh, H., Troxel, A., Rosen, J., Eskelinen, E., Mizushima, N., Ohsumi, Y., Cattoretti, G. and Levine, B. 2003 "Promotion of tumorigenesis by heterozygous disruption of the beclin 1 autophagy gene." *J Clin Invest*, *112* (12). 1809-1820.
481. Rakha, E., Maysa, E., El-Sayed, A.R., Green, A.H.S., Lee, J.F., Robertson, I.O. and Ellis, O. 2007 "Prognostic markers in triple-negative breast cancer". *Cancer 109* (1). 25-32.
482. Rakha, E., Putti, T.C., Abd El-Rehim, D.M., Paish, C., Green, A.R., Powe, D.G., Lee, A.H., Robertson, J.F. and Ellis, I.O. 2006 "Morphological and immunophenotypic analysis of breast carcinomas with basal and myoepithelial differentiation". *J Pathol.*, *208* (4). 495-506.
483. Raykhel, I., Alanen, H., Salo, K., Jurvansuu, J., Nguyen, V.D., Latva-Ranta, M. and Ruddock, L. 2007 "A molecular specificity code for the three mammalian KDEL receptors". *J Cell Biol*, *179* (6). 1193-1204.
484. Reid, B.J. 2001 "p53 and neoplastic progression in barrett's esophagus". *Am J Gastroenterol*, *96* (5). 1321-1323.
485. Reid, B.J., Blount, P.L. and Rabinovitch, P.S. 2003 "Biomarkers in Barrett's esophagus". *Gastrointest Endosc Clin N Am*, *13* (2). 369-397.
486. Rigobello, M.P., Donella-Deana, A., Cesaro, L. and Bindoli, A. 2001 "Distribution of protein disulphide isomerase in rat liver mitochondria". *Biochem J*, *356* (2). 567-570.
487. Rigobello, M.P., Donella-Deana, A., Cesaro, L. and Bindoli, A. 2000 "Isolation, purification, and characterization of a rat liver mitochondrial protein disulfide isomerase". *Free Radic Biol Med*, *28* (2). 266-272.

488. Rigobello, M.P., Turcato, F. and Bindoli, A. 1995 "Inhibition of Rat Liver Mitochondrial Permeability Transition by Respiratory Substrates". *Arch Biochem Biophys*, *319* (1). 225-230.
489. Risbud, M., Fertala, J., Vresilovic, E., Albert, T. and Shapiro, I. 2005 "Nucleus pulposus cells upregulate PI3K/Akt and MEK/ERK signaling pathways under hypoxic conditions and resist apoptosis induced by serum withdrawal". *Spine*, *30* (8). 882-889.
490. Rizzuto, R., Pinton, P., Carrington, W., Fay, F.S., Fogarty, K.E., Lifshitz, L.M., Tuft, R.A. and Pozzan, T. 1998 "Close Contacts with the Endoplasmic Reticulum as Determinants of Mitochondrial Ca2+ Responses". *Science*, *280* (5370). 1763-1766.
491. Roach, H.I. and Clarke, N.M.P. 2000 "Physiological cell death of chondrocytes in vivo is not confined to apoptosis". *J Bone Joint Surg Br*, *82-B* (4). 601-613.
492. Robertson, D.L. and Joyce, G.F. 1990 "Selection in vitro of an RNA enzyme that specifically cleaves single-stranded DNA". *Nature*, *344* (6265). 467-468.
493. Robertson, D.W., Katzenellenbogen, J.A., Long, D.J., Rorke, E.A. and Katzenellenbogen, B.S. 1982 "Tamoxifen antiestrogens. A comparison of the activity, pharmacokinetics, and metabolic activation of the cis and trans isomers of tamoxifen". *J Steroid Biochem*, *16* (1). 1-13.
494. Rojo, M., Legros, F., Chateau, D. and Lombes, A. 2002 "Membrane topology and mitochondrial targeting of mitofusins, ubiquitous mammalian homologs of the transmembrane GTPase Fzo". *J Cell Sci*, *115* (8). 1663-1674.
495. Rokhlin, O.W., Glover, R.B., Guseva, N.V., Taghiyev, A.F., Kohlgraf, K.G. and Cohen, M.B. 2006 "Mechanisms of Cell Death Induced by Histone Deacetylase Inhibitors in Androgen Receptor-Positive Prostate Cancer Cells". *Mol Cancer Res*, *4* (2). 113-123.
496. Rosenfeld, M.G. and Glass, C.K. 2001 "Coregulator Codes of Transcriptional Regulation by Nuclear Receptors". *J Biol Chem*, *276* (40). 36865-36868.
497. Roth, J., M., D., Freedman, D., T., S. and Levine, A. 1998 " Nucleo-cytoplasmic shuttling of the hdm2 oncoprotein regulates the levels of the p53 protein via a pathway used by the human immunodeficiency virus rev protein". *EMBO J*, *17* (2). 554-564.
498. Rousseau, B., Ménard, L., Haurie, V., Taras, D., JF., B., Moreau Gaudry, F., Metzler, P., Hugues, M., Boyault, S., Lemière, S., Canron, X., Costet, P., Cole, M., Balabaud, C., Bioulac Sage, P., Zucman Rossi, J. and Rosenbaum, J. 2007 "Overexpression and role of the ATPase and putative DNA helicase RuvB-like 2 in human hepatocellular carcinoma". *Hepatology*, *46* (4). 1108-1118.
499. Runnebaum, I., Nagarajan, M., Bowman, M., Soto, D. and Sukumar, S. 1991 "Mutations in p53 as potential molecular markers for human breast cancer". *Proc Natl Acad Sci U S A*, *88* (23). 10657-10661.
500. Russell, S., Hickey, G., Lowry, W., White, P. and Atkinson, R. 1990 " Allele loss from chromosome 17 in ovarian cancer." *Oncogene*, *5* (10). 1581-1583.

501. Russo, C.A., Weber, T.K., Volpe, C.M., Stoler, D.L., Petrelli, N.J., Rodriguez-Bigas, M., Burhans, W.C. and Anderson, G.R. 1995 "An Anoxia Inducible Endonuclease and Enhanced DNA Breakage as Contributors to Genomic Instability in Cancer". *Cancer Res*, *55* (5). 1122-1128.
502. Ryan, J.J., Prochownik, E., Gottlieb, C.A., Apel, I.J., Merino, R., Nu, G. and Clarke, M.F. 1994 "c-myc and bcl-2 modulate p53 function by altering p53 subcellular trafficking during the cell cycle". *PNAS*, *91* (13). 5878-5882.
503. Ryerse, J.S. 1979 "Developmental changes in Malpighian tubule cell structure". *Tissue Cell*, *11* (3). 533-551.
504. Sabbatini, P. and McCormick, F. 1999 "Phosphoinositide 3-OH Kinase (PI3K) and PKB/Akt Delay the Onset of p53-mediated, Transcriptionally Dependent Apoptosis". *J Biol Chem*, *274* (34). 24263-24269.
505. Saito, H., Inazawa, J., Saito, S., Kasumi, F., Koi, S., Sagae, S., Kudo, R., Saito, J., Noda, K. and Nakamura, Y. 1993 "Detailed deletion mapping of chromosome 17q in ovarian and breast cancers: 2-cM region on 17q21.3 often and commonly deleted in tumors." *Cancer Res*, *53* (14). 3382-3385.
506. Saito, S.i., Goodarzi, A.A., Higashimoto, Y., Noda, Y., Lees-Miller, S.P., Appella, E. and Anderson, C.W. 2002 "ATM Mediates Phosphorylation at Multiple p53 Sites, Including Ser46, in Response to Ionizing Radiation". *J Biol Chem*, *277* (15). 12491-12494.
507. Sakaguchi, K., Herrera, J.E., Saito, S.i., Miki, T., Bustin, M., Vassilev, A., Anderson, C.W. and Appella, E. 1998 "DNA damage activates p53 through a phosphorylation-acetylation cascade". *Genes Dev*, *12* (18). 2831-2841.
508. Salih, A., Larkum, A., Cox, G., Kuhl, M. and Hoegh-Guldberg, O. 2000 "Fluorescent pigments in corals are photoprotective". *Nature*, *408* (6814). 850-853.
509. Salvesen, G.S. and Dixit, V.M. 1999 "Caspase activation: The induced-proximity model". *PNAS*, *96* (20). 10964-10967.
510. Samuels Lev, Y., O'Connor, D.J., Bergamaschi, D., Trigiante, G., Hsieh, J.-K., Zhong, S., Campargue, I., Naumovski, L., Crook, T. and Lu, X. 2001 "ASPP Proteins Specifically Stimulate the Apoptotic Function of p53". *Mol Cell*, *8* (4). 781-794.
511. Sansome, C., Zaika, A., Marchenko, N.D. and Moll, U.M. 2001 "Hypoxia death stimulus induces translocation of p53 protein to mitochondria: Detection by immunofluorescence on whole cells". *FEBS Letters*, *488* (3). 110-115.
512. Saran, D., Frank, J. and Burke, D.H. 2003 "The tyranny of adenosine recognition among RNA aptamers to coenzyme A". *BMC Evol Biol*, *3*. 26.
513. Sassanfar, M. and Szostak, J.W. 1993 "An RNA motif that binds ATP". *Nature*, *364* (6437). 550-553.
514. Satoh, M., Hamamoto, T., Seo, N., Kagawa, Y. and Endo, H. 2003 "Differential sublocalization of the dynamin-related protein OPA1 isoforms in mitochondria". *Biochem Biophys Res Commun*, *300* (2). 482-493.
515. Saville, G.P., Patmanidi, A.L., Possee, R.D. and King, L.A. 2004 "Deletion of the Autographa californica nucleopolyhedrovirus chitinase KDEL motif

and in vitro and in vivo analysis of the modified virus". *J Gen Virol*, *85* (4). 821-831.

516. Scarlatti, F., Maffei, R., Beau, I., Codogno, P. and Ghidoni, R. 2008 "Role of non-canonical Beclin 1-independent autophagy in cell death induced by resveratrol in human breast cancer cells". *Cell Death Differ*, *15* (8). 1318-1329.
517. Schaefer, M., Petronczki, M., Dorner, D., Forte, M. and Knoblich, J.A. 2001 "Heterotrimeric G Proteins Direct Two Modes of Asymmetric Cell Division in the Drosophila Nervous System". *Cell*, *107* (2). 183-194.
518. Schlumpberger, M., Schaeffeler, E., Straub, M., Bredschneider, M., Wolf, D.H. and Thumm, M. 1997 "AUT1, a gene essential for autophagocytosis in the yeast Saccharomyces cerevisiae". *J Bacteriol*, *179* (4). 1068-1076.
519. Scorrano, L., Oakes, S.A., Opferman, J.T., Cheng, E.H., Sorcinelli, M.D., Pozzan, T. and Korsmeyer, S.J. 2003 "BAX and BAK Regulation of Endoplasmic Reticulum Ca2+: A Control Point for Apoptosis". *Science*, *300* (5616). 135-139.
520. Screaton, G.R., Mongkolsapaya, J., Xu, X.-N., Cowper, A.E., McMichael, A.J. and Bell, J.I. 1997 "TRICK2, a new alternatively spliced receptor that transduces the cytotoxic signal from TRAIL". *Current Biology*, *7* (9). 693-696.
521. Semenza, J.C., Hardwick, K.G., Dean, N. and Pelham, H.R.B. 1990 "ERD2, a yeast gene required for the receptor-mediated retrieval of luminal ER proteins from the secretory pathway". *Cell*, *61* (7). 1349-1357.
522. Sevier, C.S. and Kaiser, C.A. 2002 "Formation and transfer of disulphide bonds in living cells". *Nat Rev Mol Cell Biol*, *3* (11). 836-847.
523. Shamu, C.E., Cox, J.S. and Walter, P. 1994 "The unfolded-protein-response pathway in yeast". *Trends Cell Biol*, *4* (2). 56-60.
524. Shaulsky, G., Ben Zeev, A. and Rotter, V. 1990 " Subcellular distribution of the p53 protein during the cell cycle of Balb/c 3T3 cells". *Oncogene*, *5* (11). 1707-1711.
525. Shaulsky, G., Goldfinger, N., Peled, A. and Rotter, V. 1991 " Involvement of wild-type p53 protein in the cell cycle requires nuclear localization". *Cell Growth Differ*, *2* (12). 661-667.
526. Shaulsky, G., Goldfinger, N., Tosky, M., Levine, A. and Rotter, V. 1991 "Nuclear localization is essential for the activity of p53 protein". *Oncogene*, *6* (11). 2055-2065.
527. Shaw, A., Rottier, P. and Rose, J. 1988 "Evidence for the loop model of signal-sequence insertion into the endoplasmic reticulum". *Proc Natl Acad Sci U S A*, *85* (20). 7592-7596.
528. Sheahan, M., Rose, R. and McCurdy, D. 2004 "Organelle inheritance in plant cell division: the actin cytoskeleton is required for unbiased inheritance of chloroplasts, mitochondria and endoplasmic reticulum in dividing protoplasts". *Plant J*, *37* (3). 379-390.

529. Shen, X., Mizuguchi, G., Hamiche, A. and Wu, C. 2000 "A chromatin remodelling complex involved in transcription and DNA processing". *Nature*, *406* (6795). 541-544.
530. Shieh, S.Y., Taya, Y. and Prives, C. 1999 "DNA damage-inducible phosphorylation of p53 at N-terminal sites including a novel site, Ser20, requires tetramerization." *EMBO J*, *18* (7). 1815-1823.
531. Shigeaki, K., Hideki, E., Yoshikazu, M., Takuya, K., Shimami, U., Haruna, S., Shoichi, M., Yukiko, G., Eisuke, N., Hiroyuki, K., Daniel, M. and Pierre, C. 1995 "Activation of the Estrogen Receptor Through Phosphorylation by Mitogen-Activated Protein Kinase". *Science*, *270* (5241). 1491 - 1494.
532. Shih, L.-J., Lu, Y.-F., Chen, Y.-H., Lin, C.-C., Chen, J.-A. and Hwang, S.-P.L. 2007 "Characterization of the agr2 gene, a homologue of X. laevis anterior gradient 2, from the zebrafish, Danio rerio". *Gene Expr Patterns*, *7* (4). 452-460.
533. Shimizu, S., Kanaseki, T., Mizushima, N., Mizuta, T., Arakawa-Kobayashi, S., Thompson, C.B. and Tsujimoto, Y. 2004 "Role of Bcl-2 family proteins in a non-apoptotic programmed cell death dependent on autophagy genes". *Nat Cell Biol*, *6* (12). 1221-1228.
534. Shimizu, S., Narita, M., Tsujimoto, Y. and Tsujimoto, Y. 1999 "Bcl-2 family proteins regulate the release of apoptogenic cytochrome c by the mitochondrial channel VDAC". *Nature*, *399* (6735). 483-487.
535. Shimomura, O. 2005 "The discovery of aequorin and green fluorescent protein". *J Microsc*, *217* (Pt 1).
536. Shinagawa, H. and Iwasaki, H. 1996 "Processing the holliday junction in homologous recombination". *Trends Biochem Sci*, *21* (3). 107-111.
537. Shrestha, S. and Deo, S. 2006 "Anthozoa red fluorescent protein in biosensing". *Anal Bioanal Chem*, *386* (3). 515-524.
538. Sigala, B., Edwards, M., Puri, T. and Tsaneva, I.R. 2005 "Relocalization of human chromatin remodeling cofactor TIP48 in mitosis". *Exp Cell Res*, *310* (2). 357.
539. Siliciano, J.D., Canman, C.E., Taya, Y., Sakaguchi, K., Appella, E. and Kastan, M.B. 1997 "DNA damage induces phosphorylation of the amino terminus of p53". *Genes Dev*, *11* (24). 3471-3481.
540. Sirvent, J., Fortuño-Mar, A., Olona, M. and Orti, A. 2001 " Prognostic value of p53 protein expression and clinicopathological factors in infiltrating ductal carcinoma of the breast. A study of 192 patients." *Histol Histopathol*, *16* (1). 99-106.
541. Skliris, G., Leygue, E., Watson, P. and Murphy, L. 2008 " Estrogen receptor alpha negative breast cancer patients: estrogen receptor beta as a therapeutic target". *J Steroid Biochem Mol Biol*, *109* (1-2). 1-10.
542. Skulachev, V.P. 1996 "Why are mitochondria involved in apoptosis? Permeability transition pores and apoptosis as selective mechanisms to eliminate superoxide-producing mitochondria and cell". *FEBS Letters*, *397* (1). 7-10.

543. Slee, E.A., Harte, M.T., Kluck, R.M., Wolf, B.B., Casiano, C.A., Newmeyer, D.D., Wang, H.-G., Reed, J.C., Nicholson, D.W., Alnemri, E.S., Green, D.R. and Martin, S.J. 1999 "Ordering the Cytochrome c-initiated Caspase Cascade: Hierarchical Activation of Caspases-2, -3, -6, -7, -8, and -10 in a Caspase-9-dependent Manner". *J Biol Chem*, *144* (2). 281-292.
544. Smirnov, D.R., Zweitzig, B.W., Foulk, M., Miller, C., Doyle, G.V., Pienta, K.J., Meropol, N.J., Weiner, L.M., Cohen, S.J., Moreno, J.G., Connelly, M.C., Terstappen, L.W.M.M. and O Hara, S.M. 2005 "Global gene expression profiling of circulating tumor cells". *Cancer Res*, *65* (12). 4993-4997.
545. Smirnova, E., Griparic, L., Shurland, D.-L. and Van der Bliek, A.M. 2001 "Dynamin-related Protein Drp1 Is Required for Mitochondrial Division in Mammalian Cells". *Mol Biol Cell*, *12* (8). 2245-2256.
546. Smith, C.A., Farrah, T. and Goodwin, R.G. 1994 "The TNF receptor superfamily of cellular and viral proteins: Activation, costimulation, and death". *Cell*, *76* (6). 959-962.
547. Soanes, K.H., Figuereido, K., Richards, R.C., Mattatall, N.R. and Ewart, K.V. 2004 "Sequence and expression of C-type lectin receptors in Atlantic salmon (Salmo salar)". *Immunogenetics*, *56* (8). 572-584.
548. Soengas, M.S., Alarcón, R.M., Yoshida, H., Giaccia, A.J., Hakem, R., Mak, T.W. and Lowe, S.W. 1999 "Apaf-1 and Caspase-9 in p53-Dependent Apoptosis and Tumor Inhibition". *Science*, *284* (5411). 156-159.
549. Sorlie, T., Perou, C.M., Tibshirani, R., Aas, T., Geisler, S., Johnsen, H., Hastie, T., Eisen, M.B., van de Rijn, M., Jeffrey, S.S., Thorsen, T., Quist, H., Matese, J.C., Brown, P.O., Botstein, D., Lonning, P.E. and Borresen-Dale, A.-L. 2001 "Gene expression patterns of breast carcinomas distinguish tumor subclasses with clinical implications". *PNAS*, *98* (19). 10869-10874.
550. Sorlie, T., Tibshirani, R., Parker, J., Hastie, T., Marron, J.S., Nobel, A., Deng, S., Johnsen, H., Pesich, R., Geisler, S., Demeter, J., Perou, C.M., Lonning, P.E., Brown, P.O., Borresen-Dale, A.-L. and Botstein, D. 2003 "Repeated observation of breast tumor subtypes in independent gene expression data sets". *PNAS*, *100* (14). 8418-8423.
551. Spänkuch, B. and Strebhardt, K. 2008 "Combinatorial application of nucleic acid-based agents targeting protein kinases for cancer treatment". *Curr Pharm Des*, *14* (11). 1098-1112.
552. Spiess, M. 1995 "Heads or tails:what determines the orientation of proteins in the membrane". *FEBS Letters*, *369* (1). 76-79.
553. Srinivasula, S.M., Ahmad, M., Fernandes-Alnemri, T. and Alnemri, E.S. 1998 "Autoactivation of Procaspase-9 by Apaf-1-Mediated Oligomerization". *Mol Cell*, *1* (7). 949-957.
554. Srinivasula, S.M., Fernandes-Alnemri, T., Zangrilli, J., Robertson, N., Armstrong, R.C., Wang, L., Trapani, J.A., Tomaselli, K.J., Litwack, G. and Alnemri, E.S. 1996 "The Ced-3/Interleukin 1beta Converting Enzyme-like Homolog Mch6 and the Lamin-cleaving Enzyme Mch2alpha Are Substrates for the Apoptotic Mediator CPP32". *J Biol Chem*, *271* (43). 27099-27106.

555. Srinivasula, S.M., Manzoor., A., Fernandes-Alnemri, T., Litwack, G. and Alnemri, E.S. 1996 "Molecular ordering of the Fas-apoptotic pathway: The Fas/APO-1 protease Mch5 is a CrmA-inhibitable protease that activates multiple Ced-3/ICE-like cysteine proteases". *PNAS*, *93* (25). 14486-14491.
556. Srisawat, C., Goldstein, I.J. and Engelke, D.R. 2001 "Sephadex-binding RNA ligands: rapid affinity purification of RNA from complex RNA mixtures". *Nucl Acids Res*, *29* (2). e4.
557. Stendahl, M., Kronblad, A., Rydén, L., Emdin, S., Bengtsson, N. and Landberg, G. 2004 "Cyclin D1 overexpression is a negative predictive factor for tamoxifen response in postmenopausal breast cancer patients". *Br J Cancer*, *90* (10). 1942-1948.
558. Sternsdorf, T., Guldner, H., Szostecki, C., Grötzinger, T. and Will, H. 1995 "Two nuclear dot-associated proteins, PML and Sp100, are often co-autoimmunogenic in patients with primary biliary cirrhosis". *Scand J Immunol*, *42* (2). 257-268.
559. Stewart, N., Hicks, G., Paraskevas, F. and Mowat, M. 1995 "Evidence for a second cell cycle block at G2/M by p53". *Oncogene*, *10* (1). 109-115.
560. Stoltenburg, R., Reinemann, C. and Strehlitz, B. 2007 "SELEX. A (r)evolutionary method to generate high-affinity nucleic acid ligands". *Biomol Eng*, *24* (4). 381-403.
561. Strausberg, R.L., Feingold, E.A., Grouse, L.H., Derge, J.G., Klausner, R.D., Collins, F.S., Wagner, L., Shenmen, C.M., Schuler, G.D., Altschul, S.F., Zeeberg, B., Buetow, K.H., Schaefer, C.F., Bhat, N.K., Hopkins, R.F., Jordan, H., Moore, T., Max, S.I., Wang, J., Hsieh, F., Diatchenko, L., Marusina, K., Farmer, A.A., Rubin, G.M., Hong, L., Stapleton, M., Soares, M.B., Bonaldo, M.F., Casavant, T.L., Scheetz, T.E., Brownstein, M.J., Usdin, T.B., Toshiyuki, S., Carninci, P., Prange, C., Raha, S.S., Loquellano, N.A., Peters, G.J., Abramson, R.D., Mullahy, S.J., Bosak, S.A., McEwan, P.J., McKernan, K.J., Malek, J.A., Gunaratne, P.H., Richards, S., Worley, K.C., Hale, S., Garcia, A.M., Gay, L.J., Hulyk, S.W., Villalon, D.K., Muzny, D.M., Sodergren, E.J., Lu, X., Gibbs, R.A., Fahey, J., Helton, E., Ketteman, M., Madan, A., Rodrigues, S., Sanchez, A., Whiting, M., Young, A.C., Shevchenko, Y., Bouffard, G.G., Blakesley, R.W., Touchman, J.W., Green, E.D., Dickson, M.C., Rodriguez, A.C., Grimwood, J., Schmutz, J., Myers, R.M., Butterfield, Y.S., Krzywinski, M.I., Skalska, U., Smailus, D.E., Schnerch, A., Schein, J.E., Jones, S.J. and Marra, M.A. 2002 "Generation and initial analysis of more than 15,000 full-length human and mouse cDNA sequences". *Proc Natl Acad Sci U S A*, *99* (26). 16899-16903.
562. Strawbridge, A.B. and Blum, J.S. 2007 "Autophagy in MHC class II antigen processing". *Curr Opinn in Immunol*, *19* (1). 87-92.
563. Subramaniam, N., Treuter, E. and Okret, S. 1999 "Receptor Interacting Protein RIP140 Inhibits Both Positive and Negative Gene Regulation by Glucocorticoids". *J Biol Chem*, *274* (25). 18121-18127.
564. Summerhayes, I., Wong, D. and Chen, L. 1983 " Effect of microtubules and intermediate filaments on mitochondrial distribution". *J Cell Sci*, *61*. 87-105.

565. Sundararajan, R. and White, E. 2001 "E1B 19K Blocks Bax Oligomerization and Tumor Necrosis Factor Alpha-Mediated Apoptosis". *J Virol*, *75* (16). 7506-7516.
566. Suzuki, K., Takayoshi, K., Yoshiaki, K., Noboru, M., Takeshi, N. and Yoshinori, O. 2001 "The pre-autophagosomal structure organized by concerted functions of APG genes is essential for autophagosome formation." *Embo J 20*. 5971-5981.
567. Takahashi, A., Alnemri, E.S., Lazebnik, Y.A., Fernandes-Alnemri, T., Litwack, G., Moir, R.D., Goldman, R.D., Poirier, G.G., Kaufmann, S.H. and Earnshaw, W.C. 1996 "Cleavage of lamin A by Mch2alpha but not CPP32: Multiple interleukin 1beta -converting enzyme-related proteases with distinct substrate recognition properties are active in apoptosis". *PNAS*, *93* (16). 8395-8400.
568. Takimoto, G., Graham, J., Jackson, T., Tung, L., Powell, R., Horwitz, L. and Horwitz, K. 1999 "Tamoxifen resistant breast cancer: coregulators determine the direction of transcription by antagonist-occupied steroid receptors". *J Steroid Biochem Mol Biol*, *69* (1-6). 45-50.
569. Tang, J., Yu, T., Guo, L., Xie, J., Shao, N. and He, Z. 2007 "In vitro selection of DNA aptamer against abrin toxin and aptamer-based abrin direct detection". *Biosens Bioelectron*, *22* (11). 2456-2463.
570. Tao, W. and Levine, A.J. 1999 "Nucleocytoplasmic shuttling of oncoprotein Hdm2 is required for Hdm2-mediated degradation of p53". *PNAS*, *96* (6). 3077-3080.
571. Tartaglia, L.A., Ayres, T.M., Wong, G.H.W. and Goeddel, D.V. 1993 "A novel domain within the 55 kd TNF receptor signals cell death". *Cell*, *74* (5). 845-853.
572. Tazawa, H., Osman, W., Shoji, Y., Treuter, E., Gustafsson, J.-A. and Zilliacus, J. 2003 "Regulation of Subnuclear Localization Is Associated with a Mechanism for Nuclear Receptor Corepression by RIP140". *Mol Cell Biol*, *23* (12). 4187-4198.
573. Teasdale, R. and Jackson, M. 1996 " Signal-mediated sorting of membrane proteins between the endoplasmic reticulum and the golgi apparatus". *Annu Rev Cell Dev Biol*, *12*. 27-54.
574. Teng, Y., Liu, Q., Ma, J., Liu, F., Han, Z., Wang, Y. and Wang, W. 2006 "Cloning, expression and characterization of a novel human CAP10-like gene hCLP46 from CD34+ stem/progenitor cells". *Gene*, *371* (1). 7-15.
575. Terasaki, M., Chen, L. and Fujiwara, K. 1986 "Microtubules and the endoplasmic reticulum are highly interdependent structures". *J Cell Biol*, *103* (4). 1557-1568.
576. Thomas, C.J., Brown, H.L., Hawes, C.R., Lee, B.Y., Min, M.-K., King, L.A. and Possee, R.D. 1998 "Localization of a Baculovirus-Induced Chitinase in the Insect Cell Endoplasmic Reticulum". *J Virol*, *72* (12). 10207-10212.
577. Thompson, D. and Weigel, R. 1998 "hAG-2, the human homologue of the Xenopus laevis cement gland gene XAG-2, is coexpressed with estrogen

receptor in breast cancer cell lines". *Biochem Biophys Res Commun*, *251* (1). 111-116.

578. Thomson, C.S., Brewster, D.H., Dewar, J.A. and Twelves, C.J. 2004 "Improvements in survival for women with breast cancer in Scotland between 1987 and 1993: impact of earlier diagnosis and changes in treatment". *European Journal of Cancer*, *40* (5). 743-753.
579. Thorén, P., Persson, D., Karlsson, M. and Nordén, B. 2000 "The antennapedia peptide penetratin translocates across lipid bilayers - the first direct observation". *FEBS Letters*, *482* (3). 265-268.
580. Thornberry, N.A., Rano, T.A., Peterson, E.P., Rasper, D.M., Timkey, T., Garcia-Calvo, M., Houtzager, V.M., Nordstrom, P.A., Roy, S., Vaillancourt, J.P., Chapman, K.T. and Nicholson, D.W. 1997 "A Combinatorial Approach Defines Specificities of Members of the Caspase Family and Granzyme B. Functional Relationships established for key mediators of apoptosis." *J Biol Chem*, *272* (29). 17907-17911.
581. Tidow, H., Melero, R., Mylonas, E., Freund, S.M.V., Grossmann, J.G., Carazo, J.M., Svergun, D.I., Valle, M. and Fersht, A.R. 2007 "From the Cover: Quaternary structures of tumor suppressor p53 and a specific p53 DNA complex". *Proc Natl Acad Sci U S A*, *104* (30). 12324-12329.
582. Tilly, K.I., Banerjee, S., Banerjee, P.P. and Tilly, J.L. 1995 "Expression of the p53 and Wilms' tumor suppressor genes in the rat ovary: gonadotropin repression in vivo and immunohistochemical localization of nuclear p53 protein to apoptotic granulosa cells of atretic follicles". *Endocrinology*, *136* (4). 1394-1402.
583. Tiwari, B.S., Belenghi, B. and Levine, A. 2002 "Oxidative Stress Increased Respiration and Generation of Reactive Oxygen Species, Resulting in ATP Depletion, Opening of Mitochondrial Permeability Transition, and Programmed Cell Death". *Plant Physiol*, *128* (4). 1271-1281.
584. Torii, I., Morikawa, S., Nagasaki, M., Nokano, A. and Morikawa, K. 2001 "Differential endocytotic characteristics of a novel human B/DC cell line HBM-Noda: effective macropinocytic and phagocytic function rather than scavenging function". *Immunology*, *103* (1). 70-80.
585. Torregrosa, D., Bolufer, P., Lluch, A., Antonio López, J., Barragán, E., Ruiz, A., Guillem, V., Munárriz, B. and García Conde, J. 1997 "Prognostic significance of c-erbB-2/neu amplification and epidermal growth factor receptor (EGFR) in primary breast cancer and theor relation to estradiol receptor (ER) status". *Clinica Chimica Acta*, *262* (1-2). 99-119.
586. Townsley, F., Wilson, D. and Pelham, H. 1993 " Mutational analysis of the human KDEL receptor: distinct structural requirements for Golgi retention, ligand binding and retrograde transport". *EMBO J*, *12* (7). 2821-2829.
587. Travers, K.J., Patil, C.K., Wodicka, L., Lockhart, D.J., Weissman, J.S. and Walter, P. 2000 "Functional and Genomic Analyses Reveal an Essential Coordination between the Unfolded Protein Response and ER-Associated Degradation". *Cell*, *101* (3). 249-258.

588. Treuter, E., Albrektsen, T., Johansson, L., Leers, J. and Gustafsson, J.A. 1998 "A Regulatory Role for RIP140 in Nuclear Receptor Activation". *Mol Endocrinol*, *12* (6). 864-881.
589. Tsujimoto, Y. and Shimizu, S. 2000 "Bcl-2 family: Life-or-death switch". *FEBS Letters*, *466* (1). 6-10.
590. Tsukada, M. and Ohsumi, Y. 1993 "Isolation and characterization of autophagy-defective mutants of Saccharomyces cerevisiae". *FEBS Letters*, *333* (1-2). 169-174.
591. Tucker, C.E., Chen, L.S., Judkins, M.B., Farmer, J.A., Gill, S.C. and Drolet, D.W. 1999 "Detection and plasma pharmacokinetics of an anti-vascular endothelial growth factor oligonucleotide-aptamer (NX1838) in rhesus monkeys". *J Chromatogr B Biomed Sci Appl*, *732* (1). 203-212.
592. Tuerk, C. and Gold, L. 1990 "Systematic evolution of ligands by exponential enrichment: RNA ligands to bacteriophage T4 DNA polymerase". *Science*, *249* (4968). 505-510.
593. Turano, C., Coppari, S., Altieri, F. and Ferraro, A. 2002 "Proteins of the PDI family: unpredicted non-ER locations and functions". *J Cell Physiol*, *193* (2). 154-163.
594. Van de Rijn, M., Perou, C.M., Tibshirani, R., Haas, P., Kallioniemi, O., Kononen, J., Torhorst, J., Sauter, G., Zuber, M., Kochli, O.R., Mross, F., Dieterich, H., Seitz, R., Ross, D., Botstein, D. and Brown, P. 2002 "Expression of Cytokeratins 17 and 5 Identifies a Group of Breast Carcinomas with Poor Clinical Outcome". *Am J Pathol.* , *161* (6). 1991-1996.
595. Van Gestel, K., Köhler, R. and Verbelen, J. 2002 "Plant mitochondria move on F-actin, but their positioning in the cortical cytoplasm depends on both F-actin and microtubules". *J Exp Bot*, *53* (369). 659-667.
596. Vander Heiden, M.G., Chandel, N.S., Williamson, E.K., Schumacker, P.T. and Thompson, C.B. 1997 "Bcl-xL Regulates the Membrane Potential and Volume Homeostasis of Mitochondria". *Cell*, *91* (5). 627-637.
597. Vennema, H., Heijnen, L., Rottier, P.J., Horzinek, M.C. and Spaan, W.J. 1992 "A novel glycoprotein of feline infectious peritonitis coronavirus contains a KDEL-like endoplasmic reticulum retention signal". *J Virol*, *66* (8). 4951-4956.
598. Ventura, A.C. and Merajver, S.D. 2008 "Genetic Determinants of Aggressive Breast Cancer". *Annual Review of Medicine*, *59* (1). 199-212.
599. Vercammen, D., Beyaert, R., Denecker, G., Goossens, V., Van Loo, G., Declercq, W., Grooten, J., Fiers, W. and Vandenabeele, P. 1998 "Inhibition of Caspases Increases the Sensitivity of L929 Cells to Necrosis Mediated by Tumor Necrosis Factor". *J Exp Med*, *187* (9). 1477-1485.
600. Verkhusha, V.V. and Lukyanov, K.A. 2004 "The molecular properties and applications of Anthozoa fluorescent proteins and chromoproteins". *Nat Biotech*, *22* (3). 289-296.
601. Vitale, A. and Denecke, J. 1999 "The endoplasmic reticulum-gateway of the secretory pathway". *Plant Cell*, *11* (4). 615-628.

602. Vogelstein, B., Lane, D. and Levine, A.J. 2000 "Surfing the p53 network". *Nature*, *408* (6810). 307-310.
603. Von Heijne, G. 1985 "Signal sequences : The limits of variation". *J Mol Biol*, *184* (1). 99-105.
604. Wahl, G.M. and Carr, A.M. 2001 "The evolution of diverse biological responses to DNA damage: insights from yeast and p53". *Nat Cell Biol*, *3* (12). E277-E286.
605. Waldo, G.S., Standish, B.M., Berendzen, J. and Terwilliger, T.C. 1999 "Rapid protein-folding assay using green fluorescent protein". *Nat Biotech*, *17* (7). 691-695.
606. Wallis, M.G., von Ahsen, U., Schroeder, R. and Famulok, M. 1995 "A novel RNA motif for neomycin recognition". *Chem Biol*, *2* (8). 543-552.
607. Walter, P. and Johnson, A. 1994 "Signal sequence recognition and protein targeting to the endoplasmic reticulum membrane". *Annu Rev Cell Biol*, *10*. 87-119.
608. Wang, C.W. and Klionsky, D.J. 2003 "The molecular mechanism of autophagy". *Mol Med*, *9* (3-4). 65-76.
609. Wang, S., Konorev, E.A., Kotamraju, S., Joseph, J., Kalivendi, S. and Kalyanaraman, B. 2004 "Doxorubicin Induces Apoptosis in Normal and Tumor Cells via Distinctly Different Mechanisms". *J. Biol. Chem.*, *279* (24). 25535-25543.
610. Wang, X., Pai, J.-t., Wiedenfeld, E.A., Medina, J.C., Slaughter, C.A., Goldstein, J.L. and Brown, M.S. 1995 "Purification of an Interleukin-1[IMAGE] Converting Enzyme-related Cysteine Protease That Cleaves Sterol Regulatory Element-binding Proteins between the Leucine Zipper and Transmembrane Domains". *J Biol Chem*, *270* (30). 18044-18050.
611. Wang, Z., Hao, Y. and Lowe, A.W. 2008 "The Adenocarcinoma-Associated Antigen, AGR2, Promotes Tumor Growth, Cell Migration, and Cellular Transformation". *Cancer Res*, *68* (2). 492-497.
612. Wayne, W.K., Devon, A., Thompson, A., Renee, V.H. and Ronald, J.W. 1998 "Differential screening and suppression subtractive hybridization identified genes differentially expressed in an estrogen receptor-positive breast carcinoma cell line". *Nucleic Acids Res*, *26* (4). 1116-1123.
613. Wei, L.-N., Farooqui, M. and Hu, X. 2001 "Ligand-dependent Formation of Retinoid Receptors, Receptor-interacting Protein 140 (RIP140), and Histone Deacetylase Complex Is Mediated by a Novel Receptor-interacting Motif of RIP140". *J Biol Chem*, *276* (19). 16107-16112.
614. Wei, X., Yu, Z.K., Ramalingam, A., Grossman, S.R., Yu, J.H., Bloch, D.B. and Maki, C.G. 2003 "Physical and Functional Interactions between PML and MDM2". *J Biol Chem*, *278* (31). 29288-29297.
615. Weinberg, R. 1991 "Tumor suppressor genes". *Science*, *254* (5035). 1138-1146.
616. Weir, B. and Yaffe, M. 2004 "Mmd1p, a novel, conserved protein essential for normal mitochondrial morphology and distribution in the fission yeast Schizosaccharomyces pombe". *Mol Biol Cell*, *15* (4). 1656-1665.

617. Weis, K. 1998 "Importins and exportins: how to get in and out of the nucleus". *Trends Biochem Sci*, *23* (5). 185-189.
618. Weisleder, N., Taffet, G. and Capetanaki, Y. 2004 " Bcl-2 overexpression corrects mitochondrial defects and ameliorates inherited desmin null cardiomyopathy". *Proc Natl Acad Sci U S A*, *101* (3). 769-774.
619. West, S.C. 1997 "Processing of recombination intermediates by the RuvABC proteins". *Annu Rev Genet*, *31* (1). 213-244.
620. Whenham, N., D'Hondt, V. and Piccart, M. 2008 "HER2-positive breast cancer: from trastuzumab to innovatory anti-HER2 strategies". *Clin Breast Cancer*, *8* (1). 38-49.
621. Wiebe, V., Osborne, C., Fuqua, S. and DeGregorio, M. 1993 "Tamoxifen resistance in breast cancer". *Crit Rev Oncol Hematol*, *14* (3). 173-188.
622. Wilson, D., Lewis, M. and Pelham, H. 1993 "pH-dependent binding of KDEL to its receptor in vitro". *J Biol Chem*, *268* (10). 7465-7468.
623. Wiman, K. 2006 "Strategies for therapeutic targeting of the p53 pathway in cancer". *Cell Death Differ*, *13* (6). 921-926.
624. Wood, M.A., McMahon, S.B. and Cole, M.D. 2000 "An ATPase/Helicase Complex Is an Essential Cofactor for Oncogenic Transformation by c-Myc". *Mol Cell*, *5* (2). 321-330.
625. Wu, X., Bayle, J.H., Olson, D. and Levine, A.J. 1993 "The p53-mdm-2 autoregulatory feedback loop". *Genes Dev*, *7* (7a). 1126-1132.
626. Wu, Y., Tan, H., Huang, Q., Kim, Y., Pan, N., Ong, W., Liu, Z., Ong, C. and Shen, H. 2008 " Autophagy plays a protective role during zVAD-induced necrotic cell death". *Autophagy*, *4* (4). 457-466.
627. Wyllie, A.H. 1997 "Apoptosis: an overview". *Br Med Bull.*, *53* (3). 451-465.
628. Xu, Y., Piston, D.W. and Johnson, C.H. 1999 "A bioluminescence resonance energy transfer (BRET) system: Application to interacting circadian clock proteins". *Proc Natl Acad Sci U S A*, *96* (1). 151-156.
629. Yaffe, M., Harata, D., Verde, F., Eddison, M., T., T. and Nurse, P. 1996 "Microtubules mediate mitochondrial distribution in fission yeast". *Proc Natl Acad Sci U S A*, *93* (21). 11664-11668.
630. Yaffe, M., Stuurman, N. and Vale, R. 2003 "Mitochondrial positioning in fission yeast is driven by association with dynamic microtubules and mitotic spindle poles". *Proc Natl Acad Sci U S A*, *100* (20). 11424-11428.
631. Yamamoto, K., Fujii, R., Toyofuku, Y., Saito, T., Koseki, H., Hsu, V. and Aoe, T. 2001 "The KDEL receptor mediates a retrieval mechanism that contributes to quality control at the endoplasmic reticulum". *EMBO J*, *20* (12). 3082-3091.
632. Yang, D.C., Head, J.F. and Elliott, R.L. 2002 "Gene targets of antisense therapies in breast cancer". *Expert Opin Ther Targets*, *6* (3). 375-385.
633. Yang, J.-P., Hori, M., Sanda, T. and Okamoto, T. 1999 "Identification of a Novel Inhibitor of Nuclear Factor-kappa B, RelA-associated Inhibitor". *J Biol Chem*, *274* (22). 15662-15670.

634. Yang, S., Zhou, Q. and Yang, X. 2007 "Caspase-3 status is a determinant of the differential responses to genistein between MDA-MB-231 and MCF-7 breast cancer cells". *Biochim Biophys Acta*, *1773* (6). 903-911.
635. Yang, X.H., Sladek, T.L., Liu, X., Butler, B.R., Froelich, C.J. and Thor, A.D. 2001 "Reconstitution of Caspase 3 Sensitizes MCF-7 Breast Cancer Cells to Doxorubicin- and Etoposide-induced Apoptosis". *Cancer Res*, *61* (1). 348-354.
636. Yanushevich, Y.G., Staroverov, D.B., Savitsky, A.P., Fradkov, A.F., Gurskaya, N.G., Bulina, M.E., Lukyanov, K.A. and Lukyanov, S.A. 2002 "A strategy for the generation of non-aggregating mutants of Anthozoa fluorescent proteins". *FEBS Letters*, *511* (1-3). 11-14.
637. Yarbrough, D., Wachter, R.M., Kallio, K., Matz, M.V. and Remington, S.J. 2001 "Refined crystal structure of DsRed, a red fluorescent protein from coral, at 2.0-Ã resolution". *PNAS*, *98* (2). 462-467.
638. Yasumi, M., Sakisaka, T., Hoshino, T., Kimura, T., Sakamoto, Y., Yamanaka, T., Ohno, S. and Takai, Y. 2005 "Direct Binding of Lgl2 to LGN during Mitosis and Its Requirement for Normal Cell Division". *J Biol Chem*, *280* (8). 6761-6765.
639. Yethon, J.A., Epand, R.F., Leber, B., Epand, R.M. and Andrews, D.W. 2003 "Interaction with a Membrane Surface Triggers a Reversible Conformational Change in Bax Normally Associated with Induction of Apoptosis". *J Biol Chem*, *278* (49). 48935-48941.
640. Yonish-Rouach, E., Resnftzky, D., Lotem, J., Sachs, L., Kimchi, A. and Oren, M. 1991 "Wild-type p53 induces apoptosis of myeloid leukaemic cells that is inhibited by interleukin-6". *Nature*, *352* (6333). 345-347.
641. Yoon, Y., Krueger, E.W., Oswald, B.J. and McNiven, M.A. 2003 "The Mitochondrial Protein hFis1 Regulates Mitochondrial Fission in Mammalian Cells through an Interaction with the Dynamin-Like Protein DLP1". *Mol Cell Biol*, *23* (15). 5409-5420.
642. Yoshida, H., Kong, Y.-Y., Yoshida, R., Elia, A.J., Hakem, A., Hakem, R., Penninger, J.M. and Mak, T.W. 1998 "Apaf1 Is Required for Mitochondrial Pathways of Apoptosis and Brain Development". *Cell*, *94* (6). 739-750.
643. Youle, R. and Strasser, A. 2008 "The BCL-2 protein family: opposing activities that mediate cell death". *Nat Rev Mol Cell Biol*, *9* (1). 47-59.
644. Yu, F., Morin, X., Cai, Y., Yang, X. and Chia, W. 2000 "Analysis of partner of inscuteable, a Novel Player of Drosophila Asymmetric Divisions, Reveals Two Distinct Steps in Inscuteable Apical Localization". *Cell*, *100* (4). 399-409.
645. Yuan, J., Shaham, S., Ledoux, S., Ellis, H.M. and Horvitz, H.R. 1993 "The C. elegans cell death gene ced-3 encodes a protein similar to mammalian interleukin-1[beta]-converting enzyme". *Cell*, *75* (4). 641-652.
646. Yue, Z., Jin, S., Yang, C., Levine, A.J. and Heintz, N. 2003 "Beclin 1, an autophagy gene essential for early embryonic development, is a haploinsufficient tumor suppressor". *PNAS*, *100* (25). 15077-15082.

647. Zambetti, G. and Levine, A. 1993 "A comparison of the biological activities of wild-type and mutant p53". *FASEB J.*, *7* (10). 855-865.
648. Zamzami, N., Marzo, I., Susin, S., Brenner, C., Larochette, N., Marchetti, P., Reed, J., Kofler, R. and Kroemer, G. 1998 "The thiol crosslinking agent diamide overcomes the apoptosis-inhibitory effect of Bcl-2 by enforcing mitochondrial permeability transition". *Oncogene*, *16* (8). 1055-1063.
649. Zaraisky, A.G., Lukyanov, S.A., Vasiliev, O.L., Smirnov, Y.V., Belyavsky, A.V. and Kazanskaya, O.V. 1992 "A novel homeobox gene expressed in the anterior neural plate of the Xenopus embryo". *Dev Biol*, *152* (2). 373-382.
650. Zhang, J., Gong, A., Cheville, J., Smith, D. and Young, C. 2005 " AGR2, an androgen-inducible secretory protein overexpressed in prostate cancer". *Genes Chromosomes Cancer*, *43* (3). 249-259.
651. Zhao, Y., Yang, H., Zhang, X. and Chen, G. 2005 "Mutation in D-loop region of mitochondrial DNA in gastric cancer and its significance". *World J Gastroenterol*, *11* (21). 3304-3306.
652. Zheng, W., Rosenstiel, P., Huse, K., Sina, C., Valentonyte, R., Mah, N., Zeitlmann, L., Grosse, J., Ruf, N., Nurnberg, P., Costello, C.M., Onnie, C., Mathew, C., Platzer, M., Schreiber, S. and Hampe, J. 2006 "Evaluation of AGR2 and AGR3 as candidate genes for inflammatory bowel disease". *Genes Immun*, *7* (1). 11-18.
653. Zhong, J., Zhang, H., Stanyon, C.A., Tromp, G. and Finley, R.L., Jr. 2003 "A Strategy for Constructing Large Protein Interaction Maps Using the Yeast Two-Hybrid System:Regulated Expression Arrays and Two-Phase Mating". *Genome Res.*, *13* (12). 2691-2699.
654. Zhou, M., Gu, L., Findley, H.W., Jiang, R. and Woods, W.G. 2003 "PTEN Reverses MDM2-mediated Chemotherapy Resistance by Interacting with p53 in Acute Lymphoblastic Leukemia Cells". *Cancer Res*, *63* (19). 6357-6362.
655. Zhou, Q. and Salvesen, G.S. 1997 "Activation of pro-caspase-7 by serine proteases includes a non-canonical specificity". *Biochem J*, *324* (2). 361-364.
656. Zhu, W., Qin, W., P., B., A., W., Puckett, C. and Sauter, E. 2005 "Mitochondrial DNA mutations in breast cancer tissue and in matched nipple aspirate fluid". *Carcinogenesis*, *26* (1). 145-152.
657. Ziyaie, D., Hupp, T. and Thompson, A. 2000 " P53 and breast cancer". *Breast*, *9* (5). 239-246.
658. Zong, W.-X., Li, C., Hatzivassiliou, G., Lindsten, T., Yu, Q.-C., Yuan, J. and Thompson, C.B. 2003 "Bax and Bak can localize to the endoplasmic reticulum to initiate apoptosis". *J Biol Chem*, *162* (1). 59-69.
659. Zou, H., Henzel, W.J., Liu, X., Lutschg, A. and Wang, X. 1997 "Apaf-1, a Human Protein Homologous to C. elegans CED-4, Participates in Cytochrome c-Dependent Activation of Caspase-3". *Cell*, *90* (3). 405-413.
660. Zou, J., Ye, Y., Welshhans, K., Lurtz, M., Ellis, A.L., Louis, C., Rehder, V. and Yang, J.J. 2005 "Expression and optical properties of green fluorescent protein expressed in different cellular environments". *J Biotechnol*, *119* (4). 368.

661. Zou, L. and Elledge, S.J. 2003 "Sensing DNA Damage Through ATRIP Recognition of RPA-ssDNA Complexes". *Science*, *300* (5625). 1542-1548.
662. Zweitzig, D., Smirnov, D., Connelly, M., Terstappen, L., O'Hara, S. and Moran, E. 2007 "Physiological stress induces the metastasis marker AGR2 in breast cancer cells." *Mol Cell Biochem*, *306* (1-2). 255-260.

List of websites

1. Introduction
www.who.int/topics/cancer/en/

2. Materials and Methods
www.bact.wisc.edu
www.sigmaaldrich.com
www.neb.com

3. Localization of AGR-2
www.georgetown.edu
www.BDbiosciences.com
www.tsienslab.usbc
www.expasy.org
www.russell.embl-heidelberg.de